UNIVERSITY OF SOUTHAMPTON

Faculty of Engineering, Science and Mathematics

School of Mathematics

Modelling Tuberculosis Notification Data

by

Kathryn Anna Hoad

submitted for the degree of Doctor of Philosophy

May 2006

UNIVERSITY OF SOUTHAMPTON

ABSTRACT

FACULTY OF ENGINEERING, SCIENCE AND MATHEMATICS

SCHOOL OF MATHEMATICS

Doctor of Philosophy

MODELLING TUBERCULOSIS NOTIFICATION DATA.

by Kathryn Anna Hoad

This thesis describes the development of three different Tuberculosis epidemiological models: An age dependent parametric statistical model; a compartmental, age dependent, differential/difference model; and a Markov chain model that allows for location effects in the transmission of TB.

Recently collected data from countries that have experienced a long-term decline in TB incidence and in the annual risk of TB infection has exhibited a slow down in the decline of the TB notification rate. This stagnation effect has implications for projected reductions in TB incidence made by the World Health Organisation. Parametric modelling was used to carry out a preliminary analysis of TB data sets that were considered to exhibit such stagnation effects. The aim was to examine the age and time dependent effects exhibited by each data set and to identify any shared trends. This analysis was a precursor to a more structural age dependent compartmental modelling of this data.

The third model, a Markov chain model, is distinct from the previous two models described above. It is constructed to examine the relative significance of local and global effects in the transmission of TB. Examining/modelling 'household'/local effects is a relatively new branch of TB modelling that is considered important in the planning of TB control strategies and has previously been tackled with compartmental modelling. The simple Markov chain local effects model is used to examine a time-spatial TB data set from the Nyanza province in western Kenya. It is also shown how this new local/global effects model can be used in the design of community/clustered randomised trials.

Contents

List of Figures

List of Tables

Acknowledgements

I would first like to thank my supervisor Professor Russell Cheng whose assistance, advice, time and support has always been given freely and generously throughout the course of my PhD study. I would also like to thank his wife Anne for her generous support and hospitality.

Many people at the World Health Organization have helped me through the course of my PhD and I would especially like to thank Dr Brian Williams and Dr Chris Dye for their help and support. I would also like to thank the people at the Centers for Disease Control and Prevention (CDC) and Kenya Medical Research Institute (KEMRI) for their support. I am indebted to the Kenya Ministry of Health/National Leprosy and Tuberculosis Program for availing their TB surveillance data.

I am also grateful to the EPSRC who funded me throughout this research.

I would also like to thank Emily Webb, Christine Currie, Naomi, Jenny, Sarah, Ronni, James and Georgie for their invaluable friendship and support.

I would also like to acknowledge and thank the many people in the maths faculty and various support services of the University of Southampton who have been so supportive and helpful to me.

I would very much like to thank my parents, whose continued uncritical support and patience throughout my time of study has been invaluable to me.

Last but not least I would very much like to thank Jon for his continued support, patience and for making me smile and laugh when I really needed it.

Glossary: Some key epidemiological definitions

- Modelling:
  - Deterministic model - A mathematical model in which the parameters and variables are not subject to random fluctuations, so that the system is at any time entirely defined by the initial conditions chosen.
  - Stochastic model - A mathematical model which takes into consideration the presence of some randomness in one or more of its parameters or variables. The predictions of the model therefore do not give a single point estimate but a probability distribution of possible estimates.
  - Force of infection - The per capita rate at which those susceptible to infection are infected.
  - Reproductive rate (R_0) - The average number of secondary infections produced when one infected individual is introduced into a susceptible population
- General terms:
  - Syndromic - A group of symptoms indicating a disease
  - Asymptomatic - Without obvious signs of symptoms of disease
  - Pathogenesis - The origin and development of disease.
  - Morbidity - A diseased condition or state; the incidence of a disease or of all diseases in a population.
  - Seroconversion - Development of antibodies in the blood serum as a result of infection or immunization
  - Seropositive - Showing a positive reaction to a blood serum test for a disease; Showing seroconversion

Chapter 1

Introduction

This thesis describes the development of three different Tuberculosis epidemiological models: An age dependent parametric statistical model; a compartmental, age dependent, differential/difference model; and a Markov chain model that allows for location effects in the transmission of TB.

The methodology used is based on epidemiological modelling with a fairly statistical approach of model fitting using likelihood methods for parameter estimation. Likelihood methods and resampling methods were employed in the sensitivity analysis of the various models. All three TB models were programmed in Excel/VBA language, using a modular program structure.

Recently collected data from countries that have experienced a long-term decline in TB incidence and in the annual risk of TB infection has exhibited a slow down in the decline of the TB notification rate [67]. This stagnation effect has implications for projected reductions in TB incidence made by the World Health Organisation under their TB control strategy DOTS. Parametric modelling was therefore used to carry out a preliminary analysis of TB data sets that were considered to exhibit such stagnation effects. The aim was to examine the age and time dependent effects exhibited by each data set and to find which trends were shared by these

data sets. This analysis was a precursor to the more structural age dependent compartmental modelling that followed. The parametric model shows that there are significant age and stagnation effects and that these trends are shared by all three data sets examined. But it can not indicate how these effects may arise. Compartmental models can be used to try and answer these type of questions and are therefore widely used in epidemiological modelling. It was therefore an interesting experiment to apply these same data sets to a compartmental model based upon a previously constructed W.H.O TB DOTS model [14, 15]. The reconstructed compartmental model was investigated as to how well and easily it could explain the various time and age effects exhibited in these data sets.

The third model, a Markov chain model, is distinct from the previous two models described above. It is constructed to examine the relative significance of local and global effects in the transmission of TB. Examining/modelling 'household'/local effects is a relatively new branch of TB modelling that is considered important in the planning of TB control strategies and has previously been tackled with compartmental modelling. The simple Markov chain local effects model is used to examine a time-spatial TB data set from the Nyanza province in western Kenya. It is also shown how this new local/global effects model can be used in the design of community/clustered randomised trials.

1.1 Parametric Statistical Modelling

Countries that have experienced a long-term decline in TB incidence and in the annual risk of TB infection, often exhibit a slow down in the annual decline of the crude notification rate. This behaviour is referred to as stagnation and is most often observed in middle-to-higher income countries with increasing life expectancy. As the risk of infection declines, the proportion of disease due to initial infection (primary disease) and re-infection also declines. When the risk of infection reaches

an extremely low level it is likely that most of the disease detected is endogenous re-activation disease, which does not depend on the current risk of infection. This effect is called the 'ageing of the epidemic' and can not be adjusted for in analysis by standardisation by age.

The prime objective of this section of the thesis is to analyse and investigate the age and time dependent behaviour of TB case data from three countries considered to fall into this category of countries that have an increasing life expectancy and exhibit an ageing of the TB epidemic. Thus TB data sets from the Netherlands, Morocco and UK are compared to investigate whether they exhibit any similar characteristics/trends.

The general methodology is to fit a family of parametric models to the data sets from the Netherlands, Morocco and UK. Thus, the significance of certain features of the data can be inferred from the significance of certain model parameters responsible for explaining such features.

All three data sets exhibit a decline in TB that is greatest in the younger age ranges and gradually levels off in the older age ranges. The data also exhibits a strong sigmoidal shape (with age) and a tailing off behaviour (with time) that need to be captured by the fitted model.

A family of parametric distributions are fitted to the TB data sets. The method of Maximum Likelihood is used to fit the chosen distributions and the direct search optimisation method, Nelder-mead, is used to find the maximum value of the likelihood. It is assumed that each TB data set is a set of identically distributed random variables drawn from the Normal distribution. The mean of this distribution is assumed to be a function dependent on both age and time and takes the general form of a polynomial multiplied by a logistic function. The polynomial is used to describe the tail behaviour of the TB data and the logistic function describes the sigmoidal shape of the data.

Confidence intervals for the maximum likelihood estimator values and confidence/performance bands for the model fits, are constructed using Asymptotic Theory and the Bootstrap (re-sampling) Method.

The general characteristics of the TB data sets as they vary with time and age are satisfactorily captured by this family of parametric models. There are a few more detailed characteristics that the models fail to capture. However, it is unclear whether all these characteristics are derived from true features of the data. The accuracy of the data must be questioned especially for the two oldest age ranges in the Dutch data, for very young children and for the Moroccan year data that is created by projection (1995 onwards). The parametric modelling does confirm that the data contains significant age and time dependent trends. The fact that this family of functions successfully explains all three data sets confirms that the data from these three different countries share some significant trends. Parametric modelling however does not answer the question of why/how these effects/trends might occur. The most popular method used in TB epidemiological modelling for answering such questions is to construct and employ a compartmental, difference/differential equation model. Thus a compartmental model was re-constructed and applied to two of the previously examined data sets in order to investigate how well and easily such a model can explain the age and time dependent effects exhibited by such data sets.

1.2 A compartmental, age-dependent TB Model

This model was constructed with the primary purpose of investigating the ability of such compartmental models to analyse the progression of TB in countries with an increasing life expectancy and a very low annual risk of infection, where 'aging of the epidemic' and thus stagnation effects could occur. This model is re-constructed and adapted from one developed by C.Dye et. al. [14, 15] to investigate the ef-

fect of Directly Observed Short-course Therapy (DOTS), the WHO's strategy for worldwide TB control, on tuberculosis epidemics in developing countries with a high TB burden. This deterministic, compartmental model, is set in discrete time. The population is moved through the model by difference equations. HIV is not included in this new re-constructed version of the model as the countries that are of prime interest are not considered to have a large HIV problem, thus simplifying the model. It was also considered important to allow the model to take time steps of less than 1 year to adequately capture the progression of a TB epidemic in a population.

The emphasis of this work is on examining the ability of compartmental models to fit to TB data from countries experiencing an ageing of their population and an aging of the TB epidemic. Thus, after producing a reasonable fit to TB data sets from the Netherlands and Morocco, most of the work concentrates on the sensitivity analysis of the model. The aim is to explore how varying the values of each input parameter affects the outcome variable. The outcome investigated was the number of TB cases per 100,000 of population for each of 8 age groups. The UK data set was not used as it only contains TB data for white males and the model does not make this distinction between gender and ethnicity.

It is found that the shape of the line fit for both countries does not vary significantly across the 8 age ranges. Hence, in the case of the Dutch data, the model fits well for the first three age ranges but fails to capture the 'flattening' of the curved behaviour of the data in the later age ranges. It is also unable to explain the 'tailing off' and subsequent increase in TB case numbers observed in the Moroccan data. It is also noticeable that the model was unable to fit to the initial year data well, overestimating the number of TB cases in the adult age ranges. This was most noticeable in the fit to the Dutch data although many different warm-up scenarios were tried.

Most of the parameters, when varied by a fixed amount, affected the outcome

variable as would be expected and this behaviour is explainable by the known epidemiology of TB. There were a few notable exceptions however, namely, p(for ages 15+) - the proportion of infectious susceptibles which develop progressive primary TB in 1 year; x(for ages 15+) - the proportion of re-infections which is susceptible to developing TB within 1 year; r - the rate of relapse from failed treatment to active TB. These three parameters caused the same counter-intuitive effects in the outcome variable for both countries' data sets.

All the parameters mostly behave in a non-linear way (except perhaps for very small variations in value) and interact with each other in complicated and subtle ways. It was also noticeable that varying the parameters one at a time did not significantly improve the model fit to each of the age groups over time.

Thus this age dependent compartmental model, despite the large number of parameters, struggled to explain some of the age dependent characteristics shown by the Moroccan and Dutch TB case data. These two countries are considered similar in that they have an increasing life expectancy and exhibit an ageing of the TB epidemic.

When comparing the fits of the previous parametric models to the Dutch and Moroccan data with those of the age dependent compartmental model, the parametric model successfully captured much more of the age and time dependent characteristics of these data sets.

1.3 A Markov Chain model of TB case clustering in the Nyanza Province of Western Kenya

This is a separate and distinct model from the previous two models. It is constructed to examine the relative significance of local and global effects in the transmission of TB. The simple Markov chain model is used to examine a time-spatial

TB data set from the Nyanza province in western Kenya. It is also shown how this new local/global effects model can be used in the design of community/clustered randomised trials.

The Kenyan data set analysed comprises 840 notifications of all types of TB collected in Asembo and Gem by the Kenya Ministry of Health/National Leprosy and TB program and the CDC over a six year period from 1997 to 2002. The data includes information on the treatment start-date (month and year), age, gender, and contact address (village). GIS coordinates (longitude and latitude) of the contact address (village) were added for each TB case in the data set to allow for a time/spatial analysis of the data. This detailed history of individuals allows for the possibility of investigating transmission effects, in particular whether these effects are local or global.

This model is therefore created in an attempt to identify whether the nearest reported source of possible infection is a localised one stemming from an individual's contacts with family or near neighbours or whether it arises from much more dispersed 'global' contact. The basic methodology is to construct a stochastic Markov-chain model whose behaviour is determined by a number of key parameters representing possible local and global effects on TB transmission. This model is then fitted to the Kenyan TB data using maximum likelihood and Nelder-mead optimisation to estimate these key parameter values. Markov-chain models are based on transition probabilities and are very different in approach from the type of compartmental model described in chapters 9 - 11 or the statistical parametric models described in chapters 5 - 8.

It is constructed by following the individual histories of all the individuals over the study period. It is assumed that, at any time point, the state of an individual can only be one of two prescribed states: a TB case (State 1) and non-TB case (State 0). A (single step) transition probability governs each single time-step transition made by an individual and is constructed as a parametric function that includes separate

components representing the local and global clustering of TB cases. Male/female characteristics and age dependence are also included into the transition probability structure.

The model shows that there is a significant local effect in TB transmission. The results also show that age seems to be a significant factor whereas gender on its own is not.

A number of tests of the robustness of the modelling procedure were carried out including: a demonstration that the importance of local prevalence is not simply an artifact of the modelling; testing the effect of decreasing sample size on the fitting of the model; investigating the effect of the length of the infectious period; investigating the effect of different starting parameter values in the Nelder-mead optimisation procedure; investigating the model's sensitivity to the spatial scale of disease clustering. The results of all these various robustness tests were satisfactory and indicated that this model is valid and robust.

An important possible use of the local and global effect model is in the design of a community randomized trial where geographical clusters of people are divided into two groups and the effectiveness of an intervention policy is assessed by applying it to one group but not the other. Here the model can be used to calculate the minimum difference in an outcome variable that can be detected with statistical significance, taking the effect of clustering of cases into consideration. It thereby gauges the potential effectiveness of such a trial. Such a possible application is illustrated by setting up cluster randomised trial scenarios using the western Kenyan time/spatial TB data set and applying the model.

1.4 Chapter arrangement and contents

Background Material

Chapter 2 contains basic background material on disease modelling in general. Chapter 3 introduces the human disease of Tuberculosis. It includes a brief chronological history of TB and describes the epidemiology of this widespread disease. A summary of the history of mathematical TB modelling is contained in Chapter 4.

Main Chapters

Chapters 5, 6, 7 and 8 describe the analysis, construction and fitting of a family of parametric statistical functions to TB data from the Netherlands, UK and Morocco.

Chapter 9 describes the construction of the compartmental, age-dependent TB Model, including a full list and description of the difference equations powering the model and an explanation as to how the demographic data was adapted for input into the model. Chapters 10 and 11 describe the fitting and sensitivity analysis of the compartmental, age-dependent model to TB data from the Netherlands and Morocco respectively.

Chapters 12 to 16 introduce and describe a new Markov-chain local/global effects TB model used to analyse a time-spatial TB data set from western Kenya. Chapter 17 discusses the results and possible future work regarding the local/global effects model and the analysis of the Kenyan TB data set.

Chapter 18 concludes the thesis, discussing all three different models and suggesting possible further work.

Appendices

Appendix A describes the methodology of the Nelder-mead optimisation algorithm. An introduction to Likelihood Theory is contained in Appendix B. Appendix C describes the most common methods of sensitivity and uncertainty analysis. A brief description of the bootstrap methodology is contained in Appendix D. Appendix E contains a brief history of the changing demography and health in

Morocco. Appendix F contains graphs of the fitting of exponential trend lines to log transforms of the TB data from Morocco, Netherlands and UK.

Chapter 2

An Introduction to Modelling Disease Transmission

2.1 Formulating models

Epidemiology is the study of diseases in populations and communities rather than in particular individuals. Mathematical modelling is used to help in the understanding of the biology of a problem. **Dynamical models** based on difference or differential equations are designed to take into account the actual dynamics of the disease over time. They can be constructed to simulate the actual situation that exists and are limited only by the imagination of the scientist and the current data available. They can be linear, non-linear, complex or simple and are often compartmental in construction. These models are usually designed to describe the past known history of the disease and to predict the future unknown course of the disease [25].

Once the general structure of the model has been formulated, the various parameters need to be measured and then fed into the model, usually as rates. For example:

- rate at which susceptible people become infected
- mortality rate of people with the disease (which determines the rate at which the model loses people through death.)
- birth rate (which determines the rate at which new people are recruited to the model)

All these rates can be further broken down into subgroups, for example, rates for men and women or different age groups. Using a knowledge of all these rates and the values at an initial state, the **simulation model** can then show how the different rate processes combine to determine the changes in the state of the system over time.

If the rates are measured in continuous time then they are written as **differential equations**. If they make up a simple system of equations then this can be solved using calculus. However for more complex systems, the problem is usually formulated directly into **difference equations** and programmed into a computer to run the simulation over a set number of time periods.

The kind of model starts with a certain number (or proportion) of people in each state category and then calculates the numbers in each successive time step according to our knowledge of the natural history of the disease. The model can be run for various values of the parameters to see what happens over time, for differing scenarios.

This model does not include any random effects and is therefore called a **deterministic model**. To make the simulation model more realistic, random effects can be included. These are then termed **stochastic models**. For example, where in a deterministic model $x\%$ of susceptibles would be infected in one time unit, a stochastic model would consider each individual and use a random number generator to infect each person with a probability of $x\%$.

A stochastic model therefore gives a different result each time it is run, but if it is run many times, the average result should be close to the result of a single deterministic model run. Running a stochastic model many times therefore allows the variability of the results to be determined [25].

Although compartmental models are very common there are various other methods that are used to model diseases, such as statistical models where simple or more complex parametric functions are fitted to known data, time series analysis, or Markov chain models.

2.2 Measures of disease

There are a number of indicators that are used to describe the transmission and epidemiology of a disease. The following is a list of epidemiological terminology with definitions, that are most commonly used in modelling disease [25].

- The **force of infection** is the per capita rate at which susceptibles are infected.
- The **incidence** of a disease is *the rate* at which *uninfected* people *become infected.* Incidence is most commonly measured in numbers of cases per person per year, thus,

  incidence rate =

  $$\frac{\text{number of uninfected people infected in time period}}{\text{number of uninfected people at start of time period} \times \text{time period}}$$

- The **prevalence** is the proportion of people infected with the disease in the population at any particular time. Prevalence is therefore dimensionless and is calculated by,

  $$\text{prevalence} = \frac{\text{number of people infected at point in time}}{\text{population at time}}$$

- The **change in prevalence** = (force of infection - recovery rate) $\times$ time period.

- The **risk** or **cumulative incidence** is the *proportion* of uninfected people who become infected in a given time period. So, risk = incidence $\times$ time period.

- **Period prevalence** is the proportion of people who were diseased at any time point during a given interval.

- The **odds of becoming infected** equal the number becoming infected divided by the number staying uninfected. Thus,

$$\begin{aligned} \text{odds} &= \frac{\text{number becoming infected}}{\text{number staying uninfected}} \\ &= \frac{\text{risk} \times \text{number uninfected at start}}{(1 - \text{risk}) \times \text{number uninfected at start}} \\ odds &= \frac{\text{risk}}{1 - \text{risk}} \end{aligned}$$

- The **recovery rate** can be defined as the rate at which infections are lost or people recover. Thus,

$$\text{recovery rate} = \frac{\text{number of people recovered in time period}}{\text{population} \times \text{time period}}$$

- The **mortality rate** or death rate is calculated as

$$\text{mortality rate} = \frac{\text{number of deaths}}{\text{population} \times \text{time period}}$$

- The **basic case reproduction number** (or rate), R_0, is the number of secondary cases produced by one primary case in a completely susceptible population. If no interventions are implemented to reduce the transmission rate then prevalences reach approximately $\frac{(R_0-1)}{R_0}$. In practical terms this means that if a vaccine existed for this disease, the proportion of people that would need to be vaccinated in order to control the epidemic would be $\frac{(R_0-1)}{R_0}$.

R_0 therefore describes the magnitude of the control problem. For example, Smallpox had an R_0 value of approximately 3. Thus it was only necessary to vaccinate 2/3 of the population and sustain this level for long enough in order to eradicate smallpox [25].

2.3 Estimating incidence from age-prevalence data

It is the incidence of a disease that epidemiologists are usually most interested in. But it is also very difficult if not impossible to observe directly and is therefore commonly estimated from the more easily measurable prevalence of the disease. For example the rate at which prevalence increases or decreases with age can be used to get an estimate of the incidence by effectively using age as a surrogate for time. Thus the slope of the age prevalence curve, corrected for the disease related mortality and overall growth of the epidemic, can be used to get a good measure of incidence [25].

Chapter 3

Tuberculosis

Tuberculosis is a world wide disease. It kills approximately 2 million people each year and in 1993, the World Health Organisation (WHO) declared tuberculosis a global emergency. In 2003 the WHO estimated that 31 million people are exposed to TB each year and approximately 8 million become sick with TB [51].

The following section is a chronological history of TB in humans. It illustrates how TB has long been a major cause of illness and mortality in humans and describes the significant medical discoveries in the fight against this disease.

The subsequent sections describe the epidemiology, treatments and tests for TB and explain some of the important terminology that will be used in the following chapters. These sections therefore contain information on how TB infects, acts, is identified and combatted, that is either assumed or referred to directly in the following chapters.

3.1 A brief history of TB in humans

The existence of TB (though not always known by this name) as a human disease, has been traced as far back as 2000 to 4000BC. This section provides a brief

chronological summary of the history of TB in humans.

- 2400BC to 4000BC - Egyptian mummies show definite pathological signs of tubercular decay. [4, 3, 21]
- 460BC - Hippocrates wrote that 'phthisis' (consumption) was the most prevalent disease of the times and was almost always fatal. [4, 3, 21]
- 55BC to 800AD Britain - Graves dating from the Roman Occupation of Britain show evidence of TB. [29]
- Mid 17^{th} Century - Consumption (TB) was the cause of one fifth of all deaths in London, as recorded in the 'Bills of Mortality'. It was known as the 'White Plague' as TB became epidemic in the major cities of Europe and America. [29]
- 1679 - In his 'Opera Medica' (first edition 1679), Dr Sylvius Franciscus de Le Boe, (b.1642-d.1672), was the first to recognise tuberculosis as a consistent and characteristic change in the lungs and other parts of the body in consumptive patients. He stated that tubercles are often found in the lung, and that "they softened and suppurated to form cavities". (*suppurate* $\sim$ *to ripen and generate pus*) [4, 3, 21]
- 17^{th} century Italy - The earliest mention of the infectiousness of TB is found in 17^{th} century Italian medical literature. Indeed, in 1699 the Republic of Lucca issued a decree that "...henceforth, human health should no longer be endangered by objects remaining after the death of a consumptive. The names of the deceased should be reported to the authorities, and measures undertaken for disinfection." [4, 3, 21]
- 1700 - John Jacobus Manget created the phrase Miliary tuberculosis (TB) which refers to the clinical disease resulting from the uncontrolled spread of

Mycobacterium tuberculosis in the body. He used the term miliary because of the similarity he noticed between the appearance of millet seeds and the firm small white nodules found on the surface of the TB diseased lung. [3, 54]

- 1720 - English physician Benjamin Marten published 'A New Theory of Consumption' in which he theorised that TB could be caused by "wonderfully minute living creatures", and that these could cause the lesions and other symptoms of the disease. He also wrote, regarding the infectiousness of TB disease, "It may be therefore very likely that by an habitual lying in the same bed with a consumptive patient, constantly eating and drinking with him, or by very frequently conversing so nearly as to draw in part of the breath he emits from the Lungs, a consumption may be caught by a sound person...I imagine that slightly conversing with consumptive patients is seldom or never sufficient to catch the disease." [4, 3, 21]

- 19^{th} century - By the turn of the 19^{th} century the world TB death rate was estimated at 7 million per year. There were real fears that European civilisation would be destroyed by this pernicious disease. [29]

- 1836 - Dr George Bodington, an English physician, wrote down the idea of providing TB patients with a special diet, exercise and fresh air in a rural environment. These ideas were not supported by the medical establishment of the time. [74]

- 1850s - TB sufferer Hermann Brehmer, a Silesian botany student, advised by his doctor to find a 'healthier climate' travelled to the Himalayan mountains and returned 'cured' of TB. He subsequently switched to studying medicine and in 1854 presented his doctoral dissertation "Tuberculosis is a Curable Disease". In 1859 Dr Brehmer built the first 'sanatorium' in Gorbersdorf, in a pine forest in the mountains of Silesia, eastern Europe (*Poland*). This

became the blueprint for many subsequent sanatoria world wide. [4, 3, 74, 21]

- 1865 - Dr Jean-Antoine Villemin, a French military physician, showed that consumption (TB) could be passed from humans to cattle and from cattle to rabbits. He postulated that this disease was therefore caused by a specific microorganism and did not, as had been thought for centuries, arise spontaneously in each affected organism. [4, 3, 21]

- 1882 - German biologist, Robert Koch (b.1843 - d.1910), (*1905 awarded the Nobel Prize for Physiology or Medicine*) developed new techniques of staining bacteria which made them more easily visible and helped to identify them. He thus discovered the tubercle bacillus as well as a method of growing it in pure culture. In 1882 he published his classical work on Mycobacterium tuberculosis. With this brilliant scientific discovery the fight against TB began in earnest. [4, 3, 2]

- 1882 - In 1832, an English physician named James Carson, demonstrated in animals that injection of air into the pleural space collapsed the diseased lung, permitting it to heal (4). This method called artificial pneumothorax was finally put into practice in the treatment of TB when Italian C. Forlanini rediscovered the process in 1882 [3]. It was found that this method could be used to collapse the TB affected lung, putting it 'at rest' and thus allowing the tuberculous cavities to heal. Unfortunately this treatment did not work for patients in late-stage TB, as the advanced disease kept the lung from collapsing. A surgical treatment for late-stage TB patients was devised that consisted of removing parts of the upper ribs on one side to collapse the rib cage and hence cause the affected lung to collapse allowing it to heal. This treatment method is known as extra-pleural thoracoplasty. [52]

- 1895 - German physicist Wilhelm Konrad von Rontgen (b.1845 - d.1923)

discovered x-rays allowing the progress and severity of a patient's disease to be viewed and monitored. [4, 3, 21]

- Early 20^{th} century - Edward Archibald, a surgeon at the Royal Victoria Hospital in Montreal, Canada, was the first surgeon in North America to surgically treat late-stage TB with extra-pleural thoracoplasty. [52, 21]

- 1921 - French bacteriologist, Albert Calmette and veterinarian, Camille Guerin, while working at the Pasteur Institute produced a live, weakened strain of Mycobacterium bovis, (the bovine equivalent of Mycobacterium tuberculosis). In 1921, the Bacille Calmette Guerin (BCG) vaccine was developed for use in humans. It was first used in Britain in 1953. It remains the only vaccination available against tuberculosis. [4, 3, 1]

- 1939 - Selman A. Waksman discovered that the Actinomycetes fungi inhibited bacterial growth. [21]

- 1940 - Antibiotic Actinomycin was isolated and found to be effective against TB but was too toxic to be used on humans or animals. [21]

- 1943 - Dr Schatz, Bugie and Waksman announced the discovery of an antibiotic, streptomycin, that was successful in inhibiting M.tuberculosis and was of a low enough toxicity to be of use in humans and animals. [21]

- 20^{th} November 1944 - Streptomycin first administered to a TB patient, (a 21 year old woman known as 'Patricia'). The disease was immediately halted, she made a rapid recovery and the TB bacteria disappeared from her sputum. Unfortunately, streptomycin resistant TB strains soon started to appear. However with a rapid succession of new anti-TB drugs appearing in the following years these resistant strains were combatted by combining two or three drugs. [4, 3, 29, 21]

- 1949 to 1963 - Discovery and production of anti-TB drugs p-aminosalicylic, isoniazid, pyrazinamide, cycloserine, ethambutol and rifampicin. [3]

3.2 Epidemiology of Tuberculosis

Tuberculosis (TB) is primarily a disease of the respiratory system (Pulmonary Tuberculosis (PTB)) with varying degrees of infectiousness and usually occurs as pneumonia. But (non-infectious) TB can also occur in the brain, back, lymph nodes or other organs and bones. It is caused by being infected with the airborne bacterial germ *Mycobacterium tuberculosis*. Bacilli only live in the air for approximately two hours so individuals who have intense systematic exposure to TB bacilli in poorly ventilated areas are the most likely to become infected.

If the body is unable to protect itself from the TB Bacilli when they are first breathed in, then the germs can develop into active TB disease within weeks of being infected. In this case the active TB disease is termed *Primary disease*.

Latently infected individuals have the TB bacilli in their bodies but are not sick or infectious (inactive TB) and may never develop active TB because their body's immune system 'seals off' the TB bacilli which can lie dormant for years. Thus the Latent period can vary vastly in length. The inactive TB Bacilli can become active again when the body's defences are weakened. This can be due to a number of different reasons, including, natural aging, serious illness, drug or alcohol abuse, HIV infection, or lack of health care due to homelessness etc... If this reactivation of the TB Bacilli leads to active TB, it is termed *Re-activation disease* or *Endogenous disease*. Experts estimate that only $5 - 10\%$ of people infected with TB (and are HIV negative) will actually develop active TB in their life time. Thus, as latent individuals are not clinically ill, new cases of infection can go undiscovered for some time.

It is also possible for an already infected person to become re-infected with the TB Bacilli. If this re-infection causes active TB, it is termed *Re-infection disease* or *Exogenous disease*.

Thus clinical (active) TB may follow soon after initial infection (*primary disease*) or many years after (*post-primary disease*), either by *endogenous reactivation* or after *exogenous reinfection*. The risks of developing disease are age-dependent but the age-specific risks of developing endogenous or exogenous disease are difficult to assess and there is also a great variability in the estimates of the risk of developing primary disease between studies.

However, some groups of people are considered to have a higher risk of contracting TB than others; these include HIV positive individuals, people in close contact with those who have active infectious TB (e.g. relatives, health care workers..), those with medical conditions that weaken the body's defenses to disease (e.g. diabetes, people taking immune-suppressant drugs..), people from countries with a high TB prevalence, workers or residents of long-term care facilities (e.g. nursing homes, some hospitals or prisons..), the mal-nourished, alcoholics and IV drug users.

Incidence of active-TB in developed countries can be as low as 10 per 100,000 population or less. Conservative estimates for this rate at the beginning of the twentieth century are 300-600 per 100,000. Now most developing countries have incidences of active-TB of 30-200 per 100,000 [45]. But it is possible to have high prevalence of latent infections and low incidence of active-TB because TB has low progression rates. The likelihood of progression to active-TB depends on age of infection and on factors that correlate well with socio-economic status. The risks of developing disease are age-dependent and are higher for adolescents and adults than for children. Age at infection, chronological age and reinfection are considered three of the most important factors underlying tuberculosis morbidity in a population. TB morbidity and mortality rates are also strongly affected by

urban living conditions. Infectiousness of source case, duration and frequency of exposure, characteristics of shared environments all contribute to the overall risk of transmission per contact. The CDC estimate that one active case contributes to 9 effective identified contacts. The W.H.O estimate that someone in the world is newly infected with TB bacilli every second and overall, one-third of the world population is currently infected.

3.3 TB Treatment

There are many anti-TB drugs now available. Preventative Therapy aims to kill the dormant Bacilli and usually consists of a daily dose of isoniazid (INH), taken for anything from 6 months to a year. The W.H.O's recommended treatment regime is called DOTS: Directly Observed Short-course Therapy. It combines five elements: political commitment, microscopy services, drug supplies, monitoring systems and direct observation of treatment. Sputum positive patients are put on a course of anti-TB drugs, the most common of which are isoniazid, rifampicin, pyrazinamide, streptomycin and ethambutol. The patients are constantly monitored to ensure they finish the whole 6 to 8 month treatment. By the end of 2000, all 22 of the countries with the highest TB rates had adopted DOTS.

Once treatment has started the infectious individual should become non-infectious within a few weeks. However, if the treatment is not completed the TB disease can return and the patient can become infectious again. There is also a risk that the TB can become resistant to the anti-TB drugs. Shortly after drug treatment was first introduced single drug-resistant TB strains first appeared and strains of TB that are resistant to all major anti-TB drugs have developed more recently. Multi-drug resistant TB (MDR TB) is a very dangerous form of drug-resistant TB and is considered a significant threat to effective TB control.

3.4 Tests for Tuberculosis

The symptoms of TB are a persistent cough, coughing up blood, fevers, weight loss, constant tiredness, night sweats and loss of appetite, but these are not exclusive to TB and therefore further tests are necessary to confirm that an individual has contracted active TB.

The results of these tests are used to make up TB notification data. In order to understand the origins and possible shortcomings of TB case notification data sets that are now available for various countries, it is necessary to know a little about the medical tests and data collection methods that are employed.

The Tuberculin Mantoux PPD skin test shows if a person has been infected. A small amount of test material is placed just below the top layers of skin, usually on the forearm, and re-examined a few days later. If a bump/rash of a certain size has developed the test is considered significant and the person is assumed to have been infected with TB. In these PPD skin test positive cases a chest X-ray is usually taken to assess whether the infected individual has active TB. The X-ray should show any damage that active TB has caused to the lungs.

Sputum (i.e. 'coughed up' matter including saliva, foreign material, mucus or phlegm from the respiratory tract) can be tested to see if it contains TB bacilli. If bacilli is detected by either of the two test methods used, microscopy (also referred to as smear test) or culture, the case is classified as sputum-positive. Smear-positive cases are considered more infectious than only culture-positive cases, thus the term 'infectious TB case' is often used to mean the sputum smear-positive case. It is important to note that sputum tests in young children are not always accurate (and hence often not used) as young children rarely develop 'phlegmy' coughs. Thus sputum-positive case data may underestimate the number of TB cases in children. Therefore skin testing is more often used on children rather than the sputum test. TB verified by this skin test is referred to as primo infections. There may,

however, be more inaccurate notifications of TB made with this method than the sputum-positive tests that are considered very accurate in adults. Therefore primo infections data may contain false positive cases.

Passive case detection occurs when detection of cases is not produced by active efforts, i.e. disease detection only occurs when infected people present themselves to a health service. This is opposed to 'active case finding' which occurs when people who have the disease are actively searched for. In the case of TB this can be accomplished in various ways, e.g. testing relatives or close contacts of known active TB cases, checking people who are deemed to be at high risk of infection (people with HIV, slum dwellers, drug users...), or routine surveys of everyone in a defined area (e.g. six-monthly surveys are carried out in South African gold mining communities).

Chapter 4

Summary of the History of TB modelling

Probably the earliest use of a mathematical model to study the epidemiology of TB was presented in a 1962 paper by Hans Waaler (WHO senior statistician), Anton Geser MD (WHO epidemiologist) and Stig Anderson (WHO senior officer) [38]. They construct a simple compartmental dynamic epidemiological model using difference equations that reflect the dynamics of TB. They also show its potential for giving a time trend of TB and in evaluating TB control programs.

The model is based on five 'axioms' (assumptions), namely,

(i) TB is an infectious disease caused by transmission of Tubercle bacilli from person to person.

(ii) TB is a benign infection. Only a small proportion of those infected develop disease and only infected persons can become diseased.

(iii) Only persons with tissue destruction (cases) can transmit infection to other persons. (NB. choice of definition of a 'case' depends on purpose of model and nature of available data.)

(iv) Once infected, a person remains so for rest of life.

(v) Newborns are always infection free.

Using these axioms, the transmission dynamics of TB are expressed as a series of symbolic relationships, i.e. difference equations. Time moves in one year steps and the rate of new infections is proportional to the number of active infectious cases. Figure 4.1 shows the flow diagram of this model.

As can be seen from the flow diagram, the set of linear functions that describe the change in each class from one time step to the next are therefore:

$$I_{t/t+1} = f_1(C_t)$$
$$C_{t/t+1} = f_2(I_t)$$
$$H_{t/t+1} = f_3(C_t)$$
$$D_{Nt/t+1} = f_4(N_t)$$
$$D_{It/t+1} = f_5(I_t)$$
$$D_{Ct/t+1} = f_6(C_t)$$
$$B_{t/t+1} = f_7(P_t)$$

In order to estimate the values of the 7 parameters (f_i for $i = 1, 2, ..., 7$) Waaler, Geser and Anderson suggest observing the sets of variables in the functional relationships. For example; observe C_t, the number of cases at time t, and $I_{t/t+1}$, number of new infections over a certain time period, divide $I_{t/t+1}$ by C_t to calculate an estimate for parameter f_1.

The difference equations that govern the flow of population through the model can also be constructed from the flow diagram and the above linear functions,

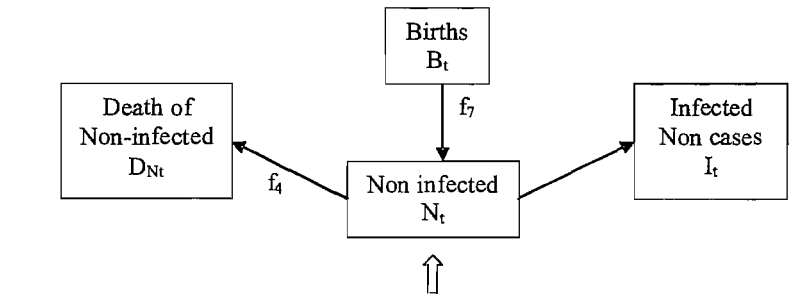

The number of non infected is disregarded as long as the proportion of non infected is high enough that lack of susceptible hosts is not a limiting factor in the spread of TB.

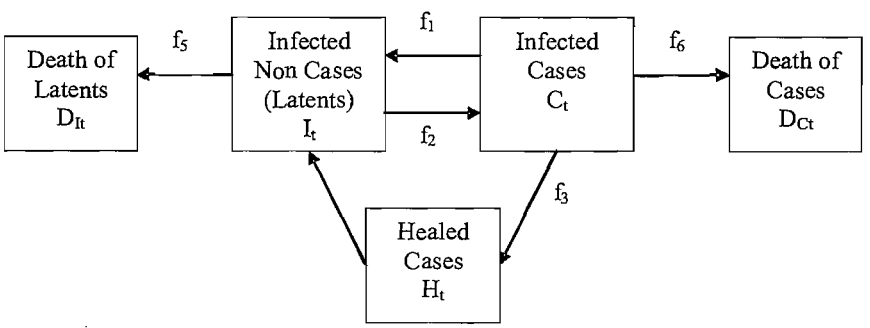

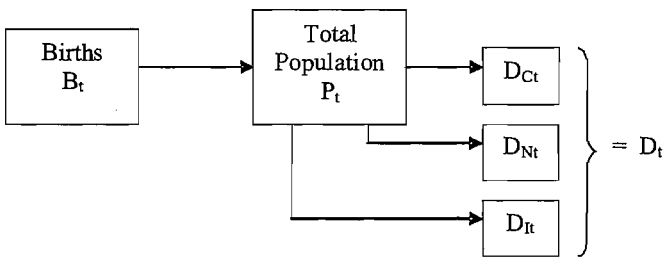

Figure 4.1: Flow diagram of the 1962 Waaler, Geser, Anderson compartmental TB model [38].

namely:

$$\begin{aligned} N_{t+1} - N_t &= B_{t/t+1} - D_{Nt/t+1} - I_{t/t+1} \\ I_{t+1} - I_t &= I_{t/t+1} + H_{t/t+1} - D_{It/t+1} - C_{t/t+1} \\ C_{t+1} - C_t &= C_{t/t+1} - D_{Ct/t+1} - H_{t/t+1} \\ P_{t+1} - P_t &= B_{t/t+1} - D_{t/t+1} \\ & \quad where\ D_{t/t+1} = D_{Ct/t+1} + D_{It/t+1} + D_{Nt/t+1} \end{aligned}$$

Although simple this model is the basis for all TB compartmental models that come after.

In 1965 S.Brogger [84] published an improved version of the previous model. He incorporated age dependence and used a combination of linear and nonlinear terms to calculate the infection rate. The model consists of six epidemiological classes: Uninfected, Infected, Pulmonary Lesions, Cases, Vaccinated and Failures. He divided the model population into 15 one year age groups for ages 0 to 14 years and into 15 five year age groups for ages 15 to 89 years. Movement between these groups was accomplished by selecting 10% of the younger age group and moving it to the older age group. Each age group is divided into the six epidemiological classes. The population then moves through the age groups within each class to simulate aging and through the six classes within each age group to simulate disease progression. Figure 4.2 shows the flow diagram of this model.

Brogger was not concerned about the Incidence of infection as he argued that the large number of infected persons (latents) already existing in most communities would cause a large time lag between when action is taken to reduce incidence and any resulting reduction. This was of particular importance to Brogger as he was most concerned with comparing the effectiveness of various control strategies. Instead, Brogger used the prevalence to influence flow rates between categories.

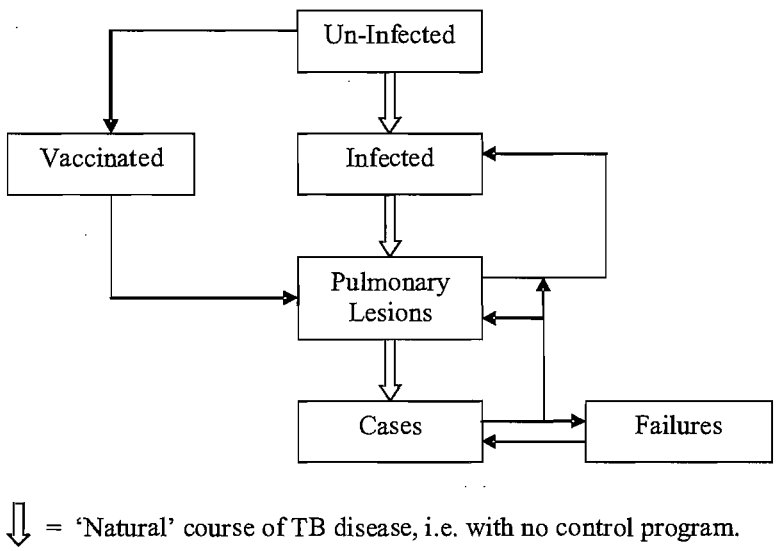

Figure 4.2: Flow diagram of the 1965 Brogger compartmental TB model [84].

He also realised that a given set of parameter values could represent a wide range of different control programs and pointed out that the operational aspects of the program are not directly specified in the model. He also confessed that the lack of quantitative information/data available to the model could cause error in the results in absolute terms (numbers). But he maintained that this does not effect the accuracy of the results on relative terms i.e. when comparing control programs against each other. Both of these observations are still relevant to current TB modelling.

Two years later ReVelle, Lynn and Feldmann (1967) [20] published a paper describing two models; a compartmental model based on the original Waaler, Geser, Anderson model, but developed as a system of non-linear ordinary differential equations; and an optimisation model derived from the first. They also, importantly, gave a full probabilistic explanation of why the infection rate depends linearly on the prevalence and set down the form of the infection rate that is currently most commonly used, namely,

$\beta\frac{S}{N}$, where,

β = a contact rate, i.e. the average number of people per unit time that any one will encounter sufficiently to cause infection.

S = Number of susceptibles $\times$ Number of active infectious cases.

N = Population number

These models were used primarily to evaluate the effectiveness of different control methods and their costs.

Waaler and Piot (1969) [37] developed an age dependent model, also with the main purpose of evaluating different control strategies. They stated that epidemiological effectiveness of control measures must be judged by the changes in transmission that they bring about.

Subsequent TB models are 'variations on a theme' using these first handful of TB models as a template. For example in 1975 Y.Azuma [95], published a simple epidemiological model (that did not require 'large' computers) to calculate annual trends in prevalence and TB incidence, TB mortality and BCG coverage. The model was used to analyse data from Japan. The model uses 15 difference equations to move the population through various state classes as shown in figure 4.3.

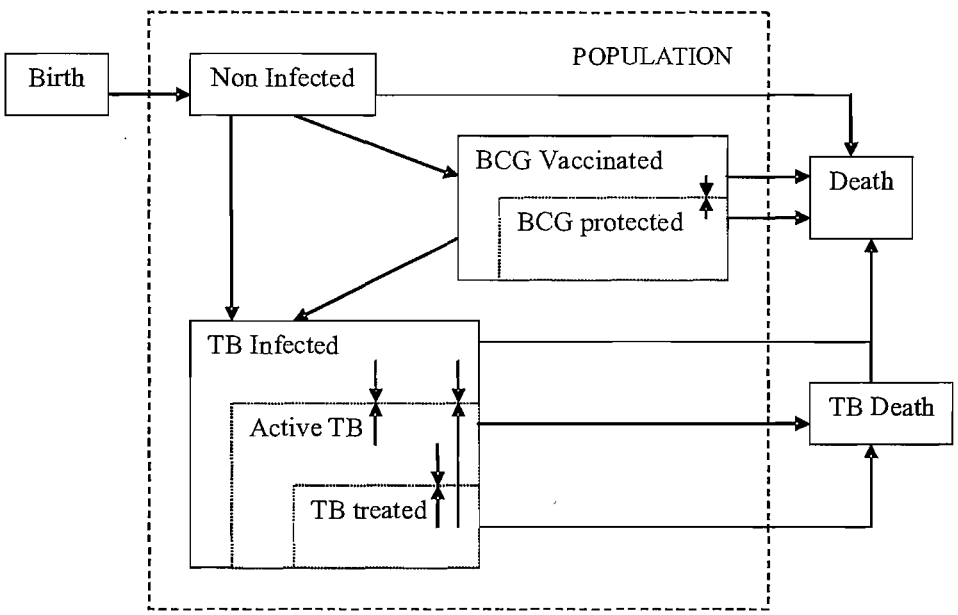

Figure 4.3: Flow diagram of the 1975 Azuma compartmental TB model [95].

As can be seen from this brief description this model differs little from the first few models already described.

Another more complicated compartmental model was constructed by Vynncky and Fine (1997) [28] to estimate the age-dependent risks of developing primary, endogenous, and exogenous tuberculosis and although it includes more of the epidemiological complexity of TB it is still easy to see from the flow diagram in figure 4.4 that it has the same basic structure as the earlier models.

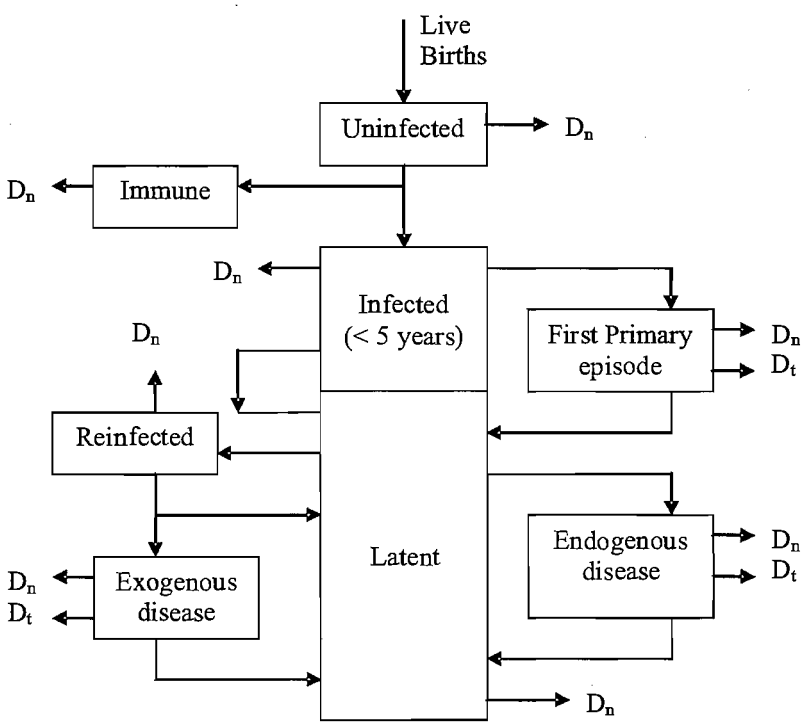

D_n = Death of sputum-negative and non-diseased people
D_t = Death of sputum-positive cases

Figure 4.4: Flow diagram of the 1997 Vynnycky, Fine compartmental TB model [28].

Further developments in TB modelling have mainly come about because of the changing threat of TB. Perhaps the most noticeable change in TB modelling came about in the early 1990s when the impact of the HIV epidemic on the incidence of TB was first taken into account. From that time onwards a large percentage of TB models constructed (compartmental and statistical) incorporate an HIV element into the dynamics of the model [5, 65, 66, 27]. However, I will not expand further on this aspect as this thesis deals with TB modelling rather than TB/HIV modelling. It should be noted however, that the 1998 papers by C.Dye et al. [14, 15] that contain the model that is re-constructed and further analysed in this thesis (see chapter 9), belong amongst this group of TB models, as it originally contained an HIV element.

Other adaptions include the modelling of antibiotic resistant TB strains that are considered to be a serious and growing threat to TB control [12, 88]; the construction of models that incorporate cluster (local or generalised household) effects and investigate the impact these cluster effects may have on TB transmission dynamics [45, 10]. This subject is explored in depth in Chapters 12 to 16.

Apart from compartmental and standard statistical modelling of collected data there have been a few attempts to utilise different modelling techniques in the study of TB transmission dynamics, including Markovian Modelling [89], use of GIS technology leading to spatial analysis [75] and the use of Bayesian networks and statistical relational models [49].

As previously mentioned chapter 9 describes the re-construction and adaptation of a compartmental, age-dependent TB Model similar to those described above [14, 15]. It is then applied to two TB data sets from Morocco and the Netherlands in chapters 10 and 11. First, however, the following chapter describes the construction of a family of parametric statistical regression models that are

used to analyse the same data sets as the compartmental model, in order to confirm the significance of age and time effects in the data. Such statistical models are useful in indicating the sort of detail that compartmental models may need to incorporate to satisfactorily capture significant features of the data.

Chapter 5

Fitting Parametric Distributions to age and time dependent TB case data

5.1 Introduction

In countries that have experienced a long-term decline in the incidence of TB and in annual risk of TB infection, a slow down in the annual decline of the crude notification rate (referred to as stagnation) is often observed. It is most often observed in middle-to-higher income countries with an increasing life expectancy rate and therefore a rapidly ageing population.

This stagnation effect can be explained by examining the natural history of TB. As the risk of infection declines, the proportion of disease due to initial infection (primary disease) and due to re-infection also declines. When the risk of infection reaches an extremely low level it is likely that most of the disease detected is due to re-activation. This effect is called the 'ageing of the epidemic' and can not be adjusted for in analysis by standardisation by age.

Re-activation disease by its very nature does not depend on the current risk of infection and the probability of occurrence of the disease is not believed to decline

significantly with lengthening time since infection. In addition, medical factors that may increase the risk of re-activation of latent TB, such as lung cancer and diabetes are predominantly found in the older generations. Therefore the incidence of this disease only declines if the latently infected cohorts either 'die off' or are given preventative therapy. Thus a country with an increasing life expectancy and a very low annual risk of infection could expect the decline in TB notifications to stagnate.

Therefore in order to analyse the progression of TB in these types of countries it is necessary to create mathematical models that can capture the essential epidemiological and demographic characteristics that are involved in the stagnation effect.

TB data sets from three countries, Netherlands, UK and Morocco, that are considered to have an aging population, low/decreasing annual risk of infection and exhibit an aging of the epidemic, are examined for similar trends/characteristics. The age and time dependent trends apparent in such data are investigated by constructing and fitting a family of parametric models to all three data sets. The form of the fitted models was chosen using knowledge of the shape and trends of known mathematical functions. The stability and fit of different variations/combinations of mathematical functions (exponential, polynomial and logistic) were compared to find the 'best' model for each data set. It was found that this decision could be easily made by simple inspection of model results. Thus, other more formal model comparison methods, such as Akaike (AIC) and Bayesian (BIC) information criteria, were not considered necessary in this case.

The rest of this chapter contains a preliminary examination and a description of the general parametric regression method used to analyse these three data sets. Chapters 6, 7 and 8 contain the specific details of the model fitted with an analysis of the results for each TB data set from the Netherlands, UK and Morocco, respectively.

5.2 Exploring trends in the TB data from the Netherlands, UK and Morocco

In order to clarify the distinguishing trends in these data sets, exponential functions were fitted to the data using a log scale for the y (TB cases) axis. This enabled an approximate value for the slope of the data for each age range to be evaluated. Using these values the relative decline in TB case numbers across the various age ranges can be assessed and compared for each country. Appendix F contains the graphs of these exponential line fits with equations for each trend line fitted, for all three countries' data.

The UK (male) data shows similar characteristics to the data from the Netherlands, in that the decline in the data is greater in the younger age ranges and begins to level off in the older age ranges (see graphs 5.1 and 5.2).

The Moroccan data shows a more extreme but similar pattern in that the younger ages exhibit a sharp decline in TB that levels off until an increase in TB is exhibited in the older age ranges (see graph 5.3).

These data sets therefore show a marked and similar age dependency.

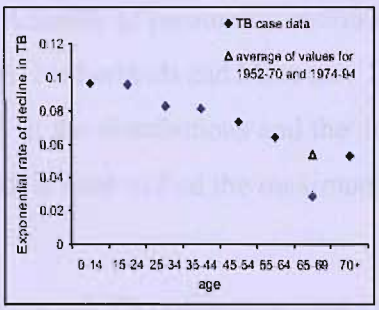

Figure 5.1: Plot of the exponential rate of decline in TB case numbers over age, for the Dutch TB data set.

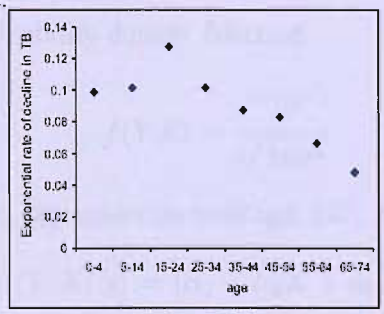

Figure 5.2: Plot of the exponential rate of decline in TB case numbers over age, for the UK TB data set.

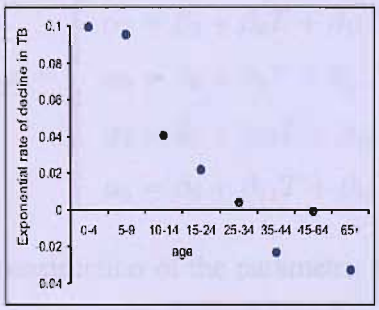

Figure 5.3: Plot of the exponential rate of decline in TB case numbers over age, for the Moroccan PTB data set.

5.3 Modelling strategy

- **Model formulation** A family of parametric distributions are fitted to the TB case data from the UK, Netherlands and Morocco. The method of Maximum Likelihood is used to fit the distributions and the direct search optimisation method, Nelder-mead, is used to find the maximum value of the likelihood, $L(\beta, y)$.

  Let Y be the set of observed TB notification case data for a specific country and β be a set of unknown parameters to be estimated. It is assumed that Y is a set of identically distributed random variables drawn from the Normal distribution with probability density function

$$f(Y, \theta) = \frac{e^{\frac{-(y-\eta)^2}{2\sigma^2}}}{\sqrt{2\pi\sigma^2}}$$

  where η is a function dependent on both age, (X), and time, (T).

  Let $\sigma = \beta_1$ and let $\eta\,(T, X, \alpha) = (\alpha_1 + \alpha_3 X + \alpha_5 X^2)\,\frac{e^{(\alpha_4 X - \alpha_2)}}{1+e^{(\alpha_4 X - \alpha_2)}}$ where α is another set of parameters dependent on β and T, such that,

$$\alpha = \begin{cases} \alpha_1 = \beta_2 + \beta_7 T + \beta_{12} T^2 \\ \alpha_2 = \beta_3 + \beta_8 T + \beta_{13} T^2 \\ \alpha_3 = \beta_4 + \beta_9 T + \beta_{14} T^2 \\ \alpha_4 = \beta_5 + \beta_{10} T + \beta_{15} T^2 \\ \alpha_5 = \beta_6 + \beta_{11} T + \beta_{16} T^2 \end{cases}$$

  This is the general construction of the parametric models fitted to the UK, Dutch and Moroccan TB data. The specific models fitted to each country are adapted by setting one or more of the β parameters to zero and by making σ a function of age and/or time.

  The logistic component of the function $\eta(T, X, \alpha)$ captures the initial rise in the TB data with age and the general sigmoidal shape. The polynomial

captures any 'tailing off' behaviour in the data. An exponential function was tried in place of the polynomial but produced a model that was hard to fit and exhibited unstable behaviour.

- **Producing confidence intervals**

  - **Asymptotic Theory** It is known that the asymptotic probability distribution of Maximum Likelihood estimates is Normal, hence as sample size $n \to \infty$, $\hat{\beta} \sim N\{\beta, V(\beta)\}$, where$V(\beta)$ is approximated by $V(\hat{\beta}) \simeq \left[-\frac{\delta^2 L(\beta,y)}{\delta\beta^2}|_{\beta=\hat{\beta}}\right]^{-1}$.

    The Hessian, $\frac{\delta^2 L(\beta,y)}{\delta\beta^2}|_{\beta=\hat{\beta}}$, is calculated numerically using a finite-difference formula for the second derivatives.

    The $(1-\alpha)100\%$ confidence interval for the parameter β_i is calculated from $\hat{\beta} \pm z_{\frac{\alpha}{2}}\sqrt{V_{ii}(\hat{\beta})}$

  - **Bootstrap Method** The basic bootstrap method was also used to create confidence intervals for the model parameters. This method samples with replacement from the original data set to create n further sets. For each of these 'new' data sets, the parametric model is fitted as before, resulting in a further n sets of MLEs. (See Appendix D for details of the Basic Bootstrap)

The chosen specific models and the results from the fitting of these models to the TB data sets for the Netherlands, Morocco and the UK are described in the following Chapters 6, 8 and 7 respectively.

5.4 Summary of results of fitting the parametric models to TB data from Netherlands, Morocco and UK

The general characteristics of the TB data sets as they vary with time and age are satisfactorily captured by this family of parametric models although there are a few that the models fail to capture. However, it is unclear whether all these characteristics are derived from true features of the data. The accuracy of the data must be questioned especially in the two oldest age ranges in the Dutch data, young children and in the Moroccan year data that is created by projection. In view of this, it is concluded that this family of parametric models is sufficiently flexible to capture the main characteristic features of these TB data sets.

Chapter 6

Parametric Modelling of Dutch TB Case Data

6.1 Model formulation

A Normal distribution model is fitted to the TB notification data for the Netherlands from 1952 to 1994:

$Y \sim \text{Normal}(\mu, \sigma)$, with pdf $\frac{1}{\sigma\sqrt{2\pi}} e^{\left(-\frac{(Y-\mu)^2}{2\sigma^2}\right)}$, where Y represents the TB notification data; $\sigma = \beta_1$; $\mu = \eta(T, X, \alpha)$; T = time; X = age and β = parameters to be estimated.

Let

$$\eta = \left(\alpha_1 + \alpha_3 X + \alpha_5 X^2\right) \frac{e^{(\alpha_4 X - \alpha_2)}}{1 + e^{(\alpha_4 X - \alpha_2)}}$$

where

$$\alpha = \begin{cases} \alpha_1 = \beta_2 + \beta_7 T + \beta_{12} T^2 \\ \alpha_2 = \beta_3 + \beta_8 T + \beta_{13} T^2 \\ \alpha_3 = \beta_4 + \beta_9 T + \beta_{14} T^2 \\ \alpha_4 = \beta_5 + \beta_{10} T + \beta_{15} T^2 \\ \alpha_5 = \beta_6 + \beta_{11} T + \beta_{16} T^2 \end{cases}$$

Note that the variance is dependent on both age and time.

6.2 Results of fitting the parametric model to the Dutch TB case data

The confidence limits for each parameter, $(\beta_i, i = 1, 2..., 16)$, produced by using asymptotic theory and bootstrapping, along with the maximum likelihood estimates for each parameter are displayed in table 6.1. The only parameter that may be insignificant is β_8, (at a very high significance level of 99%), but as this is a linear term in a quadratic function and the quadratic term β_{13} is considered significant, parameter β_8 is kept in the model.

The correlations for the 16 β parameters can be found numerically displayed in table 6.2 and graphically displayed in figures 6.1 to 6.3. The strongest correlations are between the β parameters making up the quadratic functions α_1 and α_3, α_3 and α_5 and between those in α_1 and α_5. Likewise, there is a weaker correlation between α_2 and α_4. There is also a strong correlation between the β terms within each function α; constant term with linear term and linear term with quadratic term. All these correlations are understandable as α_1, α_3 and α_5 make up the quadratic term in η and α_2 and α_4 make up the exponential term in η (see section 6.1). It also seems reasonable that the terms in a quadratic function should be correlated with each other.

Apart from the above linear correlations the scatter plots for the β parameters show a random scatter, thus there is no significant evidence that any normality assumptions made for this model would be invalid.

The fits of the parametric model to the Dutch TB case data for each of the 8 age ranges are shown in figures 6.4 (a)-(h). The model fitted well for all ages and seems to have captured well the time dependent trends for each age group. It looks

at first that the 'bump' in the model fit that first starts to appear in the fit for age group 35-44, may be as a result of the model attempting to fit to the 'jump' in the data for age group 65-69. This was of interest due to the possible inaccuracy of the data for these latter ages. The hypothesis was tested by fitting the model to the Dutch data set with the 'jump' smoothed out. The smoothing was accomplished by simply reducing the values of the data for the years 1974 onwards in age group 65-69 by a fixed amount so as to bring them in line with the trend of the preceding years. However, using this amended data set did not alter the fit and the 'bump' that can be seen in figures 6.4 (d)-(h)was still present. This confirmed that the trend seen in the model fit was a product of the model itself and not due to fitting to possibly inaccurate data.

The fits to the Dutch data for a selection of years are shown in figures 6.5 (a)-(h). The model also seems to have captured the changing age dependent trends of the data, for each time point selected, in the first 20 years of the time period. The model fits less well to the years after 1970. The shape of the data seems to suggest a cubic function may be a good fit although this was not found to be true. The parametric model however struggles to fully capture this 'cubic-like' trend in the data from 1970 to 1994.

99% performance confidence intervals and confidence bands were constructed for each of the 8 age groups, using two different methods. The first method using asymptotic theory assumes normality and the results are shown in figures 6.6 (a)-(h). The second method uses bootstrapping and the results are shown in figures 6.7 (a)-(h). It can be seen that these two methods give very similar results. All these performance confidence intervals and bands are reassuringly narrow, encasing the model fit line.

Table 6.1: Parameter MLE values with 99% asymptotic and bootstrap confidence intervals.

		Asymptotic Theory		Bootstrapping Method	
Parameters	ML Estimates	Lower 99% CI Limit	Upper 99% CI Limit	Lower 99% CI Limit	Upper 99% CI Limit
β_1	4.460	3.986	4.934	3.760	4.705
β_2	378.024	343.639	412.410	364.836	392.735
β_3	2.427	2.210	2.644	2.226	2.616
β_4	-10.110	-11.478	-8.742	-10.575	-9.609
β_5	0.224	0.194	0.253	0.203	0.245
β_6	0.082	0.069	0.095	0.077	0.086
β_7	-32.889	-37.651	-28.127	-34.413	-31.226
β_8	-0.022	-0.059	0.014	-0.051	0.015
β_9	0.766	0.569	0.963	0.732	0.797
β_{10}	-0.011	-0.013	-0.009	-0.012	-0.010
β_{11}	-0.005	-0.007	-0.003	-0.006	-0.005
β_{12}	0.981	0.747	1.215	0.881	1.086
β_{13}	0.004	0.002	0.005	0.002	0.005
β_{14}	-0.020	-0.028	-0.012	-0.022	-0.018
β_{15}	1.7E-04	1.4E-04	2.1E-04	1.5E-04	2.0E-04
β_{16}	1.1E-04	3.7E-05	1.9E-04	9.2E-05	1.3E-04

Table 6.2: Correlation matrix for the 16 parameters.

	β_1	β_2	β_3	β_4	β_5	β_6	β_7	β_8	β_9	β_{10}	β_{11}	β_{12}	β_{13}	β_{14}	β_{15}	β_{16}
β_1	1	-0.05	-2.E-03	0.06	0.03	-0.06	0.05	3.E-03	-0.05	-0.03	0.05	-0.03	0.01	0.04	0.03	-0.04
β_2	-0.05	1	-0.06	-0.98	-0.67	0.94	-0.66	0.01	0.63	0.57	-0.60	0.38	5.E-03	-0.39	-0.42	0.37
β_3	-2.E-03	-0.06	1	0.01	0.66	0.02	-0.14	-0.54	0.19	-0.64	-0.20	-4.E-03	0.13	-0.13	0.44	0.18
β_4	0.06	-0.98	0.01	1	0.59	-0.99	0.64	-5.E-04	-0.68	-0.52	0.68	-0.32	0.07	0.40	0.44	-0.43
β_5	0.03	-0.67	0.66	0.59	1	-0.54	0.20	-0.25	-0.14	-0.88	0.13	-0.12	-0.01	0.01	0.60	0.03
β_6	-0.06	0.94	0.02	-0.99	-0.54	1	-0.61	1.E-03	0.69	0.47	-0.71	0.27	-0.12	-0.39	-0.45	0.45
β_7	0.05	-0.66	-0.14	0.64	0.20	-0.61	1	0.29	-0.93	-0.13	0.83	-0.80	-0.20	0.88	0.05	-0.82
β_8	3.E-03	0.01	-0.54	-5.E-04	-0.25	1.E-03	0.29	1	-0.28	0.45	0.25	-0.08	-0.62	0.17	-0.53	-0.19
β_9	-0.05	0.63	0.19	-0.68	-0.14	0.69	-0.93	-0.28	1	0.13	-0.98	0.59	-4.E-03	-0.84	-0.20	0.90
β_{10}	-0.03	0.57	-0.64	-0.52	-0.88	0.47	-0.13	0.45	0.13	1	-0.12	0.04	-0.14	-0.02	-0.80	2.E-03
β_{11}	0.05	-0.60	-0.20	0.68	0.13	-0.71	0.83	0.25	-0.98	-0.12	1	-0.45	0.13	0.76	0.27	-0.88
β_{12}	-0.03	0.38	-4.E-03	-0.32	-0.12	0.27	-0.80	-0.08	0.59	0.04	-0.45	1	0.34	-0.87	0.19	0.69
β_{13}	0.01	5.E-03	0.13	0.07	-0.01	-0.12	-0.20	-0.62	-4.E-03	-0.14	0.13	0.34	1	-0.13	0.64	-0.06
β_{14}	0.04	-0.39	-0.13	0.40	0.01	-0.39	0.88	0.17	-0.84	-0.02	0.76	-0.87	-0.13	1	-0.01	-0.95
β_{15}	0.03	-0.42	0.44	0.44	0.60	-0.45	0.05	-0.53	-0.20	-0.80	0.27	0.19	0.64	-0.01	1	-0.12
β_{16}	-0.04	0.37	0.18	-0.43	0.03	0.45	-0.82	-0.19	0.90	2.E-03	-0.88	0.69	-0.06	-0.95	-0.12	1

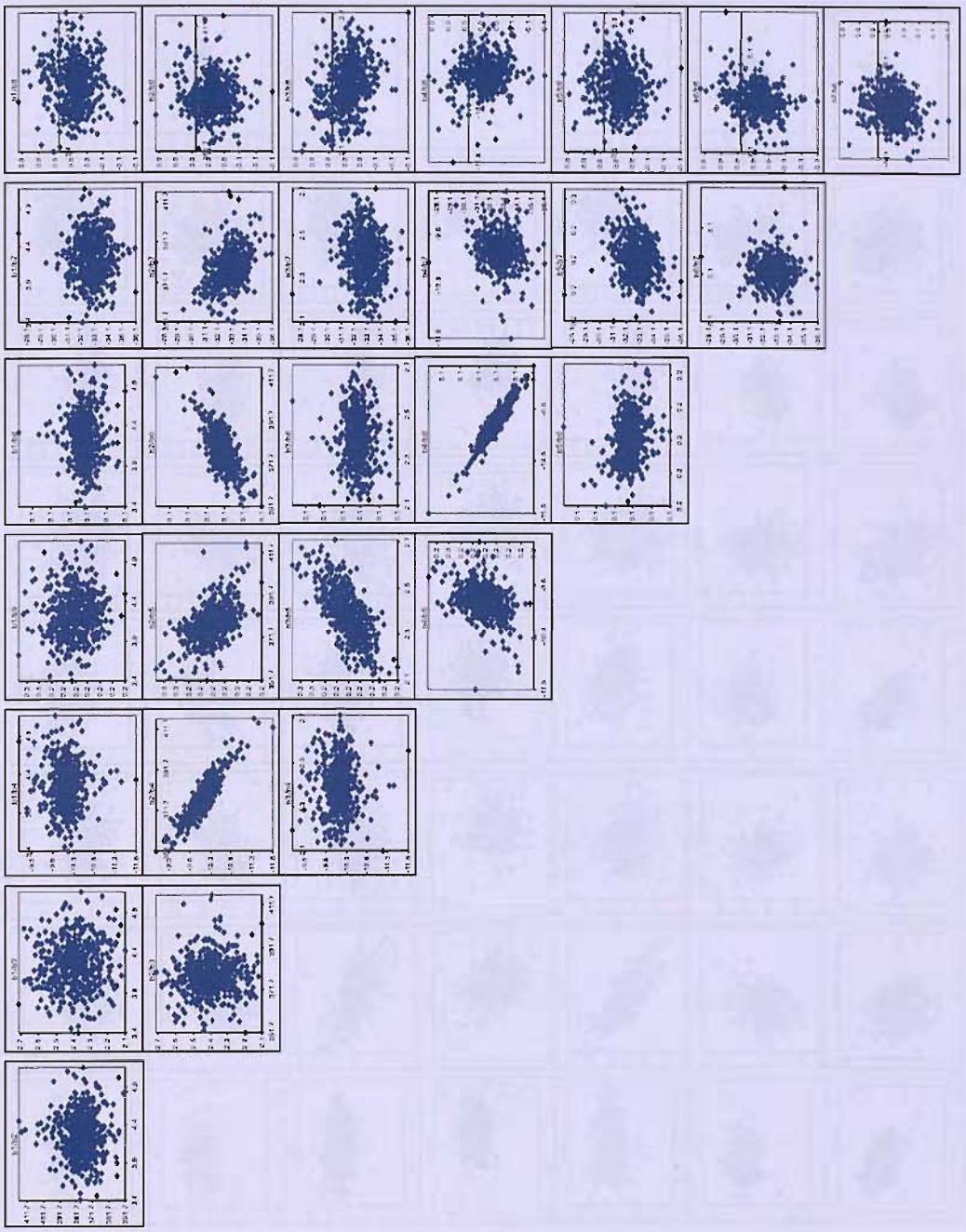

Figure 6.1: Scatter plots of the associations between the parameters $\beta_1, \ldots, \beta_7$ with $\beta_2, \ldots, \beta_8$.

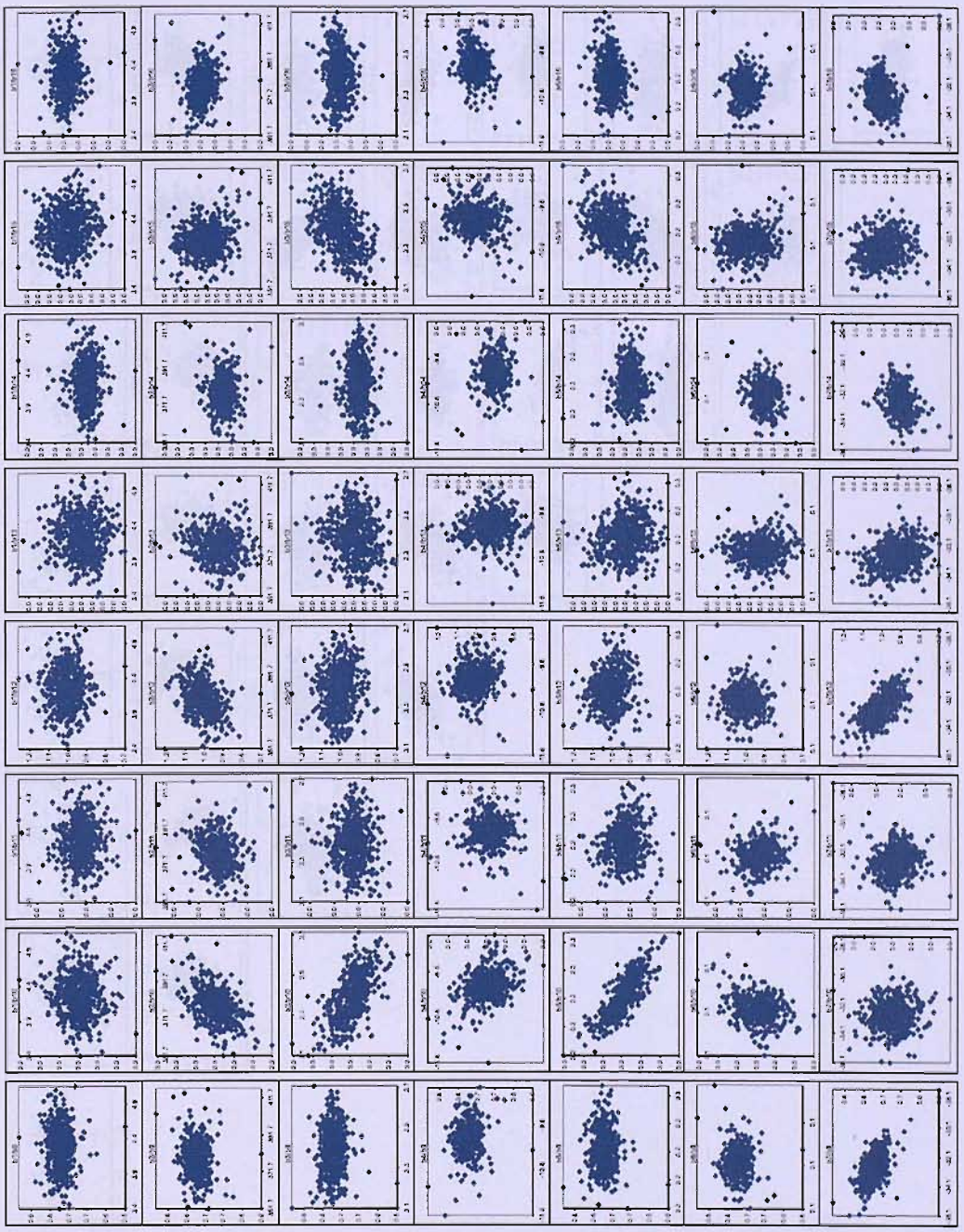

Figure 6.2: Scatter plots of the associations between the parameters $\beta_1, \ldots, \beta_7$ with $\beta_9, \ldots, \beta_{16}$.

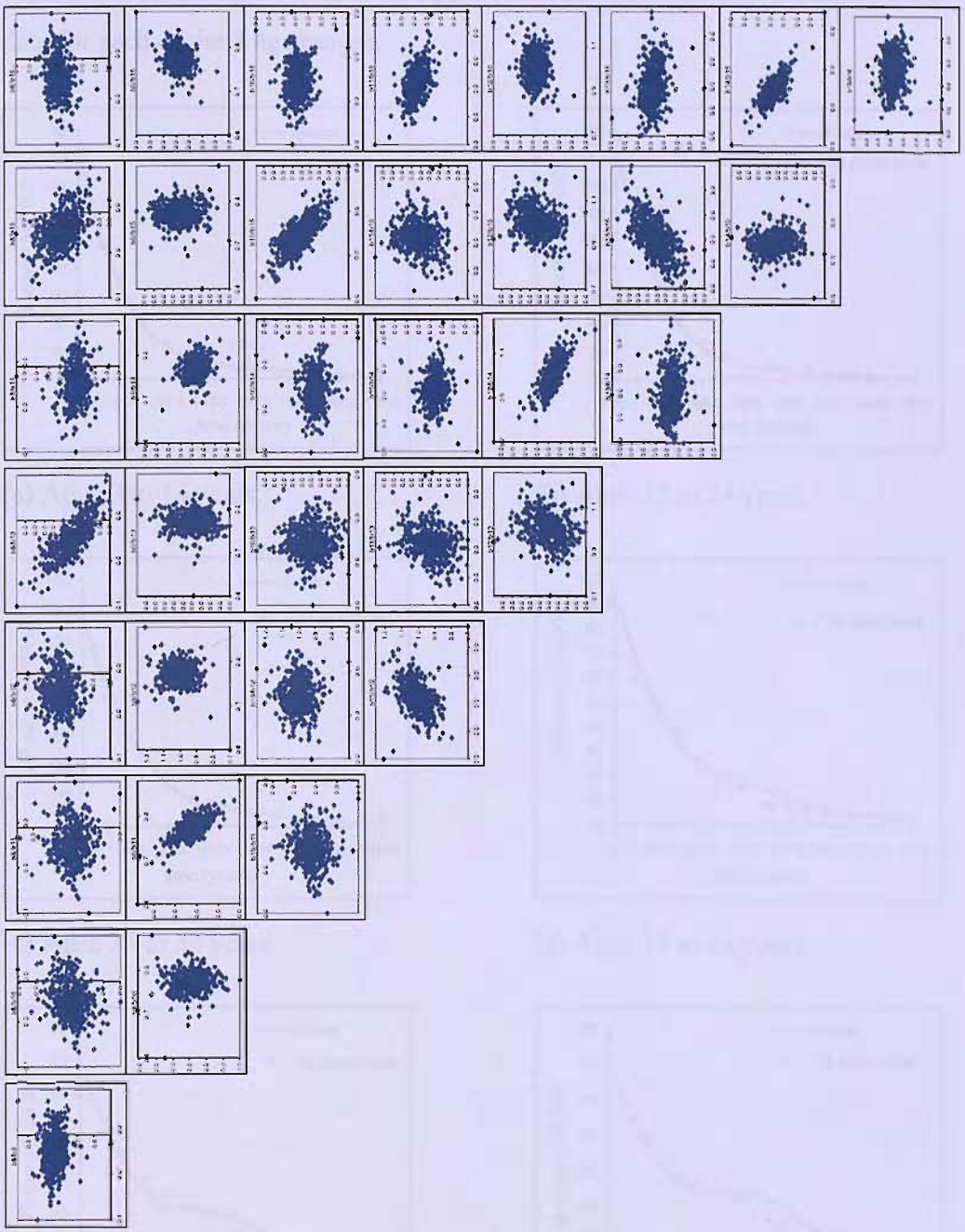

Figure 6.3: Scatter plots of the associations between the parameters $\beta_8, \ldots, \beta_{15}$ with $\beta_9, \ldots, \beta_{16}$.

Figure 6.4: (a)-(h): Plots of the fitted parametric model and Dutch TB notification data for each of the 8 age ranges.

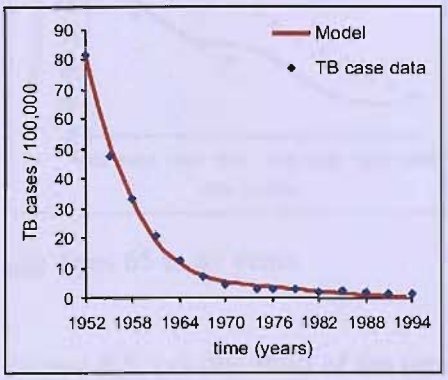

(a) Ages 0 to 14 years.

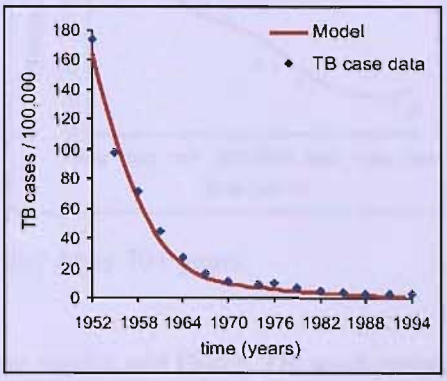

(b) Ages 15 to 24 years.

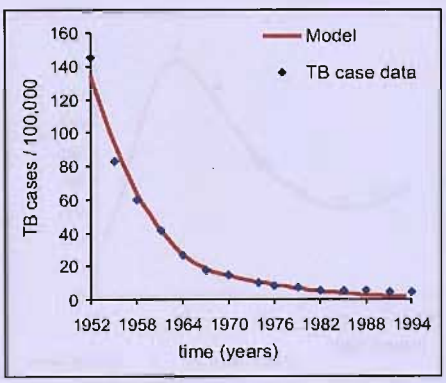

(c) Ages 25 to 34 years.

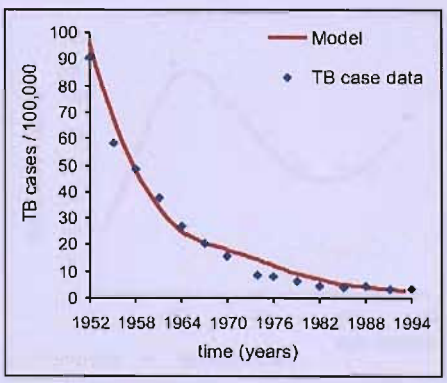

(d) Ages 35 to 44 years.

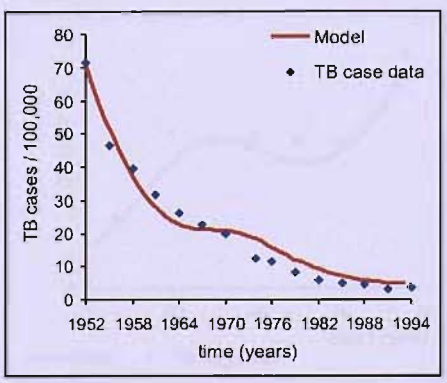

(e) Ages 45 to 54 years.

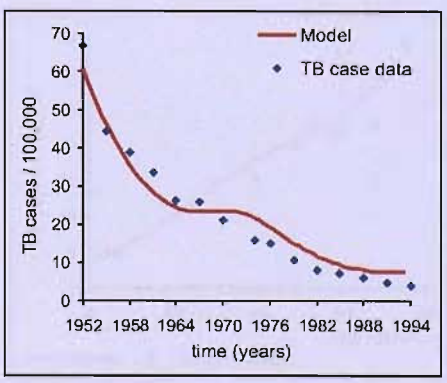

(f) Ages 55 to 64 years.

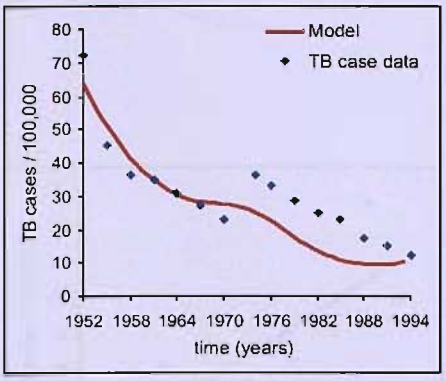

(g) Ages 65 to 69 years.

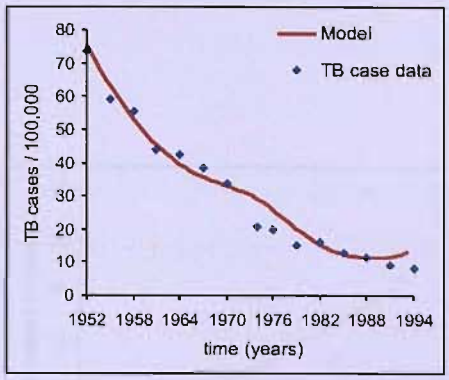

(h) Ages 70+ years.

Figure 6.5: (a)-(h): Plots of the fitted parametric model and Dutch TB notification data for a selection of years between 1952 and 1994.

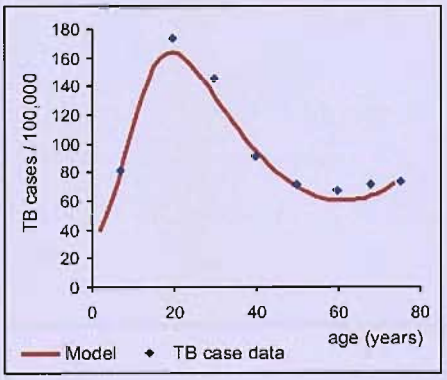

(a) 1952

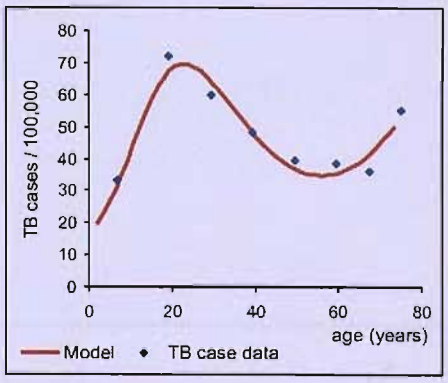

(b) 1958

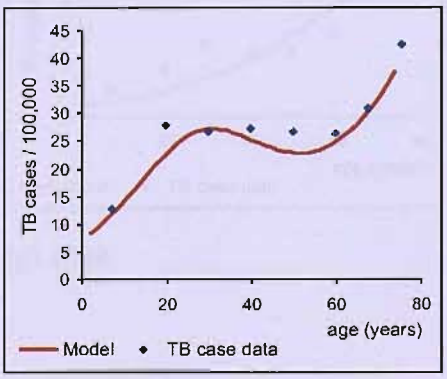

(c) 1964

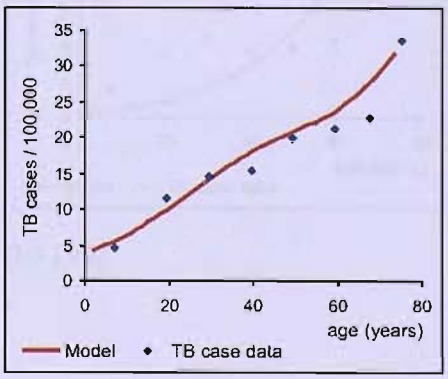

(d) 1970

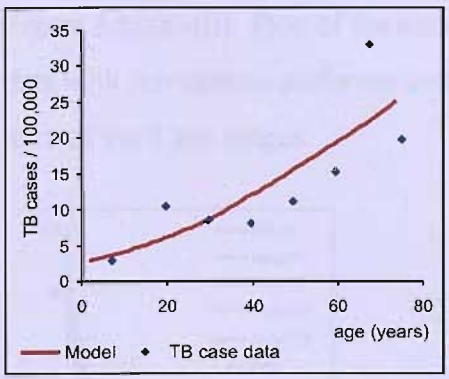

(e) 1976

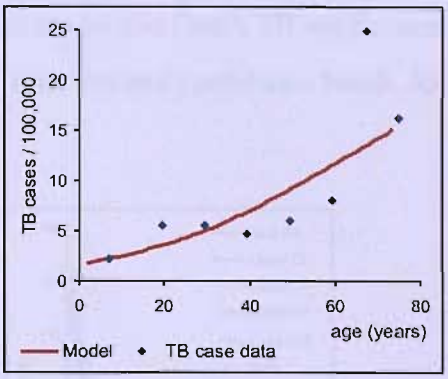

(f) 1982

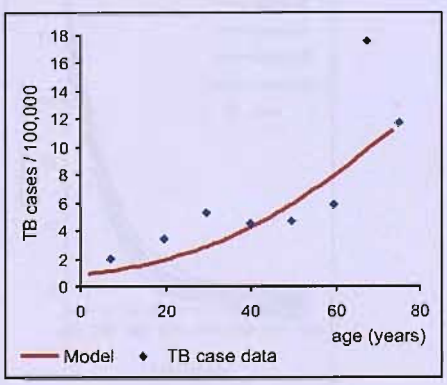

(g) 1988

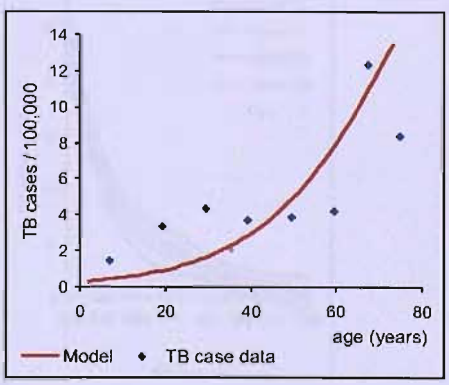

(h) 1994

Figure 6.6: (a)-(h): Plots of the fitted parametric model and Dutch TB notification data with Asymptotic performance confidence intervals and confidence bands, for each of the 8 age ranges.

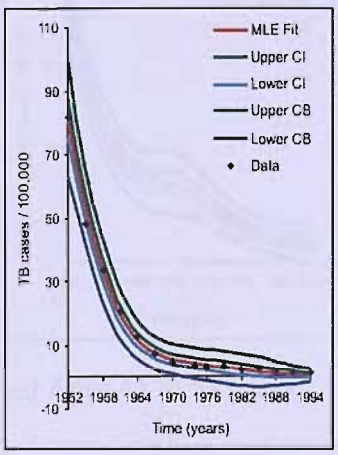

(a) Ages 0 to 14 years.

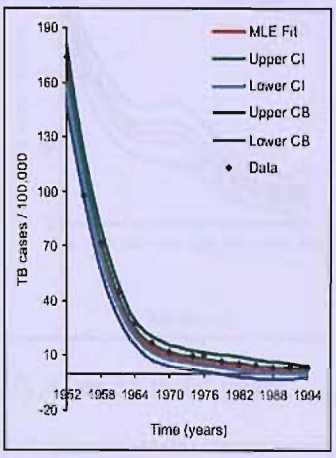

(b) Ages 15 to 24 years.

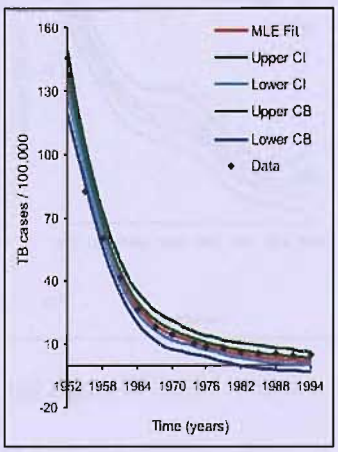

(c) Ages 25 to 34 years.

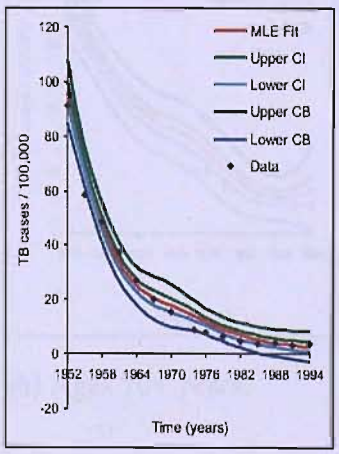

(d) Ages 35 to 44 years.

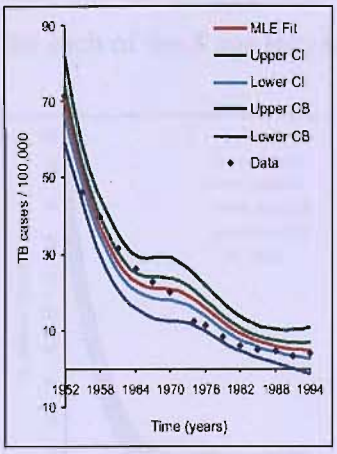

(e) Ages 45 to 54 years.

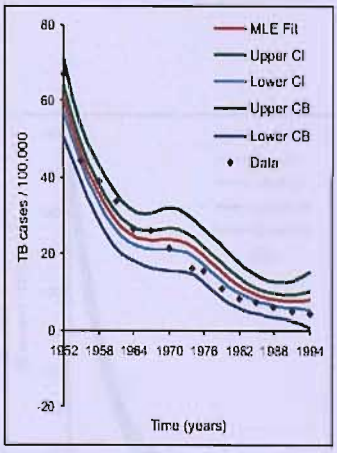

(f) Ages 55 to 64 years.

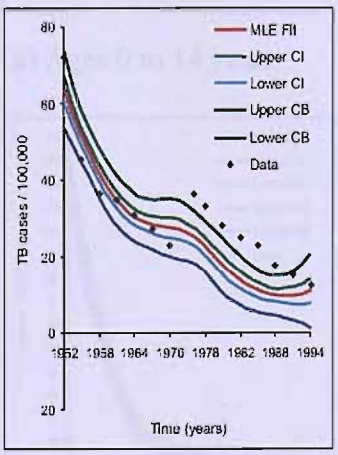

(g) Ages 65 to 69 years.

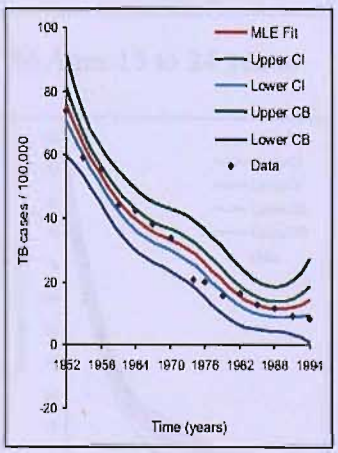

(h) Ages 70+ years.

Figure 6.7: (a)-(h): Plots of the fitted parametric model and Dutch TB notification data with bootstrapped performance confidence intervals and confidence bands, for each of the 8 age ranges.

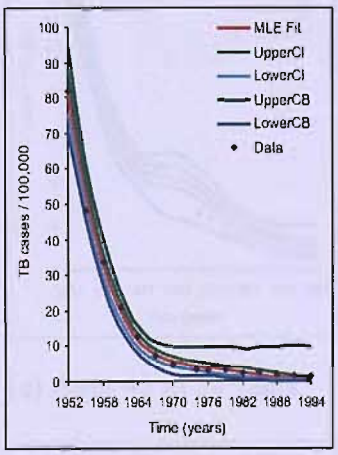

(a) Ages 0 to 14 years.

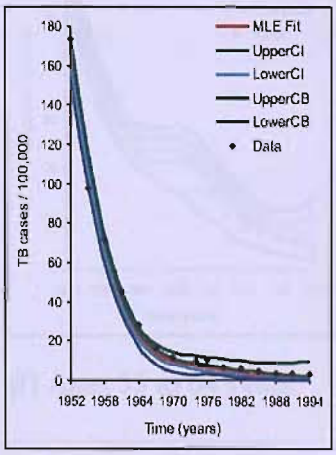

(b) Ages 15 to 24 years.

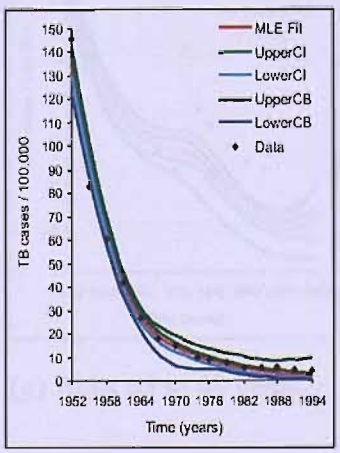

(c) Ages 25 to 34 years.

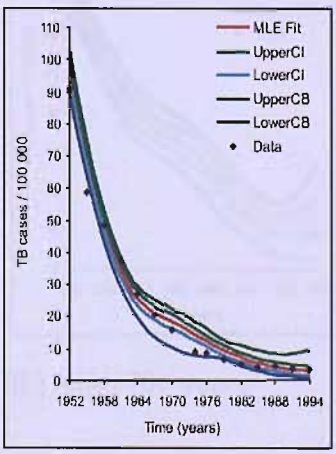

(d) Ages 35 to 44 years.

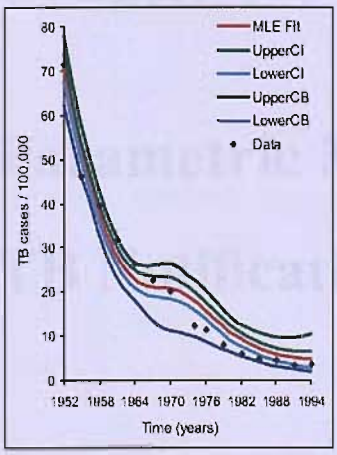

(e) Ages 45 to 54 years.

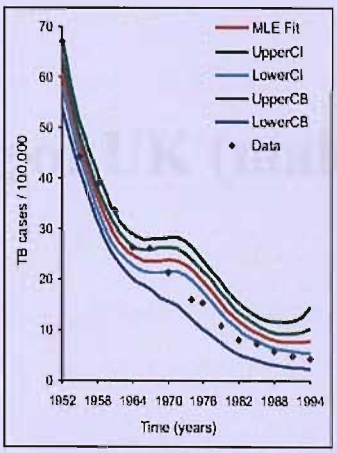

(f) Ages 55 to 64 years.

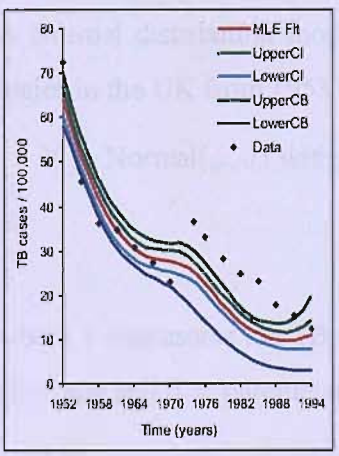

(g) Ages 65 to 69 years.

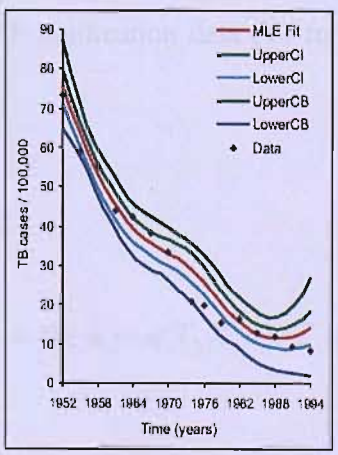

(h) Ages 70+ years.

Chapter 7

Parametric Modelling of UK (male) TB Notification Data

7.1 Model formulation

A Normal distribution model is fitted to the TB notification data (Y) for white males in the UK from 1953 to 1989:

$Y \sim \text{Normal}(\mu, \sigma)$ with pdf

$$\frac{1}{\sigma\sqrt{2\pi}} e^{\left(-\frac{(Y-\mu)^2}{2\sigma^2}\right)}$$

where Y represents the TB notification data; $\sigma = \beta_1$; $\mu = \eta(T, X, \alpha)$; T = time; X = age and β = parameters to be estimated.

Let

$$\eta = \alpha_1 \frac{e^{(\alpha_3 X - \alpha_2)}}{1 + e^{(\alpha_3 X - \alpha_2)}}$$

where

$$\alpha = \begin{cases} \alpha_1 = \beta_2 + \beta_5 T + \beta_8 T^2 \\ \alpha_2 = \beta_3 + \beta_6 T \\ \alpha_3 = \beta_4 + \beta_7 T \end{cases}$$

Note that the variance, $\beta_1 \equiv \sigma^2$, is independent of age and time.

7.2 Results of fitting the parametric model to the UK (male) TB case data

The maximum likelihood estimates as well as the confidence limits for each parameter, $(\beta_i, i = 1, 2, ..., 8)$, produced using asymptotic theory and bootstrapping methods, are displayed in table 7.2. None of the parameters seem insignificant, at a very high significance level of 99%.

The correlations for the 8 β parameters can be found numerically displayed in table 7.1 and graphically displayed in figures 7.1. The strongest correlations are between the β parameters making up the linear functions α_2 and α_3. There is also a strong correlation between the β terms within each function α. These correlations are understandable as α_2 and α_3 make up the exponential term in η. It also seems reasonable that the terms in a quadratic or linear function should be correlated with each other.

Apart from the above linear correlations the scatter plots for the β parameters show a random scatter, thus there is no significant evidence that any normality assumptions made for this model would be invalid.

The fits of the parametric model to the UK (male) TB case data for each of the 8 age ranges are shown in figures 7.2(a)-(h). The model fitted generally well and seems to have captured the time dependent trend for each age group. The model fit to the first three age groups (years 0-24) is seen to be slightly less accurate than that for the remaining ages.

The fits to the UK data for a selection of years are shown in figures 7.3 (a)-(h). The model also seems to have captured the general age dependent trends of the data, for each time point selected.

99% performance confidence intervals and confidence bands were constructed for each of the 8 age groups, using two different methods. The first method using asymptotic theory assumes normality and the results are shown in figures 7.4 (a)-(h). The second method uses bootstrapping and the results are shown in figures 7.5 (a)-(h). It can be seen that these two methods give very similar results. All these performance confidence intervals and bands are reassuringly narrow, encasing the model fit line.

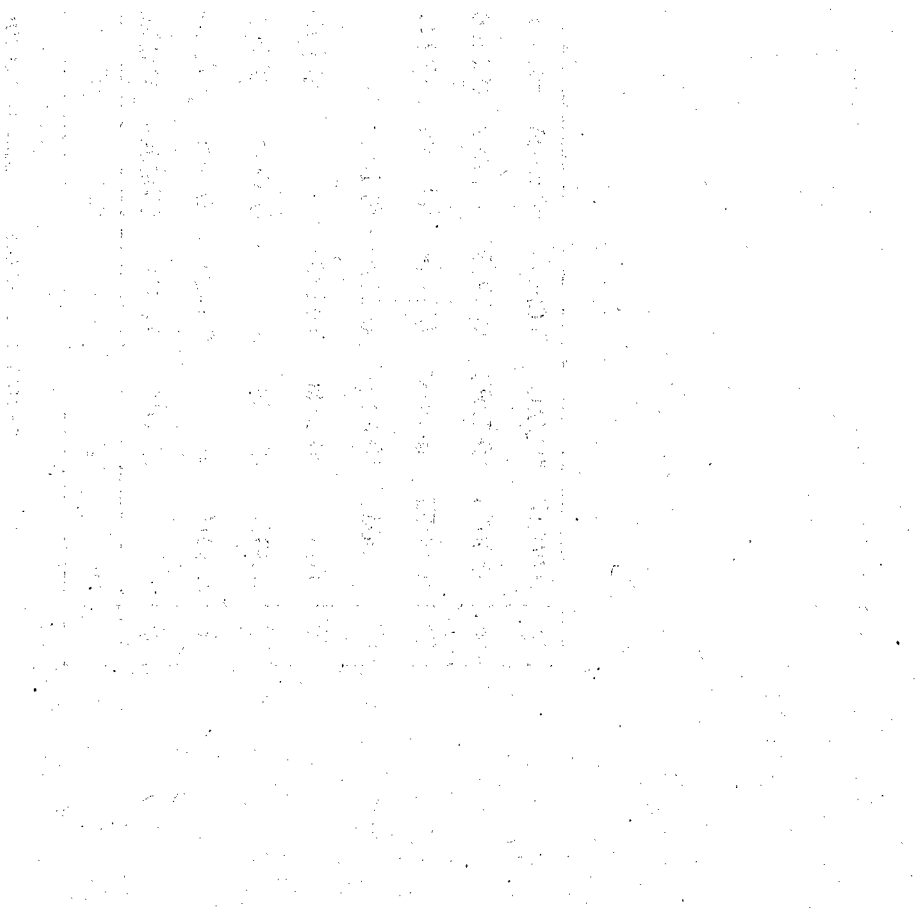

Table 7.1: Correlation matrix for the 8 parameters.

	β_1	β_2	β_3	β_4	β_5	β_6	β_7	β_8
β_1	1	0.0016	0.0018	0.0008	-0.0021	-0.0022	-0.0022	0.0020
β_2	0.0016	1	0.1531	-0.1180	-0.8403	-0.2896	-0.2062	0.7201
β_3	0.0018	0.1531	1	0.7377	-0.2180	-0.5879	-0.7523	0.0865
β_4	0.0008	-0.1180	0.7377	1	-0.1074	-0.1464	-0.7065	-0.0109
β_5	-0.0021	-0.8403	-0.2180	-0.1074	1	0.3384	0.4709	-0.9437
β_6	-0.0022	-0.2896	-0.5879	-0.1464	0.3384	1	0.7020	-0.2793
β_7	-0.0022	-0.2062	-0.7523	-0.7065	0.4709	0.7020	1	-0.4296
β_8	0.0020	0.7201	0.0865	-0.0109	-0.9437	-0.2793	-0.4296	1

Table 7.2: Parameter MLE values with 99% asymptotic and bootstrap confidence intervals.

		Asymptotic Theory		Bootstrapping Method	
Parameters	ML Estimates	Lower 99% CI Limit	Upper 99% CI Limit	Lower 99% CI Limit	Upper 99% CI Limit
$\beta_1(=\sigma)$	7.7443	6.9245	8.5642	6.625	8.6756
β_2	135.9483	129.8145	142.0822	127.7676	142.5714
β_3	0.8231	0.4451	1.2011	0.4035	1.2016
β_4	0.1288	0.1036	0.1541	0.1033	0.1581
β_5	-8.9065	-10.0688	-7.7442	-10.1811	-7.6801
β_6	0.1240	0.0856	0.1624	0.093	0.1671
β_7	-0.0021	-0.0030	-0.0011	-0.0031	-0.0009
β_8	0.2087	0.1582	0.2592	0.1575	0.2631

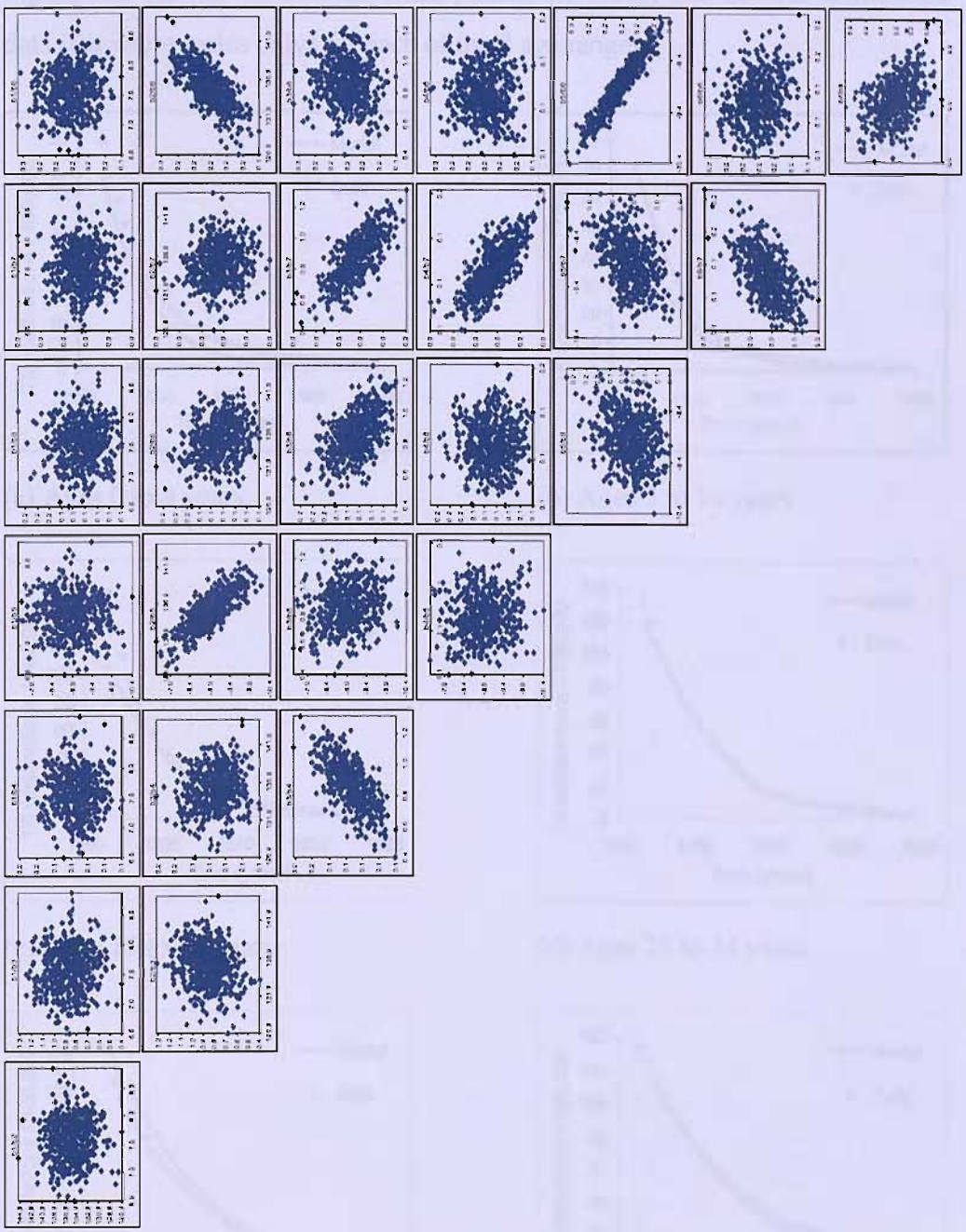

Figure 7.1: Scatter plots of the associations between the parameters $\beta_1 = \sigma$, β_2, β_3, β_4, β_5, β_6, β_7 and β_8.

Figure 7.2: (a)-(h): Plots of the fitted parametric model and UK TB notification data (for white males only) for each of the 8 age ranges.

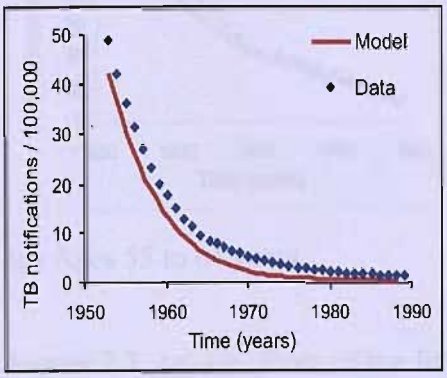

(a) Ages 0 to 4 years.

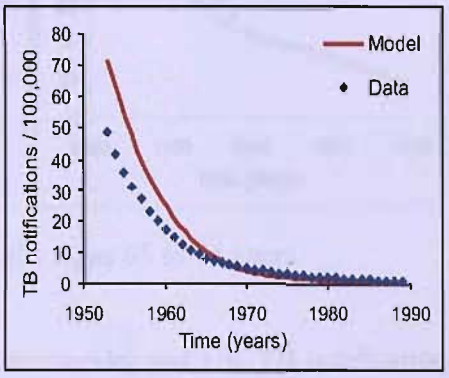

(b) Ages 5 to 14 years.

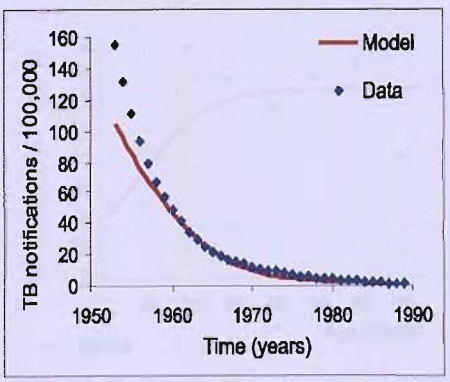

(c) Ages 15 to 24 years.

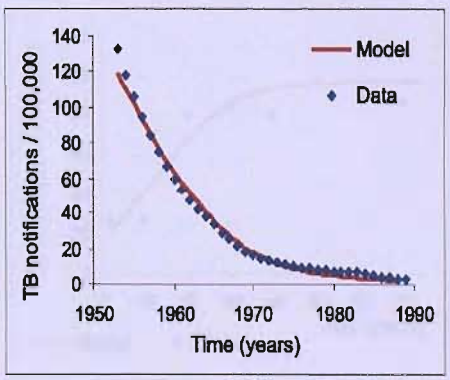

(d) Ages 25 to 34 years.

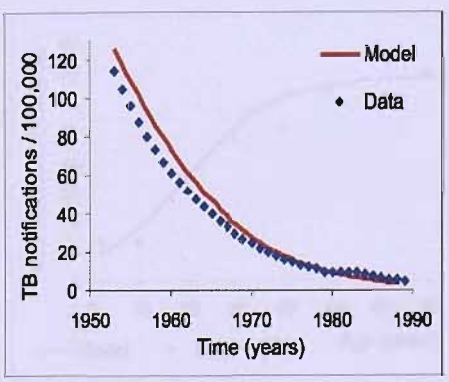

(e) Ages 35 to 44 years.

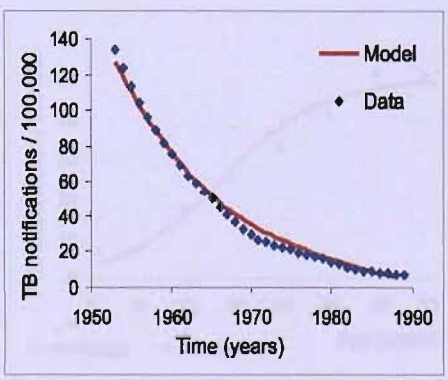

(f) Ages 45 to 54 years.

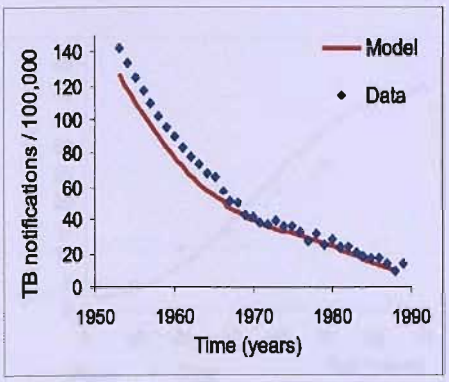

(g) Ages 55 to 64 years.

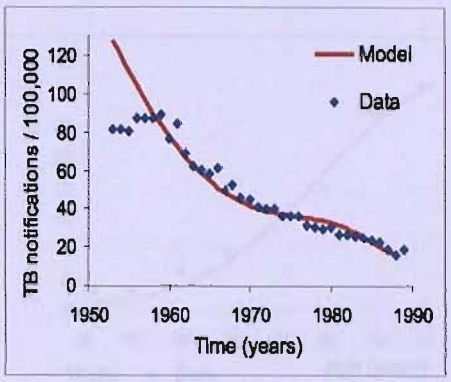

(h) Ages 65 to 74 years.

Figure 7.3: (a)-(i): Plots of the fitted parametric model and UK TB notification data (for white males only) for a selection of years between 1953 and 1989.

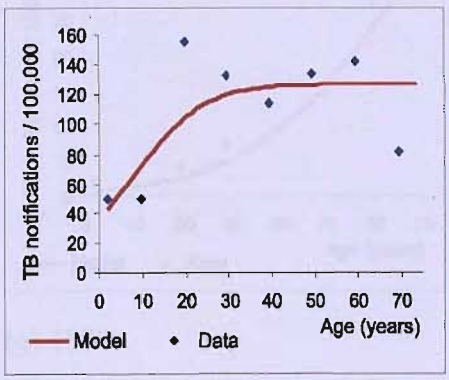

(a) 1953

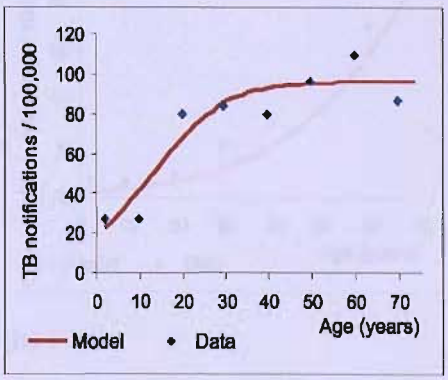

(b) 1957

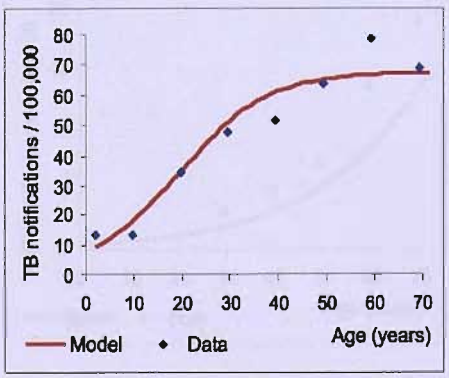

(c) 1962

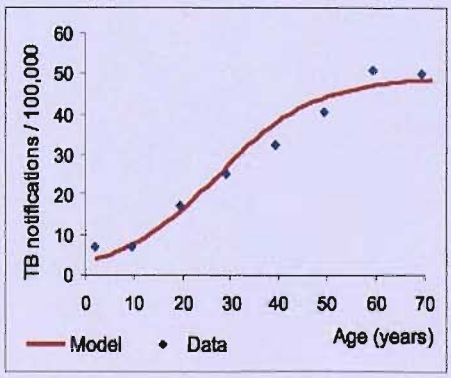

(d) 1967

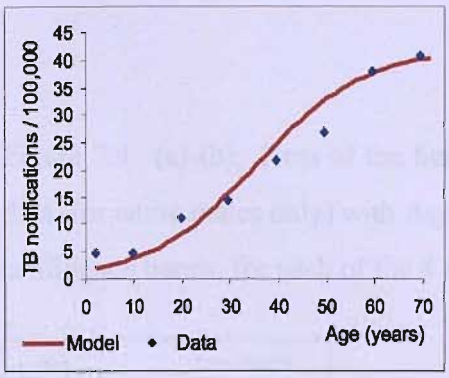

(e) 1971

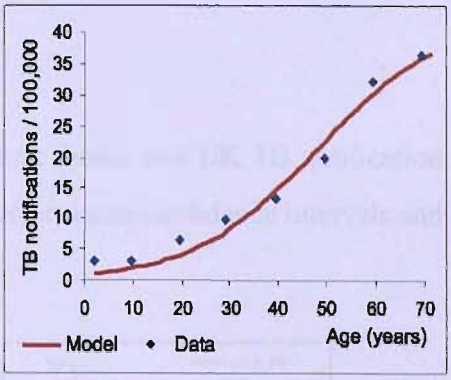

(f) 1976

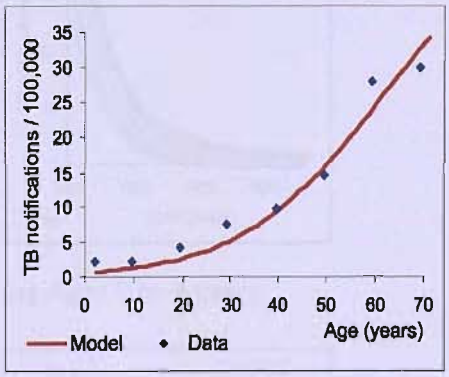

(g) 1980

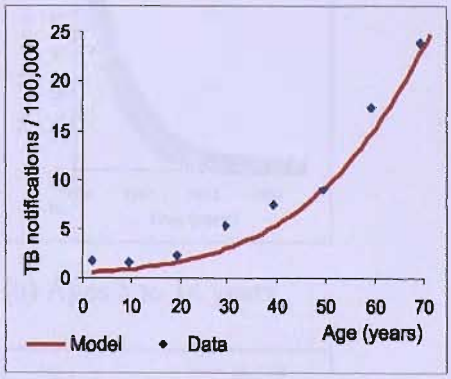

(h) 1985

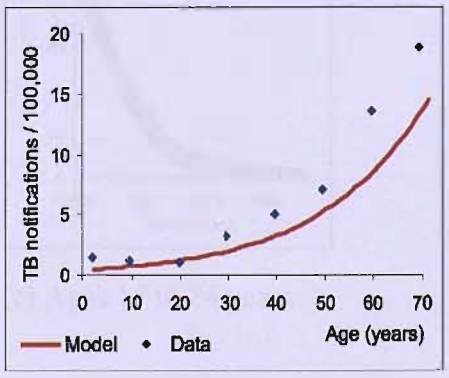

(i) 1989

Figure 7.4: (a)-(h): Plots of the fitted parametric model and UK TB notification data (for white males only) with Asymptotic performance confidence intervals and confidence bands, for each of the 8 age ranges.

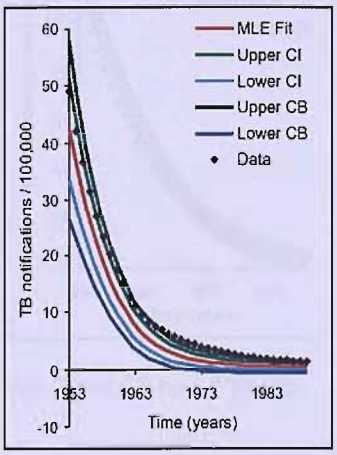

(a) Ages 0 to 4 years.

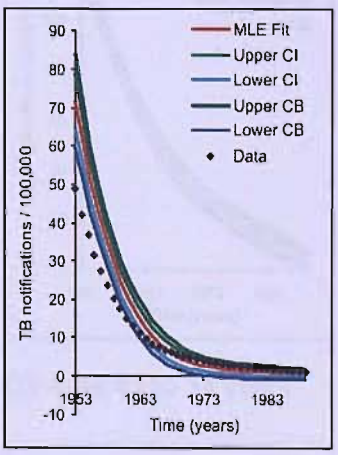

(b) Ages 5 to 14 years.

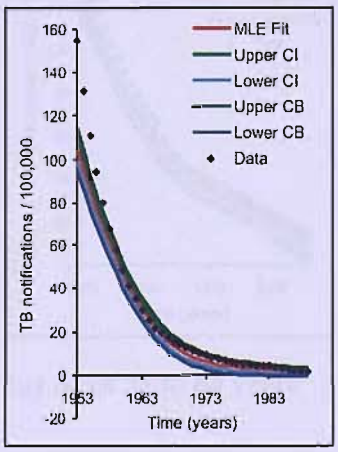

(c) Ages 15 to 24 years.

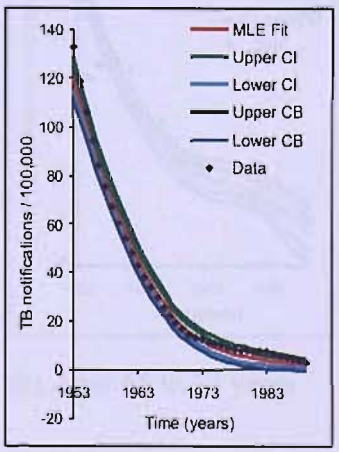

(d) Ages 25 to 34 years.

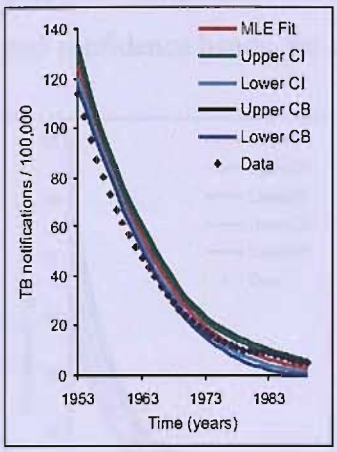

(e) Ages 35 to 44 years.

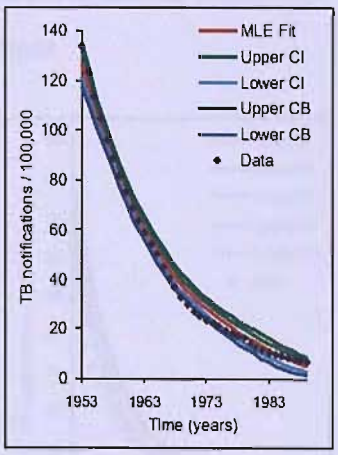

(f) Ages 45 to 54 years.

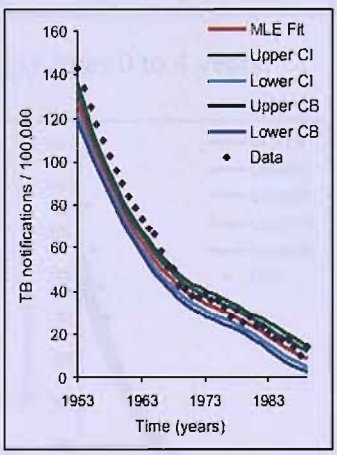

(g) Ages 55 to 64 years.

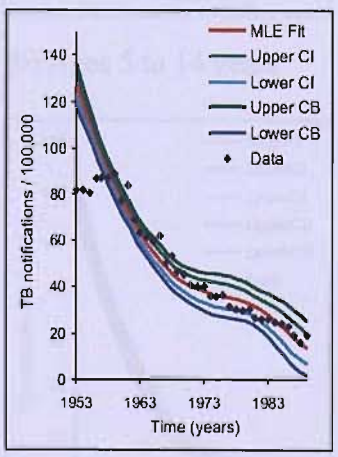

(h) Ages 65 to 74 years.

Figure 7.5: (a)-(h): Plots of the fitted parametric model and UK TB notification data (for white males only) with Bootstrapped performance confidence intervals and confidence bands, for each of the 8 age ranges.

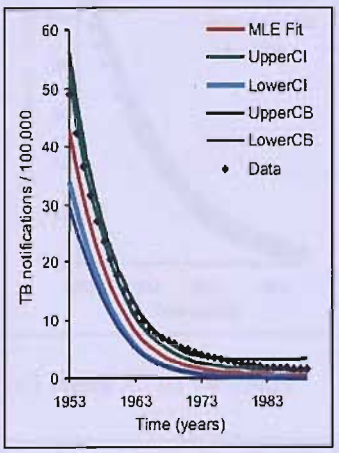

(a) Ages 0 to 4 years.

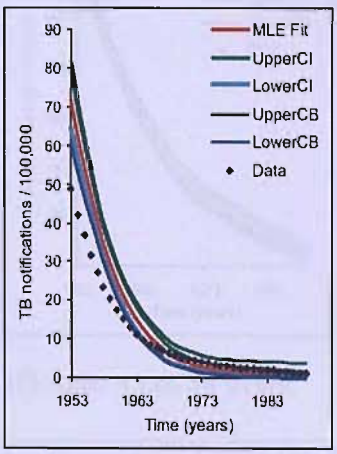

(b) Ages 5 to 14 years.

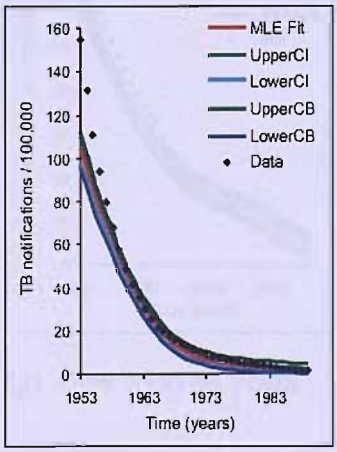

(c) Ages 15 to 24 years.

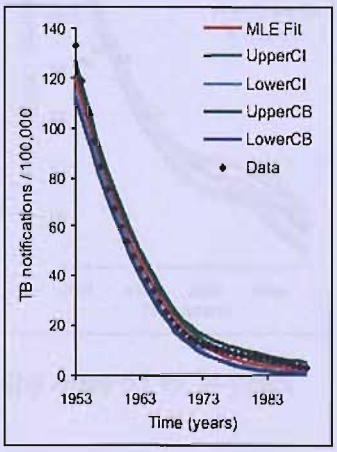

(d) Ages 25 to 34 years.

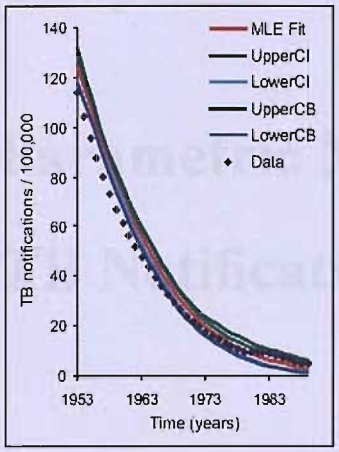

(e) Ages 35 to 44 years.

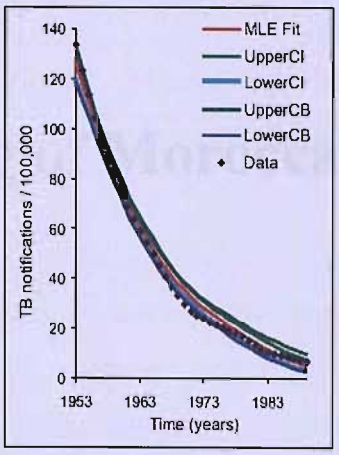

(f) Ages 45 to 54 years.

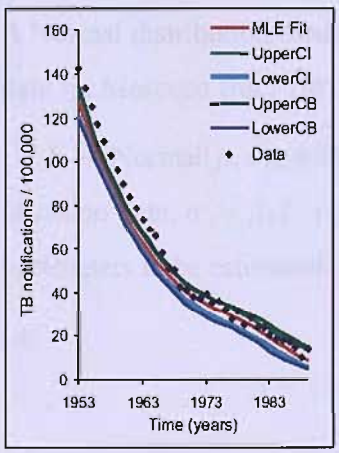

(g) Ages 55 to 64 years.

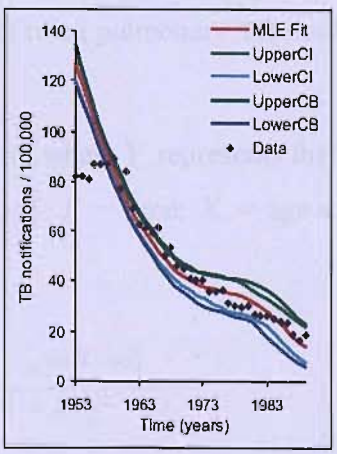

(h) Ages 65 to 74 years.

Chapter 8

Parametric Modelling of Moroccan TB Notification Data

8.1 Model formulation

A Normal distribution model is fitted to the confirmed pulmonary TB notification data for Morocco from 1980 to 2000:

$Y \sim \text{Normal}(\mu, \sigma)$, with pdf $\frac{1}{\sigma\sqrt{2\pi}} e^{\left(-\frac{(Y-\mu)^2}{2\sigma^2}\right)}$, where Y represents the TB notification data; $\sigma = \beta_1 T + \beta_{15} X$; $\mu = \eta(T, X, \alpha)$; T = time; X = age and β = parameters to be estimated.

Let

$$\eta = \left(\alpha_1 + \alpha_3 X + \alpha_5 X^2\right) \frac{e^{(\alpha_4 X - \alpha_2)}}{1 + e^{(\alpha_4 X - \alpha_2)}}$$

where

$$\alpha = \begin{cases} \alpha_1 = \beta_2 + \beta_7 T + \beta_{11} T^2 \\ \alpha_2 = \beta_3 \\ \alpha_3 = \beta_4 + \beta_8 T + \beta_{12} T^2 \\ \alpha_4 = \beta_5 + \beta_9 T + \beta_{13} T^2 \\ \alpha_5 = \beta_6 + \beta_{10} T + \beta_{14} T^2 \end{cases}$$

Note that the variance is dependent on both age and time.

8.2 Results of fitting the parametric model to the Moroccan PTB case data

The confidence limits for each parameter, $(\beta_i, i = 1, 2..., 15)$, produced by using asymptotic theory and bootstrapping, along with the maximum likelihood estimates for each parameter are displayed in table 8.1.

The parameters that may be insignificant, because their asymptotic confidence intervals include the value zero, are $\beta_4, \beta_6, \beta_8$ and β_{10} (at a very high significance level of 99%). But as these are constant and linear terms in quadratic functions and the quadratic terms β_{12} and β_{14} are considered significant, the parameters $\{\beta_i, i = 4, 6, 8, 10\}$ are kept in the model. It should be noted that the bootstrapped confidence intervals do not show evidence that any of the β parameters are insignificant and therefore strengthens the decision to keep the parametric model as formulated above.

The correlations for the 15 β parameters can be found numerically displayed in table 8.2 and graphically displayed in figures 8.1 to 8.4.

There are many strong correlations between the β parameters. From the numeric correlation values alone, all the parameters seem to be correlated with all other parameters, except for the parameters β_1, β_3 and β_{15}. β_1 and β_{15} are only correlated with each other which is reasonable as they are the two parameters of the standard deviation function. $\beta_3 \equiv \alpha_2$ is only strongly correlated with β_5, the constant term in α_4. This is also understandable as α_2 and α_4 make up the exponential term in η.

Although there are no obvious non-linear correlations that can be seen in the scatter plots for the β parameters, the large amount of correlation between the

parameters would throw doubt upon the validity of any independence assumptions.

The fits of the parametric model to the Moroccan TB case data for each of the 8 age ranges are shown in figures 8.5 (a)-(h).The model fits well for the majority of age ranges 10-44 and 65+ and seems to have captured well the time dependent characteristics for these age groups. The model seems to underestimate the number of TB cases in the younger children aged 0-9. However it must be noted that the data for children of these ages can be very unreliable (see chapter 3, section 3.4) and the numbers of cases per 100,000 is very low for these ages hence exaggerating the error in the model fit. The model struggles to fit to the data for the age group 45-64 and does not seem to adequately capture the characteristics of the data for this group.

The fits to the Moroccan data for a selection of years are shown in figures 8.6 (a)-(h). The model seems to have captured the general age dependent trends of the data, for each time point selected.

99% performance confidence intervals and confidence bands were constructed for each of the 8 age groups, using two different methods. The first method using asymptotic theory assumes normality and the results are shown in figures 8.7 (a)-(h). The second method uses bootstrapping and the results are shown in figures 8.8 (a)-(h). It can be seen that these two methods give similar results, with the asymptotic confidence intervals/bands slightly wider than those constructed by bootstrapping. This may be caused by the strong correlations between the parameters.

Table 8.1: Parameter MLE values with 99% asymptotic and bootstrap confidence intervals.

		Asymptotic Theory		Bootstrapping Method	
Parameters	ML Estimates	Lower 99% CI Limit	Upper 99% CI Limit	Lower 99% CI Limit	Upper 99% CI Limit
β_1	0.064	0.006	0.121	0.020	0.113
β_2	171.804	78.629	264.979	115.865	208.787
β_3	7.236	6.761	7.711	6.921	7.627
β_4	-3.935	-8.333	0.462	-5.763	-1.667
β_5	0.453	0.397	0.510	0.418	0.495
β_6	0.031	-0.017	0.078	0.001	0.052
β_7	24.285	3.291	45.279	19.668	29.204
β_8	-0.870	-1.850	0.109	-1.078	-0.763
β_9	-0.013	-0.022	-0.005	-0.021	-0.009
β_{10}	0.008	-0.002	0.018	0.006	0.010
β_{11}	-1.405	-2.335	-0.475	-1.607	-1.153
β_{12}	0.053	0.01	0.096	0.043	0.062
β_{13}	5.67E-04	1.89E-04	9.45E-04	3.38E-04	8.61E-04
β_{14}	-4.84E-04	-9.47E-04	-2.187E-05	-6.25E-04	-3.74E-04
β_{15}	0.219	0.166	0.272	0.164	0.256

Table 8.2: Correlation matrix for the 15 parameters.

	β_1	β_2	β_3	β_4	β_5	β_6	β_7	β_8	β_9	β_{10}	β_{11}	β_{12}	β_{13}	β_{14}	β_{15}
β_1	1	-0.15	0.36	0.14	0.3	-0.13	0.01	-0.01	-0.09	0.01	0.03	-0.03	0.06	0.03	-0.72
β_2	-0.15	1	-0.25	-0.99	-0.76	0.96	-0.86	0.86	0.83	-0.84	0.76	-0.76	-0.75	0.74	0.1
β_3	0.36	-0.25	1	0.23	0.73	-0.21	0.14	-0.13	-0.28	0.13	-0.1	0.1	0.24	-0.09	-0.3
β_4	0.14	-0.99	0.23	1	0.72	-0.99	0.84	-0.86	-0.78	0.86	-0.75	0.77	0.7	-0.76	-0.1
β_5	0.3	-0.76	0.73	0.72	1	-0.67	0.58	-0.56	-0.81	0.53	-0.51	0.49	0.73	-0.46	-0.23
β_6	-0.13	0.96	-0.21	-0.99	-0.67	1	-0.82	0.85	0.74	-0.87	0.73	-0.76	-0.66	0.77	0.09
β_7	0.01	-0.86	0.14	0.84	0.58	-0.82	1	-0.99	-0.83	0.96	-0.98	0.97	0.8	-0.94	0.02
β_8	-0.01	0.86	-0.13	-0.86	-0.56	0.85	-0.99	1	0.79	-0.99	0.97	-0.98	-0.76	0.97	-0.02
β_9	-0.09	0.83	-0.28	-0.78	-0.81	0.74	-0.83	0.79	1	-0.75	0.81	-0.77	-0.97	0.72	0.06
β_{10}	0.01	-0.84	0.13	0.86	0.53	-0.87	0.96	-0.99	-0.75	1	-0.94	0.97	0.72	-0.98	0.02
β_{11}	0.03	0.76	-0.1	-0.75	-0.51	0.73	-0.98	0.97	0.81	-0.94	1	-0.99	-0.82	0.96	-0.05
β_{12}	-0.03	-0.76	0.1	0.77	0.49	-0.76	0.97	-0.98	-0.77	0.97	-0.99	1	0.77	-0.99	0.05
β_{13}	0.06	-0.75	0.24	0.7	0.73	-0.66	0.8	-0.76	-0.97	0.72	-0.82	0.77	1	-0.73	-0.03
β_{14}	0.03	0.74	-0.09	-0.76	-0.46	0.77	-0.94	0.97	0.72	-0.98	0.96	-0.99	-0.73	1	-0.05
β_{15}	-0.72	0.1	-0.3	-0.1	-0.23	0.09	0.02	-0.02	0.06	0.02	-0.05	0.05	-0.03	-0.05	1

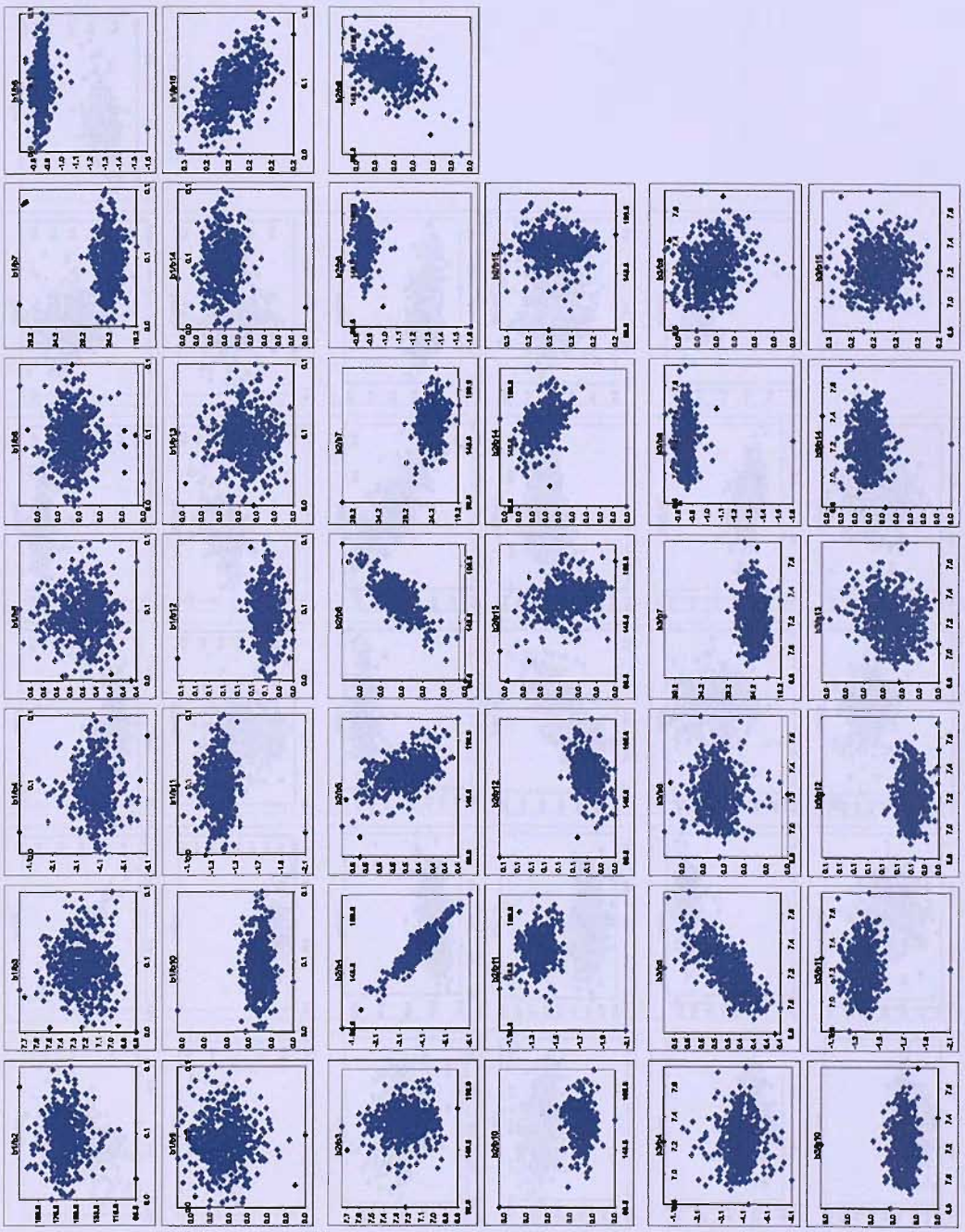

Figure 8.1: Scatter plots of the associations between the parameters β_1, β_2 and β_3, with the parameters β_2 to β_{15}.

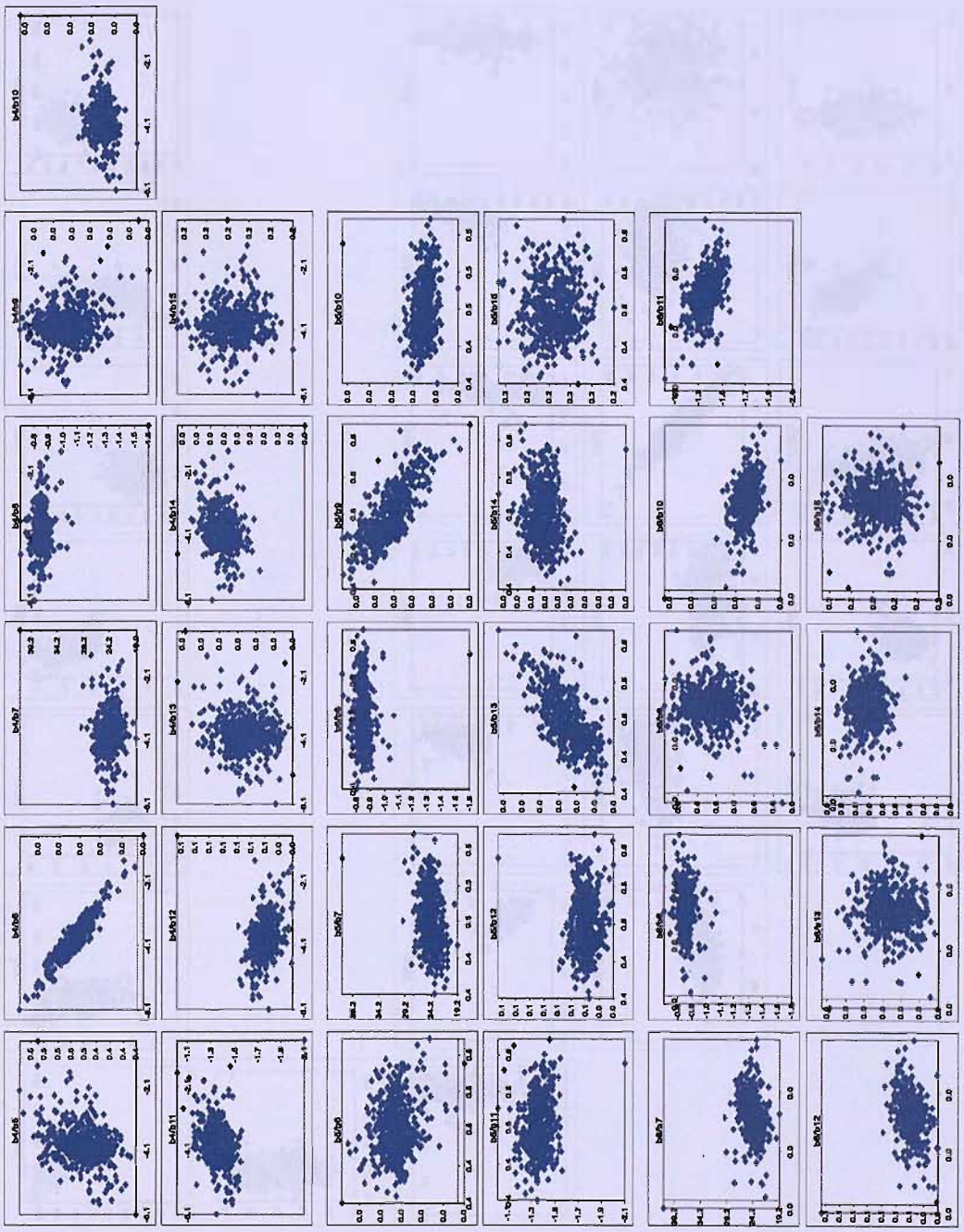

Figure 8.2: Scatter plots of the associations between the parameters β_4, β_5 and β_6, with the parameters β_5 to β_{15}.

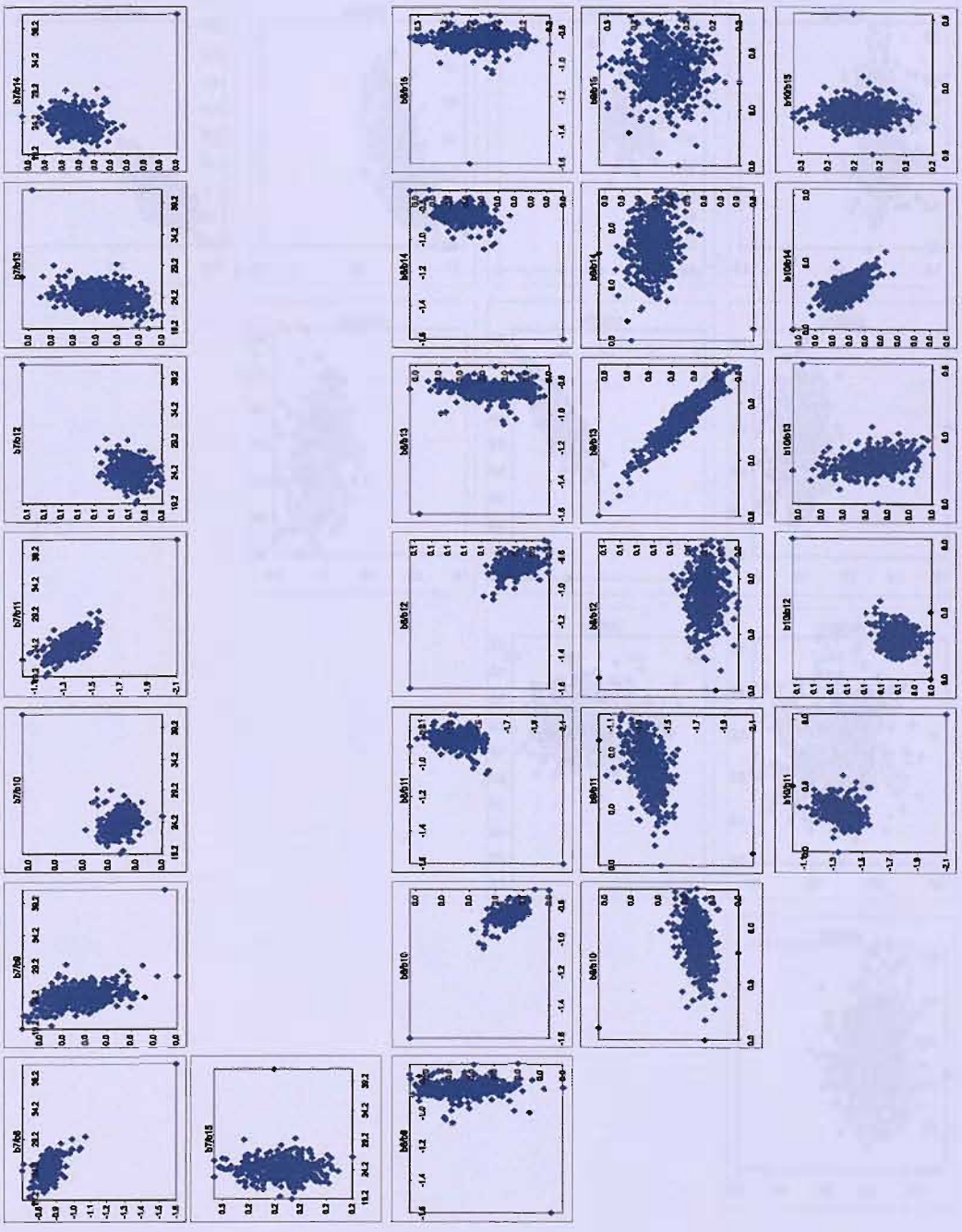

Figure 8.3: Scatter plots of the associations between the parameters β_7, β_8, β_9 and β_{10}, with the parameters β_8 to β_{15}.

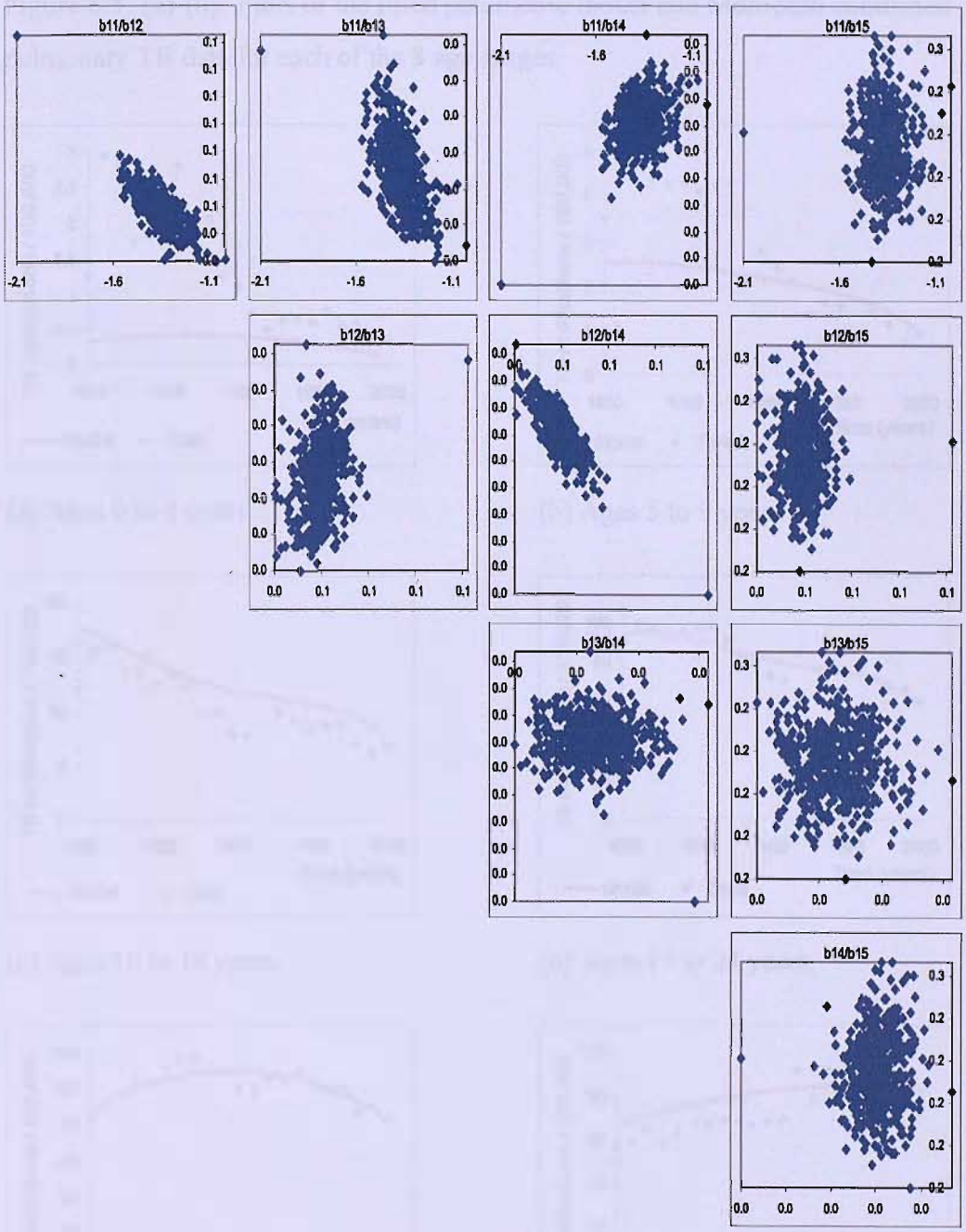

Figure 8.4: Scatter plots of the associations between the parameters β_{11}, β_{12}, β_{13} and β_{14}, with the parameters β_{12} to β_{15}.

Figure 8.5: (a)-(h): Plots of the fitted parametric model and Moroccan confirmed pulmonary TB data for each of the 8 age ranges.

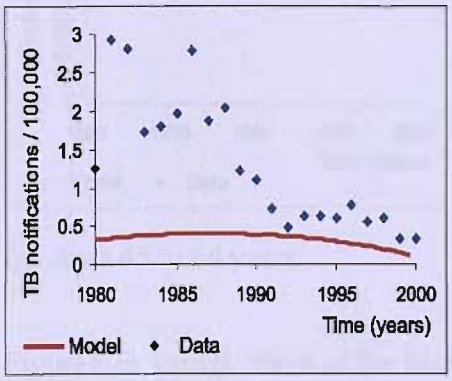

(a) Ages 0 to 4 years.

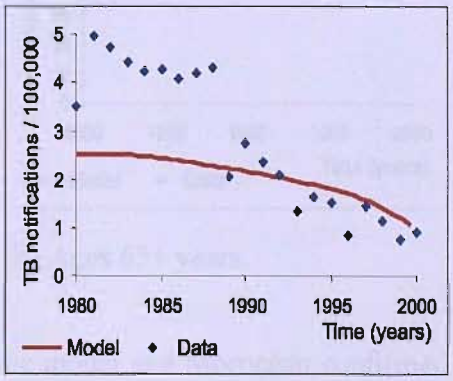

(b) Ages 5 to 9 years.

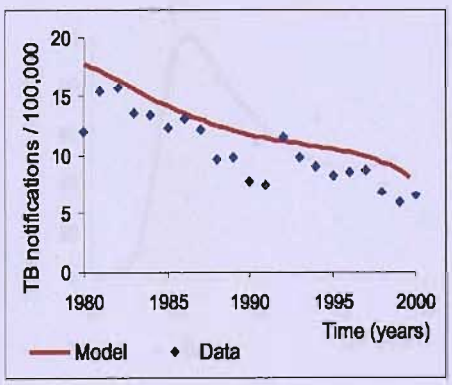

(c) Ages 10 to 14 years.

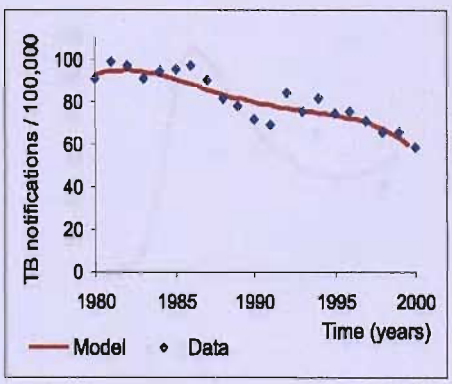

(d) Ages 15 to 24 years.

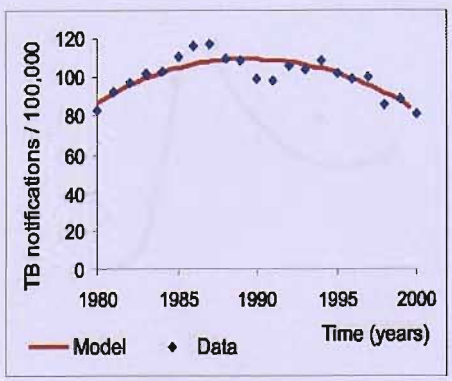

(e) Ages 25 to 34 years.

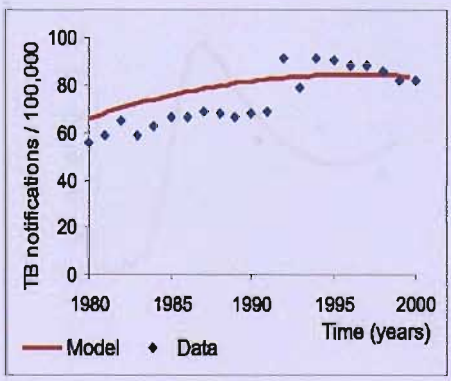

(f) Ages 35 to 44 years.

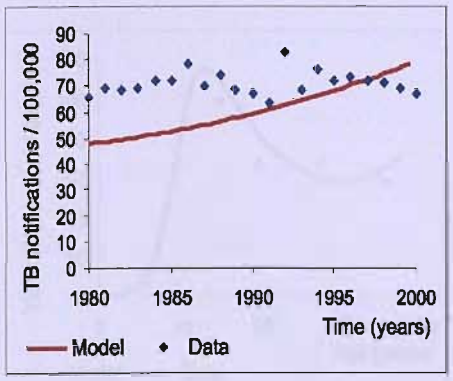

(g) Ages 45 to 64 years.

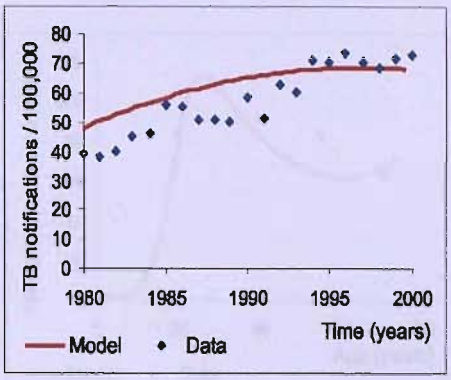

(h) Ages 65+ years.

Figure 8.6: (a)-(j): Plots of the fitted parametric model and Moroccan confirmed pulmonary TB notification data for a selection of years between 1980 and 2000.

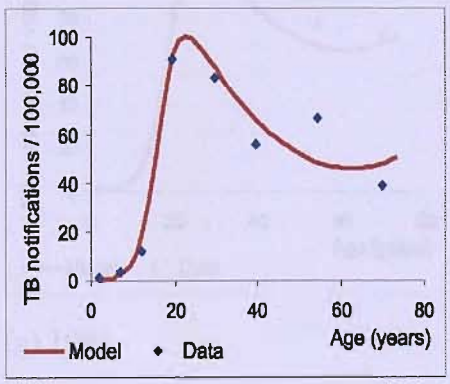

(a) 1980

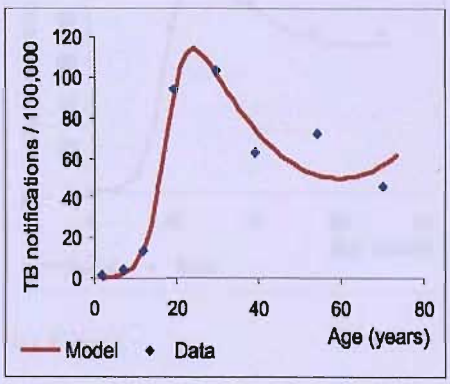

(b) 1984

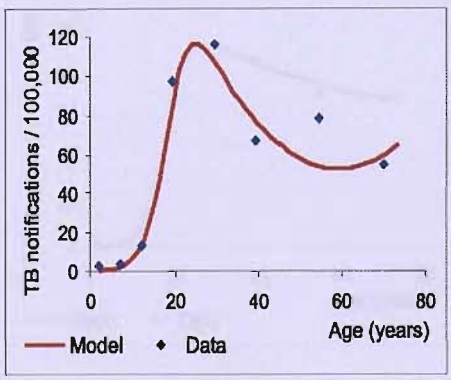

(c) 1986

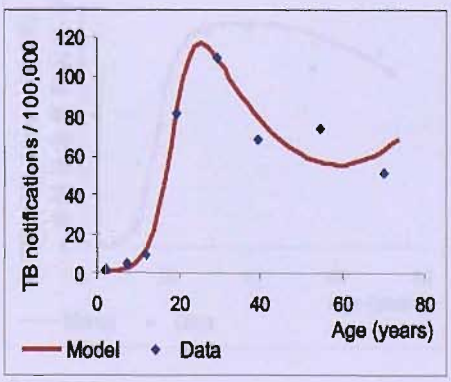

(d) 1988

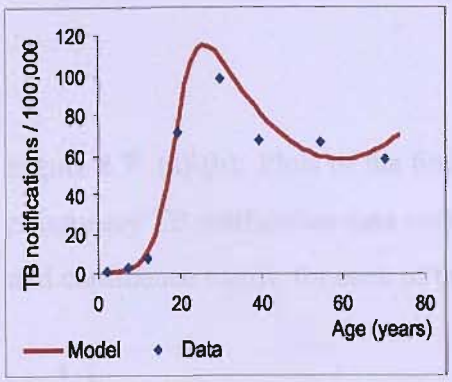

(e) 1990

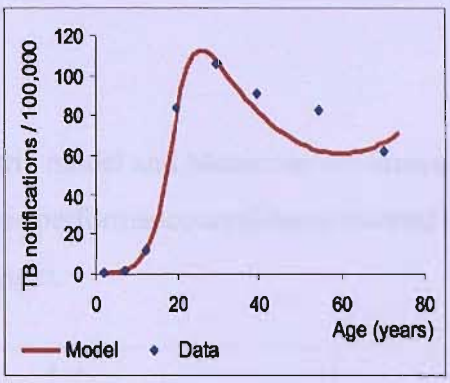

(f) 1992

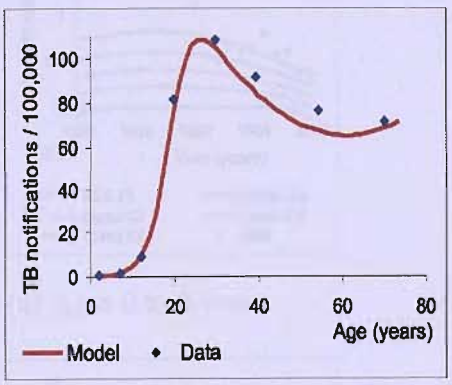

(g) 1994

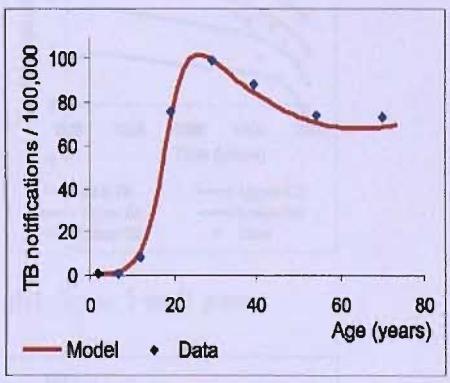

(h) 1996

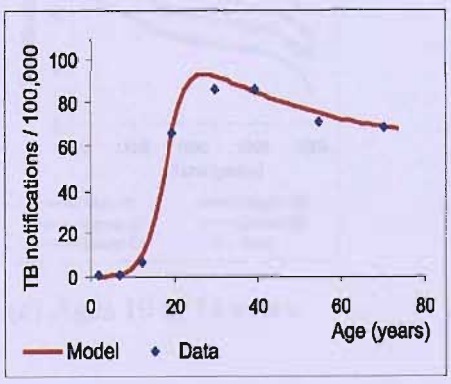

(i) 1998

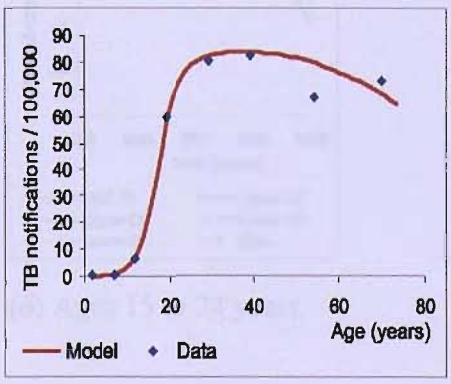

(j) 2000

Figure 8.7: (a)-(h): Plots of the fitted parametric model and Moroccan confirmed pulmonary TB notification data with Asymptotic performance confidence intervals and confidence bands, for each of the 8 age ranges.

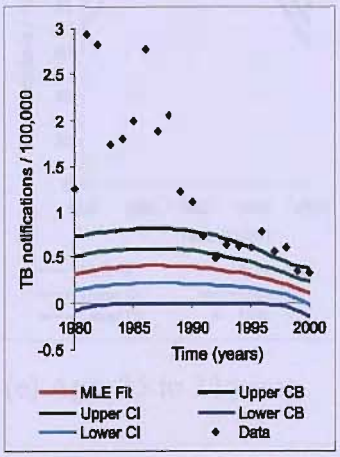

(a) Ages 0 to 4 years.

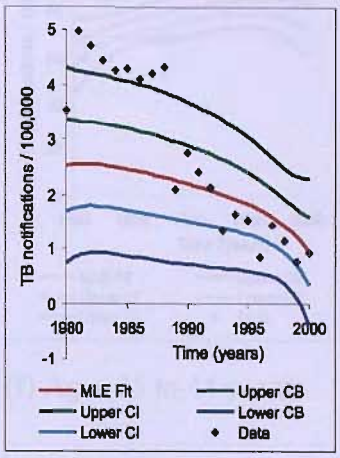

(b) Ages 5 to 9 years.

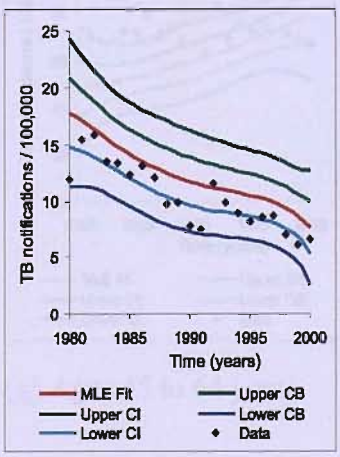

(c) Ages 10 to 14 years.

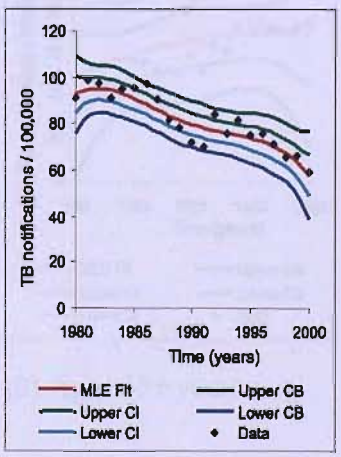

(d) Ages 15 to 24 years.

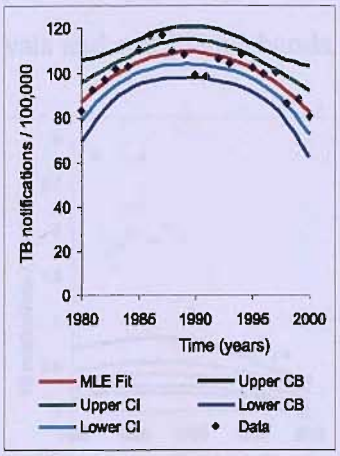

(e) Ages 25 to 34 years.

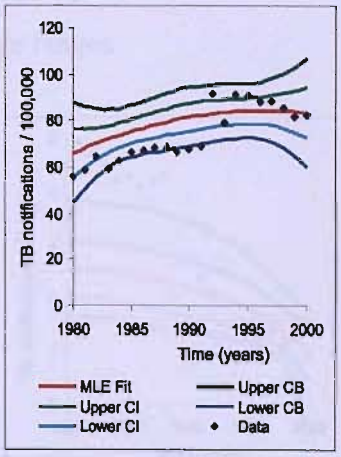

(f) Ages 35 to 44 years.

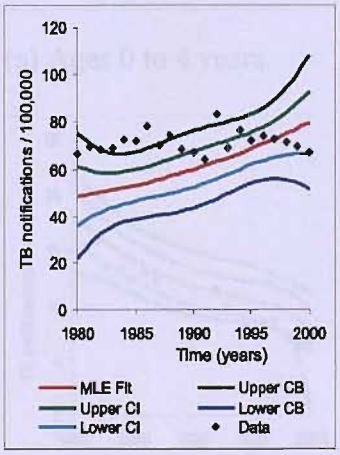

(g) Ages 45 to 64 years.

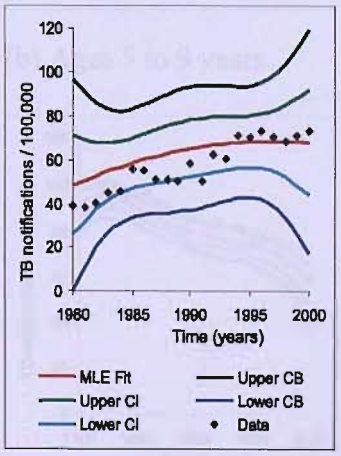

(h) Ages 65+ years.

Figure 8.8: (a)-(h): Plots of the fitted parametric model and Moroccan confirmed pulmonary TB notification data with Bootstrapped performance confidence intervals and confidence bands, for each of the 8 age ranges.

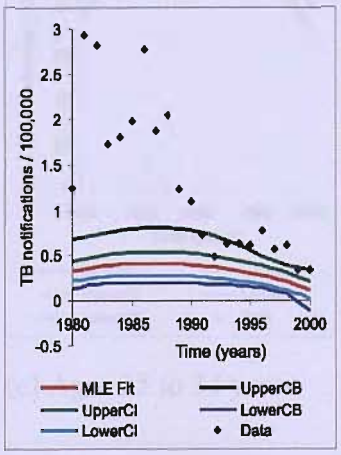

(a) Ages 0 to 4 years.

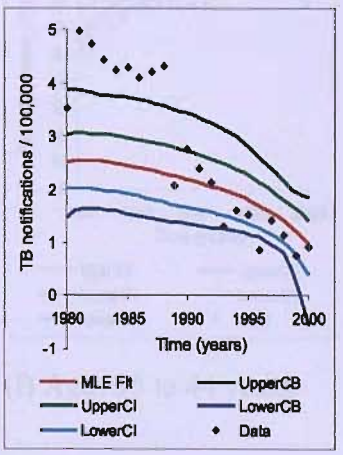

(b) Ages 5 to 9 years.

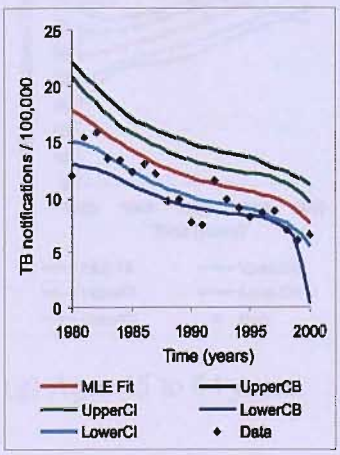

(c) Ages 10 to 14 years.

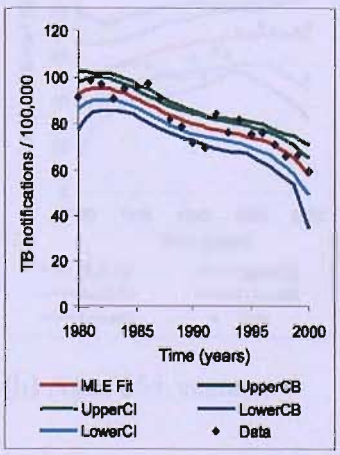

(d) Ages 15 to 24 years.

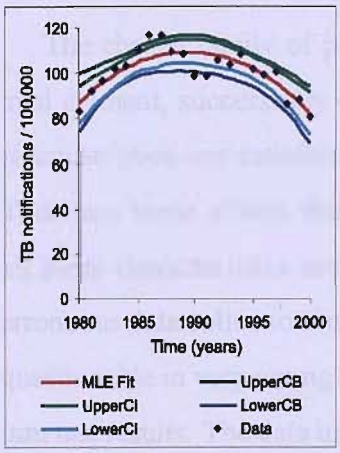

(e) Ages 25 to 34 years.

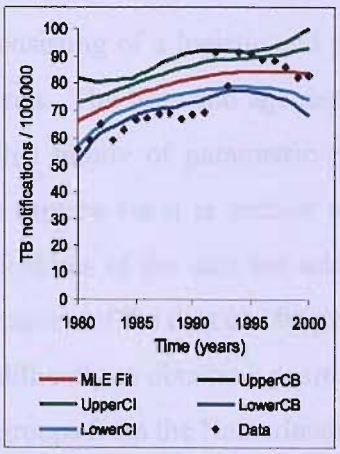

(f) Ages 35 to 44 years.

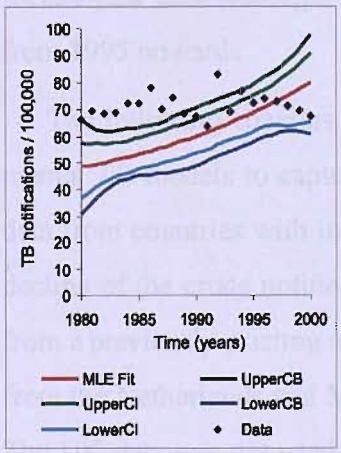

(g) Ages 45 to 64 years.

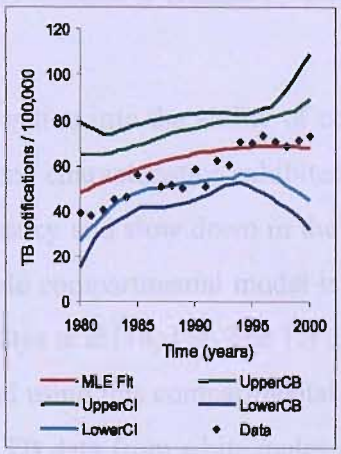

(h) Ages 65+ years.

8.3 Conclusions

The TB data sets from these three different countries, Netherlands, Morocco and UK, showed similar age and time dependent trends and characteristics. All displayed a general slowing of the decline in TB in the older age ranges.

The chosen family of parametric models consisting of a logistic and polynomial element, successfully fit to all three data sets. The time and age dependent characteristics are satisfactorily captured by this family of parametric models. There are some effects that the models fail to capture but it is unclear whether all these characteristics are derived from true features of the data but arise from erroneous data collection/manipulation. The accuracy of the data can be generally questionable in very young children due to the difficulty in obtaining positive sputum test results. The data in the two oldest age groups from the Netherlands suffer from a change in age ranges around 1972 used in the collection of data. The Moroccan year data although regarded as generally reliable is created by projection from 1995 onwards.

The following chapters describe the investigation into the ability of compartmental TB models to capture these age and time characteristics exhibited in TB data from countries with increasing life expectancy and slow down in the annual decline of the crude notification rate. A suitable compartmental model is rebuilt from a previously existing model devised by C.Dye et al [14, 15]. The TB data sets from the Netherlands and Morocco are analysed using this compartmental model. The UK data was not used as it only contains TB data from white males and the model is not built to make this distinction between gender and ethnicity.

Chapter 9

An Age-Structured Tuberculosis Model

9.1 Introduction

C.Dye et. al. [14][15] developed an age-structured mathematical model to investigate global Tuberculosis control strategy, for each of the six World Health Organisation (WHO) regions (sub-Saharan Africa, Americas, Eastern Mediterranean, Europe - divided into East and West, South East Asia, Western Pacific). In particular, it was set up to explore the effect of Directly Observed Short-course Therapy (DOTS), the WHO's strategy for worldwide TB control, on tuberculosis epidemics in those developing countries where the disease is most prevalent. Their TB model uses data from studies of the biology of TB and from the history of successful TB control in industrialised countries. The model incorporates and uses a separate HIV/AIDS model (as detailed in Garnett and Anderson, 1994 [31]) to generate HIV epidemics applicable to each of the six WHO world regions.

A newly re-constructed version of this model, adapted to enable investigation of the possible stagnation of TB in countries with an aging population, is described

in detail in the following sections and Chapters.

9.2 A description of a deterministic, compartmental, age-dependent TB Model

This model was constructed with the primary purpose of analysing the progression of TB in countries with an increasing life expectancy and a very low annual risk of infection, where 'aging of the epidemic' and thus stagnation effects could occur. It was specifically re-constructed from the age-structured mathematical model developed by C.Dye et. al. [14][15] at the W.H.O to investigate their global Tuberculosis control strategy. This re-constructed version was programmed in Excel/VBA using the two papers [14][15] that document the structure of the original TB/HIV model. The HIV element of the original WHO model [14][15] has been taken out. This somewhat simplifies the model and is not an unrealistic modification as the countries that would be of prime interest in this model are not considered to have a large HIV problem.

This deterministic, compartmental model, is set in discrete time and is run by difference equations. See Figure 9.1 for a flow diagram of the TB model and Tables 9.1, 9.2 and 9.3 for definitions of the variables and input parameters.

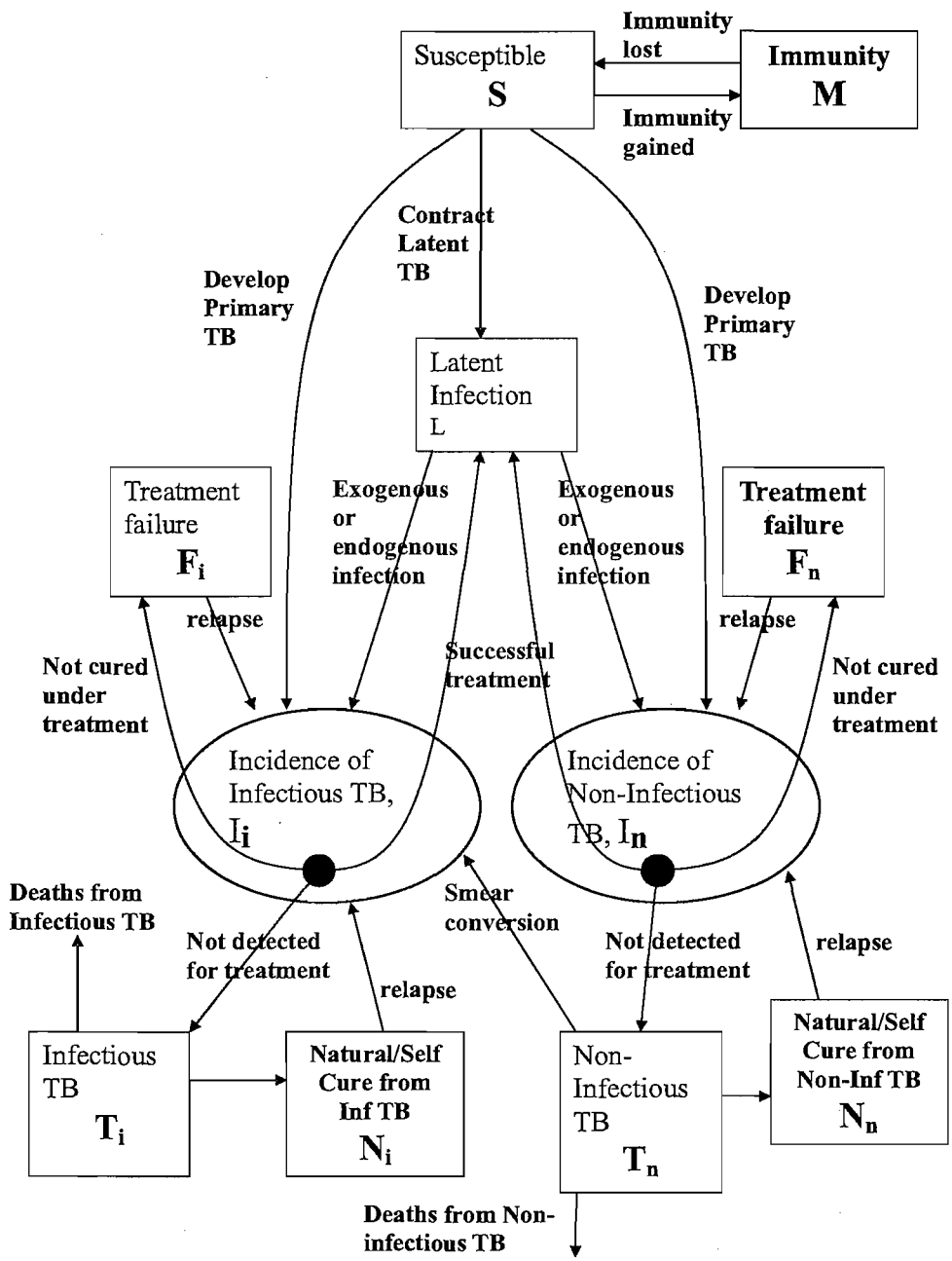

Figure 9.1: Flow diagram of the age-dependent compartmental TB model.

Variable Name	Definition
$S(t,a)$	Proportion of population who are uninfected and susceptible to infection, of age a at time t
$M(t,a)$	Proportion of population immune to infection (naturally or after vaccination), of age a at time t
$T_i(t,a)$	Proportion of population who have infectious (smear positive) TB; primary, endogenous, exogenous or relapse; of age a at time t
$T_n(t,a)$	Proportion of population who have non-infectious (smear negative) pulmonary and extra-pulmonary TB, of age a at time t
$L(t,a)$	Proportion of population who are latently infected or cured of TB under good treatment, age a at time t
$N_i(t,a)$	Proportion of population who are self-cured from infectious TB, (i.e. recover from disease naturally without medical intervention), of age a at time t
$N_n(t,a)$	Proportion of population who are self-cured from non-infectious TB, (i.e. recover from disease naturally without medical intervention), of age a at time t
$F_i(t,a)$	Proportion of incidences of infectious TB which is not cured under treatment; classed as failed, defaulted or transferred out in cohort analysis; of age a at time t
$F_n(t,a)$	Proportion of incidences of non-infectious TB which is not cured under treatment; classed as failed, defaulted or transferred out in cohort analysis; of age a at time t
$I_i(t,a)$	Incidence rate of infectious TB, for those of age a at time t
$I_n(t,a)$	Incidence rate of non-infectious TB, for those of age a at time t

Table 9.1: Name and description of variables used in the compartmental age-dependent TB model.

Variable Name	Parameter Description
timeStep	Time step (in years)
$\lambda(1)$	Initial value of the force of infection
m_+	Rate at which immunity is acquired by susceptibles
m_-	Rate at which protective immunity is lost
m	$M(1, a)$, Fraction immunised at birth
n	Rate of natural cure for infectious and non-infectious TB
μ_i	Death rate for infectious TB
μ_n	Death rate for non-infectious TB
θ	Exponential rate of decline in the contact rate β, to reflect 'socio-economic improvement'
ϕ	Proportion of failed treatment cases which are infectious
ϵ	Relative case detection rate of non-infectious cases
case_det_DOTS	Rate at which TB cases are found and treated under DOTS (or a comparable strategy)
case_cure_DOTS	Proportion of treated cases given curative chemotherapy under DOTS (or a comparable strategy)
case_det_non DOTS	Rate at which TB cases are found and treated pre-DOTS
case_cure_non DOTS	Proportion of treated cases given curative chemotherapy pre-DOTS)

Table 9.2: Name and description of parameters used in the compartmental age-dependent TB model.

Variable Name	Parameter Description
$\pi(t, a)$	Proportion of population in age class a at time t
$\beta(t)$	Per capita contact rate between T_i & rest of population, at time t
w	Rate of smear conversion from non-infectious to infectious TB
r_n	Rate of relapse after self cure to active TB
r	Rate of relapse from failed treatment to active TB
x(age≤agecut)	Proportion of re-infections which is susceptible to developing TB within one year
x(age>agecut)	(*as above*)
p(age≤agecut)	Proportion of infected susceptibles which develop progressive primary TB within one year
p(age>agecut)	(*as above*)
v(age≤agecut)	Rate at which latent infections become TB cases by endogenous reactivation
v(age>agecut)	(*as above*)
f(age≤agecut)	Proportion of progressive primary cases which become infectious
f(age>agecut)	(*as above*)

Table 9.3: Description of parameters used in the compartmental age-dependent TB model.

9.3 Assumptions behind the TB model

In order to construct this mathematical model certain assumptions were made. These assumptions were made in accordance with current scientific thinking about the epidemiology and natural history of TB. If an assumption was made in order to simplify the model it was only used if it was thought to not significantly compromise the validity of the model. The following is a list of these underlying assumptions.

- Different proportions of the model population move through the 9 states according to the corresponding governing equations and the values of the input parameters.
- Case detection is measured as the number of infectious cases diagnosed and treated per year divided by the estimated annual incidence of new infectious cases. It is assumed that cases who would otherwise have received inferior treatment are enrolled onto the DOTS programme. Extra cases are only treated when all such patients have been recruited. New DOTS programmes concentrate on achieving high cure rates first and then work on improving case detection.
- Patients who complete Short Course Chemotherapy (SCC) are assumed to be cured of TB but remain infected and move into the latent class.
- The term *treatment failure* covers all patients who do not complete treatment, i.e. those that 'fail', 'default' or 'transfer out'. They have the same death rate as those without active TB and have a higher chance of re-developing full TB than those cured. Those who 'fail' plus a proportion of the others remain infectious.

- Self-cured individuals are assumed to have a higher chance of relapsing to full TB than others.
- It is assumed that Infectious TB suffers a higher elevated death rate than non-infectious TB.
- Numerical simulations are able to be carried out with a time (t) and age (a) step of $\leq$ one year (defined by user), due to the general opinion that some changes in the TB state of an individual may occur in shorter periods than one year.
- There is no gender dependence i.e. the model does not distinguish between TB cases in males and females. This greatly simplifies the model and was not considered to significantly compromise the validity of the model.
- The age limit is input by the user (only limited by the age data available for each country of interest). It is assumed that death occurs at this limit.

9.4 Equations used in the model

Difference and other equations are used to govern the movement of the population through the various states of the TB model. The following is a list of these equations with their definitions.

1. The force of infection (or Incidence rate) is the per capita rate at which susceptibles are infected and is denoted by:

$$\lambda(t) = \beta(t) \sum_{a=0}^{agelim} \pi(t,a) \left(T_i(t,a) + \phi F_i(t,a)\right)$$

where $\beta(t) = \beta(0)e^{-\theta t}$.

$\beta(t)$ is the per capita contact rate between infectious TB cases and other

individuals. $e^{-\theta t}$ allows for a possible exponential rate of decline in $\beta(t)$, reflecting 'socio-economic improvement'. $\beta(0)$ is a chosen positive constant used to set the initial contact rate value.

To calculate the Force of Infection, the proportion of the population in age class a at time t, $\pi(t,a)$, multiplied by the sum of the proportion of population who have infectious TB, $T_i(t,a)$, and the proportion of infectious TB cases undergoing treatment who fail treatment and are left infectious, $\phi F_i(t,a)$, is summed over all age classes. This is then multiplied by the per capita contact rate between infectious TB cases and other individuals, $\beta(t)$.

2. The proportion of incidence of infectious TB in the population at time t, age a, i.e *all inputs to state T_i in the model* (see flow diagram 9.1) is calculated

as:

$$
\begin{aligned}
I_i(t,a) &= \lambda(t-1)p(a-1)f(a-1)S(t-1,a-1) \\
&\quad \text{Proportion of infected susceptibles which develop progressive primary infectious TB within 1 year} \\
&+ (v(a-1)+x(a-1)p(a-1)\lambda(t-1))f(a-1)L(t-1,a-1) \\
&\quad \text{Proportion of Latents which develop progressive primary infectious TB, by endogenous reactivation or reinfection} \\
&+ wT_n(t-1,a-1) \\
&\quad \text{Proportion of non-infectious TB population that develop infectious TB by smear conversion} \\
&+ rF_i(t-1,a-1) \\
&\quad \text{Proportion of individuals who fail treatment for infectious TB and relapse to active infectious TB} \\
&+ r_nN_i(t-1,a-1) \\
&\quad \text{Proportion of individuals who relapse from self/natural cure}
\end{aligned}
$$

3. The proportion of incidence of non-infectious TB in the population at time t, age a, i.e *all inputs to state T_n in model* (see flow diagram 9.1) is calculated

as:

$$
\begin{aligned}
I_n(t,a) &= \lambda(t-1)p(a-1)(1-f(a-1))S(t-1,a-1) \\
&\quad \text{Proportion of infected susceptibles which develop progressive} \\
&\quad \text{primary non-infectious TB within 1 year} \\
&+ (v(a-1)+x(a-1)p(a-1)\lambda(t-1))(1-f(a-1)) \\
&\quad L(t-1,a-1) \\
&\quad \text{Proportion of Latents which develop progressive primary} \\
&\quad \text{non-infectious, by endogenous reactivation or reinfection} \\
&+ rF_n(t-1,a-1) \\
&\quad \text{Proportion of individuals who fail treatment for non-infectious} \\
&\quad \text{TB and relapse to active non-infectious TB} \\
&+ r_nN_n(t-1,a-1) \\
&\quad \text{Proportion of individuals who relapse from self/natural cure}
\end{aligned}
$$

4. Hence, the proportion of incidence of both infectious TB and non-infectious TB in the population at time t, age a, is calculated as:

$$I(t,a) = I_i(t,a) + I_n(t,a) - wT_n(t-1,a-1)$$

This is simply the sum of the two separate incidences of infectious and non-infectious TB minus the proportion of individuals with non-infectious TB that develop infectious TB by smear conversion. If this was not subtracted there would be a proportion of the TB incidences that were counted twice in the formulation of I(.).

5. (i) The proportion of population aged a, in the model at time t, is simply

calculated as:

$$\begin{aligned} Agetot(t,a) &= S(t,a) + L(t,a) + T_i(t,a) + T_n(t,a) \\ &+ F_i(t,a) + F_n(t,a) + N_i(t,a) + N_n(t,a) + M(t,a) \end{aligned}$$

(ii) The proportion of the population (for all ages) in the model at time t, is therefore:

$$Gtot(t) = \sum_{\forall a} Agetot(t,a)$$

Both these equations are used to re-standardise the model values so that the proportion of the population in the model is equal to one for all t. This is necessary because the proportion of deaths that leave the model is not replenished by 'births'. Therefore after a few iterations of the model the sum of all the proportions of the population in the 9 states will be less than one.

9.4.1 Difference Equations describing the model

The following nine difference equations govern the change in the proportion of population in each of the nine state classes. They can be determined directly from the flow chart in Figure 9.1.

6. The change in the proportion of individuals who have never been infected

but are susceptible to infection is calculated by:

$$
\begin{aligned}
S(t,a) \; - \; & S(t-1,a-1) = \\
& m\_M(t-1,a-1) \\
& \text{Proportion of immune individuals who lose their protective immunity} \\
+ \; & -\lambda(t-1)S(t-1,a-1) \\
& \text{Proportion of susceptibles who become infected with TB} \\
- \; & m_{+}S(t-1,a-1) \\
& \text{Proportion of population susceptible to infection who gain} \\
& \text{immunity to infection}
\end{aligned}
$$

7. The change in the proportion of individuals who are latently infected, or cured of TB (and therefore return to the latent state) is calculated as:

$$
\begin{aligned}
L(t,a) \; - \; & L(t-1,a-1) = \\
& (1-p(a-1))\lambda(t-1)S(t-1,a-1) \\
& \text{Proportion of infected susceptibles who get a latent infection} \\
+ \; & [(det)(cure)+(detND)(cureNotDot)]I_i(t-1,a-1) \\
+ \; & \epsilon[(det)(cure)+(detND)(cureNotDot)]I_n(t-1,a-1) \\
& \text{Proportion of infectious and non-infectious TB cases who are} \\
& \text{detected and cured and therefore return to the Latent state} \\
- \; & (v(a-1)+x(a-1)p(a-1)\lambda(t-1))L(t-1,a-1) \\
& \text{Proportion of Latents which develop progressive primary infectious} \\
& \text{or non-infectious TB, by endogenous reactivation or reinfection}
\end{aligned}
$$

8. The change in the proportion of individuals who have infectious (smear positive) primary, endogenous, exogenous or relapse TB is calculated as:

$$T_i(t,a) - T_i(t-1,a-1) =$$

$$\lambda(t-1)p(a-1)f(a-1)S(t-1,a-1)$$

Proportion of infected susceptibles which develop progressive primary infectious TB within 1 year

$$+ (v(a-1)+x(a-1)p(a-1)\lambda(t-1))f(a-1)L(t-1,a-1)$$

Proportion of Latents which develop progressive primary infectious TB, by endogenous reactivation or reinfection

$$+ wT_n(t-1,a-1)$$

Proportion of individuals with non-infectious TB that develop infectious TB by smear conversion

$$+ rF_i(t-1,a-1)$$

Proportion of individuals who fail treatment for infectious TB and relapse to active infectious TB

$$+ r_nN_i(t-1,a-1)$$

Proportion of individuals who relapse from self/natural cure to active infectious TB

$$- [det + detND]I_i(t-1,a-1)$$

Proportion of incidences of infectious TB that are detected and diverted to treatment

$$- (\mu_i)T_i(t-1,a-1)$$

Proportion of infectious TB population that die a TB related death

$$- nT_i(t-1,a-1)$$

Proportion of individuals who experience a self/natural cure from active infectious TB

The proportion of individuals in state $T_i(.)$ can therefore be simplified to the proportion of all incidences of infectious TB that are not detected and diverted to treatment, minus all those with infectious TB who either die a TB related death or experience a self/natural cure from active infectious TB.

$$T_i(t,a) - T_i(t-1,a-1) \equiv$$
$$[1-(det+detND)]I_i(t-1,a-1) - (\mu_i+n)T_i(t-1,a-1)$$

9. The change in the proportion of individuals who have non-infectious (smear negative) pulmonary and extra-pulmonary TB is calculated as:

$$
\begin{aligned}
T_n(t,a) \; - \; & T_n(t-1,a-1) = \\
& \lambda(t-1)p(a-1)(1-f(a-1))S(t-1,a-1) \\
& \text{Proportion of infected susceptibles which develop} \\
& \text{progressive primary non-infectious TB within 1 year} \\
+ \; & (v(a-1)+x(a-1)p(a-1)\lambda(t-1))(1-f(a-1)) \\
& L(t-1,a-1) \\
& \text{Proportion of Latents which develop progressive primary} \\
& \text{non-infectious TB, by endogenous reactivation or reinfection} \\
+ \; & rF_n(t-1,a-1) \\
& \text{Proportion of individuals who fail treatment for} \\
& \text{non-infectious TB and relapse to active non-infectious TB} \\
+ \; & r_nN_n(t-1,a-1) \\
& \text{Proportion of individuals who relapse to active non-infectious} \\
& \text{TB from self/natural cure} \\
- \; & \epsilon[(det)+(detND)]I_n(t-1,a-1) \\
& \text{Proportion of incidences of non-infectious TB} \\
& \text{that are detected and diverted to treatment} \\
- \; & (w+\mu_n+n)T_n(t-1,a-1) \\
& \text{Proportion of non-infectious TB population that develop} \\
& \text{infectious TB by smear conversion, die a TB related death} \\
& \text{or experience self/natural cure from active non-infectious TB}
\end{aligned}
$$

The proportion of individuals in state $T_n(.)$ can therefore be simplified to the proportion of all incidences of infectious TB that are not detected and diverted to treatment, minus all those with non-infectious TB who either

die a TB related death or experience a self/natural cure from active non-infectious TB.

$$T_n(t,a) - T_n(t-1,a-1) \equiv [1-\epsilon(det+detND)]I_n(t-1,a-1) \\ -(w+\mu_n+n)T_n(t-1,a-1)$$

10. The change in the proportion of individuals with infectious TB which are not cured under treatment, is calculated as:

$$F_i(t,a) - F_i(t-1,a-1) =$$

$$[(det)(1-cure)+(detND)(1-cureND)]I_i(t-1,a-1)$$

Proportion of incidences of infectious TB that fail treatment

$$- rF_i(t-1,a-1)$$

Proportion not cured under treatment, who relapse to active infectious TB

11. The change in the proportion of individuals with non-infectious TB which are not cured under treatment, is calculated as:

$$F_n(t,a) - F_n(t-1,a-1) =$$

$$\epsilon[(det)(1-cure)+(detND)(1-cureND)]I_n(t-1,a-1)$$

Proportion of incidences of non-infectious TB that fail treatment

$$- rF_n(t-1,a-1)$$

Proportion not cured under treatment, who relapse to active non-infectious TB

12. The change in the proportion of individuals who are immune to infection,

either naturally or following vaccination, is calculated as:

$$M(t,a) - M(t-1,a-1) =$$

$$m_{+}S(t-1,a-1)$$

Proportion of susceptibles who gain immunity

$$- \; m_{-}M(t-1,a-1)$$

Proportion of immune individuals who lose their immunity

13. The change in the proportion of self-cured from infectious TB, is calculated as:

$$N_i(t,a) - N_i(t-1,a-1) =$$

$$nT_i(t-1,a-1)$$

Proportion of individuals with infectious TB who experience self/natural cure

$$- \; r_n N_i(t-1,a-1)$$

Proportion of self-cured population who relapse to active infectious TB

14. The change in the proportion of self-cured from non-infectious TB is calculated as:

$$N_n(t,a) - N_n(t-1,a-1) =$$

$$nT_n(t-1,a-1)$$

Proportion of individuals with non-infectious TB who experience self/natural cure

$$- \; r_n N_n(t-1,a-1)$$

Proportion of self-cured population who relapse to active non-infectious TB

9.5 Boundary Conditions

Boundary conditions are required as the model equations alone do not allow for an input of new people (i.e. births) into the model. The model is therefore set up so that $S(\forall t, a = 1) = 1 - m$, where $m = M(\forall t, a = 1)$. All other states at age, $a = 1$, are set to zero, for all t.

The lifespan of the model population, (*agelim*), after which age it is assumed everyone dies, is input by the user.

9.6 Equilibrium Calculations

Equilibrium values are calculated for time, $t = 1$ and age, $a = 1$ to *agelim*. A simplified set of seven equations adapted from the 9 state equations in section 9.4.1 is used to find equilibrium. The two 'Failed Treatment' states are eliminated from these equilibrium equations along with the case detection and cure parameters as it is assumed that treatment has not started before time $t = 1$.

At equilibrium:

$$\begin{aligned}
S(t, a-1) - S(t-1, a-1) &= 0 \\
L(t, a-1) - L(t-1, a-1) &= 0 \\
T_i(t, a-1) - T_i(t-1, a-1) &= 0 \\
T_n(t, a-1) - T_n(t-1, a-1) &= 0 \\
N_i(t, a-1) - N_i(t-1, a-1) &= 0 \\
N_n(t, a-1) - N_n(t-1, a-1) &= 0 \\
M(t, a-1) - M(t-1, a-1) &= 0
\end{aligned}$$

Let Ω stand for any of the above state classes.

Now if $\Omega(t, a-1) = \Omega(t-1, a-1)$

then $\Omega(t,a) - \Omega(t-1,a-1) \equiv \Omega(t,a) - \Omega(t,a-1)$.

Hence, each state equation can be written in terms of a and $a-1$ for $t=1$ and solved for each value of a:

1. Susceptibles:

$$S(1,a) - S(1,a-1) = -(\lambda(1) + m_+)S(1,a-1) + m\_M(1,a-1)$$

2. Latents:

$$\begin{aligned} L(1,a) \;-\; & L(1,a-1) = \\ & (1-p(a-1))\lambda(1)S(1,a-1) \\ - \; & (v(a-1) + x(a-1)p(a-1)\lambda(1))L(1,a-1) \end{aligned}$$

3. Infectious TB:

$$\begin{aligned} T_i(1,a) \;-\; & T_i(1,a-1) = \\ & \lambda(1)p(a-1)f(a-1)S(1,a-1) \\ + \; & (v(a-1) + x(a-1)p(a-1)\lambda(1))f(a-1)L(1,a-1) \\ + \; & wT_n(1,a-1) + r_nN_i(1,a-1) \\ - \; & (n+\mu_i)T_i(1,a-1) \end{aligned}$$

4. Non-Infectious TB:

$$\begin{aligned} T_n(1,a) \;-\; & T_n(1,a-1) = \\ & \lambda(1)p(a-1)(1-f(a-1))S(1,a-1) \\ + \; & (v(a-1) + x(a-1)p(a-1)\lambda(1))(1-f(a-1))L(1,a-1) \\ + \; & r_nN_n(1,a-1) - (n+w+\mu_n)T_n(1,a-1) \end{aligned}$$

5. Natural/self cure from Infectious TB:

$$N_i(1,a) - N_i(1,a-1) = nT_i(1,a-1) - r_n N_i(1,a-1)$$

6. Natural/self cure from non-Infectious TB:

$$N_n(1,a) - N_n(1,a-1) = nT_n(1,a-1) - r_n N_n(1,a-1)$$

7. Immunity:

$$M(1,a) - M(1,a-1) = m_+ S(1,a-1) - m_- M(1,a-1)$$

9.7 Detection Calculations in the model

The case detection rate is measured as the ratio:

$$\frac{\text{The proportion of infectious cases diagnosed and treated per year}}{\text{The proportion of incidences of new infectious cases}}$$

A non-DOTS treatment regime is introduced a set number of time steps into the model run. DOTS is then introduced a set number of time steps after that and increases the detection rate linearly until the set DOTS detection rate target is achieved. The times of introductions of these treatments and the detection rate target is input by the user.

The following algorithm describes how the varying detection rates in the model are achieved:

1. **Set initial parameter values:**

   - Let case_det_DOTS $= \alpha$ (Target detection rate under DOTS).
   - Let case_det_nonDOTS $= \beta$ (Detection rate under pre-existing (Non-DOTS) regimes).

- Let *ydot* be the time t at which the introduction of DOTS begins in the country in question.
- Let *DurationDOTS* be the number of years taken to introduce DOTS into the country; i.e. number of years from *ydot* till the DOTS target detection rate (α) is reached.

2. **Calculate the change in detection rate and put into array cdrD(t):**

   For all t:

   (a) If time $t <$ *ydot*, i.e. the present time step t is before the time at which DOTS is introduced into the country, then cdrD(t) = 0. Thus, there is no change in the detection rate from what was the existing detection rate in the country.

   (b) If *ydot* $< t <$ (*ydot* + *DurationDOTS*) i.e. the present time step t falls in the interval when DOTS is being introduced into the country, then $\text{cdrD}(t) = \frac{\alpha \times (t - ydot)}{DurationDOTS}$

   (c) If time $t >$ (*ydot* + *DurationDOTS*), then cdrD(t) = α; i.e. the DOTS target detection rate is assumed to have been achieved in the country.

3. **Re-set detection parameters, det and detND, for inclusion in the model equations, using the cdrD(t) 'change-in-rate' values calculated in 2. above:**

   - det = cdrD(t). This is the change in detection rate.
   - detND = [β - cdrD(t)]. This models DOTS taking over from a pre-existing non-DOTS regime.
   - If detND < 0, then set detND = 0. This circumstance occurs when the DOTS detection rate becomes greater than the pre-existing regime's detection rate.

In the model equations (see section 9.4) the detection rate is calculated as the sum of det and detND. Graph 9.2 shows this interaction between the parameters det = cdrD(t) and detND.

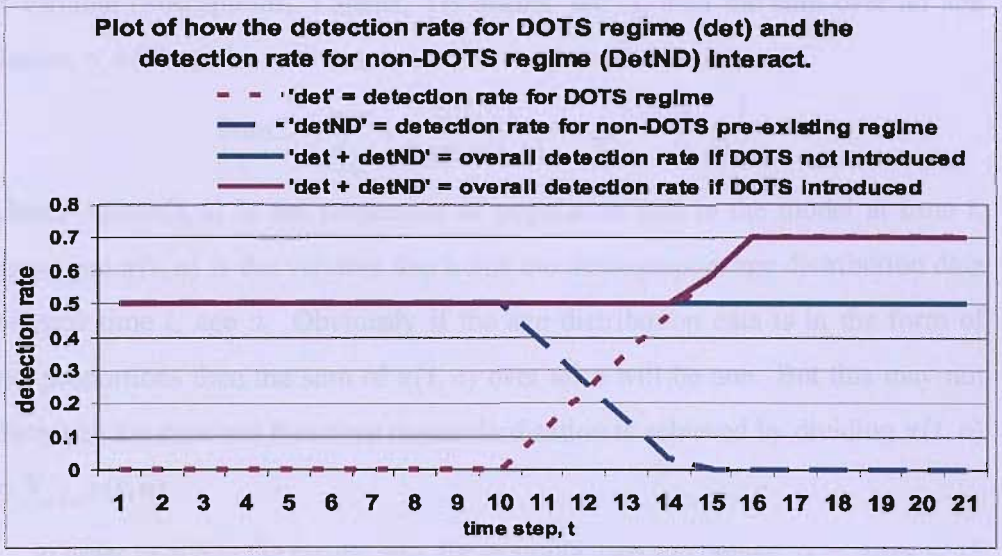

Figure 9.2: Plot of interaction between the DOTS and non-DOTS detection rates, (det = cdrD(t) and detND), with DOTS introduced at time step 10, DOTS detection rate target (α) set at 70% and the time taken to attain α set to 6 years.

9.8 Standardising age dependent results

At the end of a model run, the 'proportion' values for each t and a have been recorded for all required states and variables. However, these recorded 'proportions' may not be true proportions because the total proportion of the model population at time t may be less than one due to loss of people from the model through death. The recorded values therefore must be re-standardised to become true proportions. Then, for each t the standardised proportions belonging to each age class, are multiplied by the proportion of individuals in that particular age class accord-

ing to the age distribution data of an appropriate country. The results can then be summed over age.

For example: Let Ξ be the proportion of population in a specific TB state class or variable (Susceptibles, Latents, TB deaths, etc...), then the sum over all age classes, a, of Ξ can be written as:

$$\text{Sum}\Xi = \sum_{\forall a} \left[\frac{\Xi(t,a)}{\text{Agetot}(t,a)} \times \frac{\pi(t,a)}{\sum_{\forall a} \pi(t,a)} \right]$$

where, $\text{Agetot}(t,a)$ is the proportion of population still in the model at time t, age a, and $\pi(t,a)$ is the variable that holds the demographic age distribution data for each time t, age a. Obviously if the age distribution data is in the form of true proportions then the sum of $\pi(t,a)$ over all a will be one. But this may not always be the case and therefore re-standardisation is achieved by dividing $\pi(t,a)$ by $\sum_{\forall a} \pi(t,a)$.

In order to divide the results into, for example, two age ranges: $\alpha = \text{Ages} \leq 15$ and $\beta = \text{Ages} > 15$, the following calculations would be carried out:

$$\text{Sum}\Xi^{\alpha} = \sum_{a=0}^{15} \left[\frac{\Xi(t,a)}{\text{Agetot}(t,a)} \times \frac{\pi(t,a)}{\sum_{a=0}^{15} \pi(t,a)} \right]$$

$$\text{Sum}\Xi^{\beta} = \sum_{a=16}^{80} \left[\frac{\Xi(t,a)}{\text{Agetot}(t,a)} \times \frac{\pi(t,a)}{\sum_{a=16}^{80} \pi(t,a)} \right]$$

The theoretical basis for the above calculations can be explained in terms of probability:

Let $P(a|t)$ be the Probability of a given t, and $\pi^*(t) = \sum_{\forall a} \pi(t,a)$, then,

$$P(a|t) = \frac{P(a \cap t)}{P(t)} \equiv \frac{\pi(t,a)}{\pi^*(t)}, \text{ for the true population}$$

$$P(\Xi|a,t) = \frac{P(\Xi \cap a|t)}{P(a|t)} \equiv \frac{\Xi(t,a)}{\text{Agetot}(t,a)}, \text{ for the model population}$$

$$\begin{aligned} P(\Xi|t) &= \sum_{\forall a} P(\Xi \cap a|t) \\ &= \sum_{\forall a} P(\Xi|a,t)P(a|t) \\ &= \sum_{\forall a} \left[\frac{\Xi(t,a)}{\text{Agetot}(t,a)} \times \frac{\pi(t,a)}{\pi^*(t)} \right] \end{aligned}$$

Because the model outputs the total number of TB cases or total incidence, etc.. it is necessary to multiply the relevant output values by the respective time dependent detection rates used in the model (det + detND), before comparing the results with recorded/observed TB data.

9.9 Calculating R, The basic case reproduction number

In order to estimate R, the basic equation,

$$R = \frac{\text{number of secondary cases}}{\text{primary cases}}$$

is approximated by,

$$R = \frac{\text{Proportion of Infectious TB cases in first time period}}{\text{Proportion of people with active infectious TB}} \times \frac{1}{\text{Exit Rate}}$$

Figure 9.3 highlights the relevant part of the model flow diagram 9.1 used in calculating R.

Figure 9.3: Flow diagram of states and parameters in the TB model used to estimate the reproductive number.

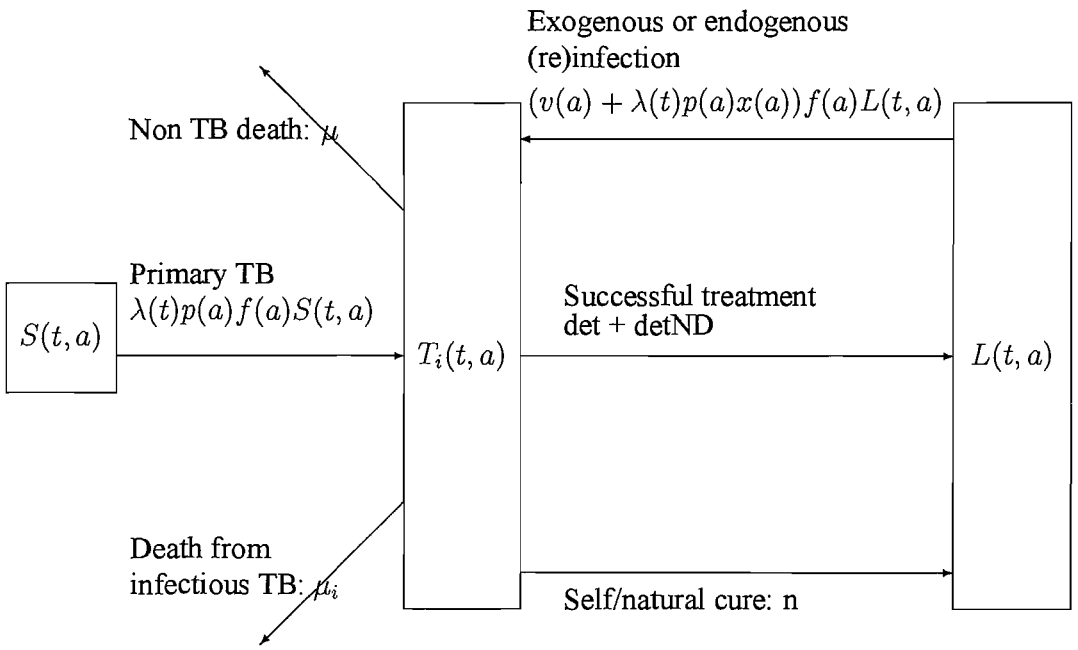

This can be simplified into one combined input to the Infectious TB state and one combined output rate:

$\hat{\theta}$ Infectious TB Incidence $\rightarrow$ Infectious TB $\rightarrow$ Exit Rate

Thus,

$$ExitRate = det + detND + n + \mu_i + \mu$$

and letting R_1 be the incidence of infectious TB,

$$R_1(t,a) = \lambda(t)pfS(t-1,a-1) + (v + \lambda(t)px)fL(t-1,a-1)$$

Standardising R_1 in the normal way and summing over a gives:

$$R_1^*(t) = \sum_a \frac{R_1(t,a) \times \frac{\pi(t,a)}{\pi(t,a)}}{Agetot(t,a)}$$

The proportion of Infectious TB at time t,

$$sumT_i = \sum_a \left[\frac{T_i(t,a)}{Agetot(t,a)} \times \frac{\pi(t,a)}{\sum_a \pi(t,a)} \right]$$

Thus,

$$R(t) = \frac{R_1^*(t)}{sumT_i \times ExitRate}$$

9.10 Calculating TB relapses

The proportion of relapses from Infectious TB, non-infectious TB and self/natural cure is calculated by the equation:

$$\begin{aligned} relapse(t,a) &= r\left(F_i(t-1,a-1) + F_n(t-1,a-1)\right) \\ &\quad + r_n\left(N_i(t-1,a-1) + N_n(t-1,a-1)\right). \end{aligned}$$

This is used to fine tune the estimate of 'new TB cases' when fitting the model output to 'new cases' recorded data.

9.11 Calculating the percentage decrease in TB Incidence

It was decided to include a calculation of the percentage decrease in TB incidence as one of the outputs of the model in order to compare with recent data collected from Morocco. This data indicates that the incidence of TB in very young children

is falling at more than 10% per year. But that TB incidence in the population as a whole is only falling at around 3 to 4%. It is reasonable to assume that children with TB must have been recently infected and it therefore seems reasonable to assume the decline in incidence in young children approximates the decline in transmission of the disease. The slower rate of decline over all ages as opposed to the decline in disease transmission seems indicative of the stagnation effects previously described. Thus, this apparent difference in the two observed rates of decline are of interest to those studying and devising TB control strategies.

Calculating the percentage decrease in TB incidence involves measuring the gradient of the decline in TB. The relationship between the model output of TB incidence per 100,000, per year, and time in years is generally exponential for each age category. Thus taking natural logs of the output produces a fairly linear relationship so that a line of best fit in the standard form of $y = mx + c$ can be fitted to the data. Here y, the response variable, is TB incidence per 100,000 and x, the explanatory variable, is time in years. The line is fitted by the least squares method and can be fitted to however many years of data seem appropriate/or of interest. The percentage decline in TB is therefore taken as the negative of the gradient of the fitted line multiplied by 100. These values are then plotted on a scatter graph.

The average rate of percentage decline is calculated by applying the same method to the average values of TB incidence taken across all age categories for each year.

9.12 Adapting demographic data for input to model

The TB compartmental age-dependent model requires age dependent demographic data as an input. It also needs to be in a specific format, namely proportions of the population in one year age steps. This section contains a description of

the smoothing techniques employed to adapt the given demographic data from Morocco and the Netherlands into the required format.

The smoothing and polynomial fitting methods described in this section are illustrated using the Moroccan age data set for 1980 to 2001.

1. The TB model does not discriminate between the sex of individuals, so the age distribution data, originally split into males and females, is first combined and then transformed into population proportions:

   Let M be the number of males in age category a in year t and let F be the number of females in age category a in year t, then, the proportion of population in age category a in year t is, $\frac{M+F}{\text{Total population in year } t}$.

Age Ranges Years	0-4	5-9	...	65-85	total
1980	0.123665388	0.122006842	...	0.046802115	1
1981	0.123745145	0.121828179	...	0.046864753	1
:			...		
:			...		
2000	0.124224901	0.122413433	...	0.04587891	1
2001	0.124211465	0.122428689	...	0.045872189	1

2. Dividing through by the range of each age category transforms the data into age categories of length 1 year:

Age	1980	Age	
0	0.024733078	:	
1	0.024733078	65	0.002228672
2	0.024733078	66	0.002228672
3	0.024733078	67	0.002228672
4	0.024733078	68	0.002228672
5	0.024401368	:	
6	0.024401368	:	
7	0.024401368	83	0.002228672
8	0.024401368	84	0.002228672
9	0.024401368	85	0.002228672

3. The proportion data is then smoothed by averaging:

   (0, 1, [2,] 3, 4,) 5, 6, 7, 8, 9, 10, 11, 12,....

   0, (1, 2, [3,] 4, 5,) 6, 7, 8, 9, 10, 11, 12,....

   where, ( ) surrounds the values to be averaged and [ ] denotes where the averaged value is to be placed.

   Three different averaging ranges were used, one after another, to take into account the increasing lengths of the original age categories: 1st averaging range = 5; 2nd averaging range = 10; 3rd averaging range = 20.

4. A polynomial is then fitted to the smoothed proportion data:

$$
\begin{aligned}
log(y_k) &= \sum_{j=1}^{11} \left[C_j \prod_{i=1, i\neq j}^{11} (k - x_i) \right] \\
\text{i.e. } log(y_k) &= C_1(k-x_2)(k-x_3)...(k-x_{11}) \\
&\quad + C_2(k-x_1)(k-x_3)...(k-x_{11})... \\
&\quad + C_{11}(k-x_1)(k-x_2)...(k-x_{10})
\end{aligned}
$$

where y_k = proportion data for age k (1 to 86), x_i = selected age values at which the polynomial passes through the respective proportion values, C_j = Coefficient values for each selected (x_i) age value.

The final population values are obtained by exponentiating $log(y_k)$ for each k.

5. Extrapolation: The coefficient values, C_j, can be used to create population data for years prior to 1980 or after 2001. This can be used to warm-up the computer model or project outcome results into the future.

9.13 Fitting the compartmental model to the TB data sets from the Netherlands and Morocco

The following chapters describe the fitting and sensitivity analysis of this compartmental model to the TB data sets from the Netherlands and Morocco, as initially analysed by the parametric regression models in chapters 5, 6 and 8. The UK data set was not used as it only contains TB data from white males and the model is not built to make this distinction between gender and ethnicity.

9.13.1 Parameter Estimation

Starting values for parameter estimates were taken from the various literature available in the area including C.Dye et. al. [14][15].

As the objective was to investigate the sensitivity and behaviour of the model it was necessary to get a reasonable initial fit to each data set. Maximum likelihood methods with the numerical optimisation algorithm Nelder-mead were used to accomplish this. The large number of parameters caused the Nelder-mead algorithm to be very slow and unstable. The parameter estimates were therefore further

adapted by hand in order to produce a fit to the data that could be used as a base line for the sensitivity analysis.

Various functions were experimented with for the different age dependent parameters. The default setting was two age-specific rates for each age dependent parameter with a cut-off age of 15. The specifics of the age dependent functions used when fitting the model to the Dutch and Moroccan data sets are described in detail in chapters 10 and 11 respectively. These two chapters also contain extensive descriptions of the model sensitivity analysis and results for each country.

Chapter 10

Fitting and Sensitivity Analysis of Compartmental TB Model using TB case data from the Netherlands

10.1 Fitting to Dutch TB notification data

The emphasis of this work is on examining the ability of a compartmental model to fit to TB data from countries experiencing an aging of their population and the aging of the TB epidemic. The Netherlands is considered to be such a country. Thus, after producing a reasonable fit to the Dutch data, most of the work in this chapter concentrates on the sensitivity analysis of the model.

The outcome investigated was the number of TB cases per 100,000 of population for each of the 8 age groups, for years, 1952 to 1994. The model estimates the case data by manipulating the TB Incidence values, I(t,a).

A selection of different starting values and age dependent functions were tried for the various model parameters. Initial fitting was carried out using a Nelder-mead optimisation algorithm to minimise the least squares error in the fit to the

data. The Nelder-mead method becomes extremely slow when attempting to optimize a 'large' number of parameters at once. Because of the large number of potentially important parameters in the model this fitting technique was only feasible to be carried out on a few of the parameters at a time. Even so, the Nelder-mead program still showed signs of instability implying a large degree of irregularity and complexity in the interactions of the parameters and resulting output of the model. The resulting parameter values from these fittings were therefore entered into the model and further fitting to the data carried out by hand.

Tables 10.1 and 10.2 contain the input parameter values that produced the fits used as the base values for subsequent sensitivity analysis. The immunity and natural/self cure variables and associated parameters were set to zero due to their insignificant effect on the model results and in order to simplify the model for analysis. Parameter 'v', rate at which latent infections become TB cases by endogenous re-activation, was calculated in the model using the age dependent function $v = v_1 e^{2\frac{ln(2)}{40}(a-30)}$, where v_1 is the initial value of the parameter shown in Table 10.1 for ages ≥ 15 and $a =$ age step. The main feature for this parameter that the selected function had to capture, was a very slow increase in ages 15 to approx 60 followed by a sharp increase in value. This mirrors the current biological understanding of the disease, that as a person ages the immune system is less likely to be able to keep latent infection at bay and thus re-activation disease is more likely to occur in the elderly than in younger healthier individuals. Figure 10.1 shows how the selected exponential function for parameter 'v' captures this age dependent trend.

It should be noted in this case that the DOTS variables and mechanisms built into the model are used to represent a **general increase** in case finding and cure rate, and **not to represent the actual DOTS regime** as put forth by the WHO.

	Fitting to Dutch TB notification data	
Parameter	Description	Initial Value
$\lambda(1)$	Force of infection	0.18
x(age$\leq$15)	Proportion of re-infections which is susceptible	0.15
x(age>15)	to developing TB within one year	0.15
p(age$\leq$15)	Proportion of infected susceptibles which	0.0371
p(age>15)	develop progressive primary TB within a year	0.1785
v(age$\leq$15)	rate at which latent infections become TB cases	1.0E-07
v(age>15)	by endogenous re-activation	2.857E-06
f(age$\leq$15)	Proportion of progressive primary cases	0.0992
f(age>15)	which become infectious	0.4439
μ_i	Death rate for infectious TB	0.3126
μ_n	Death rate for non-infectious TB	0.2307
r	Rate of relapse from failed treatment to active TB	0.3
w	Rate of smear conversion from non-infectious to infectious TB	0.0181
θ	exponential rate of decline in contact rate between TB cases and others	0.035
ϵ	Relative case detection rate of non-infectious cases	0.5
ϕ	Proportion of failed treatment cases which is infectious	0.5746

Table 10.1: Parameter values obtained by fitting TB model outputs to Dutch TB notification data.

	Fitting to Dutch TB notification data *continued*	
Parameter	Description	Initial Value
det	Rate at which TB cases are found and treated under DOTS	0.8
cure	Proportion of treated cases given curative chemotherapy under DOTS	0.9
detNotDot	Rate at which TB cases are found and treated under a previous non-DOTS regime	0.7
cureNotDot	Proportion of treated cases given curative therapy under a previous non-DOTS regime	0.75
start date of model		1952
Time step (in part of years)		0.5
finish date of model		1994
Date at which DOTS interventions begin		1965
Duration of introductory period of DOTS (in years)		10
Date at which Non-Dots interventions begin		1952
model age limit (in years)		100
model age cut off for age dependent parameters (in years)		15

Table 10.2: Parameter values obtained by fitting TB model outputs to Dutch TB notification data (*continued*).

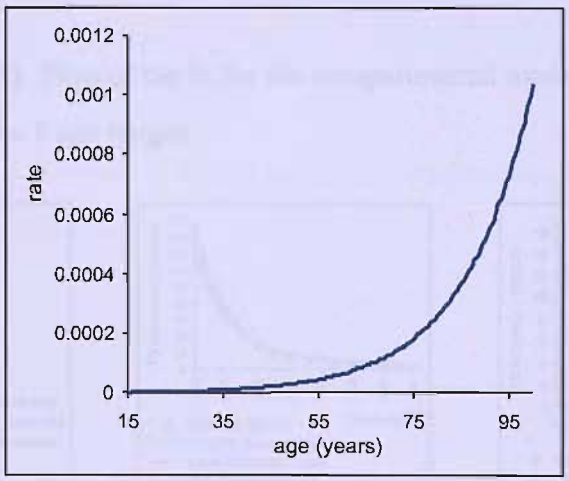

Figure 10.1: Plot of the function used for the model parameter $v = v_1 e^{2\frac{ln(2)}{40}(a-30)}$, rate at which latent infections become TB cases by endogenous re-activation; where v_1 is the initial value of the parameter for ages ≥ 15 and a = age step

The fits to the data that the above described parameter values and parameter function produce are shown in graphs 10.2 to 10.4. It is noticeable that the model was unable to fit to the initial years data (1952) for the adult age ranges, although many different warm-up scenarios were tried. It is also obvious the shape of the line fit does not vary across the 8 age ranges, hence although the fit looks good for the first three age ranges it soon fails to capture the 'flattening' of the curve in the data in the five older age groups.

Thus despite the complexity of the compartmental model it seems unable to fully capture the age dependent effects in the TB data. Thus the following sections describe the further investigation into the model's ability to fit to the time and age characteristics in the Dutch TB data.

Figure 10.2: (a)-(h): Plots of the fit for the compartmental model to the Dutch TB data, for each of the 8 age ranges.

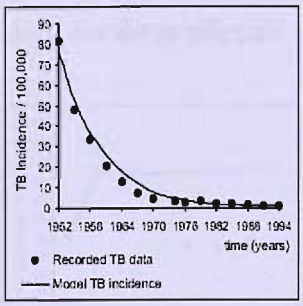

(a) Ages 0 to 14 years.

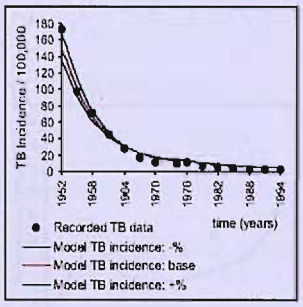

(b) Ages 15 to 24 years.

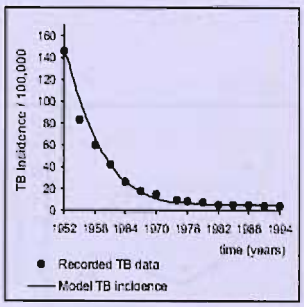

(c) Ages 25 to 34 years.

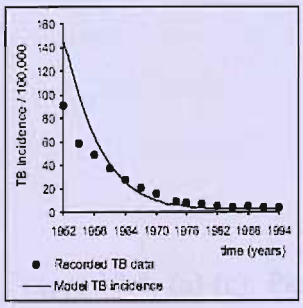

(d) Ages 35 to 44 years.

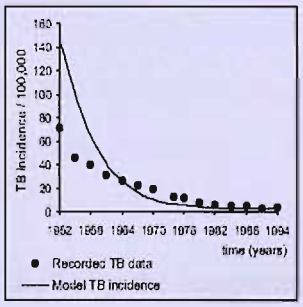

(e) Ages 45 to 54 years.

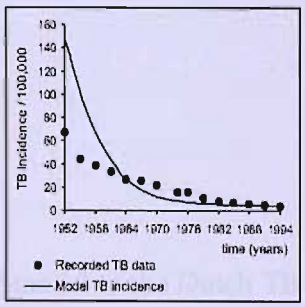

(f) Ages 55 to 64 years.

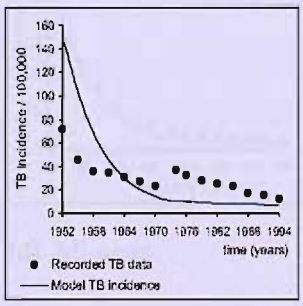

(g) Ages 65 to 69 years.

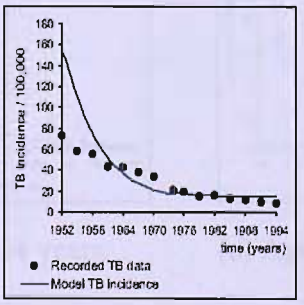

(h) Ages 70+ years.

Figure 10.3: (a)-(c): Plots of the fit for the compartmental model to the Dutch TB data, for three selected years.

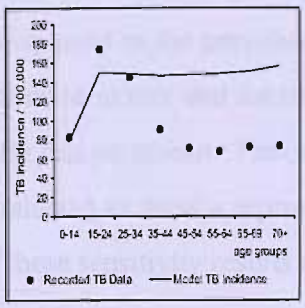

(a) 1952.

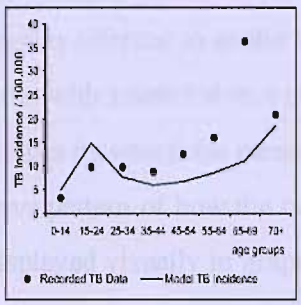

(b) 1974.

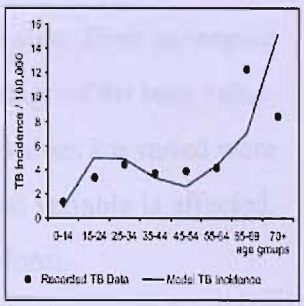

(c) 1994.

Figure 10.4: (a)-(c): Plots of the fit for the compartmental model to the Dutch TB data, over the years 1952 to 1994.

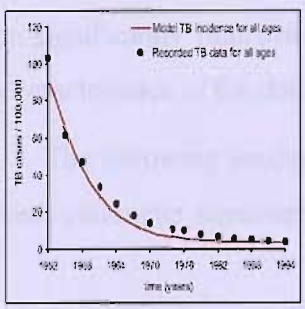

(a) All ages.

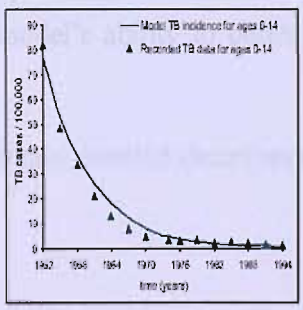

(b) Ages 0-14 years.

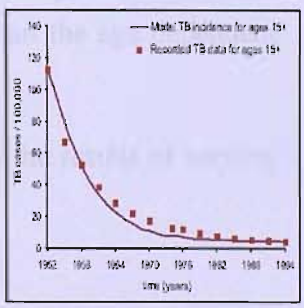

(c) Ages 15+ years.

10.2 Sensitivity analysis using Dutch TB notification data

The aim is to explore how varying the values of each input parameter affects the outcome variable. The value of each parameter used to produce a fit to the data as displayed in the previous section is referred to as the base value. Each parameter is taken in turn and the model run with a new value, a percentage of the base value, for that parameter. The percentages by which the parameter values are varied were selected to show a representative pattern of how the outcome variable is affected. These sensitivity results are displayed visually in graphical form.

The parameters were found to behave in an expected logical manner, explainable by the epidemiology of TB, apart from three notable exceptions. Varying p(for ages 15+) - the proportion of infectious susceptibles which develop progressive primary TB in 1 year, x(for ages 15+) - the proportion of re-infections which is susceptible to developing TB within 1 year, and r - the rate of relapse from failed treatment to active TB, affected the outcome in counter intuitive ways that were not easily explained by studying the model mechanisms.

Some parameters were found to be more sensitive than others and most showed a distinctly non-linear behaviour. Varying these parameters one at a time failed to significantly improve the model's ability to better explain the age dependent characteristics of the data.

The following sections contain detailed descriptions of the results of varying each parameter separately.

10.2.1 Varying parameter value $\lambda(1)$, "Initial Force of Infection".

The parameter $\lambda(1)$ is varied by 20% and 50% of its base value (see table 10.3) to explore the effect of increasing the starting value of the force of infection.

Table 10.3: Values of the parameter $\lambda(1)$, selected as input to the model

	50% of bv	80% of bv	bv	120% of bv	150% of bv
$\lambda(1)$	0.09	0.144	0.18	0.216	0.27
bv = base value					

In the first few years of the model run a 50% and 20% change in the starting value of λ produces a similar change in the outcome value (see figure 10.5(a)). At half way through the model run (1974) a nonlinear effect can be seen (see figure 10.5(b)). In general an increase and decrease in $\lambda(1)$ can be seen to increase and decrease TB incidence respectively. This effect reduces with time (figures 10.6 (a) to (c)). This behaviour seems logical; a higher initial force of infection would be expected to produce a higher TB incidence at least in the first few years until the other mechanisms (e.g. detection and cure rates) begin to have an effect. It is however interesting to note that by the middle of the time period TB incidence is virtually the same regardless of the initial force of infection value.

Figure 10.5: (a)-(b): Plots of the fit for the compartmental model to the Dutch TB data, for initial year 1952 and middle of time period 1974.

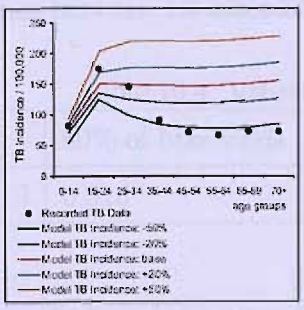

(a) 1952.

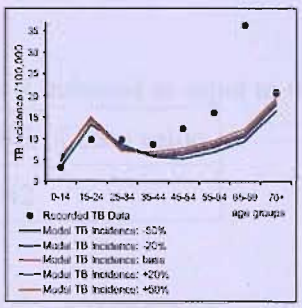

(b) 1974.

Figure 10.6: (a)-(c): Plots of the fit for the compartmental model to the Dutch TB data, over the years 1952 to 1994.

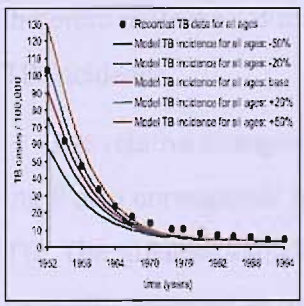

(a) All ages.

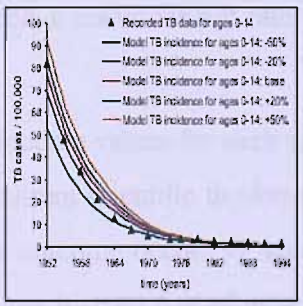

(b) Ages 0-14 years.

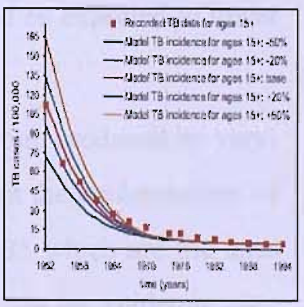

(c) Ages 15+ years.

10.2.2 Varying parameter value θ, "the exponential rate of decline in the contact rate between TB cases and others".

The parameter θ is varied by plus and minus 20% of its base value (see table 10.4) to investigate the effect of varying the exponential rate of decline in the contact rate between TB cases and others.

Table 10.4: Values of the parameter θ, selected as input to the model

	80% of base value	base value	120% of base value
θ	0.028	0.035	0.042

As there is no warm up, the θ value at time 0 (1952) has very little initial effect on the outcome variable (figure 10.7(a)). The nonlinear effect of θ increases with time as can be seen in figures 10.7 (b) and (c).

There is a larger effect for ages 15-34, which are the ages generally accepted as having a higher risk of contracting primary TB (figure 10.7 (c)). Lower values of θ and hence a slower exponential rate of decline in contact rate produce greater TB incidence. Higher values of θ and hence a greater exponential rate of decline in contact rate produce smaller values of TB incidence. These results seem logical; a higher contact rate would be expected to increase transmission of disease and therefore increase TB incidence; a lower contact rate would be expected to lower TB incidence.

The relative changes in outcome values for each age group produced by varying θ also corresponds with current scientific thinking about the epidemiology of TB. The greatest variation in outcome occurs in ages 15-35 which are the ages generally accepted as having the highest risk of infection. As the epidemic ages the TB incidence in the older age groups is thought to be predominantly fuelled by re-activation disease which would not be overly affected by contact rate.

Figure 10.7: (a)-(c): Plots of the fit for the compartmental model to the Dutch TB data, for three selected years.

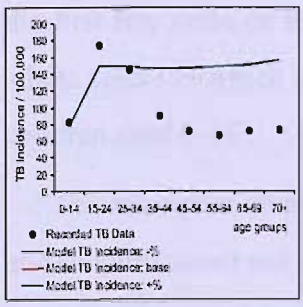

(a) 1952.

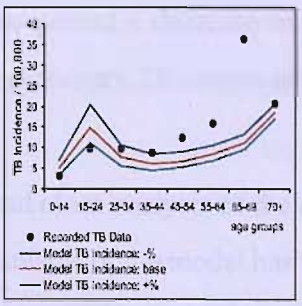

(b) 1974.

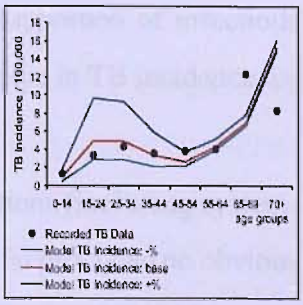

(c) 1994.

10.2.3 Varying parameter value p (for ages 15+), "the proportion of infected susceptibles which develop progressive primary TB in one year".

The parameter p (for ages 15+) is varied by 20% and 80% of its base value (see table 10.5), to investigate the effect of increasing the proportion of infected adult susceptibles which develop progressive primary TB in one year.

Table 10.5: Values of the parameter p(ages 15+), selected as input to the model

	20% of bv	80% of bv	bv	120% of bv	180% of bv
p(ages 15+)	0.036	0.143	0.179	0.214	0.321
bv = base value					

For time 0 (1952) the variation in parameter p (for ages 15+) is reflected in a linear way in the outcome values; a larger value of p produces greater TB incidence and a smaller value of p produces less TB incidence (see figure 10.8 (a)) This pattern is carried on through the time period in all ages 15 and greater, although the variation in outcome reduces with time and becomes negligible.

These results seem logical; if a higher proportion of infectious susceptibles develop progressive primary TB then it would be expected that the incidence of TB would increase. However, this trend is reversed for children aged 0-14. After the first few years of the time period a decrease in the proportion of infectious adults aged 15+ which develop primary TB causes an increase in TB incidence for children aged 0-14.

This is counter intuitive and close analysis of the equations (including systematic simplification) and mechanisms of the model has thus far produced no obvious reasons as to why this effect occurs. This would need further investigation.

Figure 10.8: (a)-(c): Plots of the fit for the compartmental model to the Dutch TB data, for three selected years.

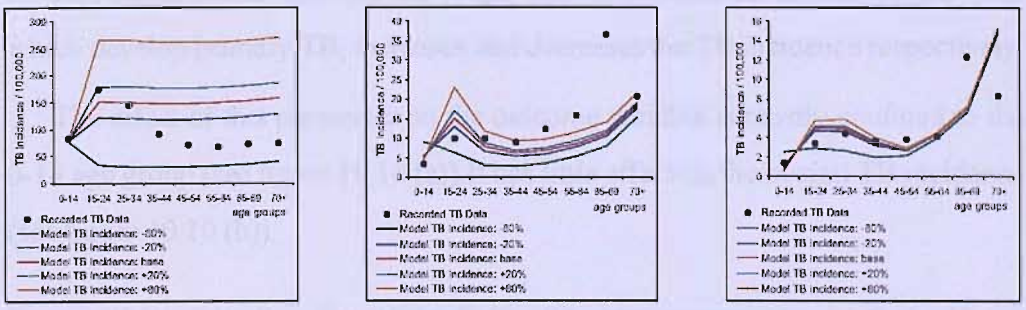

(a) 1952. (b) 1974. (c) 1994.

Figure 10.9: (a)-(c): Fits of the compartmental model to the Dutch TB data.

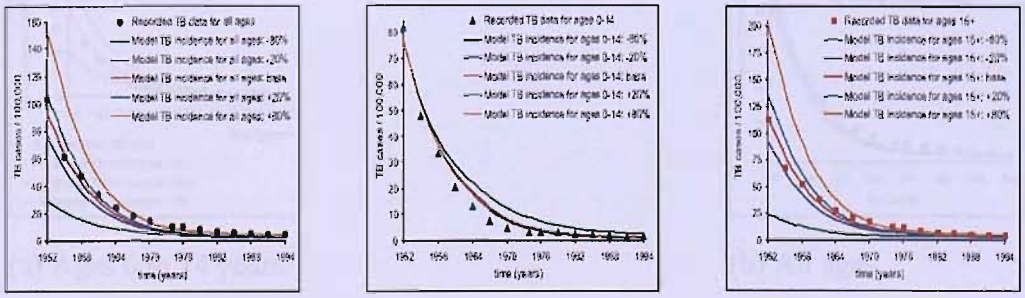

(a) All ages. (c) Ages 0-14 years. (c) Ages 15+ years.

10.2.4 Varying parameter value p (for ages 0-14), "the proportion of infected susceptibles which develop progressive primary TB in one year".

The parameter p (for ages 0-14) is varied by plus and minus 50% of its base value (see table 10.6) to investigate the effect of increasing the proportion of infected susceptibles, aged 0-14, which develop progressive primary TB in one year.

Table 10.6: Values of the parameter p(ages 0-14), selected as input to the model

	50% of base value	base value	150% of base value
p(ages 0-14)	0.0186	0.0371	0.0557

Increasing and decreasing the proportion of infected susceptibles aged 0-14 which develop primary TB, increases and decreases the TB incidence respectively.

The effect of this parameter on the outcome variable is mostly confined to the 0-14 age group (see figure 10.10 (a)).It has little effect on the overall TB incidence (see figure 10.10 (b)).

Figure 10.10: (a) - (b): Plot of the fit for the compartmental model to the Dutch TB data, over the years 1952 to 1994.

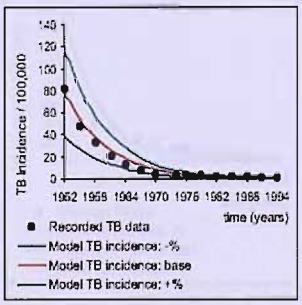

(a) Ages 0 to 14 years.

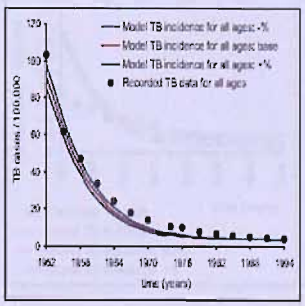

(b) All ages.

10.2.5 Varying parameter value v (ages 15+), "the rate at which latent infections become TB cases by endogenous reactivation".

The parameter v (for ages 15+) is varied by plus and minus 50% of its base value (see table 10.7) to investigate the effect of increasing the rate at which latent infections in those aged over 15 become TB cases by endogenous reactivation.

Table 10.7: Values of the parameter v(ages 15+), selected as input to the model

	50% of base value	base value	150% of base value
v(ages 15+)	1.43E-06	2.86E-06	4.3E-06

Increasing the value of v (for ages 15+) in conjunction with the exponential function for the parameter (as described at the beginning of this chapter) increases TB incidence, especially in the older age groups (see figures 10.11 (a) to (c)). This is in line with current epidemiological views of how re-activation disease occurs in an aging population.

Figure 10.11: (a)-(c): Plots of the fit for the compartmental model to the Dutch TB data, for the last 3 age ranges.

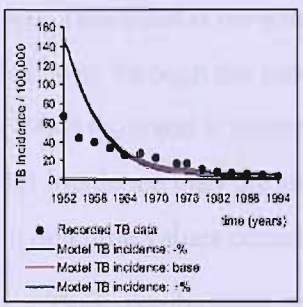

(a) Ages 55 to 64 years.

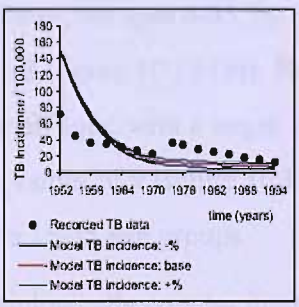

(b) Ages 65 to 69 years.

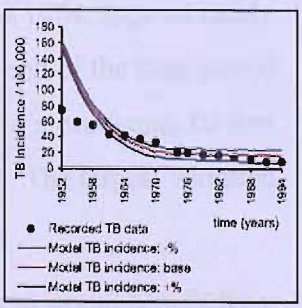

(c) Ages 70+ years.

10.2.6 Varying parameter value x (for ages 15+), "Proportion of re-infections which is susceptible to developing TB within one year".

The parameter x (for ages 15+) is varied by 20% and 70% of its base value (see table 10.8) in order to explore the effect of increasing the proportion of re-infections which are susceptible to developing TB within one year.

Table 10.8: Values of the parameter x(ages 15+), selected as input to the model

	30% of bv	80% of bv	bv	120% of bv	170% of bv
x(ages 15+)	0.045	0.12	0.15	0.18	0.255
bv = base value					

A large decrease in the value of x (for ages 15+) has a large and unexpected effect on the outcome variable, TB incidence, especially in the ages 0-45 (see figures 10.12 (a) to (d)). This effect can also be seen in figures 10.13 (a) to (c), showing the trend in TB incidence for certain years, over all 8 age groups.

At time 0 (1952), a 20% or 70% change in the value of x(ages 15+) produces a relative change in the outcome variable; with a larger value of x producing higher TB incidence and a small value of x producing lower TB incidence (figure 10.13 (a)). This trend is reversed however, for ages 0-35, by around 1974, approximately half way through the time period (figure 10.13 (b)). By the end of the time period (1994) the trend is reversed for all ages, with a larger value of x producing far less TB incidence than the smaller values of x (figure 10.13 (c)). The largest variation in outcome values occurs in the 15-35 age groups.

These results seem epidemiologically counter intuitive and would benefit from further investigation (which has not been carried out to date).

Figure 10.12: (a)-(h): Plots of the fit for the compartmental model to the Dutch TB data, for each of the 8 age ranges.

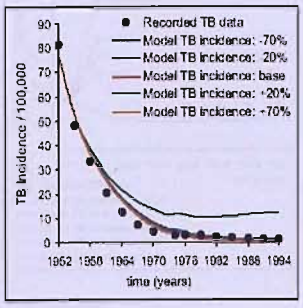

(a) Ages 0 to 14 years.

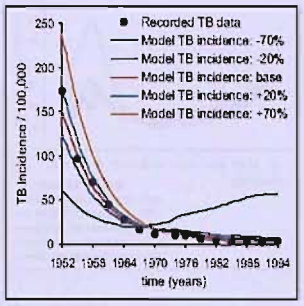

(b) Ages 15 to 24 years.

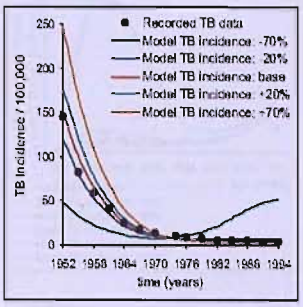

(c) Ages 25 to 34 years.

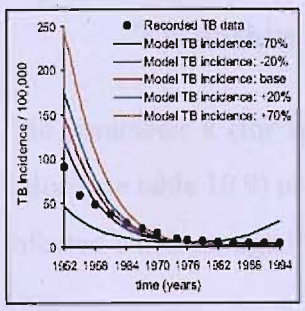

(d) Ages 35 to 44 years.

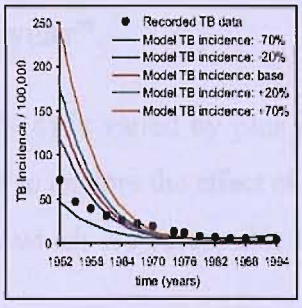

(e) Ages 45 to 54 years.

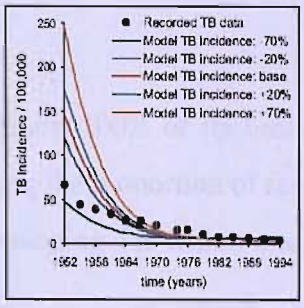

(f) Ages 55 to 64 years.

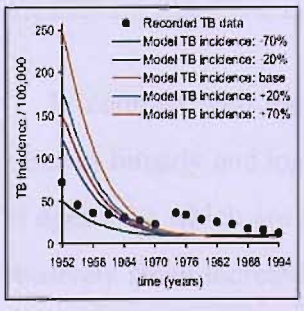

(g) Ages 65 to 69 years.

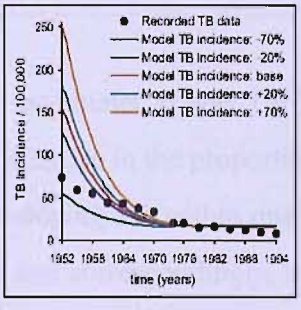

(h) Ages 70+ years.

Figure 10.13: (a)-(c): Plots of the fit for the compartmental model to the Dutch TB data, for three selected years.

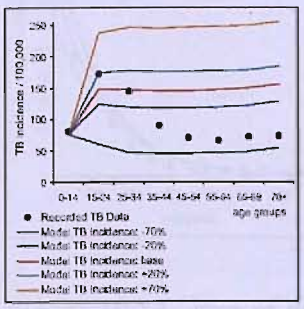

(a) 1952.

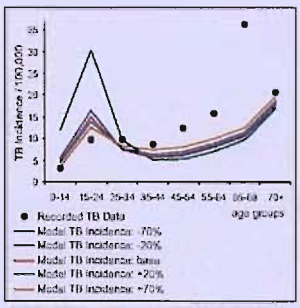

(b) 1974.

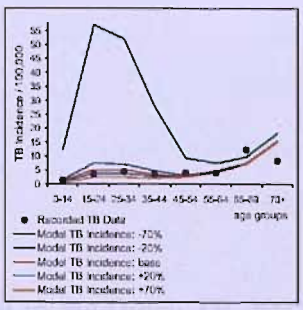

(c) 1994.

10.2.7 Varying parameter value x (for ages 0-14), "the proportion of re-infections which is susceptible to developing TB within one year".

The parameter x (for ages 0-14) is varied by plus and minus 100% of its base value (see table 10.9) in order to explore the effect of varying the proportion of re-infected children, aged 0-14, which are susceptible to developing TB within one year.

Table 10.9: Values of the parameter x(ages 0-14), selected as input to the model

	0% of base value	base value	200% of base value
x(ages 0-14)	0	0.15	0.3

In contrast with the previous related parameter x(ages 15+), this parameter behaves linearly and logically. An 100% increase in the proportion of reinfections in ages 0-14 which are susceptible to developing TB within one year, produces a relatively small increase in TB incidence and correspondingly, an 100% decrease in x(ages 0-14) produces a relatively small fall in TB incidence. This effect is only noticeable in the first half of the time period for children aged 0-14 (see figure

10.14).

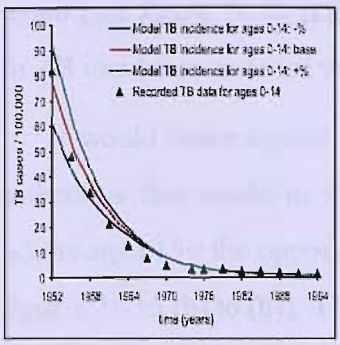

Figure 10.14: Plot of the fit for the compartmental model to the Dutch TB data, for ages 0-14.

10.2.8 Varying parameter value F (for ages 15+), "the proportion of progressive primary cases which become infectious within one year".

The parameter F (for ages 15+) is varied by plus and minus 100% of its base value (see table 10.10) to explore the effect of varying the proportion of progressive primary cases in those aged 15+ which become infectious within one year.

Table 10.10: Values of the parameter F(ages 15+), selected as input to the model

	0% of base value	base value	200% of base value
F(ages 15+)	0	0.444	0.888

Initially at time 0 (1952) an increase in F(ages 15+), the proportion of progressive primary cases in ages 15+ which become infectious within one year, causes a corresponding increase in the amount of TB incidence. Likewise, a decrease in F(ages 15+) produces a corresponding decrease in TB incidence (figure 10.16 (a)). This trend is reversed by 1974 for all ages except the very elderly (see figure 10.16

(b)) However, by the end of the time period (1994) this trend has reverted back again (see figure 10.16 (c)) so that an increase in F(ages 15+) causes an increase in TB incidence and visa versa.

It would make logical sense that if more progressive primary cases become infectious this would in turn cause an increase in TB incidence. However for adults aged 15+ the opposite occurs in the middle years (approx 1964-1980) (see figures 10.15 (b) to (h)). This phenomenon is repeated for children aged 0-15 over almost the entire time period (figure 10.15 (a)).

A possible reason for these illogical effects is that by varying the base value by 100% the resulting parameter values are well outside most ranges of values considered biologically reasonable for this parameter. For example, Styblo [48], Murray et al [18] and Dye et al [14, 15] quote a range for the parameter values of approx 0.5 to 0.65. It is therefore plausible that the values used in this sensitivity analysis are unreasonably small or large. Varying the value by less than 80% causes no visible variation in the outcome variable and can therefore be considered as not having a significant effect on the outcome.

Figure 10.15: (a)-(h): Plots of the fit for the compartmental model to the Dutch TB data, for each of the 8 age ranges.

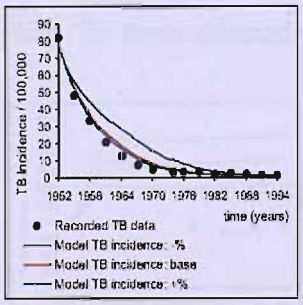

(a) Ages 0 to 14 years.

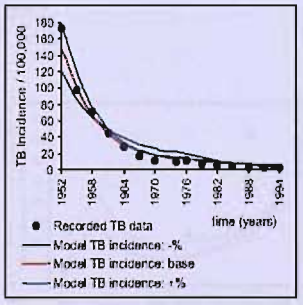

(b) Ages 15 to 24 years.

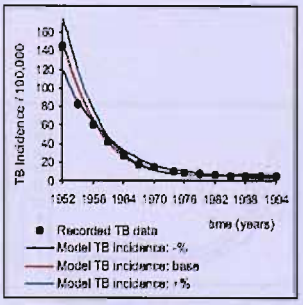

(c) Ages 25 to 34 years.

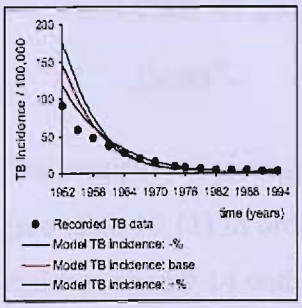

(d) Ages 35 to 44 years.

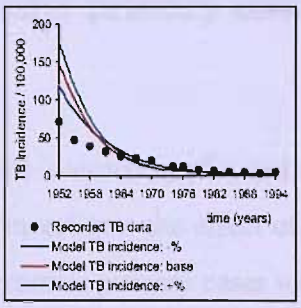

(e) Ages 45 to 54 years.

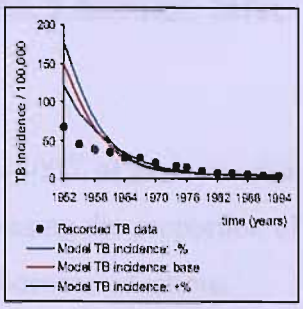

(f) Ages 55 to 64 years.

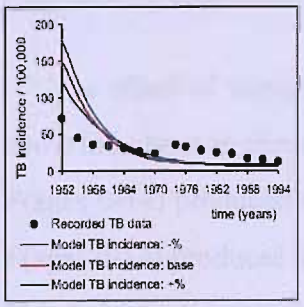

(g) Ages 65 to 69 years.

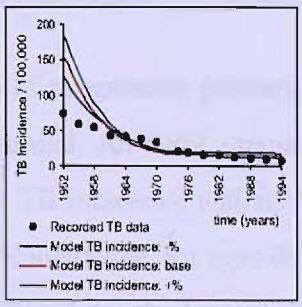

(h) Ages 70+ years.

Figure 10.16: (a)-(c): Plots of the fit for the compartmental model to the Dutch TB data, for three selected years.

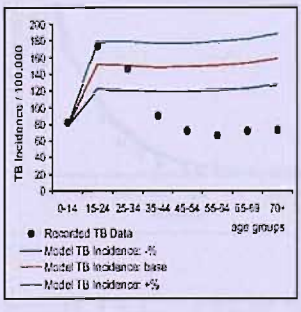

(a) 1952.

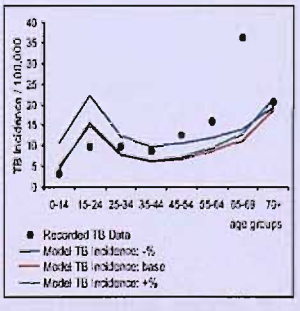

(b) 1974.

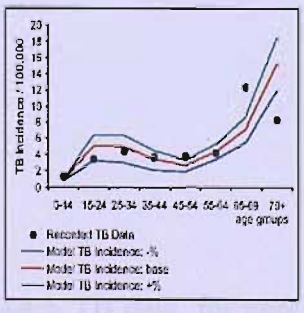

(c) 1994.

10.2.9 Varying parameter value F (for ages 0-14), "the proportion of progressive primary cases which become infectious".

The parameter F (for ages 0-14) is varied by plus and minus 100% of the base value (see table 10.11) in order to investigate the effect of increasing the proportion of children aged 0-14 with progressive primary cases which become infectious.

Table 10.11: Values of the parameter F(ages 0-14), selected as input to the model

	0% of base value	base value	200% of base value
F(ages 0-14)	0	0.099	0.198

The effect of varying the proportion of progressive primary cases which become infectious in those aged 0-14 is minimal. An 100% increase in the value of F(ages 0-14) produced a tiny increase in TB incidence and an 100% decrease in F(ages 0-14) produced a minute fall in TB incidence, for ages 0-14 (figure 10.17). This behaviour is as would be expected, in that a higher proportion of primary cases becoming infectious would be expected to cause an increase in TB incidence. Varying this variable has no visible effect on the outcome variable for those aged 15 and over.

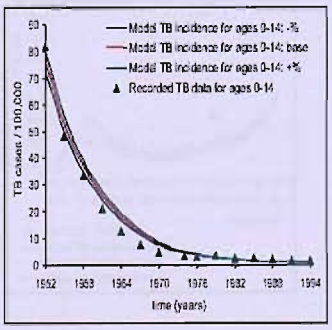

Figure 10.17: Fits of the compartmental model to the Dutch TB data, for ages 0-14.

10.2.10 Varying parameter value ϕ, "the proportion of failed treatment cases which is infectious".

The parameter ϕ is varied by plus and minus 74% of the base value (see table 10.12) in order to explore the effect of varying the proportion of failed treatment cases which is infectious.

Table 10.12: Values of the parameter ϕ, selected as input to the model

	26% of base value	base value	174% of base value
ϕ	0.1494	0.5746	0.9998
The particular value of 74% was chosen to increase the base value to approximately 1, the maximum value			

Increasing and decreasing the proportion of failed treatment cases that become infectious produced a very small corresponding increase and decrease in TB incidence. The change in outcome values were slightly larger during the middle of the time period (see figure 10.18 (a) and (b)).

Figure 10.18: (a)-(b): Plots of the fit for the compartmental model to the Dutch TB data, for selected years.

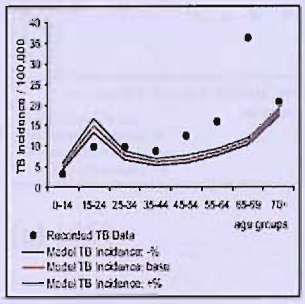

(a) 1974.

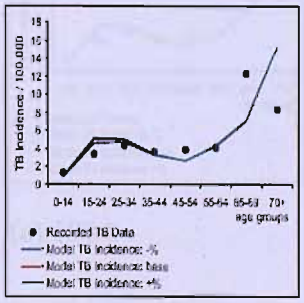

(b) 1994.

10.2.11 Varying parameter value w, "the rate of smear conversion from non-infectious to infectious TB".

The parameter w is varied by plus and minus 100% of its base value (see table 10.13) in order to examine the effect of varying the rate of smear conversion from non-infectious to infectious TB.

Table 10.13: Values of the parameter w, selected as input to the model

	0% of base value	base value	200% of base value
w	0	0.0181	0.0362

Increasing and decreasing the rate of smear conversion from non-infectious to infectious TB by 100%, produced a very small corresponding and logical increase and decrease in TB incidence. The change in outcome values is slightly larger during the first half of the time period (see figures 10.19 (a) to (c)).

Figure 10.19: (a)-(c): Plots of the fit for the compartmental model to the Dutch TB data, for three selected years.

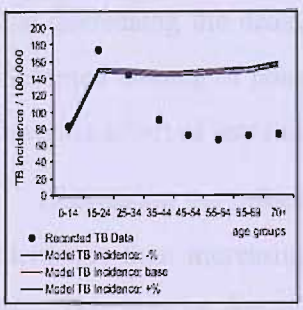

(a) 1952.

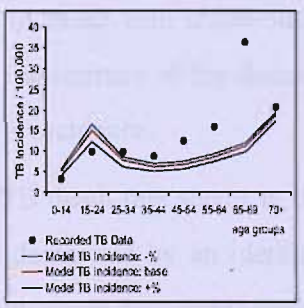

(b) 1974.

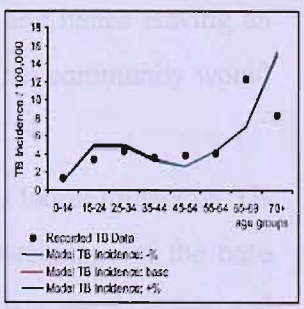

(c) 1994.

10.2.12 Varying parameter value μ_i, "the death rate for infectious TB".

The parameter μ_i is varied by plus and minus 50% of its base value (see table 10.14) to examine the effect of increasing the death rate from infectious TB.

Table 10.14: Values of the parameter μ_i, selected as input to the model

	50% of base value	base value	150% of base value
μ_i	0.156	0.313	0.469

An increase in the death rate from infectious TB, causes a decrease in TB incidence. Likewise, a decrease in the infectious TB death rate increases the incidence of TB (figures 10.21 (a) and (b)). The variation in outcome values are most pronounced in the middle of the time period (see figures 10.20 (a) and (b)).

It makes sense that increasing the death rate of those with infectious TB and hence eliminating an increased amount of potential transmitters of the disease would have the effect of decreasing TB incidence. It therefore also makes sense that decreasing the death rate of those with infectious TB and hence leaving an increased amount of potential transmitters of the disease in the community would have the effect of increasing TB incidence.

Decreasing the infectious TB death rate seems to have a larger impact on TB incidence than increasing the death rate by an identical percentage of the base rate. This may be due to an interaction with parameters such as the detection and cure rates. Decreasing μ_i leads to increased transmission but none of the other parameters that could counter act this effect and lessen TB incidence are increased in value. They are left at their base values which coped with consequences of the base value of TB death rate but not the increased rate.

Figure 10.20: (a)-(b): Plots of the fit for the compartmental model to the Dutch TB data, for years 1974 and 1994.

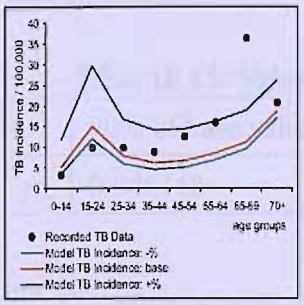

(a) 1974.

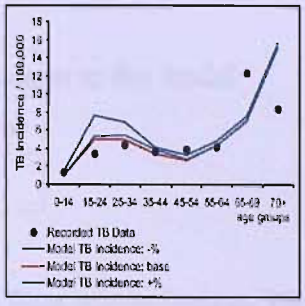

(b) 1994.

Figure 10.21: (a)-(b): Plots of the fit for the compartmental model to the Dutch TB data, over the years 1952 to 1994.

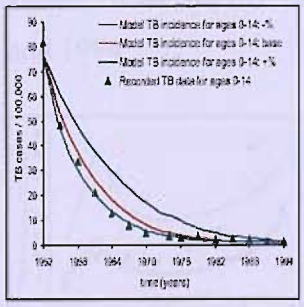

(a) Ages 0-14 years.

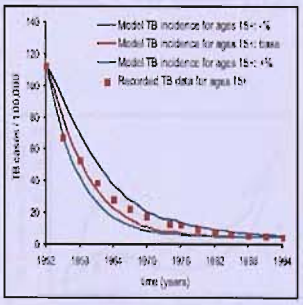

(b) Ages 15+ years.

10.2.13 Varying parameter value μ_n, "the death rate for non-infectious TB".

The parameter μ_n is varied by plus and minus 80% of its base value (see table 10.15) in order to investigate the effect of increasing the death rate from non-infectious TB.

Table 10.15: Values of the parameter μ_n, selected as input to the model

	20% of base value	base value	180% of base value
μ_n	0.046148	0.23074	0.415332

The effect of increasing and decreasing the death rate from non-infectious TB is almost identical to the effect of varying the death rate from infectious TB.

An increase in μ_n causes a decrease in TB incidence and a decrease in μ_n causes an increase in TB incidence (see figures 10.22 and 10.23). This seems to be a logical result as an increase in the death rate of those with non infectious TB would generally decrease the prevalence of non infectious TB in the population and would also therefore decrease the number of non-infectious cases becoming infectious by smear conversion.

Figure 10.22: (a)-(b): Fits of the compartmental model to the Dutch TB data, 1974 and 1994.

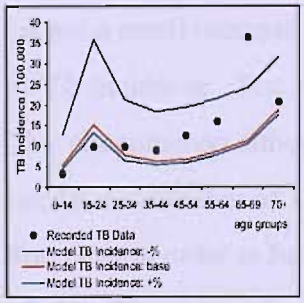

(a) 1974.

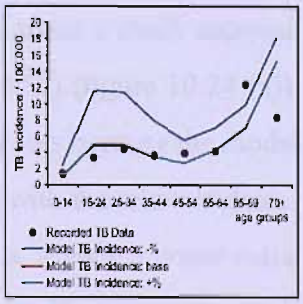

(b) 1994.

Figure 10.23: (a)-(b): Plots of the fit for the compartmental model to the Dutch TB data, over the years 1952 to 1994.

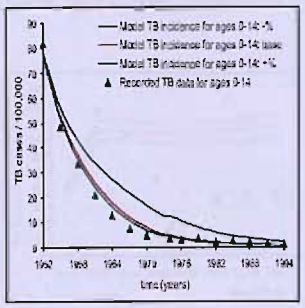

(a) Ages 0-14 years.

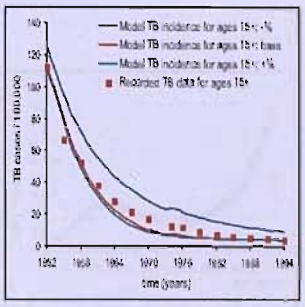

(b) Ages 15+ years.

10.2.14 Varying parameter value ϵ, "the relative case detection rate of non-infectious cases".

The parameter ϵ is varied by plus and minus 100% of its base value (see table 10.16) to investigate the effect of increasing the relative case detection rate of non-infectious cases

Table 10.16: Values of the parameter ϵ, selected as input to the model

	0% of base value	base value	200% of base value
ϵ	0	0.5	1

An 100% increase in ϵ, the relative case detection rate of non-infectious cases, causes a small increase in TB incidence. A decrease in ϵ causes a small decrease in TB incidence. The effect is most notable at time 0 (1952) (figure 10.24 (a)). This phenomenon although seeming to go against logic, occurs because the model results, i.e. number of TB cases, are multiplied by ϵ along with the relevant detection rates in order to be comparable with the observed data. Hence a larger value of ϵ would increase the value of the outcome variable. This effect is most noticeable at time 0 (1952) because there is no warm-up and therefore no time for other

factors/parameters to start reducing TB incidence.

Figure 10.24: (a)-(c): Plots of the fit for the compartmental model to the Dutch TB data, for three selected years.

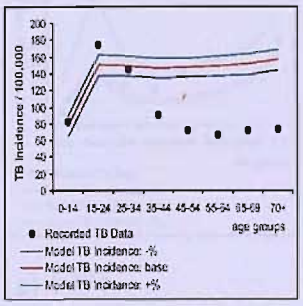

(a) 1952.

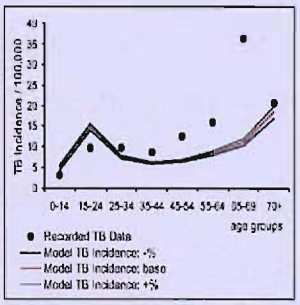

(b) 1974.

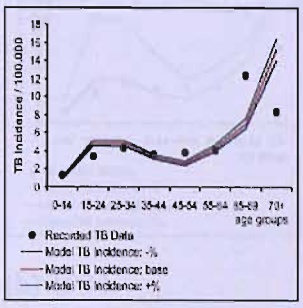

(c) 1994.

10.2.15 Varying parameter value r, "the rate of relapse from failed treatment to active TB".

The parameter r is varied by plus and minus 80% of its base value (see table 10.17) to examine the effect of increasing the rate of relapse from failed treatment to active TB.

Table 10.17: Values of the parameter r, selected as input to the model

	20% of base value	base value	180% of base value
r	0.06	0.3	0.54

A decrease in r, the rate of relapse from failed treatment to active TB, causes an increase in TB incidence. Likewise, an increase in r causes a very slight decrease in TB incidence (see figures 10.25 (a) and (b)).

This appears counter intuitive and would, like the previous parameters p(15+) and x(15+), benefit from further investigation.

Figure 10.25: (a)-(b): Plots of the fit for the compartmental model to the Dutch TB data, for selected years.

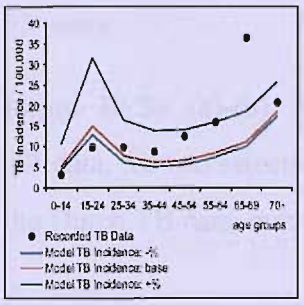

(a) 1974.

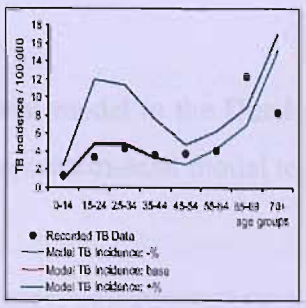

(b) 1994.

10.2.16 Varying parameter value 'det', "the rate at which TB cases are found and treated under a second improved control regime".

The parameter 'det' is varied by plus and minus 25% of its base value (see table 10.18) to investigate the effect of varying the rate at which TB cases are found and treated under a second improved control regime.

Table 10.18: Selected values of Parameter 'det', used as input to the model.

	75% of base value	base value	125% of base value
'det'	0.6	0.8	1

This new improved control regime is brought in around 1974. Increasing the detection rate initially has the effect of increasing TB incidence. This is because more (or in this case all TB cases) are being found and identified (figure 10.26 (a)) and the model results are multiplied by the time dependent detection rate in order to be comparable to the observed data. By the end of the time period (1994) the increased detection rate (in conjunction with a good cure rate) is decreasing TB incidence in the younger age ranges 0-45 years (figure 10.26 (b)). But varying this

parameter by 25% of its base value had very little over all effect on TB incidence (figures 10.26 (c)). This is probably due to the fact that the previous control regime had a good detection and cure rate and had already been in effect for the previous 13 years.

Figure 10.26: (a)-(b): Plots of the fit for the compartmental model to the Dutch TB data, for two selected years. (c) Plot of the fit for the compartmental model to the Dutch TB data, over all years, for all ages.

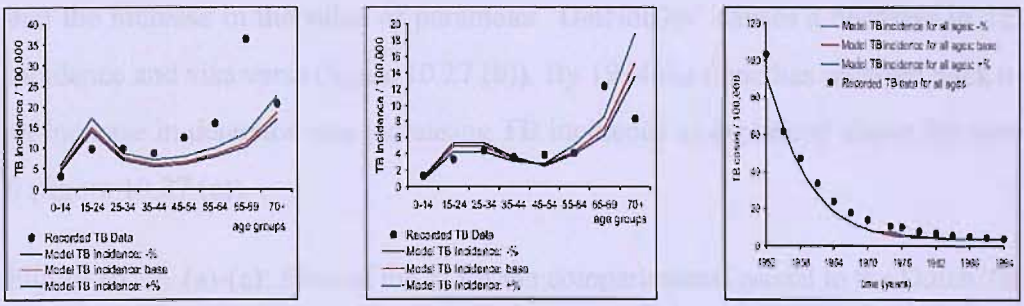

(a) 1974. (b) 1994. (c) All ages.

10.2.17 Varying parameter value 'DetNotDot', "the rate at which TB cases are found and treated under a previous (non-DOTS) less efficient regime".

The parameter 'DetNotDot' is varied by plus and minus 30% of base value (see table 10.19) to investigate the effect of varying the rate at which TB cases are found and treated under a previous (non-DOTS) less efficient regime.

Table 10.19: The values of parameter 'DetNotDot' selected as input to the model

	70% of base value	base value	130% of base value
'DetNotDot'	0.49	0.7	0.91

At time 0 (1952) the increased detection rate increases the TB incidence due

to the same reasons explained previously for parameter 'det' (figure 10.27 (a)); i.e. increased detection rates cause more cases to be identified hence inflating TB incidence and the model results are multiplied by the time dependent detection rate in order to be comparable to the observed data. By 1974 however, the new improved control regime has taken over. This new regime has a detection rate of 0.8. Thus it is detecting less cases than the previous regime's increased rate of 0.91, but more than the previous regimes base and decreased rates of 0.7 and 0.49 respectively. For these reasons we see a reversal of the trend by 1974 so that the increase in the value of parameter 'DetNotDot' causes a decrease in TB incidence and visa versa (figure 10.27 (b)). By 1994 the trend has reverted back to an increase in detection rate increasing TB incidence as explained above for time 0 (figure 10.27 (c)).

Figure 10.27: (a)-(c): Plots of the fit for the compartmental model to the Dutch TB data, for three selected years.

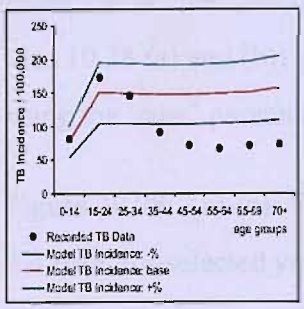

(a) 1952.

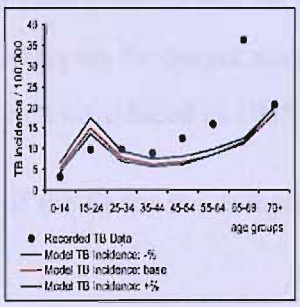

(b) 1974.

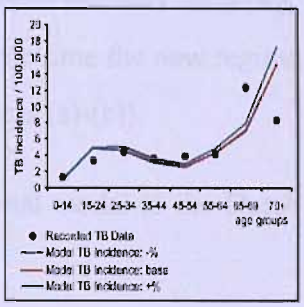

(c) 1994.

10.2.18 Varying parameter value 'cure', "the proportion of treated cases given curative chemotherapy under a second improved control regime".

The parameter 'cure' is varied by 11%, 50% and 100% of its base value (see table 10.20) in order to investigate the effect of increasing the proportion of treated cases given curative chemotherapy under a second improved control regime.

Table 10.20: Values of the parameter 'cure', selected as input to the model

	0% of bv	50% of bv	89% of bv	bv	111% of bv
'cure'	0	0.45	0.801	0.9	0.999
bv = base value					

Although the effect of increasing and decreasing the proportion of treated cases cured under a second improved regime seems non-linear it still follows a logical pattern in that increasing cure rates produce less TB incidence and visa versa (figures 10.28 (a) and (b)). The effect on the output starts at the time the new regime using the 'cure' parameter is first introduced in 1965 (figures (a)-(c)).

Figure 10.28: (a)-(b): Plots of the fit for the compartmental model to the Dutch TB data, for selected years.

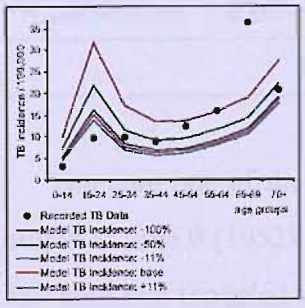

(a) 1974.

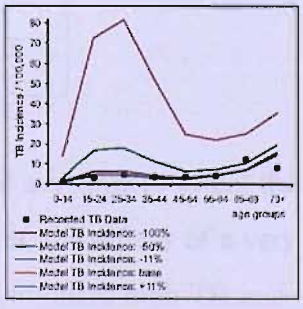

(b) 1994.

Figure 10.29: (a)-(c): Plots of the fit for the compartmental model to the Dutch TB data, over the years 1952 to 1994.

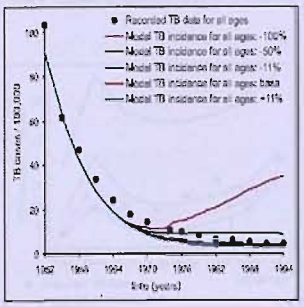

(a) All ages.

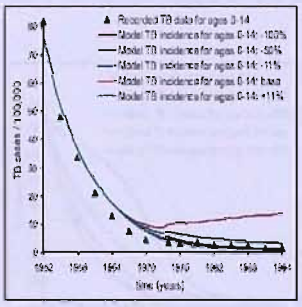

(b) Ages 0-14 years.

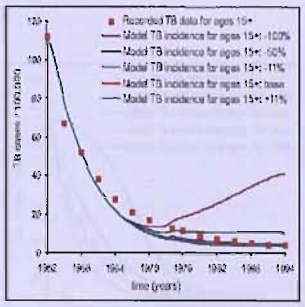

(c) Ages 15+ years.

10.2.19 Varying parameter value 'CureNotDot', "the proportion of treated cases given curative chemotherapy under a previous (non-DOTS) less efficient control regime".

The parameter 'CureNotDot' is varied by 30% and 90% of its base value (see table 10.21) to investigate the effect of increasing the proportion of treated cases given curative chemotherapy under a previous (non-DOTS) less efficient control regime.

Table 10.21: Values of the parameter 'CureNotDot', selected as input to the model

	10% of bv	70% of bv	bv	130% of bv
'CureNotDot'	0.075	0.525	0.75	0.975
bv = base value				

The cure rate of the initial control regime has not had any time to effect the output at time 0 (1952). Immediately after time 0, however, the effects of a very low cure rate (coupled with a fairly good detection rate) produces high TB incidence and a very high cure rate produces low TB incidence as would be expected (see figure 10.30 (a)-(c)).

Figure 10.30: (a): Plots of the fit for the compartmental model to the Dutch TB data, for 1974. (b)-(c): Plots of the fit for the compartmental model to the Dutch TB data, over the years 1952 to 1994, for ages 0-14 and 15+.

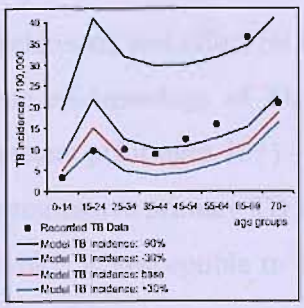

(a) 1974.

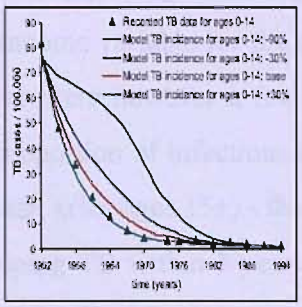

(b) Ages 0-14 years.

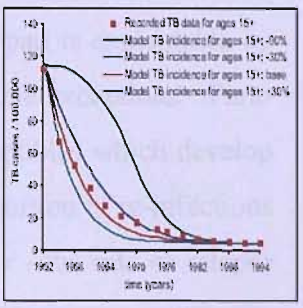

(c) Ages 15+ years.

10.3 Summary of Sensitivity Results

The parameters of the compartmental model mostly behave in a non-linear way when applied to the data from the Netherlands (except perhaps for very small variations in value where they behave approximately linearly). It is also noticeable that they interact with each other in complicated and subtle ways that are not always obvious when examining the difference equations that drive the model.

Some of the parameters produced a far greater relative effect in the outcome variable than others. In particular, ϵ - the relative case detection rate of non-infectious cases, w - the rate of smear conversion from non-infectious to infectious TB, ϕ - the proportion of failed treatment cases which is infectious, and F - proportion of progressive primary cases which become infectious within one year, have little effect on the outcome variable. However, it was found that eliminating these parameters did have a (large) effect on the output of the model, suggesting that these parameters although individually seeming relatively unimportant have significant interactions with the other model parameters.

Varying the parameters one at a time did not significantly improve the model

fit to each of the age groups over time and therefore failed to significantly improve the fit to the age dependent characteristics.

Most of the parameters caused an effect in the outcome variable, as would be expected when varied one at a time, keeping all other parameter values fixed. The behaviour and effect on the outcome variable for the most part is explainable by the epidemiology of TB. There were however a few notable exceptions. Parameters p(for ages 15+) - the proportion of infectious susceptibles which develop progressive primary TB in 1 year, x(for ages 15+) - the proportion of re-infections which is susceptible to developing TB within 1 year, and r - the rate of relapse from failed treatment to active TB, effect the outcome variable counter intuitively. Despite further examination of the model, including systematically simplifying the difference equations while noting whether the particular effect in the outcome variable was affected, no obvious reason for these anomalies was discovered. A full understanding of the model and its results would therefore benefit from further investigation of the behaviour of these particular parameters and interactions of the parameters in the model.

Chapter 11

Fitting and Sensitivity Analysis of Compartmental TB model using Pulmonary TB case data from Morocco

11.1 Fitting to Moroccan Pulmonary TB case data

The emphasis of this work as with the Dutch data (chapter 10) is on examining the ability of a compartmental model to fit to TB data from countries with an aging population and aging of the TB epidemic. Morocco is considered to fall into this category of countries. Thus, after producing a reasonable fit to the Moroccan data, most of the work in this chapter concentrates on the sensitivity analysis of the model.

The outcome investigated was the number of Pulmonary TB (PTB) cases per 100,000 of population for each of the 8 age groups, for the years 1980 to 2000. The Pulmonary TB (PTB) cases are estimated using the Infectious TB Incidence

values output by the model.

A selection of different starting values and age dependent functions were tried for the various model parameters. Initial fitting was carried out using the Nelder-mead optimisation method to minimise the least squares error in the model fit to the data. It was chosen for its general stability. However, the Nelder-mead algorithm became extremely slow when attempting to optimise the large number of potentially important parameters in the model. It was therefore only feasible to carry out this optimisation technique on a few parameters at a time. Even so, the Nelder-mead program still showed signs of instability implying a large degree of irregularity and complexity in the interactions of the parameters and resulting output of the model. The parameter values obtained from these fittings were therefore entered into the model and further fitting to the data carried out by hand. Tables 11.1 and 11.2 contain the input parameter values that were obtained and used to produce the fits used as the base values for subsequent sensitivity analysis.

The immunity and natural/self cure variables and associated parameters were set to zero due to their insignificant effect on the model results and in order to simplify the model for analysis.

Parameter 'p' (for ages 0-14), the proportion of infected susceptibles aged 0-14 which develop progressive primary TB within one year, was calculated in the model using the age dependent function $p = \left(\frac{a}{4000}\right) + \left(\frac{a^2}{7000}\right) + p_2$, where p_2 is the initial value of the parameter shown in Table 11.1 for ages ≤ 15 and $a =$ age step. The main feature for this parameter that the selected function had to capture, was a very slow increase in the parameter value in very young children with a sharper increase in value in the older ages to create a smoother transition to the p value for ages 15+. Figure 11.1 shows how the selected quadratic function for parameter 'p' (for ages 0-15) captures this age dependent trend.

The parameters 'cure' and 'cureNotDot', proportion of treated cases cured un-

der DOTS and a previous non-DOTS regime, respectively, were calculated in the model using the age dependent linear functions, cure $= c_0 + c_1 t$ and cureNotDot $= cnd_0 + cnd_1 t$; where c_0, c_1, cnd_0 and cnd_1 are the initial values and $t =$ time step. The main feature for this parameter that these selected functions had to capture, was a slow steady increase in both cure rates but with the constraint that the maximum value of 'cureNotDot' was less than the minimum value of 'cure' and that 'cure' must be less or equal to one (see figure 11.2).

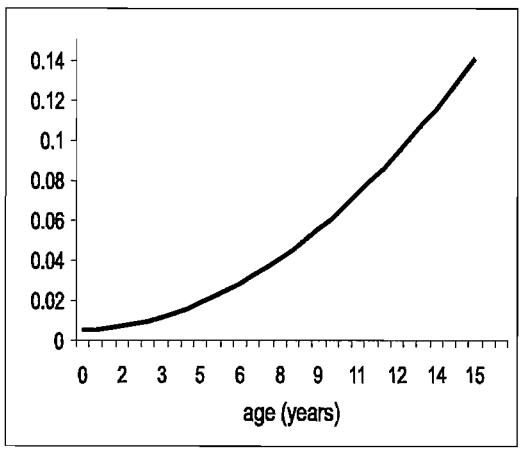

Figure 11.1: Plot of the function used for the model parameter $p = \left(\frac{a}{4000}\right) + \left(\frac{a^2}{7000}\right) + p_2$, proportion of infected susceptibles which develop progressive primary TB within one year; where p_2 is the initial value of the parameter for ages ≤ 15 and $a =$ age in half yearly steps

The fits to the data that the above described parameter values and parameter functions produce are shown in figures 11.3 to 11.5. It is noticeable that the shape of the line fit does not vary significantly across the 8 age ranges. Although the gradient of the line fit does change slightly over the age ranges, sloping in the early age ranges and leveling off in the last four age ranges, it is not a large enough change to match the gradient changes in the observed data. The fit to the percentage decrease in PTB cases (1994 to 2000) is reasonable for ages 15-65. The model

	Fitting to Moroccan PTB case data	
Parameter	Description	Initial Value
$\lambda(1)$	Force of infection	0.2
x(age$\leq$15)	Proportion of re-infections which is susceptible	0.08
x(age>15)	to developing TB within one year	0.15
p(age$\leq$15)	Proportion of infected susceptibles which	0.005
p(age>15)	develop progressive primary TB within a year	0.16
v(age$\leq$15)	rate at which latent infections become TB cases	0
v(age>15)	by endogenous re-activation	2.86E-03
f(age$\leq$15)	Proportion of progressive primary cases	0.04
f(age>15)	which become infectious	0.4439
μ	Death rate for non-TB causes	0.174
μ_i	Death rate for infectious TB	0.313
μ_n	Death rate for non-infectious TB	0.231
r	Rate of relapse from failed treatment to active TB	0.3
w	Rate of smear conversion from non-infectious to infectious TB	0.018
θ	exponential rate of decline in contact rate between TB cases and others	0.02
ϵ	Relative case detection rate of non-infectious cases	0.5
ϕ	Proportion of failed treatment cases which is infectious	0.575

Table 11.1: Parameter values obtained by fitting TB model outputs to Moroccan PTB case data.

	Fitting to Moroccan PTB case data *continued*		
Parameter	Description	Initial Value	
det	Rate at which TB cases are found and treated under DOTS	0.8	
cure	Proportion of treated cases given curative chemotherapy under DOTS	c_0 0.75	c_1 0.0015
detNotDot	Rate at which TB cases are found and treated under a previous non-DOTS regime	0.6	
cureNotDot	Proportion of treated cases given curative therapy under a previous non-DOTS regime	cnd_0 0.5	cnd_1 0.0014
warm-up period length (in years)		30	
start date of model		1980	
Time step (in part of years)		0.5	
finish date of model		2000	
Date at which DOTS interventions begin		1991	
Duration of introductory period of DOTS (in years)		3	
model age limit (in years)		85	
model age cut off for age dependent parameters (in years)		15	
Date at which non-DOTS interventions begin		1955	

Table 11.2: Parameter values obtained by fitting TB model outputs to Moroccan PTB case data (*continued*).

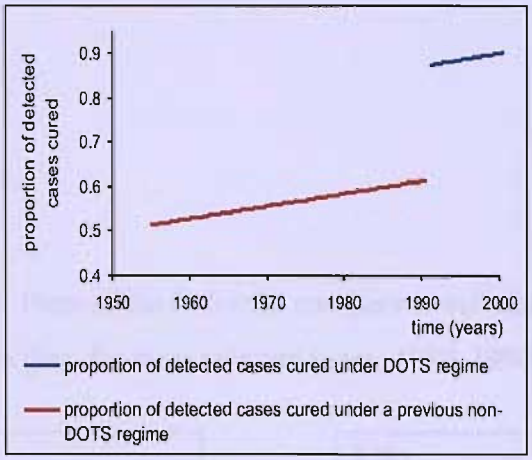

Figure 11.2: Plot of the function used for the model parameters cure $= c_0 + c_1 t$ and cureNotDot $= cnd_0 + cnd_1 t$, proportion of treated cases cured under DOTS and a previous non-DOTS regime, respectively; where c_0, c_1, cnd_0 and cnd_1 are the initial values and $t =$ time in half yearly steps

underestimates the percentage decrease in PTB for children aged 0-14 and over estimates the percentage decrease for the elderly aged 65+ (see figure 11.4 (d)).

Thus, again, despite the complexity of this compartmental model, the age dependent effects of the TB data are not fully and satisfactorily explained by this fitting of the model.

The following sections contain the further investigations into the ability of the model to capture effectively the age and time dependent trends in the Moroccan TB data set.

Figure 11.3: (a)-(c): Plots of the fit for the compartmental model to the Moroccan confirmed PTB case data, for three selected years: 1980, 1990 and 2000.

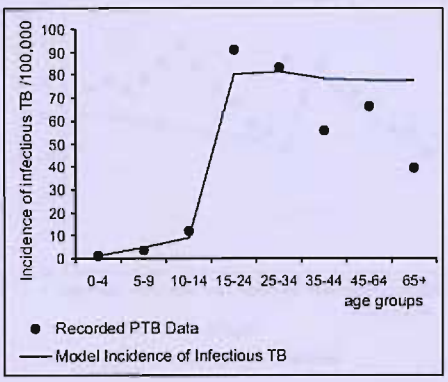

(a) 1980.

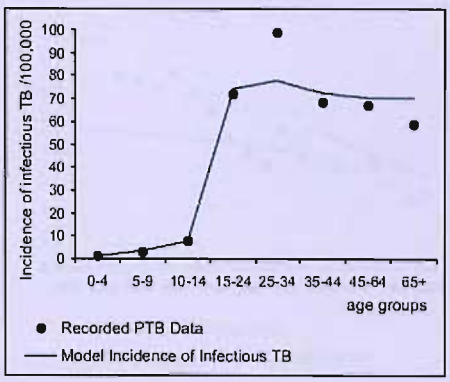

(b) 1990.

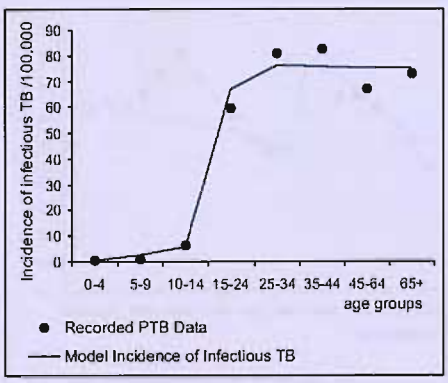

(c) 2000.

Figure 11.4: (a)-(c): Plots of the fit for the compartmental model to the Moroccan confirmed PTB case data, over the years 1980 to 2000.

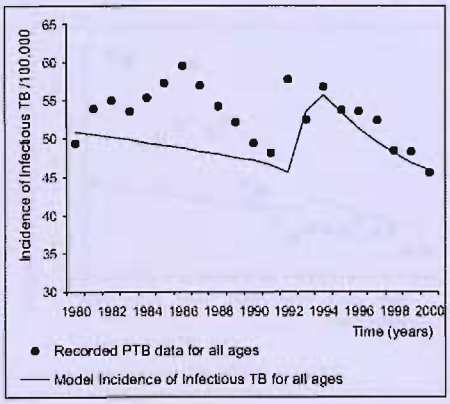

(a) All ages.

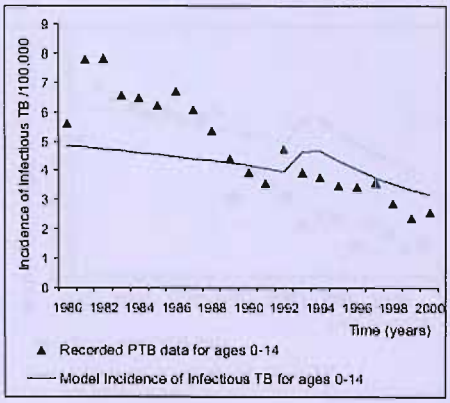

(b) Ages 0-14.

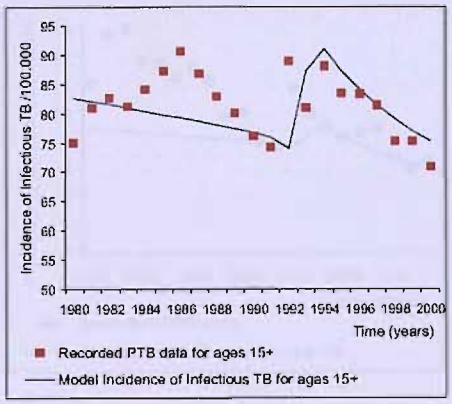

(c) Ages 15+.

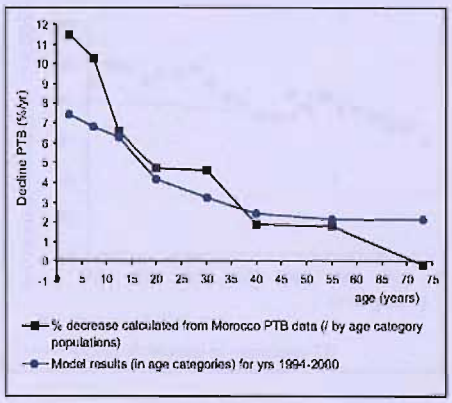

(d) Percentage decrease in PTB.

Figure 11.5: (a)-(h): Plots of the fitted age dependent model to Moroccan PTB case data, 1980-2000, for each of the eight age groups.

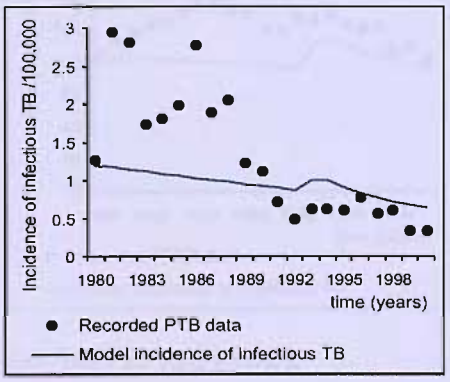

(a) Ages 0 to 4 years.

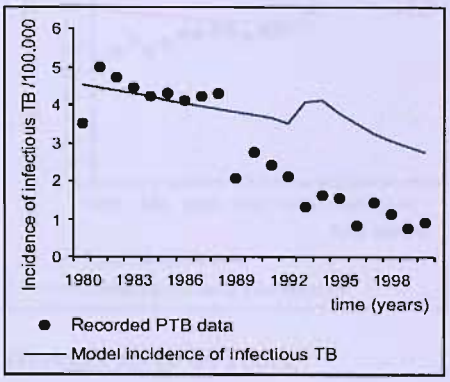

(b) Ages 5 to 9 years.

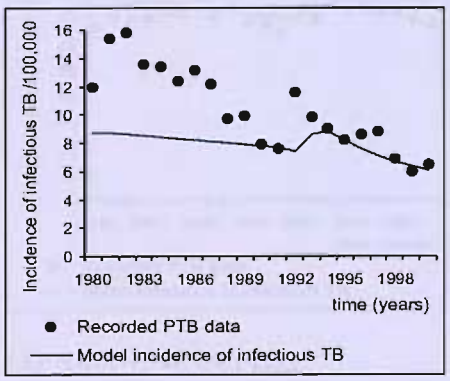

(c) Ages 10 to 14 years.

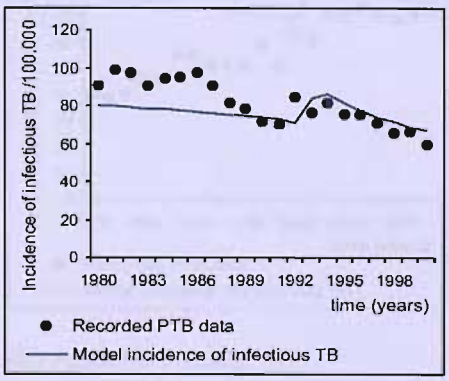

(d) Ages 15 to 24 years.

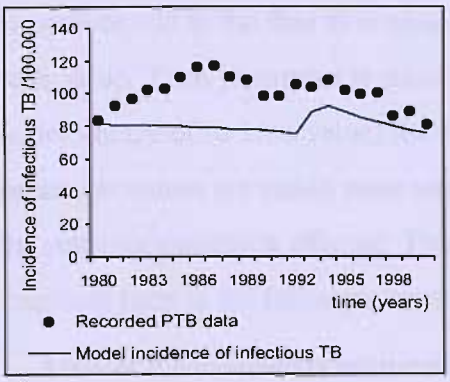

(e) Ages 25 to 34 years.

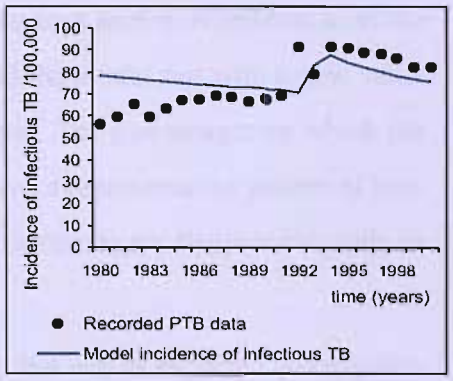

(f) Ages 35 to 44 years.

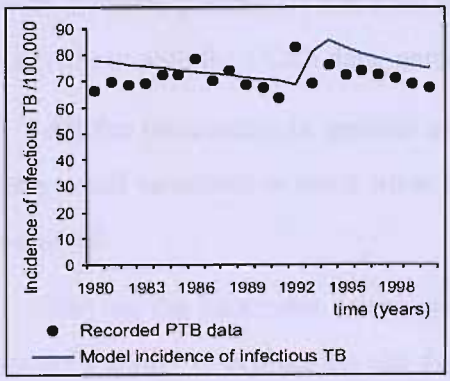

(g) Ages 45 to 64 years.

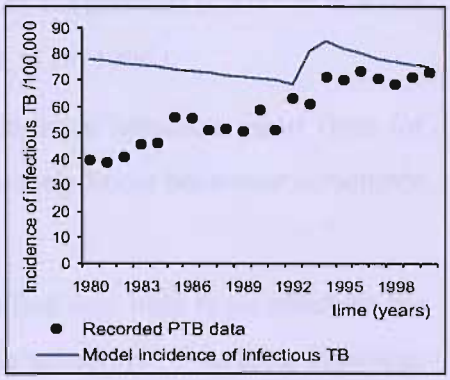

(h) Ages 65+ years.

11.2 Sensitivity analysis using Moroccan PTB case data

The aim is to explore how varying the values of each input parameter effects the outcome variables, the number of infectious TB cases/100,000 and the percentage decline in infectious TB for years 1994 to 2000. The value of each parameter used to produce a fit to the data as displayed in the previous section is referred to as the base value. Each parameter is taken in turn and the model run with a new value (a percentage of its base value) for that parameter. The percentages by which the parameter values are varied were selected to show a representative pattern of how the outcome variable is effected. These sensitivity results are displayed visually in graphical form in the following sections.

Most of the parameters exhibited behaviour that was as expected and explainable by the epidemiology of TB. There were some notable exceptions and these were the same parameters that were highlighted by the previous sensitivity analysis carried out with the Dutch data, namely, p(15+), x(15+) and r.

All the parameters in general exhibited non-linear behaviour apart from for very small variations in value when an approximately linear behaviour sometimes occurred.

Varying the parameter values one at a time had very little to no effect on the model's ability to explain the age dependent characteristics of the data. However, increasing some of the more sensitive parameters at the same time did seem to improve the fit to the data for ages 0-34.

The following sections set out the detailed results of varying the value of each parameter.

11.2.1 Varying parameter value $\lambda(1)$, "Initial Force of Infection".

The parameter $\lambda(1)$ is varied by plus and minus 30% of its base value (see table11.3) in order to investigate the effect of varying the initial value of the force of infection.

Table 11.3: Values of the parameter $\lambda(1)$, selected as input to the model

	70% of base value	base value	130% of base value
$\lambda(1)$	0.14	0.2	0.26

A 30% increase and decrease in the inital force of infection causes a relatively large corresponding increase and decrease in PTB incidence as expected (see figures 11.6 (a) and (b)).

Increasing the $\lambda(1)$ value has the effect of slightly decreasing the percentage decline in PTB over the last seven years of the time period, for ages 0-45, but slightly increasing the percentage decline for ages 45+. Decreasing the value of $\lambda(1)$ has the opposite effect (figure 11.7).

Figure 11.6: (a)-(b): Plots of the fit for the compartmental model to the Moroccan confirmed pulmonary TB data, over the years 1980 to 2000.

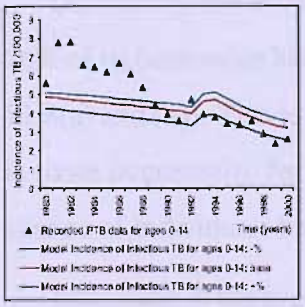

(a) Ages 0-14 years.

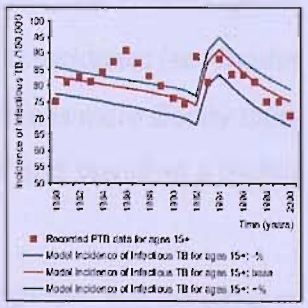

(b) Ages 15+ years.

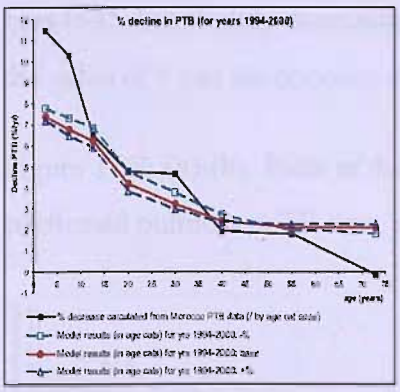

Figure 11.7: Plot of the fit for the compartmental model to the percentage decrease in the Moroccan confirmed pulmonary TB data, over the years 1994 to 2000.

11.2.2 Varying parameter value θ, "the exponential rate of decline in the contact rate between TB cases and others".

The parameter θ is varied by plus and minus 20% of its base value (see table 11.4) in order to investigate the effect of varying the exponential rate of decline in the contact rate between TB cases and others.

Table 11.4: Values of the parameter θ, selected as input to the model

	80% of base value	base value	120% of base value
θ	0.016	0.02	0.024

Decreasing and increasing the exponential rate of decline in the contact rate by 20% of its base value has a fairly large opposite effect on TB incidence (see figures 11.8(a) and (b)). This is as expected. If the contact rate declines more slowly there is more opportunity for mixing between cases and others and therefore a higher chance of individuals being infected with TB.

Increasing θ, the exponential rate of decline in the contact rate, has the effect of slightly increasing the percentage decline in PTB (over the years 1994-2000), for

ages 0-45, but slightly decreasing the percentage decline for ages 45+. Decreasing the value of θ has the opposite effect (see figure 11.9).

Figure 11.8: (a)-(b): Plots of the fit for the compartmental model to the Moroccan confirmed pulmonary TB data, over the years 1980 to 2000.

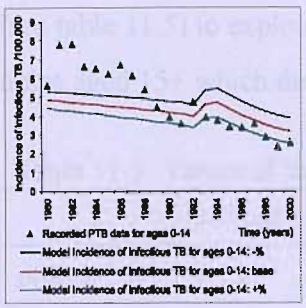

(a) Ages 0-14 years.

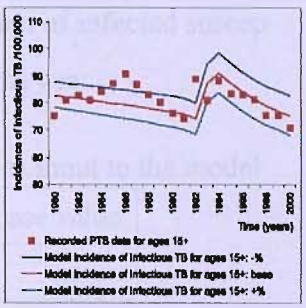

(b) Ages 15+ years.

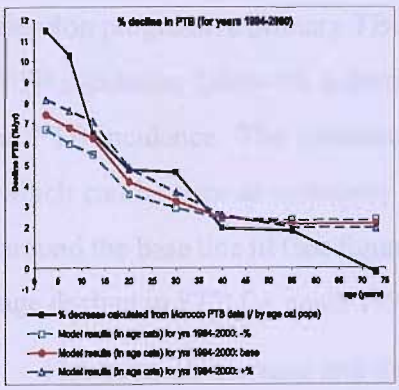

Figure 11.9: Plot of the fit for the compartmental model to the percentage decrease in the Moroccan confirmed pulmonary TB data, over the years 1994 to 2000.

11.2.3 Varying parameter value p (for ages 15+), "the proportion of infected susceptibles which develop progressive primary TB in one year".

The parameter p (for ages 15+) is varied by plus and minus 20% of its base value (see table 11.5) to explore the effect of varying the proportion of infected susceptibles aged 15+ which develop progressive primary TB in one year.

Table 11.5: Values of the parameter p(ages 15+), selected as input to the model

	80% of base value	base value	120% of base value
p(ages 15+)	0.128	0.16	0.192

For ages 15+, a small increase in the proportion of infected susceptibles which develop progressive primary TB in one year, causes a small and logical increase in PTB incidence. Likewise, a decrease in the value of p(ages 15+) causes a decrease in PTB incidence. The parameter behaves fairly linearly for this small variation which can be seen as symmetry of the two percentage decrease and increase fits around the base line fit (see figure 11.10 (b)).The trend is the same for the percentage decline in PTB for years 1994-2000 (figure 11.11).

However, an increase and decrease in p(ages 15+) causes a decrease and increase respectively in PTB incidence for children aged 0-14 (see figure 11.10 (a)). This appears counter intuitive and as for the Dutch data, could not be explained by further analysis of the model's mechanisms. This would therefore require further investigation.

Figure 11.10: (a)-(b): Plots of the fit for the compartmental model to the Moroccan confirmed pulmonary TB data, over the years 1980 to 2000.

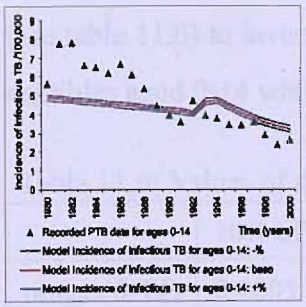

(a) Ages 0-14 years.

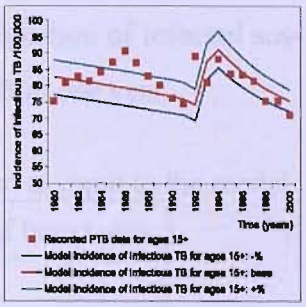

(b) Ages 15+ years.

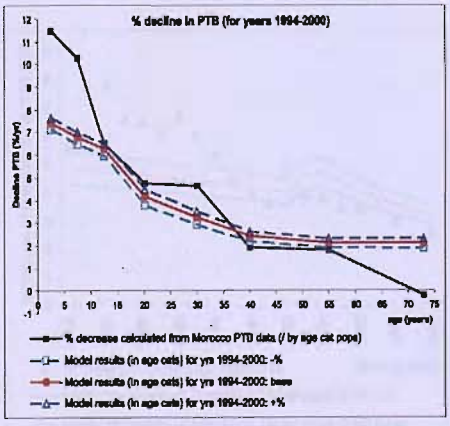

Figure 11.11: Plot of the fit for the compartmental model to the percentage decrease in the Moroccan confirmed pulmonary TB data, over the years 1994 to 2000.

11.2.4 Varying parameter value p (for ages 0-14), "the proportion of infected susceptibles which develop progressive primary TB in one year".

The parameter p (for ages 0-14) is varied by plus and minus 90% of its base value (see table 11.6) to investigate the effect of varying the proportion of infected susceptibles aged 0-14 which develop progressive primary TB in one year.

Table 11.6: Values of the parameter p(ages 0-14), selected as input to the model

	10% of base value	base value	190% of base value
p(ages 0-14)	0.0005	0.005	0.0095

A large increase and decrease in the proportion of infectious susceptibles aged 0-14 which develop progressive primary TB in one year, causes a corresponding small increase and decrease in TB incidence in children aged 0-14. This parameter therefore behaves fairly linearly and logically (see figures 11.12).

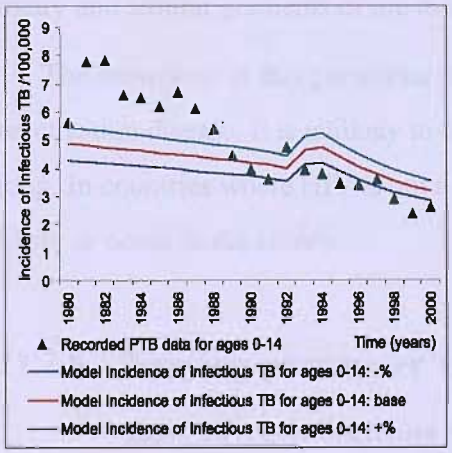

Figure 11.12: Plot of the fit for the compartmental model to the Moroccan confirmed pulmonary TB data, for ages 0-14, over the years 1980 to 2000.

11.2.5 Varying parameter value v (for ages 15+), "the rate at which latent infections become TB cases by endogenous reactivation".

The parameter v (for ages 15+) is varied by plus and minus 10% of the base value (see table 11.7) to examine the effect on the outcome variable.

Table 11.7: Values of the parameter v(ages 15+), selected as input to the model

	90% of base value	base value	110% of base value
v(ages 15+)	2.57E-03	2.86E-03	3.14E-03

For ages 15+ decreasing and increasing the rate at which latent infections become TB cases by endogenous reactivation causes a corresponding decrease and increase in TB incidence. There is very little effect on those aged under 15.

The parameter behaves fairly linearly for this small variation in value and there is very little effect on the percentage decrease of PTB as can be seen by the symmetry and similar gradients of the three fit lines in figure 11.13.

The behaviour of this parameter is in line with current scientific knowledge of reactivation disease. It is unlikely to occur in children as latent periods can be very long. In countries where HIV is not a 'large' problem, reactivation disease is more likely to occur in the elderly.

11.2.6 Varying parameter value x (for ages 15+), "the proportion of re-infections which is susceptible to developing TB within one year".

The parameter x (for ages 15+) is varied by plus and minus 40% of its base value (see table 11.8) to investigate the effect of varying the proportion of re-infections

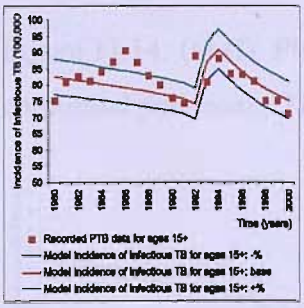

Figure 11.13: Fits of the compartmental model to Moroccan PTB data, for ages 15+, for varying values of v(15+).

in people aged 15+ which are susceptible to developing TB within one year.

Table 11.8: Values of the parameter x(ages 15+), selected as input to the model

	60% of base value	base value	140% of base value
x(ages 15+)	0.09	0.15	0.21

A decrease in x(ages 15+), the proportion of individuals aged 15+ with re-infections who are susceptible to developing TB within one year, causes an increase in TB incidence in those aged 0-14 (see figure 11.14 (a)).This trend then begins to reverse (see figure 11.14 (b) and (c)). For ages 35+ a decrease in x(ages 15+) causes a corresponding decrease in PTB incidence (see figures 11.14 (d)-(f)).

These results seem counter intuitive (as were the corresponding sensitivity results for the Dutch data set) and require further investigation.

Increasing and decreasing x(ages 15+) has the corresponding effect of increasing and decreasing the percentage decline in PTB for the years 1994-2000, as shown in figure 11.15.

Figure 11.14: (a)-(f): Plots of the fit for the compartmental model to the Moroccan confirmed pulmonary TB data, for each age range.

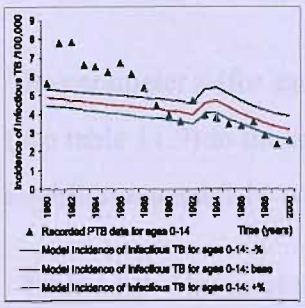

(a) Ages 0-14 years.

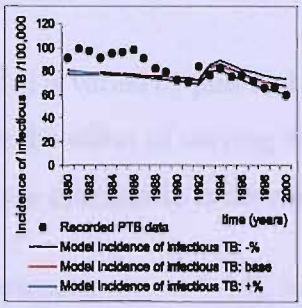

(b) Ages 15 to 24 years.

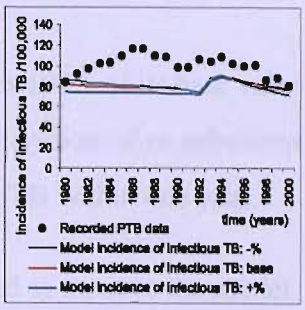

(c) Ages 25 to 34 years.

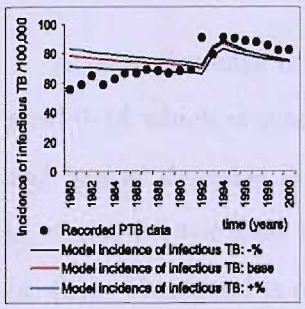

(d) Ages 35 to 44 years.

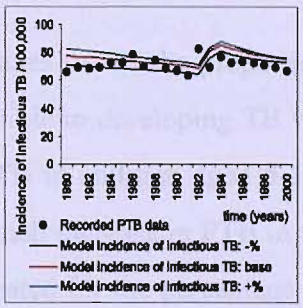

(e) Ages 45 to 64 years.

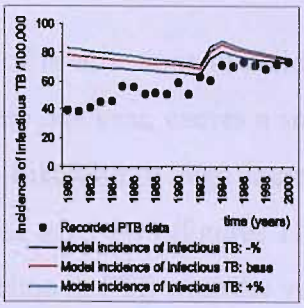

(f) Ages 65+ years.

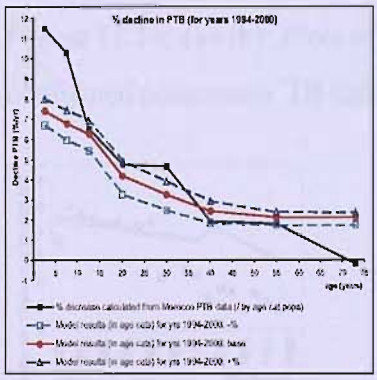

Figure 11.15: Plot of the fit for the compartmental model to the percentage decrease in the Moroccan confirmed pulmonary TB data, over the years 1994 to 2000.

11.2.7 Varying parameter value x (for ages 0-14), "the proportion of re-infections which is susceptible to developing TB within one year".

The parameter x (for ages 0-14) is varied by plus and minus 100% of its base value (see table 11.9) to investigate the effect of varying the proportion of re-infections in children aged 0-14 which are susceptible to developing TB within one year.

Table 11.9: Values of the parameter x(ages 0-14), selected as input to the model

	0% of base value	base value	200% of base value
x(ages 0-14)	0	0.08	0.16

A large decrease in x(ages 0-14), the proportion of re-infections in children aged 0-14 which is susceptible to developing TB within one year, causes a small and logical decrease in PTB in children aged 5-14. Likewise, a large increase in x(ages 0-14) causes a small increase in PTB in those aged 5-14 (figures 11.16 (a)-(b)). This trend is repeated for the percentage decline in PTB over the years 1994-2000 (figure 11.17).

Figure 11.16: (a)-(b): Plots of the fit for the compartmental model to the Moroccan confirmed pulmonary TB data, for ages 5-14.

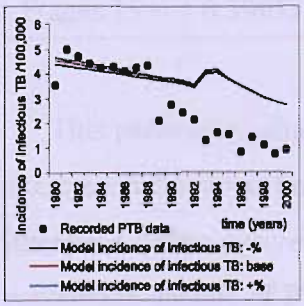

(a) Ages 5 to 9 years.

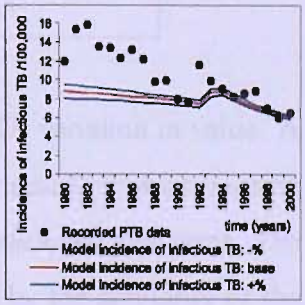

(b) Ages 10 to 14 years.

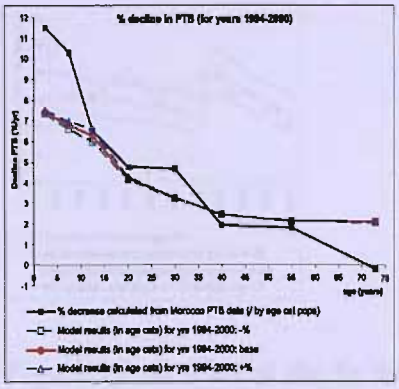

Figure 11.17: Plot of the fit for the compartmental model to the percentage decrease in the Moroccan confirmed pulmonary TB data, over the years 1994 to 2000.

11.2.8 Varying parameter value F (for ages 15+), "the proportion of progressive primary cases which become infectious within one year".

The parameter F (for ages 15+) is varied by plus and minus 10% of its base value (see table 11.10) to investigate the effect of varying the proportion of progressive primary cases for ages 15+ which become infectious within one year.

Table 11.10: Values of the parameter F(ages 15+), selected as input to the model

	90% of base value	base value	110% of base value
F(ages 15+)	0.399538	0.443932	0.488325

This parameter behaves linearly and logically for a 10% variation in value. A decrease in the proportion of progressive primary cases for ages 15+ which become infectious within one year causes a decrease in PTB incidence and visa versa. The percentage decline of PTB is not effected as can be seen by the similarity of the gradients for all three line fits (see figure 11.18)

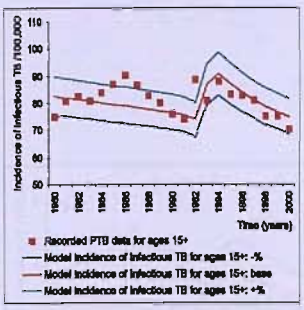

Figure 11.18: Plot of the fit for the compartmental model to the Moroccan confirmed pulmonary TB data, over the years 1980 to 2000, for ages 15+.

11.2.9 Varying parameter value F (for ages 0-14), "the proportion of progressive primary cases which become infectious".

The parameter F (for ages 0-14) is varied by plus and minus 70% of its base value (see table 11.11) in order to explore the effect of varying the proportion of progressive primary cases in children aged 0-14 which become infectious.

Table 11.11: Values of the parameter F(ages 0-14), selected as input to the model

	30% of base value	base value	170% of base value
F(ages 0-14)	0.012	0.04	0.068

A large decrease in F(ages 0-14), the proportion of progressive primary cases in children aged 0-14 which become infectious in one year, causes a relatively small decrease in PTB incidence in those aged 0-14. Likewise a large increase in F(ages 0-14) causes a relatively small increase in PTB incidence in those aged 0-14 (figure 11.19).

Decreasing F(ages 0-14) has the effect of very slightly increasing the percentage decline in PTB (over the years 1994-2000) for ages 0-14 (see figure 11.20).

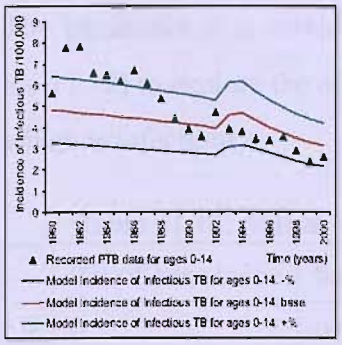

Figure 11.19: Fits of compartmental model to Moroccan PTB data, for ages 0-14.

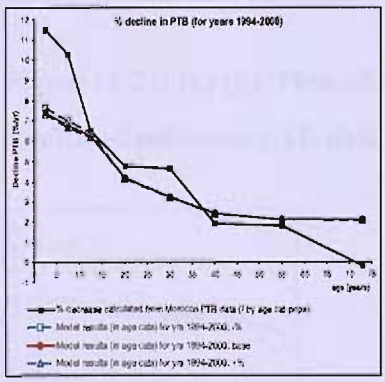

Figure 11.20: Fit for the compartmental model to the percentage decrease in the Moroccan confirmed pulmonary TB data, over the years 1994 to 2000.

11.2.10 Varying parameter value ϕ, "the proportion of failed treatment cases which is infectious".

The parameter ϕ is varied by plus and minus 100% of its base value (see table 11.12) to explore the effect of varying the proportion of failed treatment cases which is infectious.

Table 11.12: Values of the parameter ϕ, selected as input to the model

	0% of base value	base value	200% of base value
ϕ	0	0.57462	1

A large increase and decrease in ϕ, the proportion of failed treatment cases which is infectious, causes a corresponding small increase and decrease in PTB incidence (figures 11.21 (a) and (b)). It makes sense that increasing the number of infectious cases in a population increases TB incidence.

This trend is duplicated in percentage decline of PTB (over 1994-2000) for ages 0-15 and 40+, (see figure 11.22).

Figure 11.21: (a)-(b): Plots of the fit for the compartmental model to the Moroccan confirmed pulmonary TB data, over the years 1980 to 2000.

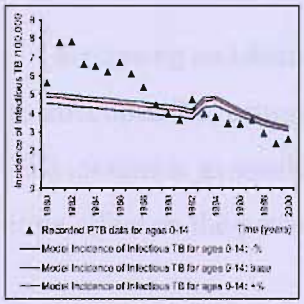

(a) Ages 0-14 years.

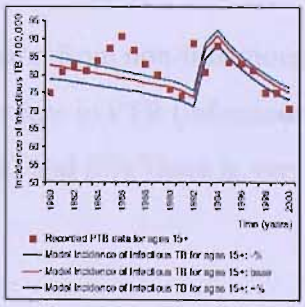

(b) Ages 15+ years.

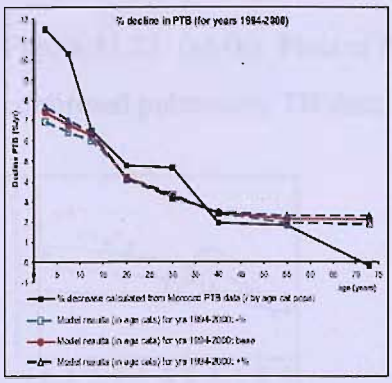

Figure 11.22: Fits for the compartmental model to the percentage decrease in the Moroccan confirmed pulmonary TB data, over the years 1994 to 2000.

11.2.11 Varying parameter value w, "the rate of smear conversion from non-infectious to infectious TB".

The parameter w is varied by plus and minus 50% of its base value (see table 11.13) to examine the effect of varying the rate of smear conversion from non-infectious to infectious TB.

Table 11.13: Values of the parameter w, selected as input to the model

	50% of base value	base value	150% of base value
w	0.009033	0.018065	0.027098

Increasing and decreasing w, the rate of smear conversion from non-infectious to infectious TB, causes a corresponding increase and decrease in PTB (infectious TB) incidence as would be expected (see figures 11.23 (a) and (b)).There is very little effect on the percentage decrease of PTB.

Figure 11.23: (a)-(b): Plots of the fit for the compartmental model to the Moroccan confirmed pulmonary TB data, over the years 1980 to 2000.

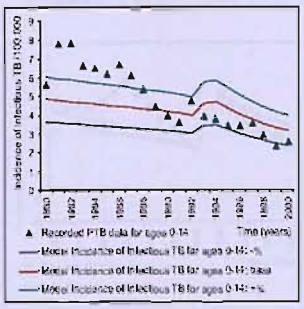

(a) Ages 0-14 years.

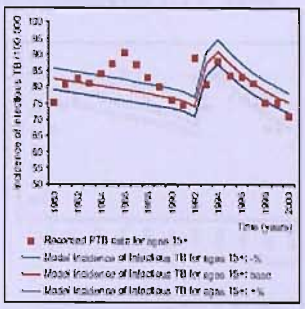

(b) Ages 15+ years.

11.2.12 Varying parameter value μ_i, "the death rate for infectious TB".

The parameter μ_i is varied by plus and minus 90% of its base value (see table 11.14) to investigate the effect of varying the death rate for infectious TB.

Table 11.14: Values of the parameter μ_i, selected as input to the model

	10% of base value	base value	190% of base value
μ_i	0.031256	0.312559	0.593862

Decreasing the death rate for infectious TB causes an increase in PTB incidence from 1994, (the year the DOTS regime takes over from the previous less efficient control regime), and onwards. This is logical as decreasing this death rate leaves an increased number of infectious TB cases in the population. Before 1994, however, a decrease in the infectious TB death rate causes a decrease in PTB incidence (see figure 11.24 (a)-(c)).This is possibly due to an interaction with the pre-DOTS and DOTS detection and cure rates.

A decrease in μ_i also causes a large decrease in the percentage decline of PTB

(over years 1994-2000). An increase in μ_i causes a small increase in the percentage decline of PTB for ages 0-20 (see figure 11.25).

Figure 11.24: (a)-(c): Fits of compartmental model to the Moroccan PTB data.

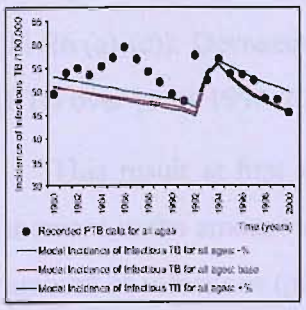

(a) All ages.

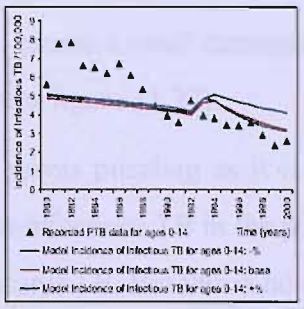

(b) Ages 0-14 years.

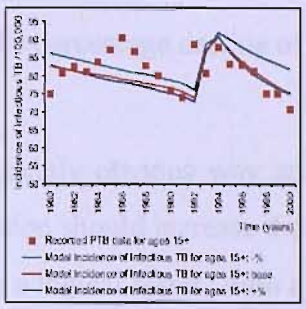

(c) Ages 15+ years.

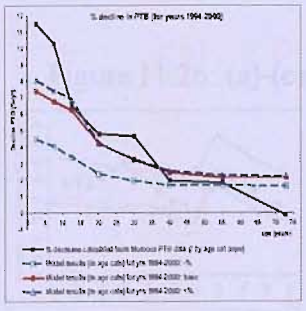

Figure 11.25: Fits for the compartmental model to the percentage decrease in the Moroccan confirmed pulmonary TB data, over the years 1994 to 2000.

11.2.13 Varying parameter value μ_n, "the death rate for non-infectious TB".

The parameter μ_n is varied by plus and minus 80% of its base value (see table 11.15) in order to investigate the effect of varying the death rate for non-infectious TB.

Decreasing the death rate from non-infectious TB causes a large increase in PTB incidence. Increasing μ_n causes a smaller decrease in PTB incidence (figure

Table 11.15: Values of the parameter μ_n, selected as input to the model

	20% of base value	base value	180% of base value
μ_n	0.046148	0.23074	0.415332

11.26 (a)-(c)). Decreasing μ_n causes a small decrease in the percentage decline of PTB over years 1994-2000, (see figure 11.27).

This result at first sight seems puzzling as it is not overly obvious why an increase in the amount of non-infectious TB in the population should increase the amount of infectious (pulmonary) TB. But this is however a logical result. With a higher prevalence of non-infectious TB, a larger number of cases are converted to infectious TB by smear conversion hence increasing PTB incidence.

Figure 11.26: (a)-(c): Fits of compartmental model to Moroccan PTB data.

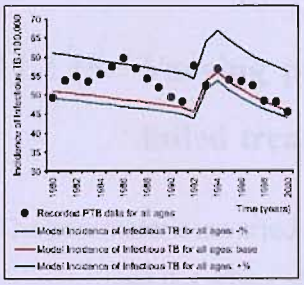

(a) All ages.

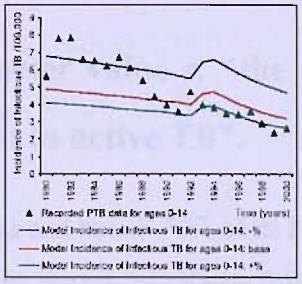

(b) Ages 0-14 years.

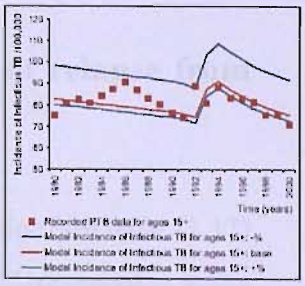

(c) Ages 15+ years.

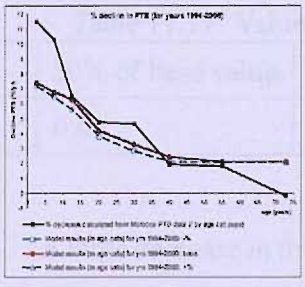

Figure 11.27: Fits for the compartmental model to the percentage decrease in the Moroccan confirmed pulmonary TB data, over the years 1994 to 2000.

11.2.14 Varying parameter value ϵ, "the relative case detection rate of non-infectious cases".

The parameter ϵ is varied by plus and minus 100% of the base value (see table 11.16) to explore the effect of varying the relative case detection rate of non-infectious cases.

Table 11.16: Values of the parameter ϵ, selected as input to the model

	0% of base value	base value	200% of base value
ϵ	0	0.5	1

Varying this parameter by 100% of its base value has little to no effect on PTB incidence.

11.2.15 Varying parameter value r, "the rate of relapse from failed treatment to active TB".

The parameter r is varied by plus and minus 70% of its base value (see table 11.17) to investigate the effect of varying the rate of relapse from failed treatment to active TB.

Table 11.17: Values of the parameter r, selected as input to the model

	30% of base value	base value	170% of base value
r	0.09	0.3	0.51

A large decrease in the rate of relapse from failed treatment to active TB causes a small increase in PTB incidence and visa versa although this effect is less pronounced (figures 11.28 (a)-(c)).This appears counter intuitive, as with the corresponding sensitivity results for the Dutch data. Therefore, like the previous pa-

rameters that produced seemingly illogical effects, this parameter would benefit from further investigation.

This parameter shows non linear characteristics and there is no clear trend for the effect of varying r on the percentage decline of PTB (figure 11.29).

Figure 11.28: (a)-(c): Plots of the fit for the compartmental model to the Moroccan confirmed pulmonary TB data, over the years 1980 to 2000.

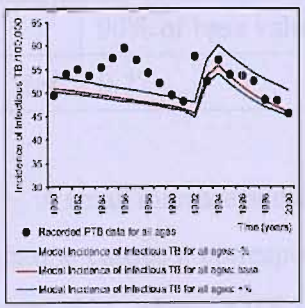

(a) All ages.

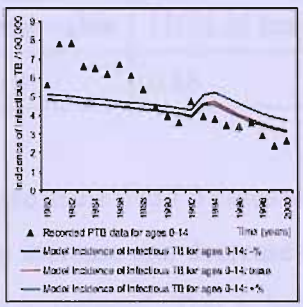

(b) Ages 0-14 years.

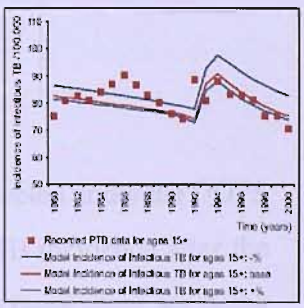

(c) Ages 15+ years.

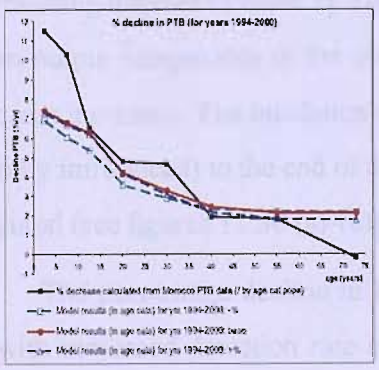

Figure 11.29: Plot of the fit for the compartmental model to the percentage decrease in the Moroccan confirmed pulmonary TB data, over the years 1994 to 2000.

11.2.16 Varying parameter value 'det', "the rate at which TB cases are found and treated under the DOTS regime".

The parameter 'det' is varied by plus and minus 10% of its base value (see table 11.18) to investigate the effect of varying the rate at which TB cases are found and treated under the DOTS regime.

Table 11.18: Values of the parameter 'det', selected as input to the model

	90% of base value	base value	110% of base value
'det'	0.72	0.8	0.88

A small increase and decrease in the rate TB cases are detected under the DOTS regime causes a corresponding increase and decrease in PTB incidence after the year 1991, when DOTS is first introduced. This is because more cases are being found and identified after this date under the new regime. The model multiplies the resulting number of cases by the time dependent detection rate in order to produce an output comparable to the observed data. Therefore at first, the number of TB cases increases. The incidence of PTB then declines from 1994 (the year DOTS is fully introduced) to the end of the time period (2000), as more cases are found and cured (see figures 11.30 (a)-(c)).

The percentage decline in PTB over this same period (1994-2000) increases with increased detection rate and decreases with decreased detection rate. This trend is most pronounced in ages 0-15, (see figure 11.31).

Figure 11.30: (a)-(c): Plots of the fit for the compartmental model to the Moroccan confirmed pulmonary TB data, over the years 1980 to 2000.

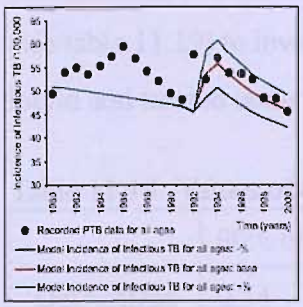

(a) All ages.

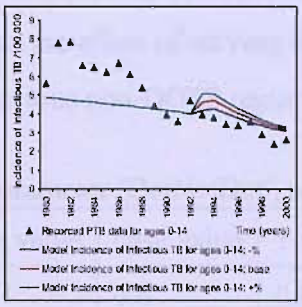

(b) Ages 0-14 years.

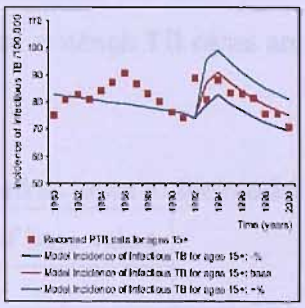

(c) Ages 15+ years.

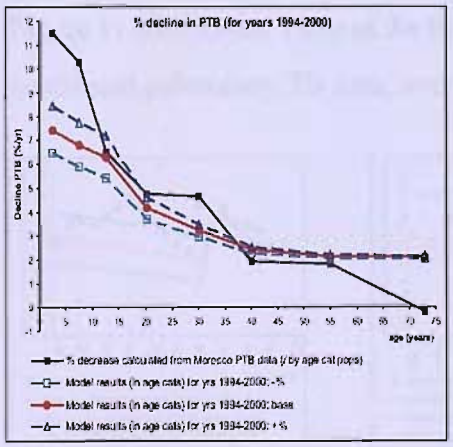

Figure 11.31: Plot of the fit for the compartmental model to the percentage decrease in the Moroccan confirmed pulmonary TB data, over the years 1994 to 2000.

11.2.17 Varying parameter value 'DetNotDot', "the rate at which TB cases are found and treated under a previous non-DOTS regime".

The parameter 'DetNotDot' is varied by plus and minus 10% of the base value (see table 11.19) to investigate the effect of varying the rate at which TB cases are found and treated under a previous non-DOTS regime.

Table 11.19: Values of the parameter 'DetNotDot', selected as input to the model

	90% of base value	base value	110% of base value
'DetNotDot'	0.54	0.6	0.66

Increasing and decreasing the detection rate of a previous less efficient non-DOTS regime produces analogous results to those for the DOTS detection rate and for the same reasons as described in the previous section (see figures 11.32 (a)-(c)).

Figure 11.32: (a)-(c): Plots of the fit for the compartmental model to the Moroccan confirmed pulmonary TB data, over the years 1980 to 2000.

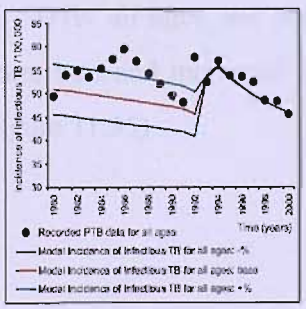

(a) All ages.

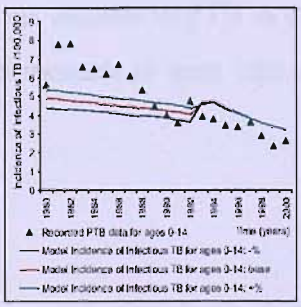

(b) Ages 0-14 years.

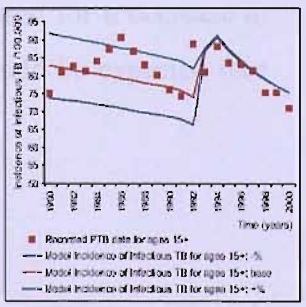

(c) Ages 15+ years.

11.2.18 Varying parameter value 'cure $= c_0 + c_1 t$', "the proportion of treated cases given curative chemotherapy under the DOTS regime".

The parameter 'cure' is varied by plus and minus 10% of its base value (see table 11.20 and figure 11.33) in order to investigate the effect of varying the proportion of treated cases given curative chemotherapy under the DOTS regime.

Table 11.20: Values of the parameter 'cure', selected as input to the model

c_0			c_1		
90% of bv	bv	110% of bv	90% of bv	bv	110% of bv
0.675	0.75	0.825	0.00135	0.0015	0.00165
bv = base value					

A decrease and increase in the cure rate under the DOTS regime cause a logical increase and decrease respectively in PTB incidence after the year 1994, the year the DOTS regime is fully introduced. The incidence of PTB declines after 1994 as the new DOTS regime is fully implemented (see figures 11.34 (a)-(c)).

Over all ages, the percentage decline in PTB is decreased for a decrease in cure rate and increased for an increase in cure rate as would be expected (see figure 11.35).

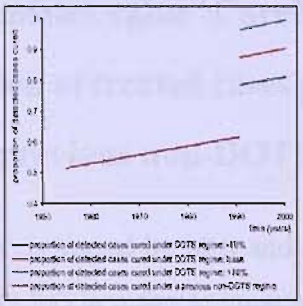

Figure 11.33: Plot of the parameter cure values.

Figure 11.34: (a)-(c): Plots of the fit for the compartmental model to the Moroccan confirmed pulmonary TB data, over the years 1980 to 2000.

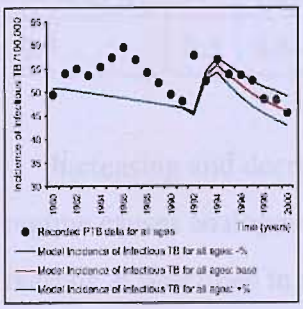

(a) All ages.

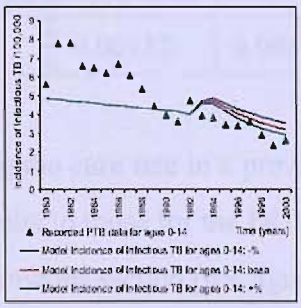

(b) Ages 0-14 years.

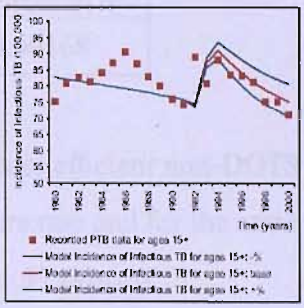

(c) Ages 15+ years.

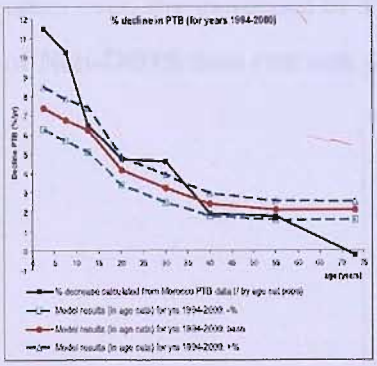

Figure 11.35: Plot of the fit for the compartmental model to the percentage decrease in the Moroccan confirmed pulmonary TB data, over the years 1994 to 2000.

11.2.19 Varying parameter value 'CureNotDot = $cnd_0 + cnd_1 t$', "the proportion of treated cases given curative chemotherapy under a previous non-DOTS regime".

The parameter 'CureNotDot' is varied by plus and minus 20% of its base value (see table 11.21 and figure 11.36) in order to investigate the effect of varying the proportion of treated cases given curative chemotherapy under a previous non-DOTS regime.

Table 11.21: Values of the parameter 'CureNotDot', selected as input to the model

cnd_0			cnd_1		
80% of bv	bv	120% of bv	80% of bv	bv	120% of bv
0.4	0.5	0.6	0.00112	0.0014	0.00168

Increasing and decreasing the cure rate in a previous less efficient non-DOTS regime causes analogous results to those for the DOTS cure rate and for the same reasons as described in the previous section (see figures 11.37 (a)-(c)).

It is interesting to note that as time moves on and the new DOTS control regime takes over, the incidence of TB values become very similar no matter what value of Non-DOTS cure rate was previously used.

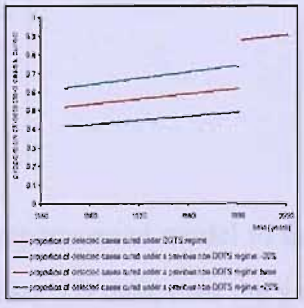

Figure 11.36: Plot of the parameter 'cureNotDot = $cnd_0 + cnd_1 t$ values.

Figure 11.37: (a)-(c): Fits of compartmental model to Moroccan PTB data.

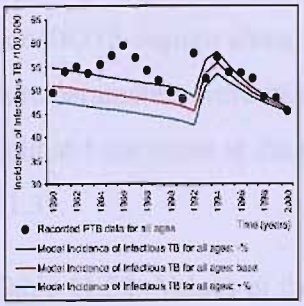

(a) All ages.

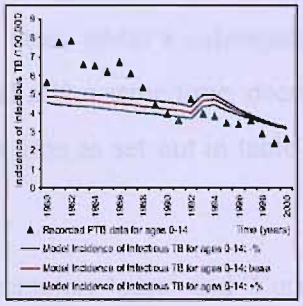

(b) Ages 0-14 years.

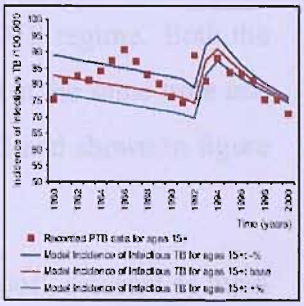

(c) Ages 15+ years.

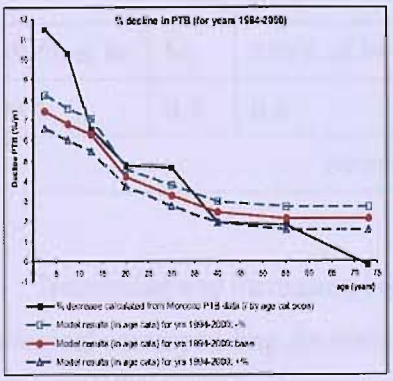

Figure 11.38: Fits of the compartmental model to the percentage decrease in the Moroccan confirmed pulmonary TB data, over the years 1994 to 2000.

11.2.20 Varying the two parameter values 'cure' and 'CureNotDot' simultaneously.

The two cure parameters are varied simultaneously to investigate the effect of varying the proportion of treated cases given curative chemotherapy under a previous non-DOTS regime along with those under a subsequent DOTS regime. Both the cure parameters were increased at the same time, decreased at the same time and held at base value at the same time as set out in table 11.22 and shown in figure 11.39.

Table 11.22: Values of the parameters 'cure' and 'CureNotDot', selected as input to the model

'cure'					
c_0			c_1		
90% of bv	bv	110% of bv	90% of bv	bv	110% of bv
0.675	0.75	0.825	0.00135	0.0015	0.00165
'CureNotDot'					
cnd_0			cnd_1		
80% of bv	bv	120% of bv	80% of bv	bv	120% of bv
0.4	0.5	0.6	0.00112	0.0014	0.00168
$bv = base\ value$					

Decreasing and increasing both non-DOTS and DOTS cure rates together causes a logical corresponding decrease and increase in PTB incidence (see figures 11.40 (a)-(c)). The percentage decline in PTB (over years 1994-2000) is only minimally effected.

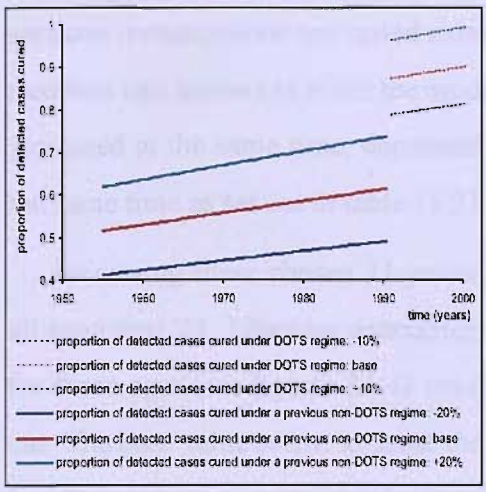

Figure 11.39: Plot of the parameters 'cure' and 'cureNotDot' values.

Figure 11.40: (a)-(c): Fits of compartmental model to Moroccan PTB data.

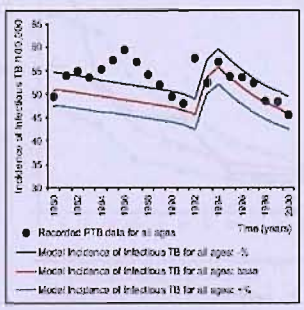

(a) All ages.

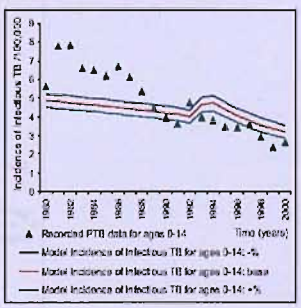

(b) Ages 0-14 years.

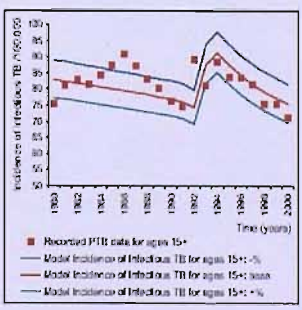

(c) Ages 15+ years.

11.2.21 Varying 11 parameter values simultaneously

The parameters established as the most interesting and sensitive by the previous sections investigations are varied simultaneously to give an idea of how these parameters can interact to effect the model outcomes. All the parameters varied were increased at the same time, decreased at the same time and held at base value at the same time as set out in table 11.23.

Increasing these chosen 11 parameters together increases PTB incidence for all ages over 24. Likewise decreasing all 11 parameters decreases PTB incidence for these ages (see figures 11.42 (e)-(h)). For ages 0-24 the results are less clear cut. The base value seems to cause the most PTB incidence with an increase in the parameters causing a sharper decline in PTB incidence, especially in the 5-9 year age range (see figures 11.42 (a)-(d)).

An increase/decrease in the parameter values caused a marked increase/decrease in the percentage decline in PTB for years 1994-2000 (see figure 11.41).

It is obvious that these parameters interact with each other in complicated and subtle non-linear ways that are not obvious by examining the difference equations that drive the model.

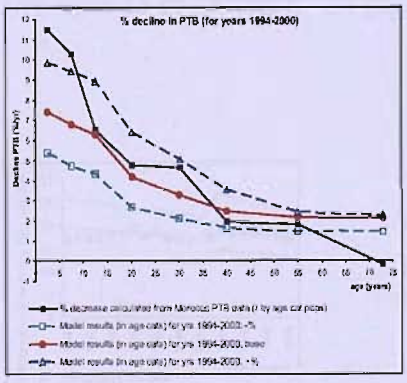

Figure 11.41: Fits for the compartmental model to the percentage decrease in the Moroccan confirmed pulmonary TB data, over the years 1994 to 2000.

Figure 11.42: (a)-(h): Plots of the fit for the compartmental model to the Moroccan confirmed pulmonary TB data, for each of the 8 age ranges.

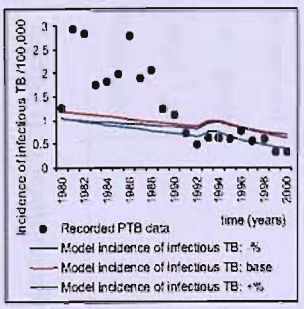

(a) Ages 0 to 4 years.

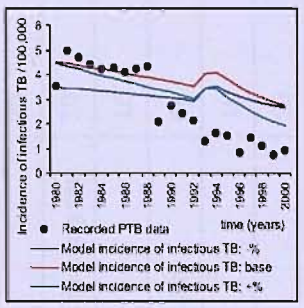

(b) Ages 5 to 9 years.

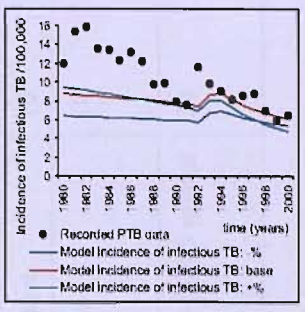

(c) Ages 10 to 14 years.

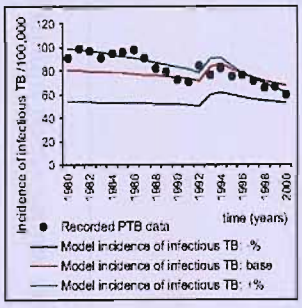

(d) Ages 15 to 24 years.

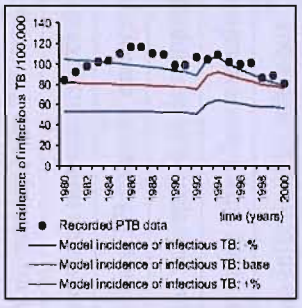

(e) Ages 25 to 34 years.

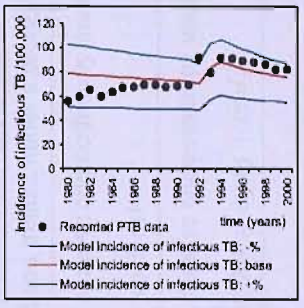

(f) Ages 35 to 44 years.

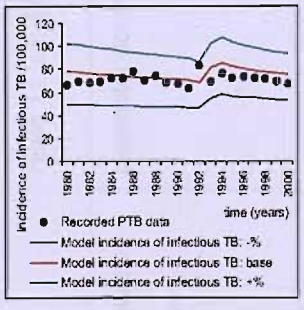

(g) Ages 45 to 64 years.

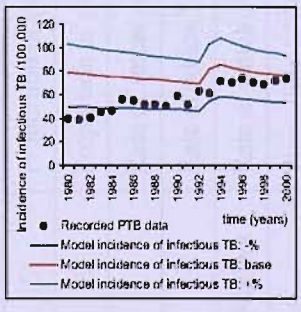

(h) Ages 65+ years.

Table 11.23: Details of parameter values varied simultaneously to investigate interaction effects.

parameter name	parameter description	percentage of base value used to vary parameter value
$\lambda(1)$	Initial value of force of infection	30
θ	Exponential rate of decline in contact rate between TB cases and others	20
p(> 15)	Proportion of infected susceptibles which develop progressive primary TB within one year	20
v(> 15)	Rate at which latent infections become TB cases by endogenous reactivation	10
x(> 15)	Proportion of re-infections which is susceptible to developing TB within one year	40
F(> 15)	Proportion of progressive primary cases which become infectious	10
w	Rate of smear conversion from non-infectious to infectious TB	50
det	Rate at which TB cases are found and treated under the DOTS regime	10
detNotDot	Rate at which TB cases are found and treated under a previous non-DOTS regime	10
cure	Proportion of treated cases given curative chemotherapy under the DOTS regime Time dependent function: cure $= c_0 + c_1 t$	10
cureNotDot	Proportion of treated cases given curative chemotherapy under a previous non-DOTS regime Time dependent function: cureNotDot $= cnd_0 + cnd_1 t$	20

11.3 Summary of Sensitivity Analysis

Most of the parameters behaviour was as expected and explainable by the epidemiology of TB. There were however some notable exceptions, namely, p(for ages 15+) - the proportion of infectious susceptibles which develop progressive primary TB in 1 year; x(for ages 15+) - the proportion of re-infections which is susceptible to developing TB within 1 year; r - the rate of relapse from failed treatment to active TB. These three parameters showed the same illogical effects with the Moroccan PTB data as they did when applied to the Dutch TB data set. Further examination of the model provided no obvious explanations for these results.

The parameters again showed non-linear characteristics, except for very small variations in value where they behave approximately linearly. Varying parameters x(ages 0-14), ϕ and ϵ had a relatively small effect on the outcome variable as compared with other parameters.

It is noticeable that varying the parameters one at a time did not significantly improve the model fit to the age dependent characteristics. The model therefore still struggled to fully capture the age characteristics especially in the older age groups. However, increasing the 11 selected parameters at the same time did have the effect of varying the gradient and placement of the fitted line so that it gave a better fit to the data for ages 0-34 (see figures 11.42 (a)-(e)).

Chapter 12

Modelling Local and Global Effects in the Transmission of TB Observed in Asembo and Gem, Kenya: Designing a Spatial Model of TB Case Clustering.

This third model, a Markov chain model, is distinct from the previous two parametric and compartmental models previously described. It is constructed to examine the relative significance of local and global effects in the transmission of TB. The simple Markov chain local effects model is used to examine a time-spatial TB data set from the Nyanza province in western Kenya. It is also shown how this new local/global effects model can be used in the design of community/clustered randomised trials.

12.1 Introduction

The following Chapters describe the background, design and application of a Markov Chain model of TB case clustering in the Nyanza Province of western Kenya. The model is created in an attempt to identify whether the nearest reported source of possible infection is a localised one stemming from an individual's contacts with family or near neighbours or whether it arises from a much more dispersed contact with people in a much less localised way.

The basic methodology is to construct a stochastic Markov-chain model whose behaviour is determined by a number of key parameters and then fit this model to the data using maximum likelihood to estimate these key parameter values. Markov-chain models are based on transition probabilities and are very different in approach from the type of compartmental model described in chapter 9.

The rest of this chapter sets out the background and detail of the Kenyan TB data set analysed by this new local/global effects model. Chapter 13 introduces and gives a brief history of modelling space-time clustering of disease. Chapter 14 contains the detail of the Markov-chain local/global effects model construction. Chapter 15 contains the application of this new model to the Kenyan TB data set described below. Chapter 16 sets out a possible use of this local/global effects model in the design of cluster randomised trials.

12.2 The Kenyan Space-Time TB Data

A demographic surveillance system (DSS) exists in the Nyanza Province of western Kenya as part of the Centers for Disease Control and Prevention (CDC) and Kenya Medical Research Institute (KEMRI) research operations. It covers approximately 500 km^2 of land including 217 villages, 75 of which are in Asembo in the Rarieda Division of the Bondo District and the rest are in Gem in the Wagai and

Yala Divisions of the Siaya District. There is global information systems (GIS) positional information (including longitude and latitude coordinates) and annual population statistics for each village in the demographic surveillance area (DSA). Figure 12.2 contains a map of Asembo and Gem showing the location of each of the 217 villages and their allocated identifying number.

Over 95% of the residents in Asembo and Gem are Luo. Poverty occurs throughout the demographic surveillance area (DSA) which is an area of endemic Malaria and high HIV prevalence (approximately 22%). Asembo has a high prevalence of HIV in the region around Lake Victoria due to lakeside prostitution whereas Gem has a generally lower prevalence of HIV. In Asembo the ratio of female to male TB prevalence is almost 1 to 1 in the middle age categories (ages 25 to 34). This is in contrast to Gem where there is higher TB prevalence among females in the 25-30 age category and higher prevalence among males in the 30-34 age category. The TB notification data set that will be studied and analysed in the following chapters is taken from this DSA.

The data set comprises 840 notifications of all types of TB collected in Asembo and Gem by the Kenya Ministry of Health/National Leprosy and TB program and the CDC over a six year period from 1997 to 2002. Data on the treatment start-date (month and year), age, gender, and contact address (village) were abstracted from district TB registers for patients whose contact address (village) was within the DSS area. For any missing time periods in the district registers, TB registers of health facilities in the area were consulted. GIS coordinates (longitude and latitude) of the contact address (village) were added for each TB case in the data set to allow for a time/spatial analysis of the data. Figure 12.1 shows the geographical distribution of the TB notifications in the data set for the entire study period and a summary of the population demography of this study area over the same period, 1997 to 2002, is shown in table 12.1.

For input to our local and global effects model as described in Chapter 14, the

TB notification data was written in the form of a *history matrix* (as formulated in equation 14.4). Table 12.3 consists of an example history matrix formed from a sample of the western Kenyan TB data displayed in table 12.2.

Table 12.1: Summary of the population demography (age/gender) of the study area, averaged over the study period, 1997 to 2002.

% of population	Male	Female	Male and Female
≤ 15	22.6	22.7	45.3
$16 - 64$	21.3	27.9	49.2
65+	2.4	3.1	5.5
All ages	46.3	53.7	100

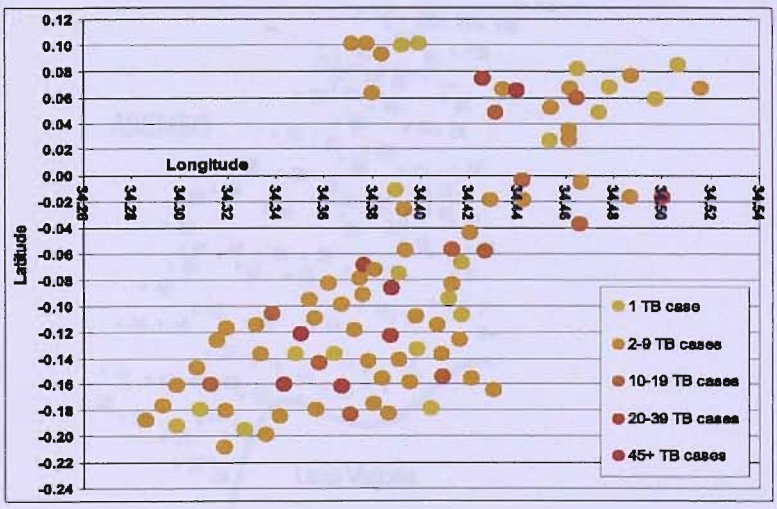

Figure 12.1: Geographical (longitude and latitude) location of the TB notifications.

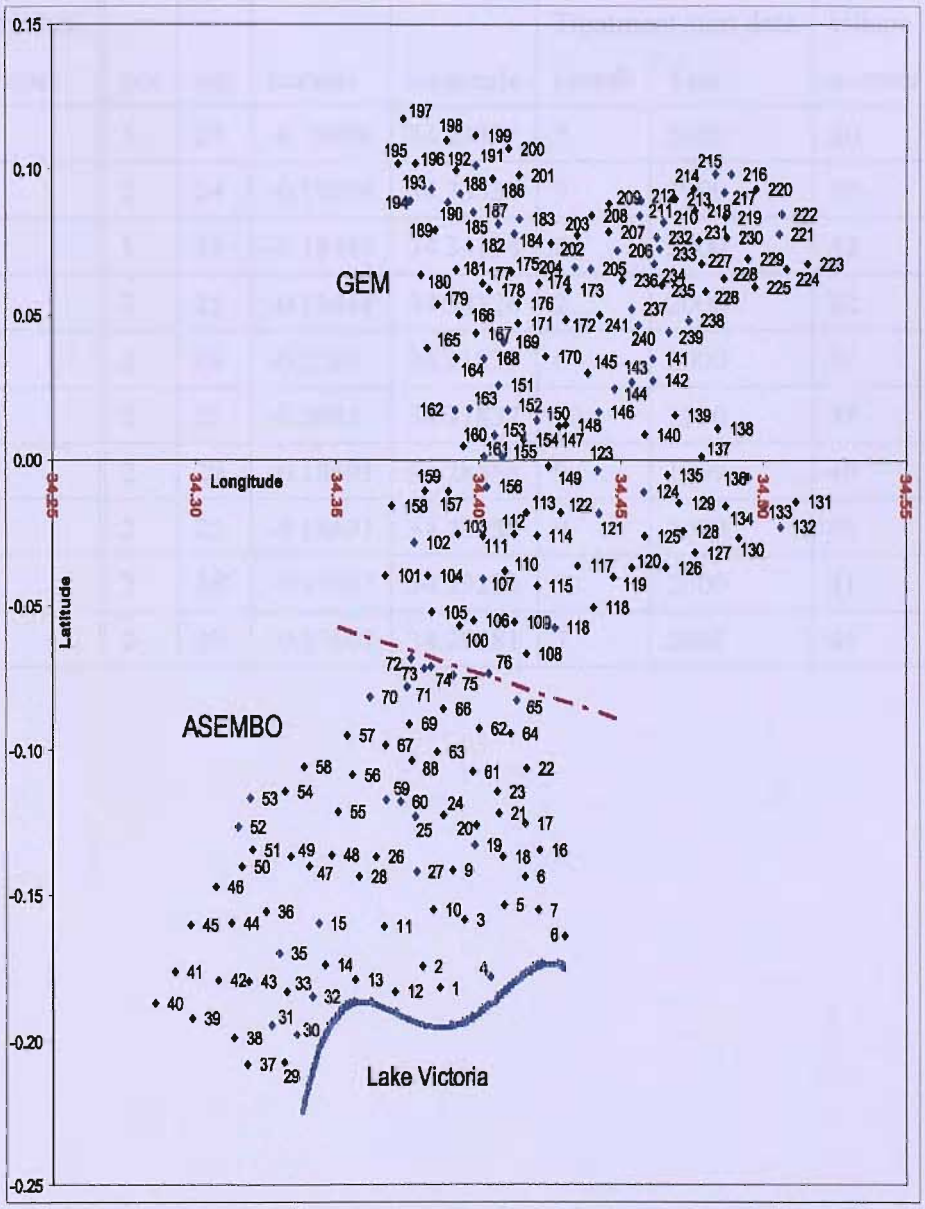

Figure 12.2: Geographical (longitude and latitude) location of the villages in the Asembo and Gem regions.

Table 12.2: Example sample of western Kenyan TB data set.

Individual Number	sex	age	latitude	longitude	Treatment start date		village number
					Month	Year	
1	1	20	-0.19806	34.33531	7	2000	30
2	2	24	-0.19806	34.33531	9	1999	30
3	1	33	-0.18448	34.34124	6	2000	32
4	2	25	-0.18448	34.34124	2	2000	32
5	2	19	-0.2083	34.31837	6	2000	37
6	2	21	-0.2083	34.31837	10	2000	37
7	2	29	-0.18691	34.28558	9	1999	40
8	2	25	-0.18691	34.28558	9	2000	40
9	2	56	-0.17607	34.29281	9	2000	41
10	2	29	-0.17607	34.29281	7	2001	41

Table 12.3: Example History Matrix.

Year	1999										2000												2001					
Month	3	4	5	6	7	8	9	10	11	12	1	2	3	4	5	6	7	8	9	10	11	12	1	2	3	4	5	6
Individual 1	0	0	0	0	0	0	0	0	0	0	1	1	1	1	1	1	0	0	0	0	0	0	0	0	0	0	0	0
Individual 2	1	1	1	1	1	1	0	0	0	0	0	0	0	0	0	0	0	0	0	0	0	0	0	0	0	0	0	0
Individual 3	0	0	0	0	0	0	0	0	0	1	1	1	1	1	1	0	0	0	0	0	0	0	0	0	0	0	0	0
Individual 4	0	0	0	0	0	1	1	1	1	1	1	0	0	0	0	0	0	0	0	0	0	0	0	0	0	0	0	0
Individual 5	0	0	0	0	0	0	0	0	0	1	1	1	1	1	1	0	0	0	0	0	0	0	0	0	0	0	0	0
Individual 6	0	0	0	0	0	0	0	0	0	0	0	0	0	1	1	1	1	1	1	0	0	0	0	0	0	0	0	0
Individual 7	1	1	1	1	1	1	0	0	0	0	0	0	0	0	0	0	0	0	0	0	0	0	0	0	0	0	0	0
Individual 8	0	0	0	0	0	0	0	0	0	0	0	0	1	1	1	1	1	1	0	0	0	0	0	0	0	0	0	0
Individual 9	0	0	0	0	0	0	0	0	0	0	0	0	1	1	1	1	1	1	0	0	0	0	0	0	0	0	0	0
Individual 10		0	0	0	0	0	0	0	0	0	0	0	0	0	0	0	0	0	0	0	0	0	1	1	1	1	1	1

0 = non-TB case; 1 = TB case.

It is assumed that an individual is infectious for 6 months before treatment starts and then becomes non-infectious.

Chapter 13

Space Time Clustering

Space-time clustering of disease is described as the interaction between the places and times of disease onset, i.e. clusters occur when cases which are close in space are also close in time [53]. The existence of such clusters is regarded as evidence of the infectiousness of the disease under study. Knox [24] considered the difficult problem of deciding whether or not a disease can be regarded as being contagious or epidemic and was the first to propose a test statistic for detecting space-time interactions/clustering. He proposed examining all possible pairs of cases, in a time/spatial data set, to ascertain whether they occurred within some fixed time distance δ of each other and whether their dates of onset were within some fixed time τ of each other. The number of pairs, X, satisfying both criteria would then be compared with the number of pairs that would be expected to satisfy the space-time criteria if the cases were randomly distributed in time and space. A value of X greater than this expectation value is therefore considered as evidence of space-time interaction and therefore clustering. Subsequently, Mantel [68], Pike and Smith [53], Symons et al. [55], Raubertas [78], Diggle et al [73], Jacquez [32], Baker [76] and Kulldorff and Hjalmars [59] have all proposed different tests for space-time interaction/clustering but the majority of methods only produce a single test statistic that rejects or supports the existence of space-time clustering but does

not detect or specify the size and location of any statistically significant clusters.

Pike and Smith [53] extend and generalise Knox's approach to incorporate the analysis of disease with a long latent period. Mantel [68] proposes a space-time interaction test where each pair of cases is assigned a value describing their geographic and temporal closeness. The test statistic is then the sum of the products of these values over all case pairs. A large value of this statistic implies the existence of space-time interaction. Symons et al. [55] used a different approach by using disease occurrence data to classify space-time cells as low-risk or high-risk cells. The high-risk cells are categorised as disease clusters, but it is only after the cells have been thus classified that a combinatorial test is used to check whether a larger number occur next to each other than would otherwise be expected if they were to be randomly distributed. Raubertas [78] proposes a method related to spatial autocorrelation techniques which are widely used to analyse geographical data [7]. However, in contrast with the preceding methods, as well as proposing tests for clustering, the analysis also specifies the contributions to clustering that is made by each time-space cell.

Kulldorff et al. [59] revisits the problem of space-time analysis with the proposal of the space-time permutation scan statistic which has been incorporated into the software package SaTScan [60]. This free software program can be used to test whether a disease is randomly distributed over time and space and to evaluate the statistical significance of reported space-time disease clusters. (The software also carries out purely spatial or temporal analysis and can perform repeated time-periodic disease surveillance for the early detection of disease outbreaks [60] [61]). The space-time scan statistic takes the form of a cylinder in space and time where the base represents the spatial dimension and the height represents the temporal dimension. The circular base is centered on each grid point in turn throughout the study region. At each of these points the radius of the base is varied continuously from zero to an upper limit determined by the user. For each grid point and size

of geographical base the height of the cylinder is also varied continuously, so that the cylinder moves through time and space covering the whole study region with an infinite number of overlapping cylinders of different sizes and shapes. Each of these cylinders denotes a possible cluster.

The space-time permutation model compares the number of cases observed in a cluster with the number expected if there was no space-time interaction. This model automatically adjusts for any purely spatial or temporal clusters. It is necessary to note that space-time clustering can also be caused by an increased risk of disease at different times and location or by changes in the distribution of the population. Due to these possible confounding factors and the fact that the space-time permutation model does not require 'population at risk' data, it is advisable to take care with the interpretation of the results when analysing case data collected over more than one year.

The SaTScan software was used to analyse the set of TB notifications collected in Asembo and Gem in western Kenya, as described in the previous chapter. Figure 13.1 shows the clusters that were detected. It should be noted that this data is collected over more than one year and therefore the above health warning regarding interpreting these results is relevant.

Tuberculosis (TB) is primarily a disease of the respiratory system with variable degrees of infectiousness. It is caused by being infected with the airborne bacterial germ *Mycobacterium tuberculosis*. Bacilli only live in the air for approximately 2 hours so individuals who have intense contact with TB bacilli in poorly ventilated areas are the most likely to become infected. TB morbidity and mortality rates are strongly affected by living conditions. Infectiousness of the source case, duration and frequency of exposure and characteristics of shared environments, all contribute to the overall risk of transmission [45].

Such characteristics of TB transmission can contribute to clustering in the in-

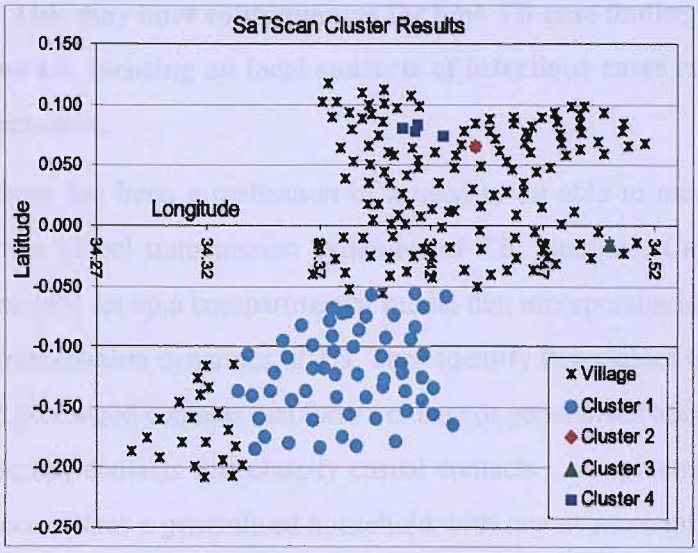

Figure 13.1: Results of analysing the Kenyan TB data set with SaTScan, using the space-time permutation model

cidence of the disease. Local factors such as a willingness to seek medical care, distance to the nearest health facility, or the skill of health care providers could cause clustering by influencing recognition and reporting of cases of tuberculosis.

Space-time clustering refers here to the interaction between places and the times of the onset of disease, i.e. cases which are close in space tend to be close in time. When this occurs it is likely, but not certain, that it reflects clustering in transmission events. Most cluster analysis investigates whether the data of interest supports a time/spatial structure or pattern and if possible seeks to establish the cause of such a pattern. However, it is already known that TB is infectious. The more important question is whether transmission in areas with high TB prevalence is fueled predominantly by the over-lying global transmission rate or can be seen to be a more localised effect.

In summary, we are concerned with determining whether a clustering (local) effect is as strong or stronger than a general global effect in respect of TB

transmission. This may have consequences for how TB case finding strategies are undertaken i.e. focusing on local contacts of infectious cases rather than the entire population.

Recently there has been a realisation of a need to be able to model the local effects on the global transmission dynamics of TB. Aparicio, Capurrio and Castillo-Chavez [45] set up a compartmental model that incorporates local effects on the global transmission dynamics of TB. They identify two classes of contacts, close daily and prolonged contacts that form a cluster or generalised household and close but infrequent contacts that classify casual contacts. An epidemiologically active cluster constitutes a generalised household with one or more infectious individuals. Deterministic epidemiological compartmental models are developed to evaluate the relative importance of TB transmission in populations with epidemiologically active clusters. Song, Castillo-Chavez and Aparicio [10] extend this work to explore the varying time scales involved. They classify TB as a 'slow' disease in that it has long and variable latency periods lasting for decades on average and relatively short infectious periods lasting for months or years. Population and individual-level transmission processes that operate on different time scales are used to construct TB epidemic models with two levels of mixing. This approach is based on the assumption that an individual's risk of infection is significantly higher from within an epidemiologically active cluster than from the general population.

In the next chapter I introduce a stochastic Markov-chain parametric model that specifically includes possible local or more dispersed global effects on the risk of contracting a communicable disease. The explicit application is to the transmission dynamics of tuberculosis, and the model is used to analyse the previously described set of TB notifications collected in Asembo and Gem in western Kenya.

Chapter 14

Kenya Model construction

14.1 Designing a Spatial Model of Disease Case Clustering.

The following is an attempt at modelling disease case clustering that focuses on trying to identify whether the nearest reported source of possible infection is a localised one stemming from an individual's contacts with family or near neighbours or whether it arises from a much more dispersed contact with people in the wider community. The model is constructed using the previously described TB data set for western Kenyan.

The basic methodology is to construct a stochastic Markov-chain model whose behaviour is determined by a number of key parameters and then fit this model to the data using the classical method of maximum likelihood (ML) in order to estimate these key parameter values (see Kendall and Stuart [58] for example). Markov-chain models are based on transition probabilities and are very different in approach from compartmental models. Examples of such latter models are given by Dye and Williams [13] and Dye et al. [15].

The model is designed to be as simple as possible whilst allowing it to distin-

guish between local and global effects.

The data comprises M (840) cases of all types of TB registered with the national tuberculosis program in the study area, in a population of some N (approximately 130,000) over a given period T (approx six years). The location (village) and date of occurrence of each notification is recorded. Population statistics (annual) are also available for each of the villages. There are V (approx 217) villages.

The model could be formulated with time treated as being continuous, however for ease of calculation time is treated as discrete. For simplicity of exposition, let the basic time step be unity and the study period be

$$t = 0, 1, 2, \ldots T. \tag{14.1}$$

A possible time step might be one month or a quarter of a year.

We also treat the population size, N, as being fixed over the period of interest. This is a reasonable simplification as the variation in population size over the study period is only 7%.

The model is constructed by following the *individual histories* of all the individuals over the study period. We write the *history* of the ith individual as the row vector

$$\underline{z}^{(i)} = \left(z_0^{(i)}, z_1^{(i)}, \ldots, z_T^{(i)}\right) \tag{14.2}$$

where $z_t^{(i)}$ is the *state* of the ith individual at time t.

It is assumed that, at any time point, the state of an individual can only be one of two prescribed states. Some TB epidemiological models allow for a large number of possible states, for example: *susceptible, latent (inactive TB), infectious, undergoing treatment, dead.* [28, 93] For simplicity our model has just two states: *case* (State 1) and *non-case* (State 0). Our model is described in terms of this two-state version.

We shall also write

$$\underline{z}_t = \left(z_t^{(1)}, z_t^{(2)}, \ldots, z_t^{(N)}\right)^T \tag{14.3}$$

to denote the column vector giving the state of all individuals at time t. Thus $\underline{z}_t$ specifies the overall state of the epidemic at time t. (The superscript T denotes transposition, so that we regard $\underline{z}_t$ as a *column* vector.)

We can therefore regard

$$\underline{Z} = (\underline{z}_0, \underline{z}_1, \ldots, \underline{z}_T) \tag{14.4}$$

as being a matrix giving a discretised form of the complete data set, with columns giving the state of the epidemic at different time points, and rows giving the histories of each individual. This shall be referred to as the *History matrix*.

$$\begin{aligned} \text{Let } a^{(i)}(k|j, \underline{z}_t) = {} & \Pr(\text{Individual } i \text{ moves to state } k \text{ in the next time step} \\ & \text{given that she/he is currently in state } j, \text{ and that} \\ & \text{the current state of the epidemic is } \underline{z}_t \,) \end{aligned} \tag{14.5}$$

This (*single step*) *transition probability* governs the individual single time-step transitions made by an individual. Notice that $a^{(i)}(k|j, \underline{z}_t)$ does not depend on t explicitly, but it will vary with time through its dependence on $\underline{z}_t$, the state of the epidemic at time t.

We now consider the form of the transition probabilities, $a^{(i)}\left(z_{t+1}^{(i)}|z_t^{(i)}, \underline{z}_t\right)$. As there are only two possible states, 0 (non-case) and 1 (case), the only possible transitions correspond, in the notation of equation 14.5, to just the four cases $(j,k) = (0,0), (0,1), (1,0), (1,1)$. Moreover the four corresponding transition probabilities must satisfy

$$a^{(i)}(0|0, \underline{z}_t) = 1 - a^{(i)}(1|0, \underline{z}_t) \tag{14.6}$$

and

$$a^{(i)}(1|1,\underline{z}_t) = 1 - a^{(i)}(0|1,\underline{z}_t) \tag{14.7}$$

i.e. Using the notation abbreviation $a_{\alpha\beta} = a^{(i)}(\alpha|\beta,\underline{z}_t), \{\alpha = 0,1; \beta = 0,1\}$ the two transition probabilities a_{00} and a_{11} can be written in terms of the other two probabilities a_{10} and a_{01}:

$$\begin{aligned} a_{00} &= \text{(probability of staying a non-case from one time step to the next)} \\ &= 1 - a_{10} \\ &= 1 - \text{(probability of moving from being a non-case to being a case} \\ &\qquad \text{in one time step.)} \end{aligned}$$

and

$$\begin{aligned} a_{11} &= \text{(probability of staying a case from one time step to the next)} \\ &= 1 - a_{01} \\ &= 1 - \text{(probability of moving from being a case to being a non-case} \\ &\qquad \text{in one time step.)} \\ &= 1 - \text{(probability of recovery in one time step)} \\ &= 1 - \left(\frac{\text{time step}}{b_2}\right), \\ &\qquad \text{where } b_2 = \text{ period of infection (specified in same units as time step)} \\ &= 1 - b_2^* \end{aligned}$$

Thus we need only specify $a^{(i)}(1|0,\underline{z}_t)$ and $a^{(i)}(0|1,\underline{z}_t)$. Figure 14.1 contains an example graphical representation of these four transition probabilities.

In terms of the propagation of TB, $a^{(i)}(1|0,\underline{z}_t)$ is the key probability as it gives the probability that a non-case (effectively, in this simple model, a susceptible) individual will become a TB case over the next time step. We can thus introduce a *parametric form* for this transition probability that enables us to include *separate*

components for the *global* and *local* clustering of TB. There are various possibilities here. A very simple form is

$$a^{(i)}(1|0,\underline{z}_t) = b_0 m_0(\underline{z}_t) + b_1 m_1^{(i)}(\underline{z}_t) + c_0 \quad (14.8)$$

where $b_0 m_0(\underline{z}_t)$ and $b_1 m_1^{(i)}(\underline{z}_t)$ are probabilities due respectively to a global effect and to a local effect, and c_0 is a generalised positive constant reflecting a background incidence component or could be thought of as the reactivation rate for TB cases. In practice c_0 can be very small and in terms of the fitted model is effectively zero. However, its retention in the model greatly simplifies the estimation process. Without c_0 the transition probability 14.8 would have to be specially redefined for the situation where the local and global prevalences both happen to be zero, and thus the transition probability 14.8 is zero which in practice causes the Loglikelihood to be inappropriately defined.

The global and local unknown (positive) parameters, b_0 and b_1, are to be estimated from the data, and $m_0(\underline{z}_t)$ and $m_1^{(i)}(\underline{z}_t)$ are measures of the prevalence of TB at the global and local level that are the cause of the respective corresponding effects.

It is important to note that the local measure of prevalence, $m_1^{(i)}(\underline{z}_t)$, is *highly dependent* on the location of the individual i. It can, for example, simply be the prevalence of TB, at time t, in the village to which i belongs. This is easily calculated from $\underline{z}_t$. Alternatively if more information is available about the activities of the individual, then possible transmission arising from regular attendance at a particular market town, work place etc.. can be modelled by taking $m_1^{(i)}(\underline{z}_t)$ to be the measure of the prevalence of TB, at time t, in the population at these locations.

The other transmission probability required is $a^{(i)}(0|1,\underline{z}_t)$, which is simply the probability of recovery in any given time step. We assume that this is not location dependent. Indeed, in our simple model, we assume that it is an unknown constant, $a^{(i)}(0|1,\underline{z}_t) = b_2^* = \frac{\text{time step}}{b_2}$. The notifications of the TB cases will be assumed

as the moment when treatment starts and the individual becomes, in the framework of the simple two-state model, non-cases and therefore 'non-infectious'. If this is correct then what is needed is an estimate of how long an individual might have been infectious for, *prior* to this notification time. In constructing the history matrix, the period of infection, b_2, is set, at present, at a notional, deterministic, six months. Thus the history matrix is built using what is effectively a prior estimate of b_2. (Although the value of b_2 is fixed it is also treated as the fourth parameter to be estimated and its resulting MLE is output as a check to the correct programming of the model).

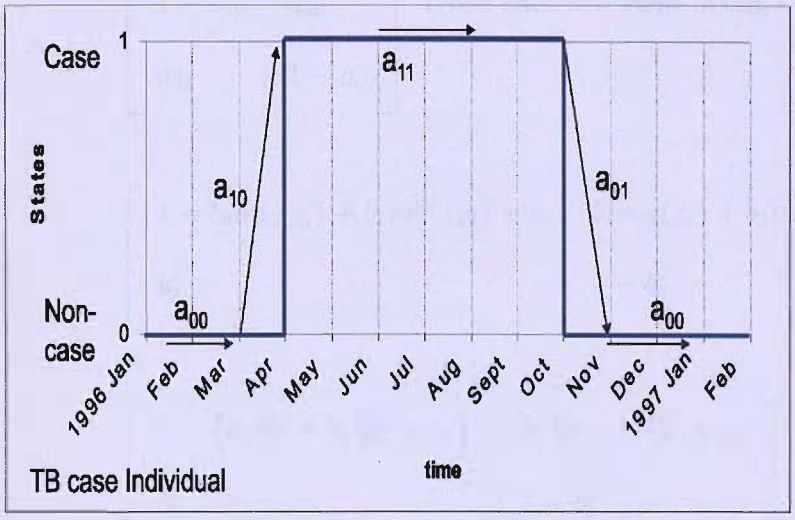

Figure 14.1: Graphical representation of the four transition probabilities for an example history of a TB case individual, using the abbreviation of notation, $a_{\alpha\beta} = a^{(i)}(\alpha|\beta, \underline{z}_t), \{\alpha = 0, 1; \beta = 0, 1\}$.

Hence this two state Markov model can be summarized by the transition probability matrix:

$$p_{t,v}^{(i)} = \begin{array}{c} \text{Current} \\ \text{State} \end{array} \begin{array}{c} \\ 0 \\ 1 \end{array} \begin{array}{c} \begin{array}{cc} \text{Next Future} & \\ \text{State} & \\ 0 & 1 \end{array} \\ \begin{bmatrix} a_{00} & a_{10} \\ a_{01} & a_{11} \end{bmatrix} \end{array}$$

$$= \begin{bmatrix} 1 - a_{10} & a_{10} \\ a_{01} & 1 - a_{01} \end{bmatrix} \quad \text{(Note each row sums to one.)}$$

$$= \begin{bmatrix} 1 - b_0 m_0\left(\underline{z}_t\right) + b_1 m_1^{(i)}\left(\underline{z}_t\right) + c_0 & b_0 m_0\left(\underline{z}_t\right) + b_1 m_1^{(i)}\left(\underline{z}_t\right) + c_0 \\ b_2^* & 1 - b_2^* \end{bmatrix}$$

$$= \begin{bmatrix} 1 - \left(b_0 \frac{M_t}{N} + b_1 \frac{M_t^v}{N^v} + c_0\right) & b_0 \frac{M_t}{N} + b_1 \frac{M_t^v}{N^v} + c_0 \\ b_2^* & 1 - b_2^* \end{bmatrix}$$

where $a_{\alpha\beta} = a^{(i)}\left(\alpha|\beta, \underline{z}_t\right); \quad \alpha = 0, 1; \beta = 0, 1$

$$\frac{M_t}{N} = \frac{\text{Total number of TB notifications at time } t}{\text{Total population}}$$

$$\frac{M_t^v}{N^v} = \frac{\text{Number of TB notifications in locality } v \text{ at time } t}{\text{Population in locality } v}$$

The *likelihood* of $\underline{z}^{(i)}$, the history of the ith individual, is defined to be the *probability of the occurrence of this particular history.* If we assume that the transitions forming $\underline{z}^{(i)}$ is a sequence of mutually independent events then this likelihood is the product of the individual transition probabilities, so that

$$lik\left(\underline{z}^{(i)}\right) = p\left(z_0^{(i)}\right)\prod_{t=0}^{T-1} a^{(i)}\left(z_{t+1}^{(i)}|z_t^{(i)},\underline{z}_t\right) \tag{14.9}$$

where $p\left(z_0^{(i)}\right)$ is the probability that the initial state of the ith individual is $z_0^{(i)}$. In practice, when coding this model in excel/VBA, the first term $p\left(z_0^{(i)}\right)$ is left out. This is a reasonable simplification due to the large number of time points used in running the model.

The total likelihood of all the histories is therefore

$$lik\left(\underline{Z}\right) = \prod_{i=1}^{N} lik\left(\underline{z}^{(i)}\right) \tag{14.10}$$

It is usually easier to work with the *loglikelihood*,

$$\begin{aligned} L\left(\underline{Z}\right) = loglik\left(\underline{Z}\right) &= \sum_{i=1}^{N}\log\left[p\left(z_0^{(i)}\right)\right] \\ &\quad + \sum_{i=1}^{N}\sum_{t=0}^{T-1}\log\left[a^{(i)}\left(z_{t+1}^{(i)}|z_t^{(i)},\underline{z}_t\right)\right] \end{aligned} \tag{14.11}$$

If b_2 is given and we use (14.8) for $a^{(i)}\left(1|0,\underline{z}_t\right)$, then the likelihood (14.11) is a function of just the three parameters b_0, b_1 and c_0, i.e.

$$L = L\left(b_0, b_1, c_0|\underline{Z}\right) \tag{14.12}$$

The *maximum likelihood estimate*(MLE) [58] of b_0, b_1 and c_0 are those that maximize $L = L\left(b_0, b_1, c_0|\underline{Z}\right)$ and are conventionally denoted $\hat{b}_0, \hat{b}_1$ and $\hat{c}_0$. It is necessary to use a numerical procedure to maximize L. The Nelder-mead optimisation method was used due to its stability and for ease of programming.

Standard asymptotic theory [81] can be used to establish the distributional properties of the MLEs $\hat{b}_0, \hat{b}_1$ and $\hat{c}_0$, including their significance. The confidence intervals for each parameter were calculated from the information matrix calculated from the negative of the inverse of the Hessian of second derivatives.

An important practical point to note is that the ML method requires the log-likelihood to be calculated repeatedly for different values of b_0, b_1 and c_0. Each loglikelihood calculation involves a summation over N, the size of the entire population. This may seem prohibitively expensive given the size of N. However the only detailed calculations required are those involving the M individuals contracting TB. The remaining $N - M$ individuals can be grouped according to the village to which they belong, so that the likelihood calculations for these non-TB individuals need only be carried out at the village level. This calculation is therefore only of order V, the number of villages, and not of order $N - M$.

Thus the total Loglikelihood, L, is calculated in practice as

$$L = \sum_{i=1}^{M} L + \sum_{j=1}^{v} n_j L_j^N$$

where L_i = log likelihood for TB case individual i; L_j^N = log likelihood for a non-case individual in locality j; and n_j = number of non-cases in locality j.

The above model formulation omits separate modelling of male/female characteristics and of age dependence, but these can be added using a more detailed transition probability structure. This is discussed in the next subsection.

14.1.1 Modeling of male/female characteristics and of age dependence

We now consider the effect of gender and age on an individual, for those individuals who do become cases during the period of study. Let $g = 1, 2$ denote the gender

(male, female), and $h = 1, 2$ denote the age-category ('child':15 years or under, 'adult':16 or over) at which notification occurs. At any time point individuals who are cases can belong to one of four categories $\{(g, h), g = 1, 2, h = 1, 2\}$.

14.1.1.1 Conditional form of the local effect coefficient

The transition probability 14.8 can be refined to

$$a^{(i)}(1|0, g, h, \underline{z}_t) = b_0 m_0(\underline{z}_t) + \sum_{j=1}^{2}\sum_{k=1}^{2} b_1(g, h|j, k)\, m_1^{(i)}(\underline{z}_t|j, k) + c_0 \quad (14.13)$$

where $m_1^{(i)}(\underline{z}_t|j, k)$ is the prevalence of those individuals in category (j = gender, k = age category), at time t, in the village of individual i, and where $b_1(g, h|j, k)$is the coefficient corresponding to the degree of influence this category (j = gender, k = age category) has on the probability that a non-case individual in category (g = gender, h = age category) will become a case in the next time step.

One problem with this formulation is that the number of unknown $b_1(.|.)$ coefficients jumps from a single unknown, in equation 14.8 to 16 unknowns: $b_1(g, h|j, k), g = 1, 2, h = 1, 2, j = 1, 2, k = 1, 2$. This is almost certainly unacceptably large.

A possible way of reducing this proliferation of coefficients is to examine the gender on its own using the model:

$$a^{(i)}(1|0, g, \underline{z}_t) = b_0 m_0(\underline{z}_t) + \sum_{j=1}^{2} b_1(g|j)\, m_1^{(i)}(\underline{z}_t|j) + c_0 \quad (14.14)$$

where the arguments g and j in $b_1(g|j)$ and $m_1^{(i)}(\underline{z}_t|j)$ refer to gender categories only. Likewise the age effect can be examined on its own using the model

$$a^{(i)}(1|0,h,\underline{z}_t) = b_0 m_0(\underline{z}_t) + \sum_{k=1}^{2} b_1(h|k)\, m_1^{(i)}(\underline{z}_t|k) + c_0 \quad (14.15)$$

where the arguments h and k in $b_1(h|k)$ and $m_1^{(i)}(\underline{z}_t|k)$ refer to age categories only. Each of these two models has only four $b_1(.|.)$ coefficients.

This conditional form of the model was found to be flawed. The results of running the age dependent model showed significance in two categories: transmission of TB from children to adults, and adults to adults. Table 14.1 shows the Maximum Likelihood Estimates for the parameters in this (two category) Age model. The significance of child to adult transmission went against all biological knowledge of TB transmission and led to a thorough re-examination of the model. It was thought that the current form of the local effect coefficient caused a misleading interpretation of the results in that it imposed a conditional causal effect.

An unconditional form of the model was subsequently formulated.

Age model:	b_0	$b_1(1,1)^*$	$b_1(1,2)^*$	$b_1(2,1)^*$	$b_1(2,2)^*$	c_0
Upper 95% CL	0.052	0.08	0.023	0.277	0.21	8.06E-06
MLE	0.043	0.032	0.015	0.189	0.19	5.48E-06
Lower 95% CL	0.034	-0.016	0.007	0.101	0.171	2.9E-06

**where,* $1 =$ *aged* ≤ 15 *and* $2 =$ *aged* $16+$.

b_2(length of infectious period) is set to 6 months.

Time step is set to one month.

Starting parameter values in optimisation procedure,for all parameters, is 0.0001.

Table 14.1: Maximum Likelihood Estimates for the conditional form of the (two category) age dependent model.

14.1.1.2 Non-conditional form of local effect coefficient

By not allowing the local effect coefficient to take conditional form the 16 previous coefficients in equation 14.13 $\{b_1(g,h|j,k) : g = 1,2, h = 1,2\}$, reduce to just four, $\{b_1(g,h) : g = 1,2; h = 1,2\} = \{b_1(1,2), b_1(2,1), b_1(1,1), b_1(2,2)\}$.

Then transition probability (14.8) can be refined to

$$\begin{aligned} a^{(i)}(1|0,g,h,\underline{z}_t) &= b_0 m_0(\underline{z}_t) \\ &\quad + b_1(g,h)\, m_1^{(i)}(\underline{z}_t) + c_0 \end{aligned} \tag{14.16}$$

where $m_1^{(i)}(\underline{z}_t)$ is the prevalence, at time t in the village of individual i and where $b_1(g,h)$ is the coefficient corresponding to the degree of influence gender and age has on the probability that a non-case individual in category (g,h) will become a case in the next time step.

An even simpler formulation with only two unknown $b_1(.|.)$ coefficients can be used to separately examine gender,

$$a^{(i)}(1|0,g,\underline{z}_t) = b_0 m_0(\underline{z}_t) + b_1(g)\, m_1^{(i)}(\underline{z}_t) + c_0 \tag{14.17}$$

and age,

$$a^{(i)}(1|0,h,\underline{z}_t) = b_0 m_0(\underline{z}_t) + b_1(h)\, m_1^{(i)}(\underline{z}_t) + c_0 \tag{14.18}$$

Further extensions included constructing models incorporating three and five age categories respectively, and a model that is both age (five categories) and gender dependent, in order to reflect age and gender dependent differences in TB and human immunodeficiency virus (HIV) incidence. However using the formulation in (14.13), a combined gender/age model with five age categories has ten unknown b_1 coefficients. This is almost certainly an unacceptably large number of parameters to have to estimate. A possible way of reducing this proliferation of coefficients is to construct two separate models: an age/male model and an age/female

model. In the first model only the TB notifications for males are used to calculate the loglikelihood and only female notifications in the second model. The global and local prevalence values are calculated using both male and female data for both models. Thus the male/age effect can be examined using the model

$$a^{(i)}(1|0,h,\underline{z}_t) = b_0 m_0(\underline{z}_t) + b_1(h|male)\, m_1(\underline{z}_t) + c_0 \qquad (14.19)$$

and the female/age effect can be examined in the same way using the model

$$a^{(i)}(1|0,h,\underline{z}_t) = b_0 m_0(\underline{z}_t) + b_1(h|female)\, m_1(\underline{z}_t) + c_0 \qquad (14.20)$$

The argument h in $b_1(h|male)$ and in $b_1(h|female)$ refers to the five age categories.

A further adaptation to the model was made by clustering the villages into 16 zones. These zones were created by grouping neighbouring villages together so that the number of people residing in each zone were roughly equal. The previously described models were then run with zones as the 'locality' marker rather than individual villages. Figure 14.2 shows the geographical (longitude and latitude) location of the villages and the 16 zone groupings for the Asembo and Gem, western Kenyan TB data set.

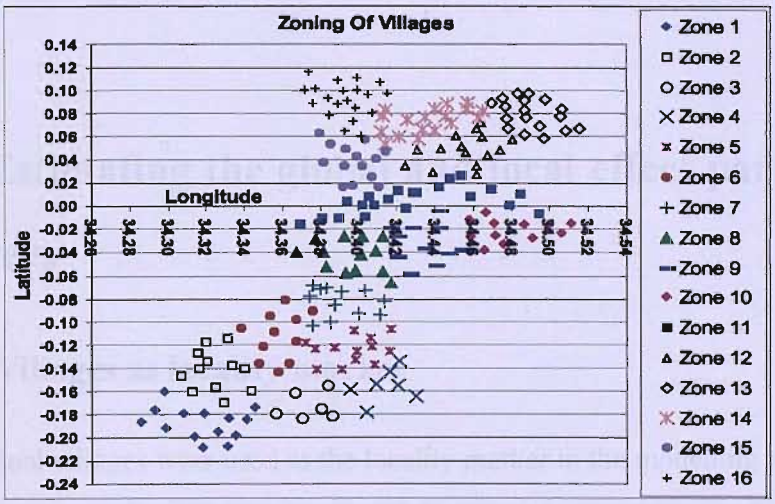

Figure 14.2: Geographical (longitude and latitude) location of the villages and the 16 zone groupings.

Chapter 15

Kenyan Model Results

15.1 Estimating the global and local effect parameters

15.1.1 Villages as locality marker

The individual villages were used as the locality marker in the modelling process. The transmission probability was structured as shown in equations (14.8) for the simple model, (14.14) for the gender model, (14.15) for the age model (with two, three or five age categories), (14.16) for the mixed age/male model and (14.17) for the mixed age/female model. Table 15.1 and 15.2 shows the Maximum Likelihood Estimates, $\hat{b}_0, \hat{b}_1$ and $\hat{c}_0$ and their corresponding 95% confidence intervals for the parameters in these seven model variations.

The transition probability of becoming a case in the next time step, (a_{10}), can be constructed using these estimated parameter values (see tables 15.3 to 15.9).

Table 15.1: Maximum Likelihood Estimates and 95% confidence intervals for the parameters in village models: Simple model, Gender model, Age model: (2 categories, 3 categories, 5 categories).

	b_0	b_1(local)					c_0
Simple model:							
Upper 95% CL	0.054	0.119					7.9E-06
MLE	0.045	0.109					5.4E-06
Lower 95% CL	0.036	0.1					2.8E-06
Gender model:		Male		Female			
Upper 95% CL	0.054	0.129		0.118			7.9E-06
MLE	0.045	0.115		0.105			5.4E-06
Lower 95% CL	0.036	0.1		0.092			2.8E-06
Age model: 1		≤ 15		16+			
Upper 95% CL	0.052	0.023		0.207			8.0E-06
MLE	0.043	0.017		0.19			5.5E-06
Lower 95% CL	0.034	0.01		0.173			2.9E-06
Age model: 2		≤ 24	$25-34$			35+	
Upper 95% CL	0.052	0.051	0.464			0.206	8.1E-06
MLE	0.043	0.043	0.405			0.182	5.5E-06
Lower 95% CL	0.034	0.035	0.346			0.157	2.9E-06
Age model: 3		≤ 15	$16-24$	$25-34$	$35-64$	65+	
Upper 95% CL	0.051	0.023	0.126	0.464	0.259	0.04	8.2E-06
MLE	0.042	0.017	0.105	0.405	0.228	0.02	5.6E-06
Lower 95% CL	0.034	0.01	0.084	0.346	0.197	-3.2E-04	3.0E-06

b_2(length of infectious period) is set to 6 months. Time step is set to one month. Starting parameter values in optimisation procedure, for all parameters, is 0.0001.

Table 15.2: Maximum Likelihood Estimates and 95% confidence intervals for the parameters in village models: Mixed Age/Male model, Mixed Age/Female model.

	b_0	b_1(local)					c_0
Age/Male model:		≤ 15	$16-29$	$30-34$	$35-64$	$65+$	
Upper 95% CL	0.06	0.019	0.143	0.85	0.398	0.085	1.2E-05
MLE	0.042	0.011	0.114	0.671	0.338	0.043	8.1E-06
Lower 95% CL	0.029	0.003	0.086	0.491	0.278	5.4E-04	3.7E-06
Age/Female model:		≤ 15	$16-24$	$25-30$	$31-64$	$65+$	
Upper 95% CL	0.055	0.032	0.176	0.526	0.207	0.018	6.3E-06
MLE	0.043	0.022	0.143	0.421	0.175	0.002	3.2E-06
Lower 95% CL	0.032	0.012	0.11	0.316	0.143	-0.013	2.2E-07

b_2(length of infectious period) is set to 6 months. Time step is set to one month.

Starting parameter values in optimisation procedure, for all parameters, is 0.0001.

Table 15.3: Estimated probability of becoming a case in the next time step (a_{10}) for the simple model with villages as the locality marker.

a_{10} = probability of becoming a case in next time step $m_1^{(v)}$ = (Local) TB prevalence in village v m_0 = (Global) TB prevalence in whole study area			
a_{10} =	0.045 m_0 +	0.109 $m_1^{(v)}$ +	5.4E-06
95% Confidence Intervals	(0.036, 0.054)	(0.1, 0.119)	(2.8E-06, 7.93E-06)
Standard deviations	0.005	0.005	1.3E-06

Table 15.4: Estimated probability of becoming a case in the next time step (a_{10}) for the gender model with villages as the locality marker.

a_{10}^{M} = probability of a male becoming a case in next time step a_{10}^{F} = probability of a female becoming a case in next time step $m_1^{(v)}$ = (Local) TB prevalence in village v m_0 = (Global) TB prevalence in whole study area			
a_{10}^{M} =	0.045 m_0 +	0.115 $m_1^{(v)}$ +	5.4E-06
95% Confidence Intervals	(0.036, 0.054)	(0.1, 0.129)	(2.8E-06, 7.9E-06)
a_{10}^{F} =	0.045 m_0 +	0.105 $m_1^{(v)}$ +	5.4E-06
95% Confidence Intervals	(0.036, 0.054)	(0.092, 0.118)	(2.8E-06, 7.9E-06)

Table 15.5: Estimated probability of becoming a case in the next time step (a_{10}) for age model (two categories) with villages as the locality marker.

$a_{10}^{(\leq 15)}$ = probability of a child (aged ≤ 15) becoming a case in next time step $a_{10}^{(16+)}$ = probability of an adult (aged ≥ 16) becoming a case in next time step $m_1^{(v)}$ = (Local) TB prevalence in village v m_0 = (Global) TB prevalence in whole study area			
$a_{10}^{(\leq 15)}$ =	0.043 m_0 +	0.017 $m_1^{(v)}$ +	5.5E-06
95% Confidence Intervals	(0.034, 0.052)	(0.01, 0.023)	(2.9E-06, 8.0E-06)
$a_{10}^{(16+)}$ =	0.043 m_0 +	0.19 $m_1^{(v)}$ +	5.5E-06
95% Confidence Intervals	(0.034, 0.052)	(0.173, 0.207)	(2.9E-06, 8.0E-06)

Table 15.6: Estimated probability of becoming a case in the next time step (a_{10}) for age model (three categories) with villages as the locality marker.

$a_{10}^{(\leq 24)}$ = probability of a person aged ≤ 24 becoming a case in next time step $a_{10}^{(25-34)}$ = probability of a person aged 25-34 becoming a case in next time step $a_{10}^{(35+)}$ = probability of a person aged 35 or over becoming a case in next time step $m_1^{(v)}$ = (Local) TB prevalence in village v m_0 = (Global) TB prevalence in whole study area			
$a_{10}^{(\leq 24)}$ =	0.043 m_0 +	0.043 $m_1^{(v)}$ +	5.5E-06
95% Confidence Intervals	(0.034, 0.052)	(0.035, 0.051)	(2.9E-06, 8.1E-06)
$a_{10}^{(25-34)}$ =	0.043 m_0 +	0.405 $m_1^{(v)}$ +	5.5E-06
95% Confidence Intervals	(0.034, 0.052)	(0.346, 0.464)	(2.9E-06, 8.1E-06)
$a_{10}^{(35+)}$ =	0.043 m_0 +	0.182 $m_1^{(v)}$ +	5.5E-06
95% Confidence Intervals	(0.034, 0.052)	(0.157, 0.206)	(2.9E-06, 8.1E-06)

Table 15.7: Estimated probability of becoming a case in the next time step (a_{10}) for age model (five categories) with villages as the locality marker.

$a_{10}^{(\leq 15)}$ = probability of a child aged ≤ 15 becoming a case in next time step
$a_{10}^{(16-24)}$ = probability of a person aged 16-24 becoming a case in next time step
$a_{10}^{(25-34)}$ = probability of a person aged 25-34 becoming a case in next time step
$a_{10}^{(35-64)}$ = probability of a person aged 35-64 becoming a case in next time step
$a_{10}^{(65+)}$ = probability of a person aged 65 or over becoming a case in next time step
$m_1^{(v)}$ = (Local) TB prevalence in village v
m_0 = (Global) TB prevalence over whole study area

$a_{10}^{(\leq 15)}$ =	0.042 m_0 +	0.017 $m_1^{(v)}$ +	5.6E-06
95% Confidence Intervals	(0.034, 0.051)	(0.01, 0.023)	(3.0E-06, 8.2E-06)
$a_{10}^{(16-24)}$ =	0.042 m_0 +	0.105 $m_1^{(v)}$ +	5.6E-06
95% Confidence Intervals	(0.034, 0.051)	(0.084, 0.126)	(3.0E-06, 8.2E-06)
$a_{10}^{(25-34)}$ =	0.042 m_0 +	0.405 $m_1^{(v)}$ +	5.6E-06
95% Confidence Intervals	(0.034, 0.051)	(0.346, 0.464)	(3.0E-06, 8.2E-06)
$a_{10}^{(35-64)}$ =	0.042 m_0 +	0.228 $m_1^{(v)}$ +	5.6E-06
95% Confidence Intervals	(0.034, 0.051)	(0.197, 0.259)	(3.0E-06, 8.2E-06)
$a_{10}^{(65+)}$ =	0.042 m_0 +	0.02 $m_1^{(v)}$ +	5.6E-06
95% Confidence Intervals	(0.034, 0.051)	(-3.2E-04, 0.04)	(3.0E-06, 8.2E-06)

Table 15.8: Estimated probability of becoming a case in the next time step (a_{10}) for male/age model (five categories) with villages as the locality marker.

$a_{10}^{M(\leq 15)}$ = probability of a boy aged ≤ 15 becoming a case in next time step
$a_{10}^{M(16-29)}$ = probability of a man aged 16-29 becoming a case in next time step
$a_{10}^{M(30-34)}$ = probability of a man aged 30-34 becoming a case in next time step
$a_{10}^{M(35-64)}$ = probability of a man aged 35-64 becoming a case in next time step
$a_{10}^{M(65+)}$ = probability of a man aged 65 or over becoming a case in next time step
$m_1^{(v)}$ = (Local) TB prevalence in village v
m_0 = (Global) TB prevalence over whole study area

$a_{10}^{M(\leq 15)}$ =	0.042 m_0 +	0.011 $m_1^{(v)}$ +	8.1E-06
95% Confidence Intervals	(0.029, 0.06)	(0.003, 0.019)	(3.7E-06, 1.2E-05)
$a_{10}^{M(16-29)}$ =	0.042 m_0 +	0.114 $m_1^{(v)}$ +	8.1E-06
95% Confidence Intervals	(0.029, 0.06)	(0.086, 0.143)	(3.7E-06, 1.2E-05)
$a_{10}^{M(30-34)}$ =	0.042 m_0 +	0.671 $m_1^{(v)}$ +	8.1E-06
95% Confidence Intervals	(0.029, 0.06)	(0.491, 0.85)	(3.7E-06, 1.2E-05)
$a_{10}^{M(35-64)}$ =	0.042 m_0 +	0.338 $m_1^{(v)}$ +	8.1E-06
95% Confidence Intervals	(0.029, 0.06)	(0.278, 0.398)	(3.7E-06, 1.2E-05)
$a_{10}^{M(65+)}$ =	0.042 m_0 +	0.043 $m_1^{(v)}$ +	8.1E-06
95% Confidence Intervals	(0.029, 0.06)	(5.4E-04, 0.085)	(3.7E-06, 1.2E-05)

Table 15.9: Estimated probability of becoming a case in the next time step (a_{10}) for female/age model (five categories) with villages as the locality marker.

$a_{10}^{F(\leq 15)}$ = probability of a girl aged ≤ 15 becoming a case in next time step $a_{10}^{F(16-24)}$ = probability of a woman aged 16-24 becoming a case in next time step $a_{10}^{F(25-30)}$ = probability of a woman aged 25-30 becoming a case in next time step $a_{10}^{F(31-64)}$ = probability of a woman aged 31-64 becoming a case in next time step $a_{10}^{F(65+)}$ = probability of a woman aged 65 or over becoming a case in next time step $m_1^{(v)}$ = (Local) TB prevalence in village v m_0 = (Global) TB prevalence over whole study area

$a_{10}^{F(\leq 15)}$ =	0.043 m_0 +	0.022 $m_1^{(v)}$ +	3.2E-06
95% Confidence Intervals	(0.032, 0.055)	(0.012, 0.032)	(2.2E-07, 6.3E-06)
$a_{10}^{F(16-24)}$ =	0.043 m_0 +	0.143 $m_1^{(v)}$ +	3.2E-06
95% Confidence Intervals	(0.032, 0.055)	(0.11, 0.176)	(2.2E-07, 6.3E-06)
$a_{10}^{F(25-30)}$ =	0.043 m_0 +	0.421 $m_1^{(v)}$ +	3.2E-06
95% Confidence Intervals	(0.032, 0.055)	(0.316, 0.526)	(2.2E-07, 6.3E-06)
$a_{10}^{F(31-64)}$ =	0.043 m_0 +	0.175 $m_1^{(v)}$ +	3.2E-06
95% Confidence Intervals	(0.032, 0.055)	(0.143, 0.207)	(2.2E-07, 6.3E-06)
$a_{10}^{F(65+)}$ =	0.043 m_0 +	0.002 $m_1^{(v)}$ +	3.2E-06
95% Confidence Intervals	(0.032, 0.055)	(-0.013, 0.018)	(2.2E-07, 6.3E-06)

The local transmission coefficient is larger than the global coefficient in all the model variations. The gender dependent model shows no significant difference between males and females. However, the age dependent models show significant differences between the various age groups. In general, the local transmission coefficient, b_1, takes a larger value in adults (ages 16+) than in children (ages $\leq$ 15). It peaks in the age range of 25-34 without gender dependence. This coefficient also takes particularly large values in the age/gender models in the expected age ranges of 30-34 for males and 25-30 in females.

The estimated correlations between the parameters for the simple model are shown in Table 15.10. The estimator for the infection period length, b_2, is effectively uncorrelated with the other parameter estimates, which is desirable. Correl$(b_0, c_0) = -0.55$ indicates, quite sensibly, that both the global effect parameter, b_0 and the background incidence component, c_0 are estimating the same global influence. Correl$(b_0, b_1) = -0.18$ indicates a small compensating relationship between the global and local effect parameters. Correl$(b_1, c_0) = 0.04$ suggests an extremely weak or no association between these parameters.

Table 15.10: Correlation matrix for the parameters in the simple village model.

	b_0	b_1	b_2	c_0
b_0	1	-0.18361	3.51E-10	-0.55122
b_1	-0.18361	1	-1.6E-10	0.03855
b_2	3.51E-10	-1.6E-10	1	-4.5E-10
c_0	-0.55122	0.03855	-4.5E-10	1

15.1.2 Zone as locality marker

The villages were assigned to 16 different zones as shown in Figures 14.2 and 15.1. This zoning was then used as the new locality marker in the modelling process. Tables 15.11 and 15.12 show the MLEs with 95% confidence intervals for the parameters in models: simple model; gender model; two, three and five category age models; mixed age/male model; mixed age/female model.

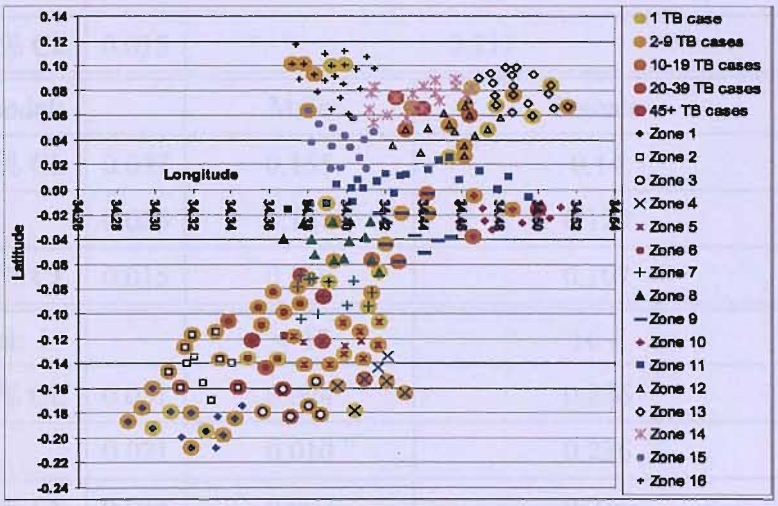

Figure 15.1: Geographical (longitude and latitude) location of the villages in the original 16 zone groupings with TB case distribution overlaid.

No significance in the models is lost by the transition to using zones rather than villages as the locality marker. There is a slight increase in the local effect and reduction in the global effect. The local transmission coefficient, b_1, peaks in the expected age ranges of 25-64 without gender dependence. This coefficient also takes particularly large values in the age/gender models in the expected age ranges of 30-34 for males and 25-30 in females.

The transition probability of becoming a case in the next time step, (a_{10}), can be constructed using these estimated parameter values (see tables 15.13 to 15.19).

Table 15.11: Maximum Likelihood Estimates for the parameters in '16 zone' models: Simple model, Gender model, Age model: (2 categories, 3 categories, 5 categories).

	b_0	b_1(local)					c_0
Simple model:							
Upper 95% CL	0.037	0.143					6.8E-06
MLE	0.026	0.13					4.5E-06
Lower 95% CL	0.015	0.117					2.2E-06
Gender model:		Male		Female			
Upper 95% CL	0.037	0.155		0.14			6.8E-06
MLE	0.026	0.137		0.123			4.5E-06
Lower 95% CL	0.015	0.119		0.107			2.2E-06
Age model: 1		≤ 15		16+			
Upper 95% CL	0.031	0.024		0.256			6.5E-06
MLE	0.021	0.016		0.236			4.3E-06
Lower 95% CL	0.011	0.007		0.216			2.2E-06
Age model: 2		≤ 24	$25-34$			35+	
Upper 95% CL	0.031	0.061	0.548			0.252	7.2E-06
MLE	0.021	0.051	0.484			0.223	4.8E-06
Lower 95% CL	0.011	0.040	0.42			0.194	2.5E-06
Age model: 3		≤ 15	$16-24$	$25-34$	$35-64$	65+	
Upper 95% CL	0.028	0.025	0.161	0.55	0.32	0.043	6.9E-06
MLE	0.019	0.016	0.136	0.487	0.284	0.02	4.7E-06
Lower 95% CL	0.009	0.008	0.111	0.423	0.248	-0.002	2.4E-06

b_2(length of infectious period) is set to 6 months. Time step is set to one month. Starting parameter values in optimisation procedure, for all parameters, is 0.0001.

Table 15.12: Maximum Likelihood Estimates for the parameters in '16 zone' models: Mixed Age/Male model, Mixed Age/Female model.

	b_0	b_1(local)					c_0
Age/Male model:		≤ 15	$16-29$	$30-34$	$35-64$	$65+$	
Upper 95% CL	0.03	0.023	0.186	0.909	0.501	0.095	1.1E-05
MLE	0.016	0.012	0.152	0.728	0.431	0.047	7.2E-06
Lower 95% CL	0.002	6.8E-04	0.118	0.547	0.362	-6E-04	3.3E-06
Age/Female model:		≤ 15	$16-24$	$25-30$	$31-64$	$65+$	
Upper 95% CL	0.035	0.034	0.225	0.631	0.246	0.018	4.4E-06
MLE	0.022	0.021	0.186	0.516	0.209	3E-06	2.2E-06
Lower 95% CL	0.009	0.008	0.147	0.401	0.173	-0.018	-1E-07

b_2(length of infectious period) is set to 6 months. Time step is set to one month.

Starting parameter values in optimisation procedure, for all parameters, is 0.0001.

Table 15.13: Estimated probability of becoming a case in the next time step (a_{10}) for the simple model with zone as the locality marker.

a_{10} = probability of becoming a case in next time step $m_1^{(z)}$ = (Local) TB prevalence in zone z m_0 = (Global) TB prevalence in whole study area			
a_{10} =	0.026 m_0 +	0.13 $m_1^{(z)}$ +	4.5E-06
95% Confidence Intervals	(0.015, 0.037)	(0.117, 0.143)	(2.2E-06, 6.8E-06)
Standard deviations	0.006	0.007	1.2E-06

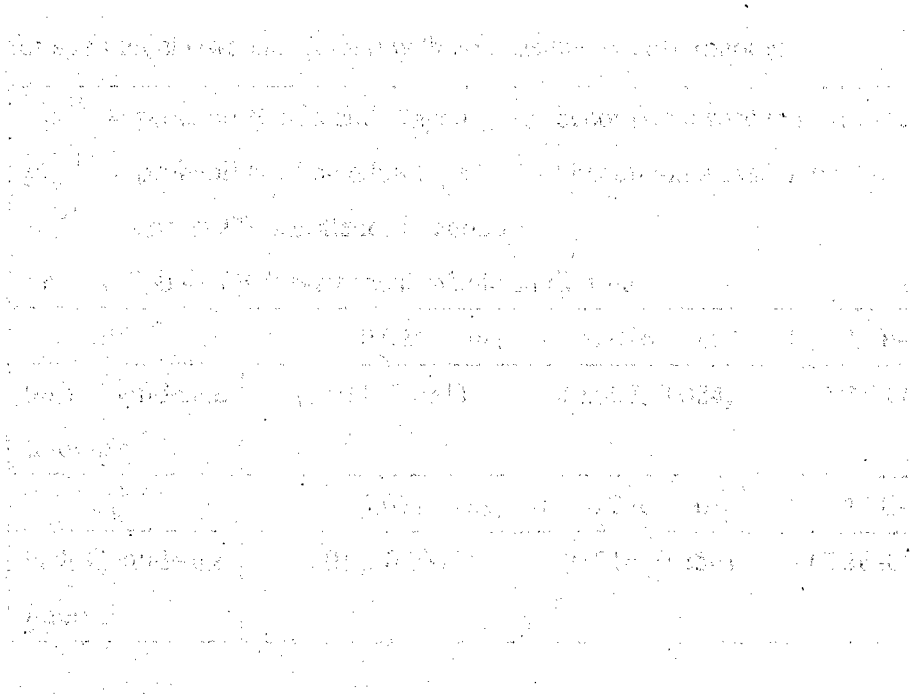

Table 15.14: Estimated probability of becoming a case in the next time step (a_{10}) for the gender model with zone as the locality marker.

a_{10}^{M} = probability of a male becoming a case in next time step a_{10}^{F} = probability of a female becoming a case in next time step $m_1^{(z)}$ = (Local) TB prevalence in zone z m_0 = (Global) TB prevalence in whole study area			
a_{10}^{M} =	0.026 m_0 +	0.137 $m_1^{(z)}$ +	4.5E-06
95% Confidence Intervals	(0.015, 0.037)	(0.119, 0.155)	(2.2E-06, 6.8E-06)
a_{10}^{F} =	0.026 m_0 +	0.123 $m_1^{(z)}$ +	4.5E-06
95% Confidence Intervals	(0.015, 0.037)	(0.107, 0.14)	(2.2E-06, 6.8E-06)

Table 15.15: Estimated probability of becoming a case in the next time step (a_{10}) for age model (two categories) with zone as the locality marker.

$a_{10}^{(\leq 15)}$ = probability of a child (aged $\leq$ 15) becoming a case in next time step $a_{10}^{(16+)}$ = probability of an adult (aged $\geq$ 16) becoming a case in next time step $m_1^{(z)}$ = (Local) TB prevalence in zone z m_0 = (Global) TB prevalence in whole study area			
$a_{10}^{(\leq 15)}$ =	0.021 m_0 +	0.016 $m_1^{(z)}$ +	4.3E-06
95% Confidence Intervals	(0.011, 0.031)	(0.007, 0.024)	(2.2E-06, 6.5E-06)
$a_{10}^{(16+)}$ =	0.021 m_0 +	0.236 $m_1^{(z)}$ +	4.3E-06
95% Confidence Intervals	(0.011, 0.031)	(0.216, 0.256)	(2.2E-06, 6.5E-06)

Table 15.16: Estimated probability of becoming a case in the next time step (a_{10}) for age model (three categories) with zones as the locality marker.

$a_{10}^{(\leq 24)}$ = probability of a person aged ≤ 24 becoming a case in next time step $a_{10}^{(25-34)}$ = probability of a person aged 25-34 becoming a case in next time step $a_{10}^{(35+)}$ = probability of a person aged 35 or over becoming a case in next time step $m_1^{(z)}$ = (Local) TB prevalence in zone z m_0 = (Global) TB prevalence in whole study area			
$a_{10}^{(\leq 24)}$ =	0.021 m_0 +	0.051 $m_1^{(z)}$ +	4.8E-06
95% Confidence Intervals	(0.011, 0.031)	(0.04, 0.061)	(2.5E-06, 7.2E-06)
$a_{10}^{(25-34)}$ =	0.021 m_0 +	0.484 $m_1^{(z)}$ +	4.8E-06
95% Confidence Intervals	(0.011, 0.031)	(0.42, 0.548)	(2.5E-06, 7.2E-06)
$a_{10}^{(35+)}$ =	0.021 m_0 +	0.223 $m_1^{(z)}$ +	4.8E-06
95% Confidence Intervals	(0.011, 0.031)	(0.194, 0.252)	(2.5E-06, 7.2E-06)

Table 15.17: Estimated probability of becoming a case in the next time step (a_{10}) for age model (five categories) with zones as the locality marker.

$a_{10}^{(\leq 15)}$ = probability of a child aged ≤ 15 becoming a case in next time step
$a_{10}^{(16-24)}$ = probability of a person aged 16-24 becoming a case in next time step
$a_{10}^{(25-34)}$ = probability of a person aged 25-34 becoming a case in next time step
$a_{10}^{(35-64)}$ = probability of a person aged 35-64 becoming a case in next time step
$a_{10}^{(65+)}$ = probability of a person aged 65 or over becoming a case in next time step
$m_1^{(z)}$ = (Local) TB prevalence in zone z
m_0 = (Global) TB prevalence over whole study area

$a_{10}^{(\leq 15)}$ =	0.019 m_0 +	0.016 $m_1^{(z)}$ +	4.7E-06
95% Confidence Intervals	(0.009, 0.028)	(0.008, 0.025)	(2.4E-06, 6.9E-06)
$a_{10}^{(16-24)}$ =	0.019 m_0 +	0.136 $m_1^{(z)}$ +	4.7E-06
95% Confidence Intervals	(0.009, 0.028)	(0.111, 0.161)	(2.4E-06, 6.9E-06)
$a_{10}^{(25-34)}$ =	0.019 m_0 +	0.487 $m_1^{(z)}$ +	4.7E-06
95% Confidence Intervals	(0.009, 0.028)	(0.423, 0.55)	(2.4E-06, 6.9E-06)
$a_{10}^{(35-64)}$ =	0.019 m_0 +	0.284 $m_1^{(z)}$ +	4.7E-06
95% Confidence Intervals	(0.009, 0.028)	(0.248, 0.32)	(2.4E-06, 6.9E-06)
$a_{10}^{(65+)}$ =	0.019 m_0 +	0.02 $m_1^{(z)}$ +	4.7E-06
95% Confidence Intervals	(0.009, 0.028)	(-0.002, 0.043)	(2.4E-06, 6.9E-06)

Table 15.18: Estimated probability of becoming a case in the next time step (a_{10}) for male/age model (five categories) with zones as the locality marker.

$a_{10}^{M(\leq 15)}$ = probability of a boy aged ≤ 15 becoming a case in next time step
$a_{10}^{M(16-29)}$ = probability of a man aged 16-29 becoming a case in next time step
$a_{10}^{M(30-34)}$ = probability of a man aged 30-34 becoming a case in next time step
$a_{10}^{M(35-64)}$ = probability of a man aged 35-64 becoming a case in next time step
$a_{10}^{M(65+)}$ = probability of a man aged 65 or over becoming a case in next time step
$m_1^{(z)}$ = (Local) TB prevalence in zone z
m_0 = (Global) TB prevalence over whole study area

$a_{10}^{M(\leq 15)}$ =	0.016 m_0 +	0.012 $m_1^{(z)}$ +	7.2E-06
95% Confidence Intervals	(0.002, 0.03)	(6.8E-04, 0.023)	(3.3E-06, 1.1E-05)
$a_{10}^{M(16-29)}$ =	0.016 m_0 +	0.152 $m_1^{(z)}$ +	7.2E-06
95% Confidence Intervals	(0.002, 0.03)	(0.118, 0.186)	(3.3E-06, 1.1E-05)
$a_{10}^{M(30-34)}$ =	0.016 m_0 +	0.728 $m_1^{(z)}$ +	7.2E-06
95% Confidence Intervals	(0.002, 0.03)	(0.547, 0.909)	(3.3E-06, 1.1E-05)
$a_{10}^{M(35-64)}$ =	0.016 m_0 +	0.431 $m_1^{(z)}$ +	7.2E-06
95% Confidence Intervals	(0.002, 0.03)	(0.362, 0.501)	(3.3E-06, 1.1E-05)
$a_{10}^{M(65+)}$ =	0.016 m_0 +	0.047 $m_1^{(z)}$ +	7.2E-06
95% Confidence Intervals	(0.002, 0.03)	(-6E-04, 0.095)	(3.3E-06, 1.1E-05)

Table 15.19: Estimated probability of becoming a case in the next time step (a_{10}) for female/age model (five categories) with zones as the locality marker.

$a_{10}^{F(\leq 15)}$ = probability of a girl aged ≤ 15 becoming a case in next time step
$a_{10}^{F(16-24)}$ = probability of a woman aged 16-24 becoming a case in next time step
$a_{10}^{F(25-30)}$ = probability of a woman aged 25-30 becoming a case in next time step
$a_{10}^{F(31-64)}$ = probability of a woman aged 31-64 becoming a case in next time step
$a_{10}^{F(65+)}$ = probability of a woman aged 65 or over becoming a case in next time step
$m_1^{(z)}$ = (Local) TB prevalence in zone z
m_0 = (Global) TB prevalence over whole study area

$a_{10}^{F(\leq 15)}$ =	0.022 m_0 +	0.021 $m_1^{(z)}$ +	2.2E-06
95% Confidence Intervals	(0.009, 0.035)	(0.008, 0.034)	(-1E-07, 4.4E-06)
$a_{10}^{F(16-24)}$ =	0.022 m_0 +	0.186 $m_1^{(z)}$ +	2.2E-06
95% Confidence Intervals	(0.009, 0.035)	(0.147, 0.225)	(-1E-07, 4.4E-06)
$a_{10}^{F(25-30)}$ =	0.022 m_0 +	0.516 $m_1^{(z)}$ +	2.2E-06
95% Confidence Intervals	(0.009, 0.035)	(0.401, 0.631)	(-1E-07, 4.4E-06)
$a_{10}^{F(31-64)}$ =	0.022 m_0 +	0.209 $m_1^{(z)}$ +	2.2E-06
95% Confidence Intervals	(0.009, 0.035)	(0.173, 0.246)	(-1E-07, 4.4E-06)
$a_{10}^{F(65+)}$ =	0.022 m_0 +	3E-06 $m_1^{(z)}$ +	2.2E-06
95% Confidence Intervals	(0.009, 0.035)	(-0.018, 0.018)	(-1E-07, 4.4E-06)

The estimated correlations between the parameters in the simple model are shown in Table 15.20. As with the village results, the estimator for the infectious period length, b_2, is effectively uncorrelated with the other parameter estimates. Correl$(b_0, c_0) = -0.46$ again indicates that both b_0 and c_0 are estimating the same global influence and Correl$(b_0, b_1) = -0.54$ indicates a stronger compensating relationship between the global and local effect coefficients than when the individual villages was used as the locality measure. This is to be expected because the local effect is now measured over a larger geographical area and therefore the distinction between local and global influences are not as marked as before.

Table 15.20: Correlation matrix for the parameters in the simple 16 zones model.

	b_0	b_1	b_2	c_0
b_0	1	-0.53631	5.45E-10	-0.46115
b_1	-0.53631	1	-2.5E-10	0.089507
b_2	5.45E-10	-2.5E-10	1	-3.4E-10
c_0	-0.46115	0.089507	-3.4E-10	1

15.1.3 Testing the robustness of the modelling procedure.

In this section a number of tests are presented which were used to test the robustness of the model.

The first test is simply to demonstrate that the importance of local prevalence was not simply an artifact of the modelling. The TB notifications were randomly assigned to the 217 villages and the simple model then fitted to this new data. This was repeated several times. The resulting MLE values and 95% CIs were similar in each run. Table 15.21 shows a typical set of results and in these tests the local effect becomes not significant.

Table 15.21: Maximum Likelihood Estimates for the parameters in the simple model when TB cases are randomly assigned to the 217 villages.

	b_0	b_1	c_0
Upper 95% CL	0.165	0.011	6.4E-06
MLE	0.15	0.005	4.0E-06
Lower 95% CL	0.136	-0.001	1.6E-06

b_2(length of infectious period) is set to 6 months.

Time step is set to one month.

Starting parameter values in optimisation procedure, for all parameters, is 0.0001.

15.1.3.1 The effect of decreasing sample size (M) on the fitting of the simple model.

To examine the effect of changes in the observed prevalence in the data, TB notification data was randomly deleted and the MLEs of b_0, b_1 and c_0 and their 95% CIs calculated for differing M. As the number of TB notification data points decreases, the significance of local TB prevalence is lost in the model and superseded by the global prevalence. The background prevalence parameter c_0 decreases in negative correlation with the global parameter b_0 as expected. These results can be used to estimate the sample size (M) required to detect significant effects. Figures 15.2 to 15.7 show the resulting estimated parameter values. Although only two representative runs are depicted for brevity, results of repeated runs remain very similar in that the confidence interval widths remain stable for the larger sample sizes. For the local and global parameter estimates, $\hat{b}_1$ and $\hat{b}_0$, these intervals remain distinct until M has decreased to approximately 350. This gives a clear indication that M needs to be of this order to detect a difference between local and global effects of the size observed. The confidence intervals for $\hat{b}_2$ increase in width with decreasing sample size M as would be expected. In contrast, it is interesting to note that

the confidence intervals for $\hat{c}_0$ decrease in width as sample size decreases. This may be due to the negative correlation between c_0 and global parameter b_0. As the $\hat{b}_0$ value and 95% confidence interval width both increase, the $\hat{c}_0$ value and 95% confidence interval width both decrease.

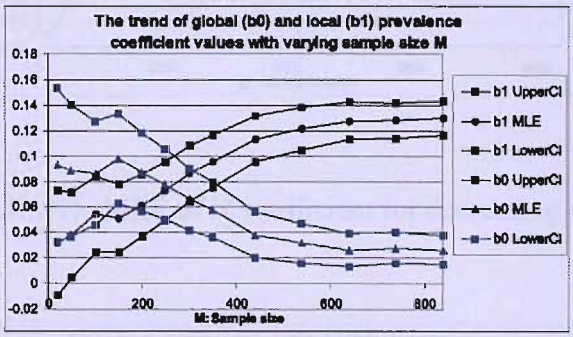

Figure 15.2: RUN1: MLE of global and local prevalence coefficients b_0 and b_1 for decreasing sample sizes.

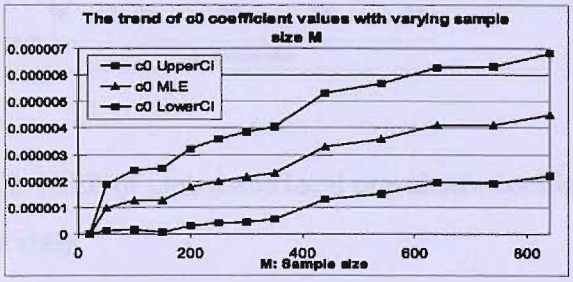

Figure 15.3: RUN1: MLE of c_0 coefficient for decreasing sample sizes.

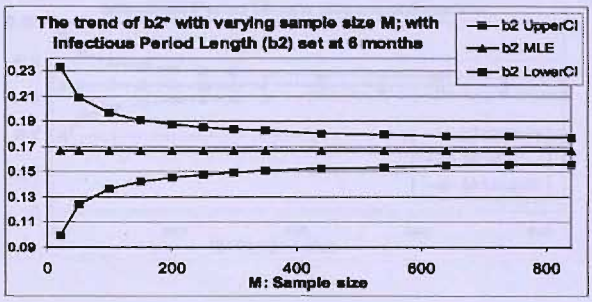

Figure 15.4: RUN1: MLE of b_2^* coefficient for decreasing sample sizes.

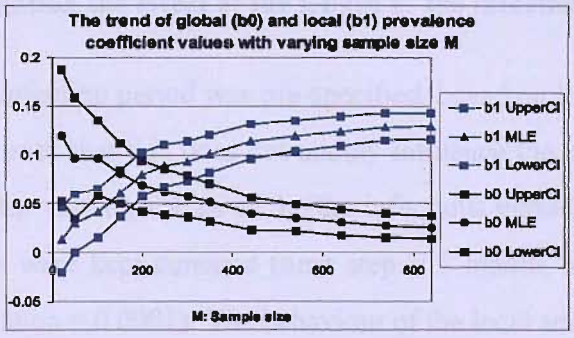

Figure 15.5: RUN2: MLE of global and local prevalence coefficients b_0 and b_1 for decreasing sample sizes.

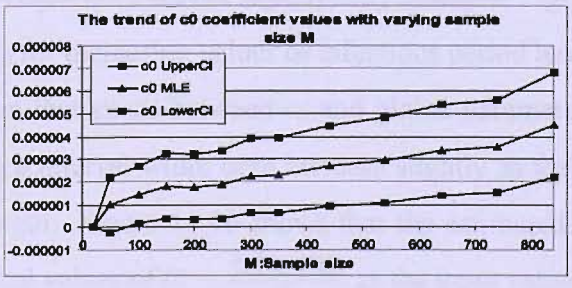

Figure 15.6: RUN2: MLE of c_0 coefficient for decreasing sample sizes.

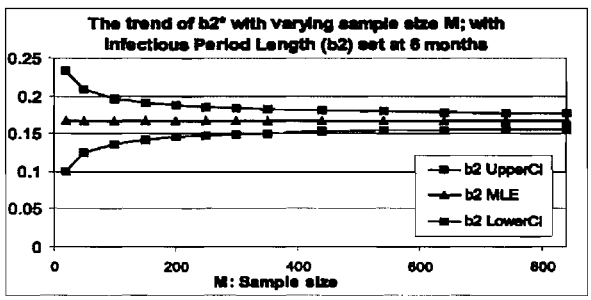

Figure 15.7: RUN2: MLE of b_2^* coefficient for decreasing sample sizes.

15.1.3.2 Investigating the effect of the length of the infectious period b_2

The length of the infection period was pre-specified, based on known characteristics of TB. As a check that this does not unduly influence the results, the simple model was fitted for varying values of b_2 (the infectious period length) while all other input values were kept constant (time step = 1 month, starting parameter values for optimisation = 0.0001). The behaviour of the local and global effect parameters, b_1 and b_0 (shown in Figure 15.8) is consistent with how we would expect them to behave as b_2 changes. With a longer infectious period length, the model would expect there to be more TB notifications than the 840 provided. Thus, the values of b_1 and b_0 decrease as the length of the infectious period increases. However their relative magnitudes are not significantly changed. Figure 15.9 shows the estimated values $\hat{c}_0$ for increasing values of infectious period length b_2. Due to the negative correlation that exists between c_0 and global parameter b_0, the $\hat{c}_0$ value and 95% confidence interval width both increase slightly as the infectious period b_2 increases in length. Figure 15.10 shows that the estimated values $\hat{b}_2^*$ closely match the theoretical values of $b_2^* = \frac{\text{time step}}{b_2}$ as the input value of b_2 increases.

This investigation was also carried out with the 5 category age model and very similar results were obtained as is shown in figures 15.9 to 15.18.

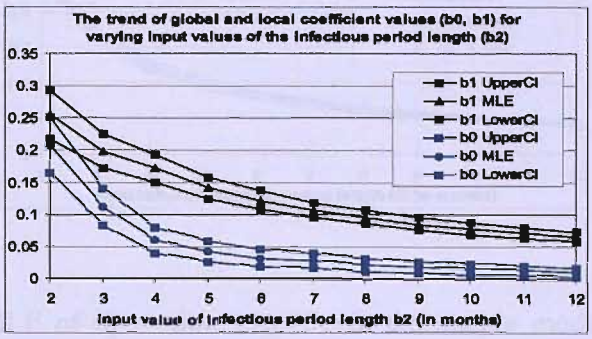

Figure 15.8: MLE of global and local prevalence coefficients (b_0, b_1)in the simple model, for increasing infectious period length b_2.

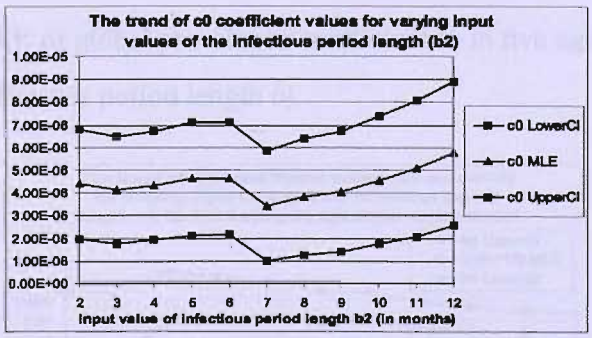

Figure 15.9: MLE of c_0 coefficient in the simple model, for increasing infectious period length b_2.

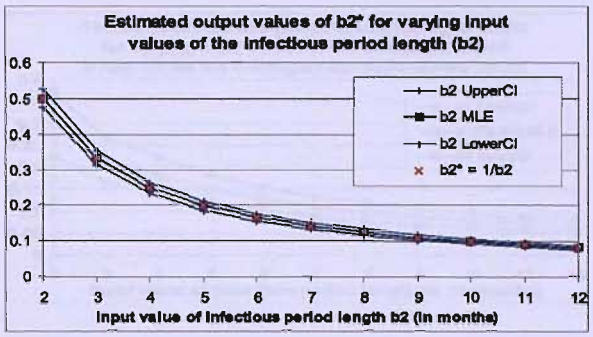

Figure 15.10: MLE of $b_2^* =$ time step$/b_2$, in the simple model, for increasing infectious period length b_2.

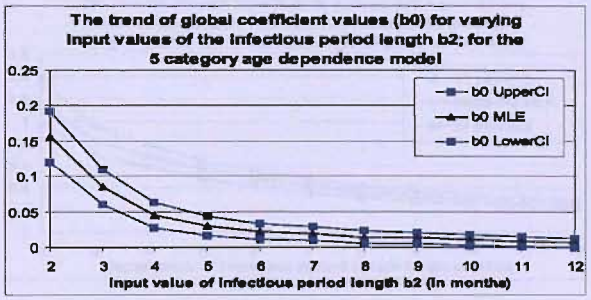

Figure 15.11: MLE of global prevalence coefficient b_0 in five age category model, for increasing infectious period length b_2.

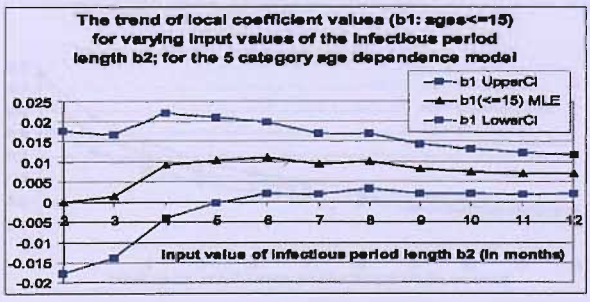

Figure 15.12: Age Model results: MLE of local prevalence coefficient b_1: ages 0-15, for increasing infectious period length b_2.

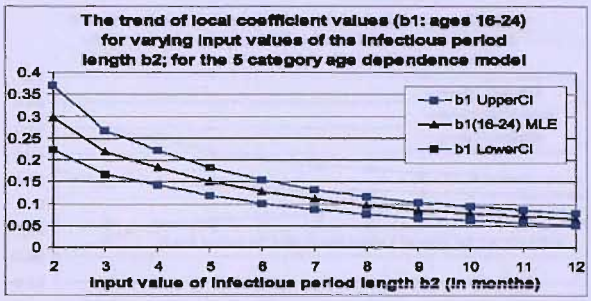

Figure 15.13: Age Model results: MLE of local prevalence coefficient b_1: ages 16-24, for increasing infectious period length b_2.

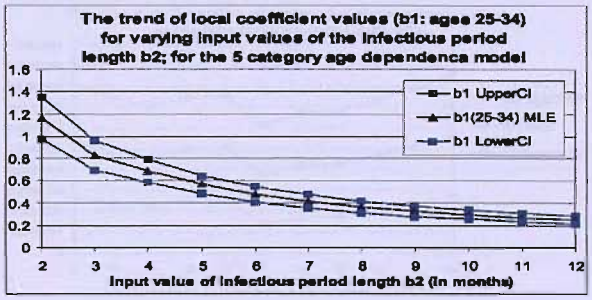

Figure 15.14: Age Model results: MLE of local prevalence coefficient b_1: ages 25-34, for increasing infectious period length b_2.

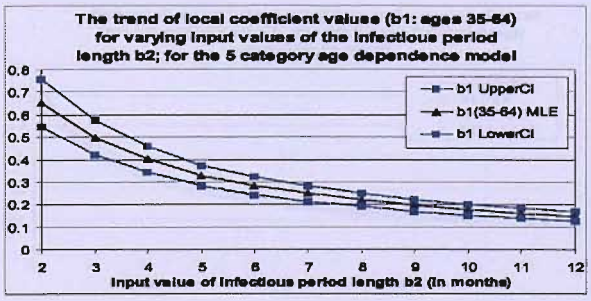

Figure 15.15: Age Model results: MLE of local prevalence coefficient b_1: ages 35-64, for increasing infectious period length b_2.

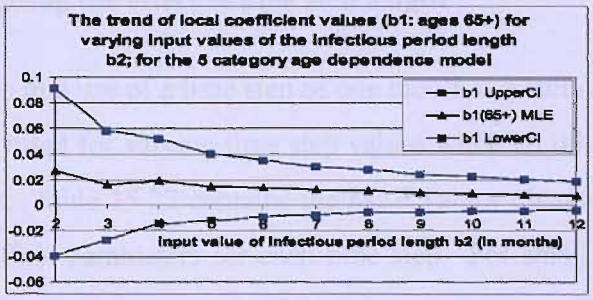

Figure 15.16: Age Model results: MLE of local prevalence coefficient b_1: ages $65+$, for increasing infectious period length b_2.

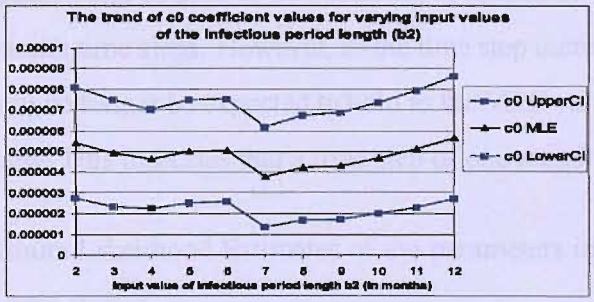

Figure 15.17: MLE of coefficient c_0 in the five age category model, for increasing infectious period length b_2.

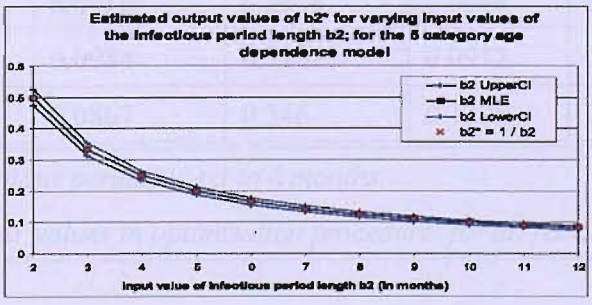

Figure 15.18: MLE of $b_2^* = \text{time step}/b_2$ in the five age category model, for increasing infectious period length b_2.

15.1.3.3 Investigating the effect of time step length

The next test shows that use of a time step of one month is a suitable choice. The simple model was fitted for varying time step values while all other input values were kept constant. Table 15.22 contains the MLE values obtained for both the global and local effect parameters for each time step. For small time steps the transition probabilities can be considered to behave in a linear fashion because in this situation the linear term dominates quadratic and higher order terms, this becoming progressively more marked as the step size decreases. Therefore if the time step is doubled the parameter values would be expected to approximately double also. This pattern can be seen to be occurring in figures 15.19 to 15.21 for the two and three month time steps. However, as the time step increases in size the linearity property can no longer be expected to hold as the MLE values for the four month time step show. This indicates that a time step of one month is satisfactory.

Table 15.22: Maximum Likelihood Estimates of the parameters in the simple model for varying lengths of time step.

Time step (ts) length (in months)	Global effect MLE (b_0)	Local effect MLE (b_1)	ts $\times b_0^{(ts=1)}$	ts $\times b_1^{(ts=1)}$
1	0.0324	0.1214		
2	0.0619	0.2338	0.0648	0.2427
3	0.0984	0.3262	0.0972	0.3641
4	0.0867	0.346	0.1295	0.4854

b_2(length of infectious period) is set to 6 months.

Starting parameter values in optimisation procedure, for all parameters, is 0.0001.

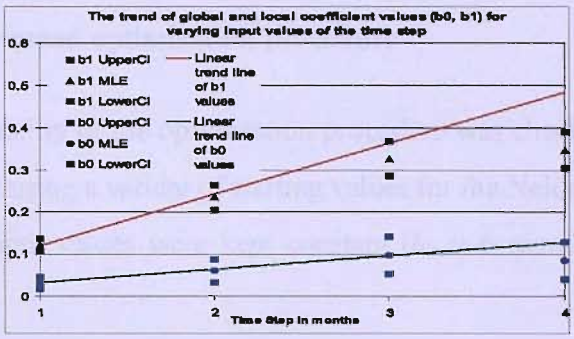

Figure 15.19: MLE of Local and Global effect coefficient for varying time step lengths.

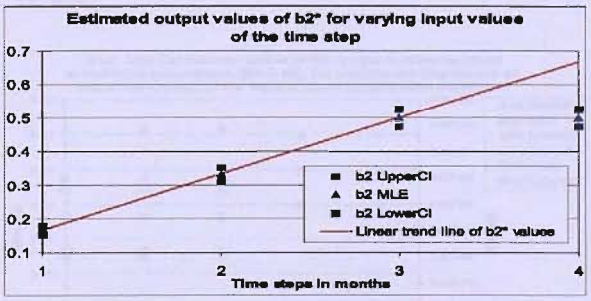

Figure 15.20: MLE of $b_2^* = \text{time step}/b_2$ for varying time step lengths.

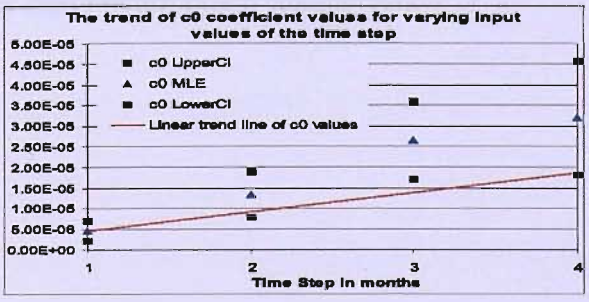

Figure 15.21: MLE of c_0 coefficient for varying time step lengths.

15.1.3.4 Investigating the effect of different starting parameter values in the Nelder-mead optimisation procedure

The numerical stability of the optimisation procedure was checked for the simple model by fitting it using a variety of starting values for the Nelder-mead algorithm while all other input values were kept constant (b_2 = 6 months, time step = 1 month).

The starting value of c_0 seemed to be the most influential prompting a complimentary change in the MLEs of both c_0 and b_0 as illustrated in Figure 15.22. This is not surprising in light of the negative correlation between these two parameters. Parameter estimates for b_1 and b_2^* were hardly affected as can be seen in figures 15.23 and 15.24.

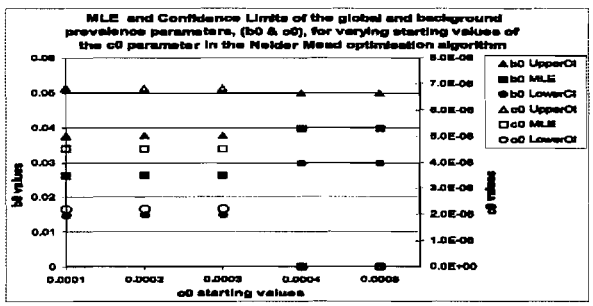

Figure 15.22: MLE of Global and background prevalence coefficients (b_0 and c_0) for varying Nelder-mead optimisation starting values of c_0.

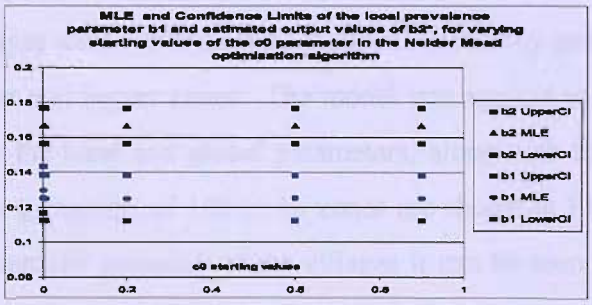

Figure 15.23: MLE of local prevalence coefficient b_1 and parameter b_2^* for varying Nelder-mead optimisation starting values of c_0.

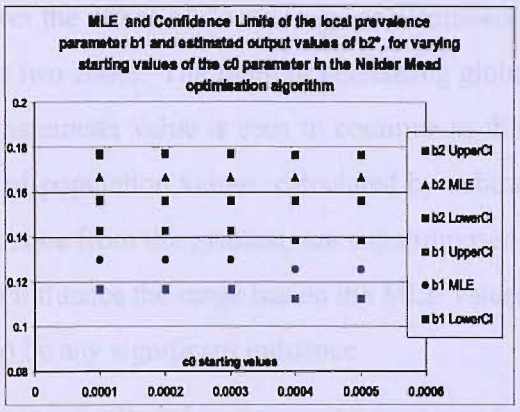

Figure 15.24: MLE of local prevalence coefficient b_1 and b_2^* for varying Nelder-mead optimisation starting values of c_0, between 0.0001 and 0.0005.

15.1.3.5 Investigating the effect of different sizes of zone

In order to investigate the model's sensitivity to the spatial scale of disease clustering the 240 villages were systematically grouped together by gathering adjacent villages into bigger and bigger zones. The model was applied to each grouping and the MLEs for the local and global parameters, along with their 95% confidence intervals for groupings of 108 to 16 zones are shown in Figure 15.26. In this particular systematic grouping of the villages it can be seen that the global and local MLE values stay relatively consistent up to the grouping of 40 zones. After this point, as the number of zones decrease (and the zone size increases), the global parameter value decreases as the local parameter shows a slight increasing trend. A control was also set up where the villages were randomly assigned to progressively larger zones. The corresponding results for these random groupings are shown in Figure 15.27. The random zoning did not show the same trend as the systematic zoning. For large zone size (and therefore small numbers of zones, 20 or less) the global and local effects become less distinct.

Figure 15.25 shows the effect of decreasing zone numbers from the original 16 zones down to just two zones. The trend of decreasing global parameter value and increasing local parameter value is seen to continue as the number of zones decrease. The range of population values, calculated by subtracting the smallest population value in a zone from the greatest, are superimposed in figure 15.25 to investigate how much influence the range has on the MLE values. From this graph there does not seem to be any significant influence.

The MLE $\hat{b}_2^*$ value is not affected by increasing zone size for either systematic or random groupings of villages, (see figures 15.28 to 15.30).

The coefficient $\hat{c}_0$ value for both systematic and random groupings of villages is relatively consistent until the number of zones is decreased to approximately 20. The $\hat{c}_0$ value then seems to decrease in negative correlation with the $\hat{b}_0$ value.

This trend is more pronounced when the villages are systematically grouped (see figures 15.31 to 15.33).

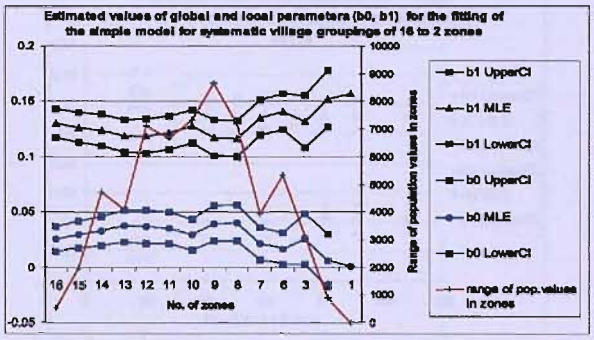

Figure 15.25: MLE of global and local prevalence coefficients, b_0, b_1, for the systematic grouping of villages into increasing zone sizes (and thus decreasing numbers of zones: 16 to 2).

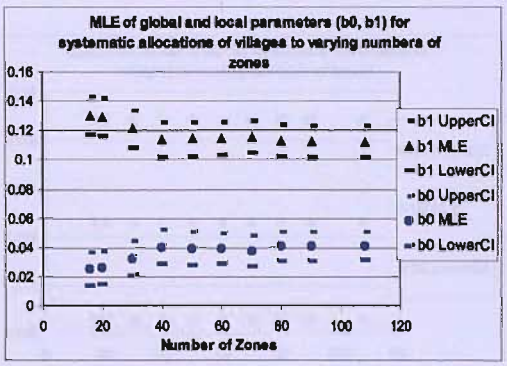

Figure 15.26: MLE of global and local prevalence coefficients, b_0, b_1, for the systematic grouping of villages into increasing zone sizes (and thus decreasing numbers of zones: 108 to 16).

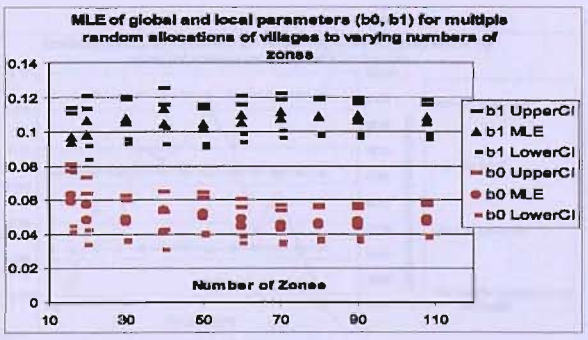

Figure 15.27: MLE of global and local prevalence coefficients, b_0, b_1, for the random grouping of villages into increasing zone sizes (and thus decreasing numbers of zones).

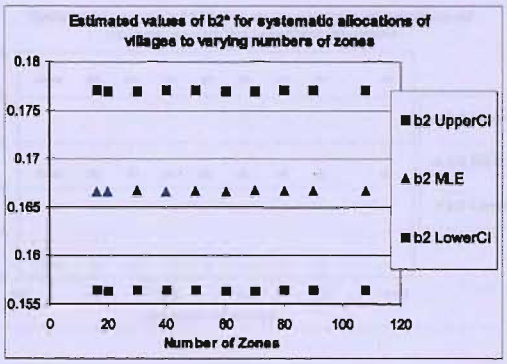

Figure 15.28: MLE of b_2^* coefficient for the systematic grouping of villages into increasing zone sizes (and thus decreasing numbers of zones: 108 to 16).

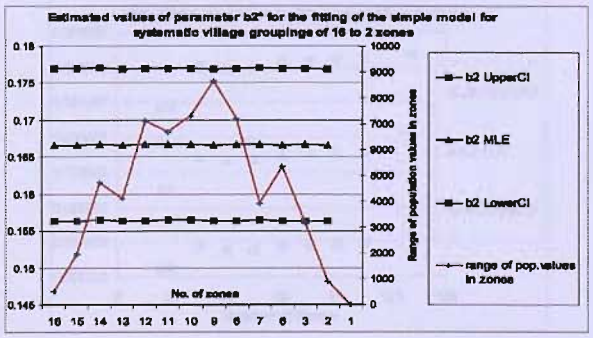

Figure 15.29: MLE of b_2^* coefficient for the systematic grouping of villages into increasing zone sizes (and thus decreasing numbers of zones: 16 to 2).

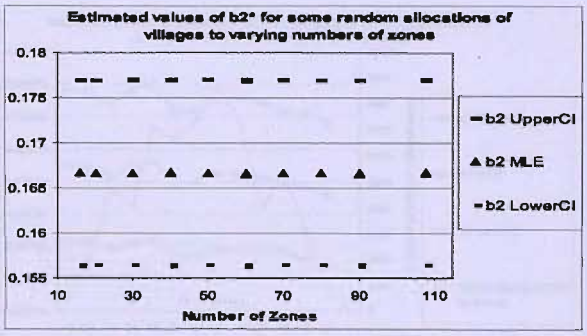

Figure 15.30: MLE of b_2^* coefficient for the random grouping of villages into increasing zone sizes (and thus decreasing numbers of zones).

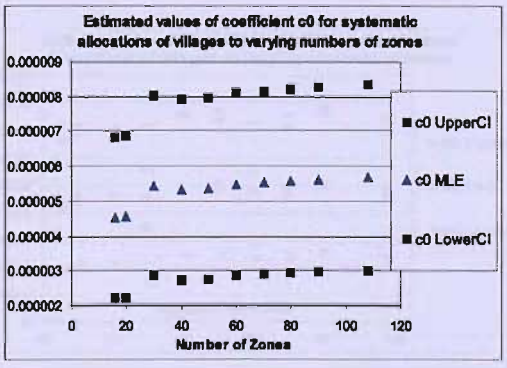

Figure 15.31: MLE of c_0 coefficient for the systematic grouping of villages into increasing zone sizes (and thus decreasing numbers of zones: 108 to 16).

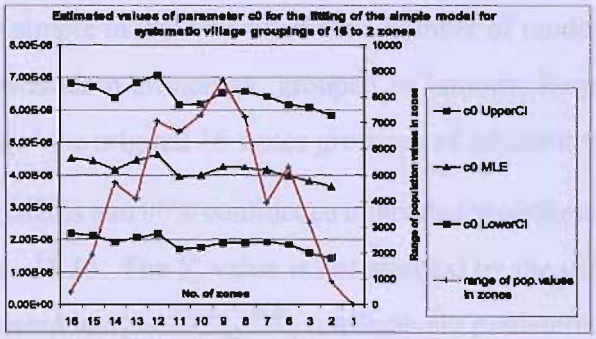

Figure 15.32: MLE of c_0 coefficient for the systematic grouping of villages into increasing zone sizes (and thus decreasing numbers of zones: 16 to 2).

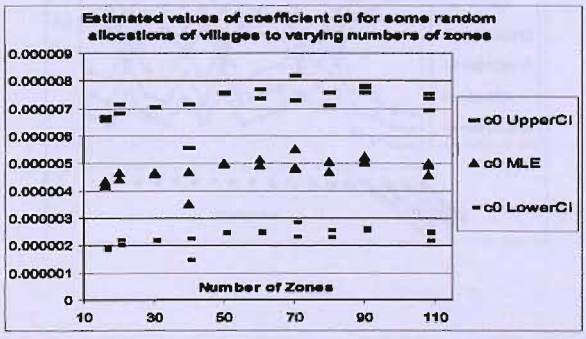

Figure 15.33: MLE of c_0 coefficient for the random grouping of villages into increasing zone sizes (and thus decreasing numbers of zones).

15.1.3.6 Effect of different groupings of villages into 16 zones

In order to explore whether the way the 217 villages were grouped effected the model results the simple model was fitted for a number of random groupings plus a further four non-random groupings: grouped by latitude; longitude; in order of village number; and the original 16 zones grouping of adjacent villages.

The resulting MLEs and 95% confidence intervals for each parameter are shown in graphs 15.34 to 15.36. The $\hat{b}_2^*$ value is not affected by the different groupings. This is to be expected as $\hat{b}_2^* = \frac{\text{time step}}{b_2}$, is effectively predetermined.

The coefficient $\hat{c}_0$ value can again be seen to behave in direct negative correspondence with the value of the global coefficient $\hat{b}_0$.

The values of the local and global coefficients, $\hat{b}_1$ and $\hat{b}_0$, are visibly more distinct from each other when any geographic based grouping is applied. This implies the model is picking up the local geographic effect of the TB case clustering.

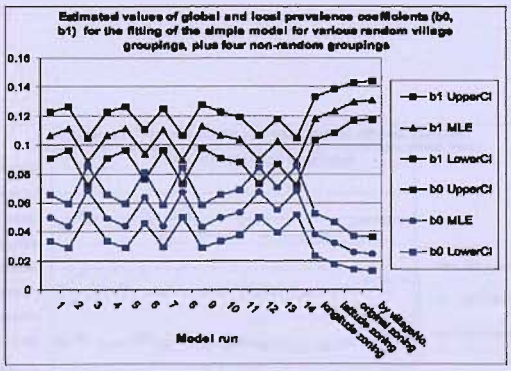

Figure 15.34: MLE of global and local prevalence coefficients, b_0, b_1, for various different groupings of the 217 villages.

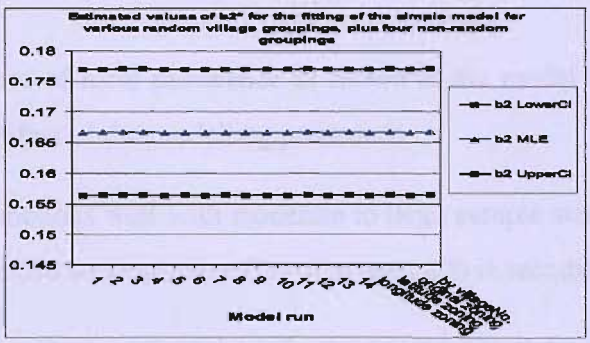

Figure 15.35: MLE of parameter b_2^* for various different groupings of the 217 villages.

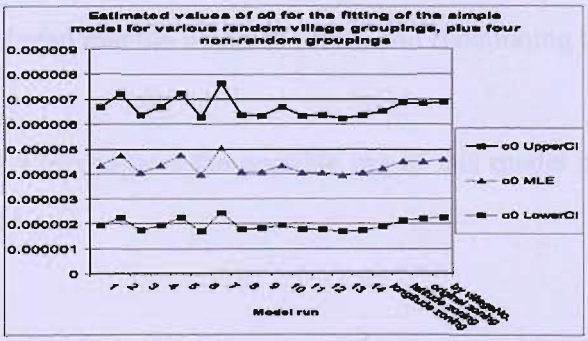

Figure 15.36: MLE of parameter c_0 for various different groupings of the 217 villages.

15.1.3.7 Summary of robustness tests of model

The various test results show that:

- the importance of local prevalence as shown in the model results was not simply an artifact of the modelling procedure.
- the model functions well with moderate to large sample sizes (M). The results indicate that a sample size (M) of at least 400 is recommended.
- Pre-specifying the length of the infectious period b_2 at 6 months does not unduly influence the model output.
- the chosen time step length of 1 month is satisfying.
- the stability of the optimisation procedure and therefore the validity of the MLE values resulting from it.
- the model reacts predictably and logically to varying sizes of groupings (zones) and ways of grouping the locality measure (villages).

It is therefore concluded that the model is robust and functioning in a satisfactory manner.

The next chapter investigates the possible use of this model in the design of cluster randomised trials.

Chapter 16

Cluster Randomised Trial Design

16.1 Introduction

Cluster or group randomised trials are used to assess the relative effectiveness of alternative interventions. They occur when the trial subjects (e.g. patients) are randomised to a certain intervention at the group level but the resulting data is analysed at the individual level. For example, in a group randomised trial of two different health interventions, A and B, 10 health centres are randomly assigned to carry out intervention A and another 10 health centres are assigned to carry out intervention B. The resulting data set consists of the individual patient responses to the interventions. Thus, here the trial subjects are the patients, who are clustered/grouped according to the health facility they attend, but the health centres rather than the individual patients were randomly assigned to the interventions. Usually a significance test is applied to the collected data from such a study in order to statistically assess the performance of one intervention over another. The statistical power of a trial is defined as the probability of rejecting a false statistical null hypothesis given the collected data. This probability that a trial will have a significant result, i.e produce a p-value of less than the specified significance level (alpha, usually set at 5%) is calculated under the assumption that the difference

in intervention results equals the minimal detectable difference (i.e the smallest difference believed clinically important or biologically plausible).

A power analysis should always be carried out at the planning/design stage of a trial in order to estimate the required sample size, significance level and size of observed effect that it is desirable to detect. The larger the effect size, sample size and/or significance level, the greater the likelihood that the trial will result in detecting a statistically significant effect.

A well designed trial ensures that the statistical power is high enough to detect reasonable departures from the null hypothesis while taking into account the aims of the trial and the resources available (e.g. time, money, available workforce size etc..). When carrying out a power analysis for a clustered randomised trial the clustering effect must be taken into account, especially when estimating the required sample size. People within a group/cluster are likely to have more similarities with each other than with people from another group, e.g. geographic, socioeconomic, health facilities, racial, sexual, political, age and gender similarities. A clustering effect occurs when these group similarities lead to a decreased variation among the responses of people in the same group/cluster (within-cluster variation) as opposed to the variation of responses between the groups/clusters (between-cluster variation). Within cluster-variation can therefore increase the differences in responses observed between groups and introduce bias. Cluster randomisation can thus reduce the effective sample size (ESS) of the trial and it is necessary to adjust for this at the design stage.

An important possible use of the local and global effect model (introduced and described in the chapter 14) is in just such a design of a community randomised trial where geographical clusters of people are divided into two groups and the effectiveness of an intervention policy is assessed by applying it to one group but not the other. Here the model can be used to calculate the minimum difference in an outcome variable that can be detected with statistical significance, taking

the effect of clustering of cases into consideration. It thereby gauges the potential effectiveness of such a trial. Such a possible application is illustrated by setting up cluster randomised trial scenarios using the western Kenyan time/spatial TB data set and applying the model.

16.2 Splitting zones into two groups representing two different treatment groups in a group randomised trial

In order to design a group or community-randomized trial to evaluate the impact of a specific intervention policy on tuberculosis transmission in an area with a high tuberculosis burden, information to estimate the effect of local versus global transmission is required. Communities should be large enough to encompass most TB transmission but enough communities are needed to ensure statistical power. TB prevalence is chosen to be the outcome variable as a substitute for the true variable of interest, TB transmission, due to the difficulties of measuring transmission directly. The 16 original zones were divided into two different groupings of 8 zones each and the simple model was then fitted to this data. (The infectious period length, b_2, was set to 6 months, the time step to one month and the starting parameter values in the optimisation procedure to 0.0001). This fitting was repeated for a variety of different groupings of the original 16 zones. The difference between the prevalence of TB in each group was systematically varied in order to try to identify the minimum difference that could be detected with statistical significance. Figure 16.1 shows the resulting MLE values for the local and global parameters. The minimum detectable difference in TB prevalence is at the point where the two 95% confidence intervals for the two groupings separate and no longer overlap. This occurs at approximately 0.007.

In order to explore the effect of decreasing the number of zones in each grouping, zones were merged together with the effect that no TB case data was lost. The simple model was then fitted to the new groupings. Figures 16.2 and 16.3 show the resulting MLE values of the local and global parameters for 6 and 4 zones in each grouping.

In order to further explore the effect of decreasing the number of zones in each grouping along with the sample data size, zones with their corresponding TB case data were systematically deleted and the simple model fitted to the new groupings. The Figures 16.4 to 16.6 show the resulting MLE values of the local and global parameters for 7, 6 and 4 zones in each grouping. A summary of all the groupings results is displayed in Table 16.1.

Table 16.1: The estimated minimum difference in TB prevalence detectable by the simple model when 16, 14, 12 and 8 zones are assigned equally to two different groups.

Number of zones in each group (method used to reduce zone numbers)	TB prevalence in Group1	TB prevalence in Group2	Approximate minimum detectable difference in TB prevalence
8	0.003	0.01	0.007
6 (merging zones)	0.0037	0.011	0.0073
4 (merging zones)	0.0023	0.0104	>0.0081
7 (deleting 2 zones)	0.0041	0.0104	0.0063
6 (deleting 4 zones)	0.0055	0.011	0.0055
4 (deleting 6 zones)	0.0054	0.0131	>0.0077
The minimum detectable difference is calculated using: |Group 1 TB prevalence – Group 2 TB prevalence|			

The overall prevalence in the total population remains constant for the first three results in Table 16.1 where the sample size was kept constant. From these results it seems that as the number of zones in the groupings decrease the minimum difference in TB prevalence that is detectable by the model increases. This is what would be expected in a group randomised trial where there is a considerable clustering effect.

Decreasing the number of zones in each grouping by deletion of zones and therefore sample data produces varying total overall TB prevalence values. For 7 zones in each grouping the total overall prevalence is 0.0072. For 6 zones the total overall prevalence is 0.0082 and for 4 zones it is 0.0093. There seems to be less of a pattern to the results for these groupings, possibly due to the confounding factor of decreasing amounts of sample data available to the model and thus varying TB prevalence in the total population.

In all the different grouping runs, as the local parameter MLE decreases the global MLE increases to compensate, as can be seen in figures 16.1 to 16.6.

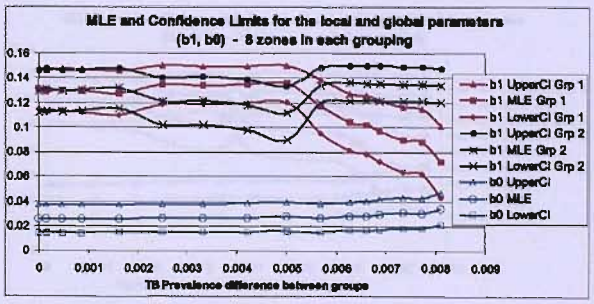

Figure 16.1: MLE of local and global effect coefficients for varying differences in the TB prevalence between two groupings of 8 zones.

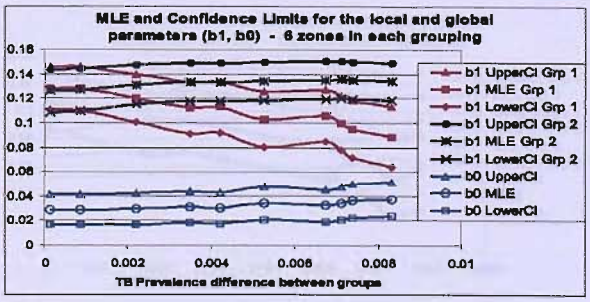

Figure 16.2: Merging of zones: MLE of local and global effect coefficients for varying differences in the TB prevalence between two groupings of 6 zones.

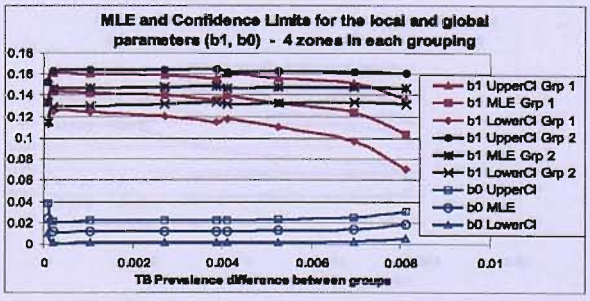

Figure 16.3: Merging of zones: MLE of local and global effect coefficients for varying differences in the TB prevalence between two groupings of 4 zones.

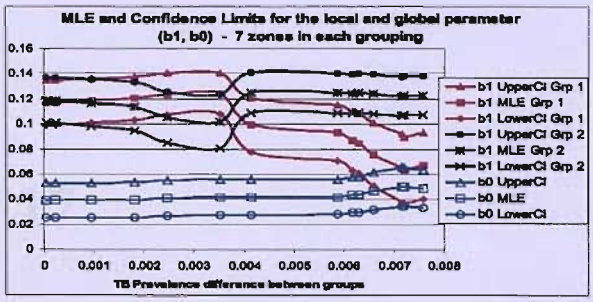

Figure 16.4: Deletion of zones: MLE of local and global prevalence coefficients for varying differences in the TB prevalence between two groupings of 7 zones.

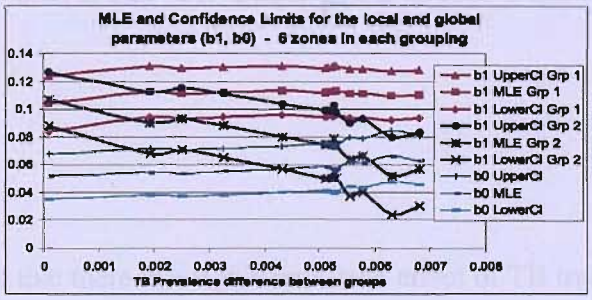

Figure 16.5: Deletion of zones: MLE of local and global prevalence coefficients for varying differences in the TB prevalence between two groupings of 6 zones.

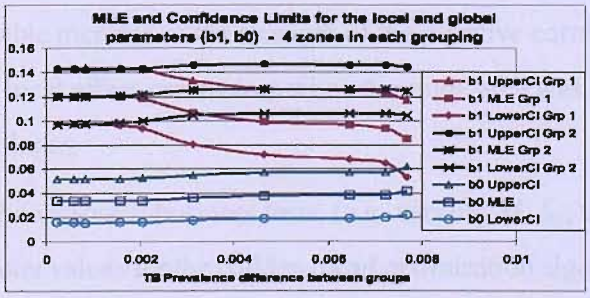

Figure 16.6: Deletion of zones: MLE of local and global prevalence coefficients for varying differences in the TB prevalence between two groupings of 4 zones.

Chapter 17

Discussion and Conclusions for the Markov-chain local/global effects model

The model showed that there is a significant local effect of TB transmission with a larger local transition coefficient (b_1) than the global coefficient (b_0) in all the different model variations. Age seems to be a significant factor whereas gender on its own is not. The two mixed age/gender models show significant local prevalence in the anticipated age classes: males aged 30-34 and females aged 25-30. There was an understandable increase in the strength of the negative correlation between the two global and local effect parameters when the study area was divided into 16 zones instead of villages.

The results of the various robustness tests, (e.g. varying M, b_2, time step length and starting parameter values for the Nelder-mead optimisation algorithm) indicate that the model is robust.

There are several limitations to the interpretation of the results for this particular TB data set. First, routine TB surveillance program data was used. This

data does not represent the full spectrum of cases in the study area. It is estimated that the Kenyan national program detects only 47% of TB cases. There are no data available to allow comparison of those detected and those not detected on such factors as health seeking behaviours, accuracy of diagnosis, and survival. TB cases reported in the register are from people who self report to a government health facility, are correctly diagnosed, and survive to start treatment. It is therefore likely that some of the clustering effect detected could be due to patchy reporting. Some district health centres may be more active in advertising their services or provide better quality services than others and so capture a higher fraction of patients. This could cause an apparent cluster of TB cases around these health centres and therefore cause bias in the local effect parameter. In addition, the home address in the registers is recorded for defaulter tracing purposes and does not necessarily reflect the place where the person contracted or spread TB. There may be misclassification of location in the data.

Despite the above data limitations it has been shown that this model does detect significant local clustering effects (whatever their true cause may be). It has also been shown that it is possible to use the model in the design of a cluster randomised trial where clusters of subjects are divided into two groups and the effectiveness of an intervention policy is assessed by applying it to one group but not the other. Here the model can be used to calculate the minimum difference in an outcome variable that can be detected with statistical significance, given a certain available sample size. It can thereby be used to gauge the potential effectiveness of such a trial, taking into account the effect of clustering.

Chapter 18

Conclusions and discussion of Thesis regarding all three TB models

This thesis has described the development of three different Tuberculosis epidemiological models: A family of age dependent parametric statistical models; a compartmental, age dependent, difference equations model; and a Markov chain model that allows for location effects in the transmission of TB.

18.1 Parametric Statistical TB modelling

In countries that have experienced a long-term decline in the incidence of TB and in annual risk of TB infection, a slow down in the annual decline of the crude notification rate (referred to as stagnation) is often observed. It is most often observed in middle-to-higher income countries with an increasing life expectancy rate and therefore a rapidly ageing population.

This stagnation effect can be explained by the epidemiology of TB. As the risk of infection declines, the proportion of disease due to initial infection (primary disease) and due to re-infection also declines. When the risk of infection reaches

an extremely low level it is likely that most of the disease detected is re-activation disease. This effect is called the 'ageing of the epidemic'.

Re-activation disease by its very nature does not depend on the current risk of infection and the probability of occurrence of the disease is not believed to decline significantly with lengthening time since infection. In addition, medical factors that may increase the risk of re-activation of latent TB, such as lung cancer and diabetes are predominantly found in the older generations. Therefore the incidence of this disease only declines if the latently infected cohorts either 'die off' or are given preventative therapy. Thus a country with an increasing life expectancy and a very low annual risk of infection could expect the decline in TB notifications to stagnate.

In order to analyse the progression of TB in these types of countries it is necessary to create mathematical models that can capture the essential epidemiological and demographic characteristics that are involved in the stagnation effect.

TB data sets from three countries, Netherlands, UK and Morocco, that are considered to have an aging population, low/decreasing annual risk of infection and exhibit an aging of the epidemic, are examined for similar trends/characteristics.

The UK (male) data shows similar characteristics to the data from the Netherlands, in that the rate of decline in the data is greater in the younger age ranges and begins to level off in the older age ranges.

The Moroccan data shows a more extreme but similar pattern in that the younger ages exhibit a sharp decline in TB that levels off until an increase in TB is exhibited in the older age ranges.

The age and time dependent trends apparent in the data are investigated by constructing and fitting a family of parametric models to all three data sets as described in chapters 5 to 8. The method of Maximum Likelihood is used to fit the distributions and the direct search optimisation method, Nelder-mead, is used to

find the maximum value of the likelihood. Confidence intervals for the maximum likelihood estimator values and confidence/performance bands for the model fits, are constructed using Asymptotic Theory and the Bootstrap Method.

The general characteristics of the TB data sets as they vary with time and age are satisfactorily captured by this family of parametric models. There are some effects that the models fail to capture but it is unclear whether all these characteristics are derived from true features of the data or arise from erroneous data collection/manipulation. The accuracy of the data can be generally questionable in very young children due to the difficulty in obtaining positive sputum test results. The data in the two oldest age groups from the Netherlands suffer from a change in age ranges around 1972 used in the collection of data. The Moroccan year data although regarded as generally reliable is partly created by projection.

The parametric model therefore gives a clear indication of the general features of age dependency that any subsequent TB model would need to be able to capture.

18.2 Compartmental age-dependent TB model

The emphasis of this part of the work is on investigating the ability of compartmental TB models to capture the age and time characteristics exhibited in TB data from countries with increasing life expectancy, aging of the TB epidemic and a slow down in the annual decline of the crude notification rate. A suitable compartmental model is rebuilt from a previously existing model devised by C.Dye et al [14, 15]. The TB data sets from the Netherlands and Morocco are analysed using this compartmental model. The UK data was not used as it only contains TB data from white males and the model is not built to make this distinction between gender and ethnicity.

For the Netherlands the outcome investigated was the number of TB cases per

100,000 of population for each of the 8 age groups, for years, 1952 to 1994. For Morocco the outcome investigated was the number of Pulmonary TB (PTB) cases per 100,000 of population for each of the 8 age groups, for the years 1980 to 2000.

The model was unable to fit well to the initial year data, overestimating the number of TB cases in the adult age groups. This was most noticeable in the fit to the Dutch data. It is also obvious the shape of the line fit for both countries does not vary significantly across the 8 age ranges. Hence, in the case of the Dutch data, although the model fits well for the first three age groups it soon fails to capture the 'flattening' of the curvature in the data. It is also unable to explain the 'tailing off' and subsequent increase in TB case numbers observed in the Moroccan data. But it does successfully capture the majority of time dependent trends in the data.

After describing a reasonable fit to the data most of the work concentrates on the sensitivity analysis of the model. The aim is to explore how varying the values of each input parameter effects the outcome variables. The value of each parameter used to produce the original fits to the data is referred to as the base value. Each parameter is taken in turn and the model run with a new value (a percentage of its base value) for that parameter. The percentages by which the parameter values are varied were selected to show a representative pattern of how the outcome variable is affected.

The parameters of the compartmental model mostly behave in a non-linear way except for very small variations in value where they often behave approximately linearly. It is also noticeable that they interact with each other in complicated and subtle ways that are not always obvious when examining the difference equations that drive the model.

Most of the parameters caused an effect in the outcome variable, as would be expected, when varied one at a time keeping all other parameter values fixed. The behaviour and effect on the outcome variable for the most part is explainable by

the epidemiology of TB. There were however a few notable exceptions. Parameters p(for ages 15+) - the proportion of infectious susceptibles which develop progressive primary TB in 1 year, x(for ages 15+) - the proportion of re-infections which is susceptible to developing TB within 1 year, and r - the rate of relapse from failed treatment to active TB, effect the outcome variable counter intuitively. Despite further examination of the model, including systematically simplifying the difference equations while noting whether the particular effect in the outcome variable was affected, no obvious reason for these anomalies was discovered. A full understanding of the model and its results would therefore benefit from further investigation of the behaviour of these particular parameters and the interactions of all the parameters in the model.

When fitting to the Dutch data some of the parameters produced a far smaller relative effect in the outcome variable than others. In particular, ϵ - the relative case detection rate of non-infectious cases, w - the rate of smear conversion from non-infectious to infectious TB, ϕ - the proportion of failed treatment cases which is infectious, and F - proportion of progressive primary cases which become infectious within one year, have little effect on the outcome variable. Likewise, when fitting to the Moroccan data a variation in the values for parameters x(ages 0-14) - the proportion of re-infections which is susceptible to developing TB within 1 year, ϕ and ϵ had a relatively small effect on the outcome variable as compared with other parameters. However, it was found that eliminating these parameters did have a (large) effect on the output of the model, suggesting that these parameters although individually seeming relatively unimportant have significant interactions with the other model parameters.

Varying the parameters one at a time did not significantly improve the model fit to each of the age groups over time and therefore failed to significantly improve the fit to the age dependent characteristics. However, for the Moroccan data, increasing the 11 selected parameters at the same time did have the effect of varying

the gradient and placement of the fitted line so that it gave a better fit to the data for ages 0-34. But the model still failed to capture fully the age characteristics in the data especially in the older age groups. Therefore, despite the apparent flexibility and large number of parameters of this compartmental model, there are still age dependent features of these TB data sets which would need further modelling to capture.

It would be possible in theory to get a better fit to the data with more robust and sophisticated optimisation/fitting techniques and building in an even more sophisticated age/time dependency e.g more age/time dependent functions for the parameters. It could also be useful to construct another way to obtain equilibrium, so that the model starts with the same age distribution for the output variable as the observed data (with or without a warm-up). If the characteristics observed in these countries' TB data sets and captured by the parametric modelling are considered important, it could be useful to devise a way to directly build these trends into the age dependent compartmental model. But the large number of parameters in the model (which would increase rapidly with a more sophisticated internal age/time dependent structure) make the model very unwieldy and difficult to optimise. It should also be noted that the data sets that could be applied to this kind of model may not be very large, so it is important that the model not become over complicated.

The accuracy of model results is always going to be limited by the form of epidemiological, behavioural and intervention data that are available to inform the structure and input values of the model. Perhaps one of the most valuable aspects of constructing a compartmental model is that it produces insight into and clarification of the real biological system being modelled.

One of the advantages of carrying out compartmental analysis is the ability to assign biological or physiological meaning to the rate/proportion parameters that underlie the movement of the population through the model. Parameter estimation,

however, is not particularly easy, with research into this aspect arguably lagging behind research into model formulation. In the case of diseases such as Tuberculosis, the estimation of many parameters is further complicated because when individuals are infected but not infectious they may not be distinguished from susceptibles. Research into overcoming this and other parameter estimation problems is currently being carried out within a Bayesian framework (using MCMC) [34, 35, 40, 91, 33].

As the work in this part of the thesis shows, analysis of non-linear compartmental models is not simple. Particular attention should be paid to ensure that the complicated internal structure does not produce spurious results. It is particularly important in analysing possible stagnation effects in TB notification data that age dependency characteristics are sufficiently captured in the structure of the model.

18.3 Modelling Local and Global Effects in the Transmission of TB Observed in Asembo and Gem, Kenya: Designing a Spatial Model of TB Case Clustering.

Most current epidemiological TB models are homogeneous, in that an infected individual is equally likely to infect any of the susceptible individuals in the model population. This is in effect assuming that an infectious individual in Southampton is as likely to infect someone in Glasgow as someone else in Southampton. This assumption has been found to be adequate for diseases such as influenza, in which the disease can be transmitted via casual contact. However, the validity of this assumption is generally agreed to be questionable for diseases in which each individual has a limited number of potentially infectious contacts. Tuberculosis is

such a disease.

With this in mind, a Markov-chain model is created in an attempt to identify whether the nearest reported source of possible infection is a localised one stemming from an individual's contacts with family or near neighbours or whether it arises from much more dispersed 'global' contact. Thus, we are concerned with determining whether a clustering (local) effect is as strong or stronger than a general global effect in respect of TB transmission. This may have consequences for how TB case finding strategies are undertaken i.e. focussing on local contacts of infectious cases or on the entire population.

The basic methodology is to construct a stochastic Markov-chain model whose behaviour is determined by a number of key parameters representing possible local and global effects on TB transmission. This model is then fitted to Kenyan time-spatial TB data using maximum likelihood to estimate these key parameter values.

The model showed that there is a significant local effect of transmission with a larger local transition coefficient (b_1) than the global coefficient (b_0). Age was identified as a significant factor whereas gender on its own was not. The two mixed age/gender models also showed significant local prevalence in the anticipated age classes: males aged 30-34 and females aged 25-30.

A number of tests of the robustness of the modelling procedure were carried out including: a demonstration that the importance of local prevalence is not simply an artifact of the modelling; testing the effect of decreasing sample size on the fitting of the model; investigating the effect of the length of the infectious period; investigating the effect of different starting parameter values in the Nelder-mead optimisation procedure; investigating the model's sensitivity to the spatial scale of disease clustering. The results of all these various robustness tests were more than satisfactory.

It has also been shown that it is possible to use the model in the design of

a cluster randomised trial where clusters of subjects are divided into two groups and the effectiveness of an intervention policy is assessed by applying it to one group but not the other. Here the model can be used to calculate the minimum difference in an outcome variable that can be detected with statistical significance, given a certain available sample size. It can thereby be used to gauge the potential effectiveness of such a trial, taking into account the effect of clustering.

The model was formulated to match the complexity of the model with the quality of the data available. The model assumes an equal period and degree of infectiousness for all identified cases. However, not all notified cases are necessarily infectious or equally infectious and indeed the data used for the study combined different types of TB (e.g. smear positive, smear negative, and extra pulmonary). Additionally, information about the HIV status of each individual in the study was not available although it is estimated that HIV prevalence is approximately $20-25\%$ in the study area. HIV positive people are more likely than HIV negative people to have active TB disease, to be smear negative, to have shorter survival, but to be less infectious for TB. HIV could therefore influence TB prevalence by influencing transmission and acquisition of active TB. It is interesting to note that in the model results the magnitude of the local effect was greatest in the age groups that have the greatest prevalence of HIV. It is therefore possible that the register data shows HIV clustering more than clustering of TB due to the infectiousness of TB cases. This would lead to bias in the local effect, making it larger than if HIV was not present. However, the relevance of the model results in the design of a cluster randomised trial is not effected by the reason for clustering.

With more detailed data it may be possible to refine the model to incorporate a larger number of states (rather than just case and non-case). Much of the interest in active case finding concerns transmission in households therefore data for individual families or households would be preferable. If HIV status data was available this could also be incorporated into the model. Another component of the model

that requires further development is the way the length of infectious period (b_2) is handled. The assumption that recovery time is independent of location may be flawed. The rate of recovery is dependent on HIV co-infection and drug resistance, both of which may be location dependent. In future models it would be preferable to include this as a parameter to be estimated.

Appendix A

Maximising the posterior - Using Least squares/Neldermead Simplex methods

The objective is to minimise the error between the actual recorded data and the model output, thus finding the optimal values of the input parameters.

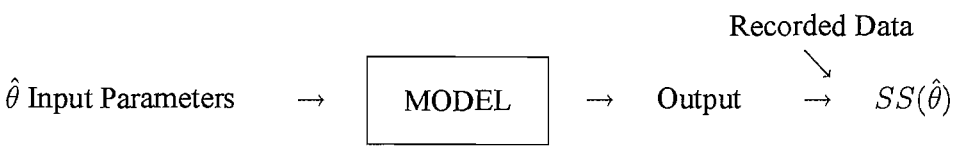

Using the Nelder-mead Simplex algorithm, the input parameter values are systematically varied until an optimal fit for the data is found (i.e the objective function for the error term is minimised).

In the simple case, the objective function to be minimised is the Sum of Squares:

$$SS = \sum_{\forall i} (\hat{y}_i(\theta) - y_i)^2$$

where $\hat{y}_i$ is the model output and y_i is the recorded data.

A.1 Nelder-mead Simplex Algorithm

(with reference to the paper "Convergence Properties of the Nelder-mead Simplex Method in Low Dimensions" - J.C.Lagarias et. al. [42])

The Nelder-mead simplex algorithm was first published in 1965 and is an extremely popular direct search method for carrying out unconstrained minimisation of non-linear functions in multi-dimensions. Direct Search methods are a class of minimisation methods that do not require the use of derivatives. They rely exclusively on calculating the value of the objective function and comparing it with the best previous value [82]. The fact that the Nelder-mead algorithm is relatively simple to program for computer calculation adds to its popularity.

The standard Nelder-mead algorithm uses four scalar parameters:

- Reflection: $\rho = 1$
- Expansion: $\chi = 2$
- Contraction: $\gamma = 1/2$
- Shrinkage: $\sigma = 1/2$

in order to minimise an objective function, $f(\theta)$.

An iteration step of the algorithm:

Each iteration step begins with a non degenerate simplex Δ and its n+1 vertices, (i.e n+1 points in R^n).

1. **Order:** The n+1 vertices are ordered and labelled, $x_1, x_2, \ldots, x_n, x_{n+1}$, so that the objective function values satisfy:

$$f(x_1) \leq f(x_2) \leq \ldots \leq f(x_n) \leq f(x_{n+1})$$

Because the purpose of this algorithm is to minimise the objective function, the vertex x_1 is the "best" point, x_{n+1} is the "worst" point and $f(x_{n+1})$ is the "worst" function value.

2. **REFLECT:**

   The Reflection point, x_r, is calculated from:

$$\begin{aligned} x_r &= \overbrace{\sum_{i=1}^{n} \frac{x_i}{n}}^{\text{centroid of the n best points}} + \rho[(\sum_{i=1}^{n} \frac{x_i}{n}) - x_{n+1}] \\ &= (1+\rho)(\sum_{i=1}^{n} \frac{x_i}{n}) - \rho x_{n+1} \end{aligned}$$

   Evaluate $f(x_r)$.

   If $f(x_1) \leq f(x_r) \leq f(x_n)$, accept the reflected point, x_r, and end the iteration.

3. **If $f(x_r) \leq f(x_1)$ then EXPAND:**

   The Expansion point, x_e, is calculated from:

$$\begin{aligned} x_e &= \overbrace{\sum_{i=1}^{n} \frac{x_i}{n}}^{\text{centroid of the n best points}} + \chi(x_r - \sum_{i=1}^{n} \frac{x_i}{n}) \\ &= (1+\rho\chi)(\sum_{i=1}^{n} \frac{x_i}{n}) - \rho\chi x_{n+1} \end{aligned}$$

   Evaluate $f(x_e)$.

   If $f(x_e) \leq f(x_r)$, accept the expansion point, x_e, and end the iteration.
   else **If $f(x_e) \geq f(x_r)$, accept the reflection point, x_r, and end the iteration.**

4. **If $f(x_r) \geq f(x_n)$ then CONTRACT between the centroid, $\sum_{i=1}^{n} \frac{x_i}{n}$, and the "better" of x_{n+1} and x_r:**

(a) **If** $f(x_n) \leq f(x_r) < f(x_{n+1})$ **then calculate the Contraction point,** x_{c1}**:**

$$\begin{aligned} x_{c1} &= \overbrace{\sum_{i=1}^{n} \frac{x_i}{n}}^{\text{centroid of the n best points}} + \gamma(x_r - \sum_{i=1}^{n} \frac{x_i}{n}) \\ &= (1+\rho\gamma)(\sum_{i=1}^{n} \frac{x_i}{n}) - \rho\gamma x_{n+1} \end{aligned}$$

Evaluate $f(x_{c1})$.

If $f(x_{c1}) \leq f(x_r)$**, accept the contraction point,** x_{c1}**, and end the iteration.** *else* **If** $f(x_{c1}) > f(x_r)$**, go to step 5, i.e. perform a shrink operation.**

(b) **If** $f(x_r) \geq f(x_{n+1}) < f(x_{n+1})$ **then calculate the Contraction point,** x_{c2}**:**

$$\begin{aligned} x_{c2} &= \overbrace{\sum_{i=1}^{n} \frac{x_i}{n}}^{\text{centroid of the n best points}} - \gamma[(\sum_{i=1}^{n} \frac{x_i}{n}) - x_{n+1}] \\ &= (1+\gamma)(\sum_{i=1}^{n} \frac{x_i}{n}) + \gamma x_{n+1} \end{aligned}$$

Evaluate $f(x_{c2})$.

If $f(x_{c2}) < f(x_{n+1})$**, accept the contraction point,** x_{c2}**, and end the iteration.** *else* **If** $f(x_{c2}) \geq f(x_r)$**, go to step 5, i.e. perform a shrink operation.**

5. **Perform a SHRINK operation:**

Evaluate $f(\alpha_i)$ at the n points, $\alpha_i = x_1 + \sigma(x_i - x_1)$, where $i = 2, 3, \ldots, n, n+1$.

Thus, the vertices of the simplex at the next iteration, before ordering, will be: $x_1, v_2, v_3, \ldots, v_{n+1}$

The algorithm terminates when the function values at the vertices of the simplex satisfy some predetermined stopping condition, e.g. a tolerance value for the variance of the n+1 function values.

The Nelder-mead paper [39] did not explain how to order the vertices when equal function values were produced. This has led to differences in interpretation of the Nelder-mead algorithm. An example of a set of tie-breaking rules can be found in the 1998 paper by Lagarius et. al. [42].

Nelder-mead's algorithm is economical in the number of times it evaluates the function at each iteration. In practice it often only needs one or two function evaluations to construct a new simplex and is often able to find reasonably good solutions fairly rapidly. However, its convergence properties are not particularly well understood. Only limited results exist for particular classes of problems based in one or two dimensions. Although there are recent attempts to expand these results including the 2002 paper by Price, Coope and Byatt [17] which introduces a convergent variant of the Nelder-mead algorithm.

Appendix B

An Introduction to Likelihood Theory

Let $\underline{\theta}$ be the unknown input parameters to a model. The "most likely" value of $\underline{\theta}$, i.e. the value that makes the observed data the "most probable", is called the *maximum likelihood estimate* (m.l.e) of $\underline{\theta}$ because it maximises the likelihood function, $f_{\underline{x}}(\underline{x}, \underline{\theta})$. Let $\hat{\underline{\theta}}$ denote this m.l.e. $\hat{\underline{\theta}}$ is dependent on the observed data, $\underline{x}$, as different data samples give different likelihood functions. A very useful property of the m.l.e is its coherence, i.e. if $\hat{\underline{\theta}}$ is the m.l.e of $\underline{\theta}$, then for any function, $g(\underline{\theta})$, the m.l.e is $g(\hat{\underline{\theta}})$. Calculating the m.l.e is fairly straightforward and consists of maximising the likelihood function. When maximising the likelihood function, $f_{\underline{x}}(\underline{x}, \underline{\theta})$, it is usual and easier to work with the log likelihood, $\log f_{\underline{x}}(\underline{x}, \underline{\theta})$. Maximising the log likelihood function is achieved by finding a stationary point in the normal way: by differentiating $\log f_{\underline{x}}(\underline{x}, \underline{\theta})$ with respect to $\underline{\theta}$, setting the results equal to 0 and solving. To check that this stationary point is indeed a maximum it is necessary to show that the Hessian matrix, a matrix of second derivatives with elements $[H(\underline{\theta})]_{ij} = \frac{\partial^2}{\partial\theta_i \partial\theta_j} \log f_{\underline{x}}(\underline{x}, \underline{\theta})$, is negative definite at $\underline{\theta} = \hat{\underline{\theta}}$.

One reason for the Maximum Likelihood estimation's wide popularity is the usefulness of the m.l.e's asymptotic behaviour:

- Let $\underline{x}$ be n observations of i.i.d random variables $\underline{X}$, whose joint p.d.f, $f_{\underline{X}}(\underline{x}, \underline{\theta}) = \sum_{i=1}^{n} f_{\underline{X}}(x_i, \underline{\theta})$, is completely specified except for the values of the unknown parameters, $\underline{\theta}$. Let $\hat{\underline{\theta}}$ be the maximum likelihood estimator of $\underline{\theta}$.

  Then, as $n \rightarrow \infty$, the distribution of the m.l.e, $\hat{\underline{\theta}}$, tends to a multivariate normal distribution $N[\underline{\theta}, I(\underline{\theta})^{-1}]$.

  The variance in this multivariate normal distribution is called the asymptotic variance covariance matrix.

B.1 Calculating the Asymptotic variance covariance matrix:

$I(\underline{\theta})^{-1}$ can be calculated from the Hessian matrix:

- $I(\underline{\theta})^{-1} = E[-\frac{\partial^2}{\partial\theta_i \partial\theta_j} \log f_{\underline{x}}(\underline{x}, \underline{\theta})]^{-1}$

where the variances of $\underline{\theta}$ are the leading diagonal elements and the covariances are the off diagonal elements.

From this covariance matrix the **correlation matrix** can be calculated:

$$Corr(\theta_i, \theta_j) = \frac{Cov(\theta_i, \theta_j)}{\sqrt{Var(\theta_i), Var(\theta_j)}}$$

Appendix C

Sensitivity and Uncertainty Analysis

(Referencing the paper "Sensitivity and Uncertainty Analysis of Complex Models of Disease Transmission..." - Blower and Dowlatabadi [87])

C.1 Complex Models of disease transmission:

Simple models can be solved analytically but the behaviour of more complex models can only be understood by numerical analysis. Uncertainty analysis and sensitivity analysis are used because these models have a complex structure and a high degree of uncertainty in estimating the values of many of the input parameters.

Model Characteristics:

- Many uncertain parameters
- Outcome variables are non-linear functions of the parameters
- The full range of each input parameter needs investigating
- The models are computationally taxing. Therefore the ability to complete sensitivity analysis with the minimum possible number of computer runs is desirable.

Uncertainty and Sensitivity Analysis:

- Uncertainty Analysis is used to assess the variability (prediction imprecision) in the outcome variable that is due to the uncertainty in estimating the input values.
- Sensitivity Analysis extends the uncertainty analysis by identifying which parameters are important (due to their own estimation uncertainty) in contributing to the prediction imprecision; i.e. it tries to answer the question: how do changes in the values of the input parameters alter the value of the outcome variable?

C.2 Summary of Sampling Schemes:-

In order to carry out uncertainty or sensitivity analysis, a large sample of the model outcomes and input parameter values have to be collected. The following is a list of some of the more popular sampling designs:

1. Full Factorial Design: This uses every value of each parameter and forms every possible combination of parameter values. This therefore explores the entire parameter space but is extremely time consuming and hence highly impractical, especially for models with large numbers of parameters.
2. Alternative Factorial Design: For a K parameter model, fix the values of K-1 parameters and vary only the value of the Kth parameter over a specified range. This is very quick and simple. Its main disadvantages are that only one parameter can be varied at a time and therefore only a small subset of the K-dimensional parameter space can be explored and the values of the K-1 parameters have to be estimated with a high degree of precision.

3. Latin Hypercube Sampling (LHS): One of the designs that allow for the simultaneous variation of the values of all the input parameters. Latin Hypercube Sampling (LHS) scheme is an efficient sampling design proposed by McKay, Conover and Beckman (1979). It is a type of stratified Monte Carlo sampling and can be seen as an extension of Latin Square sampling. It has been demonstrated that if the outcome variable is a monotonic function of each of the input functions, the LHS design is the most efficient design compared with simple random and fractional stratified sampling designs, for estimating the mean value and the cumulative distribution function of the output variable. It has also been shown that even if the monotonicity assumption doesn't hold, but the sample sizes are large, then LHS is more efficient than the simple random sampling design.

Appendix D

Bootstrapping

The Bootstrap method is a computer-based method of statistical inference [9] and belongs to a large class of methods called resampling methods because they re-sample from the original sample data set [63].

Bootstrapping was given its name by Efron [8] who borrowed it from the phrase "to pull oneself up by one's bootstrap". This saying commonly refers to succeeding without help from others. The Bootstrap method can be thought of as doing just that, in that it aims to carry out statistical calculations, standard errors, confidence intervals etc... using no further information than the already available sample data set.

The following is an explanation of the simple nonparametric bootstrap method [43].

D.1 Nonparametric Bootstrap

Let $S = \{X_1, X_2, ..., X_n\}$ be a random sample drawn from a population $P = \{x_1, x_2, ..., x_N\}$. Suppose $T = t(S)$ is a statistic that is used to estimate the population parameter of interest, $\theta = t(P)$, such as the population mean or standard

error for example.

The traditional approach to estimating the sampling distribution of this statistic T requires making assumptions about the structure of the population P (e.g. normality) and either deriving the exact distribution of T or if this is not possible deriving the asymptotic distribution. This method can produce inaccurate results if the assumptions are incorrect or, if using asymptotic results, the sample data set is 'too' small.

The bootstrap method avoids these problems and allows us to estimate the sampling distribution of T empirically. The algorithm for carrying out the non-parametric bootstrap is as follows:

For $i = 1$ to M
Draw a random sample $S_i^* = \{X_{i1}^*, X_{i2}^*, ..., X_{in}^*\}$ of size n from S, using sampling with replacement.
Compute statistic T for each bootstrap sample: $T_i^* = t(S_i^*)$.
Next i

Hence, the distribution of the bootstrap statistic, T^*, can then be used as an estimate for the distribution of the true population parameter of interest, θ.

In principle, all possible bootstrap samples of size n could be collected from S. Unfortunately, the number of possible S^* is n^n, which is prohibitively large unless n is extremely small. In order to minimise any possible error in bootstrap inference by not using all possible bootstrap samples the number of bootstrap replications, M, should be made 'sufficiently' large [43, 9](Ch6, pgs 51-53).

D.2 Bootstrap Confidence Intervals

There are many different methods of constructing bootstrap confidence intervals. This section sets out two of the most common and easiest to implement.

- The normal-theory interval method assumes that statistic T is normally distributed and hence constructs a $100(1-\alpha)\%$ confidence interval as follows,

$$\begin{aligned}
\left(T - \hat{B}^*\right) &\pm z_{1-\frac{\alpha}{2}} \hat{SE}^*(T^*) \\
\text{where } \hat{B}^* &= \bar{T}^* - T \text{ is an estimate of the bias of } T; \\
\hat{SE}^*(T^*) &= \sqrt{\hat{V}^*(T^*)}; \\
\text{where } \hat{V}^*(T^*) & \quad \text{is the estimated bootstrap variance of } T^* : \\
\hat{V}^*(T^*) &= \frac{\sum_{i=1}^{M} \left(T_i^* - \bar{T}^*\right)^2}{M-1}; \\
\text{and } \bar{T}^* & \quad \text{is the estimate of the expectation of } T^* : \\
T^* &= \frac{\sum_{i=1}^{M} T_i^*}{M}
\end{aligned}$$

- The bootstrap percentile interval method creates a confidence interval, $\left(T^*_{(\text{lower})}, T^*_{(\text{upper})}\right)$, using the lower and upper quantiles of $T*$. The bootstrap replicates are put in order, $\left\{T^*_{(1)}, T^*_{(2)}, ..., T^*_{(M)}\right\}$, and the lower and upper quantiles calculated using: lower $= \left[(M+1)\frac{\alpha}{2}\right]$; upper $= \left[(M+1)(1-\frac{\alpha}{2})\right]$.

Appendix E

Demography and Health in Morocco

E.1 A brief history of the changing demography and health in Morocco

This information was partly gathered in a discussion with Salah-Eddine Ottmani MD, MPH, Medical Officer, TB Strategy and Operations (TBS) - Stop TB Communicable Diseases (CDS), (ottmanis@who.int); upon my first visit to the WHO in Geneva, November 2002.

E.1.1 Demography

There has been a rapid decrease in infant mortality in recent times and life expectancy has been rapidly increasing. It is now estimated at around 69 years. Demographic and various TB data collected in Morocco is regarded as being fairly reliable for the years 1980 to present day. The last Census was taken in 1994 and all subsequent year data is by projection. For the year 2000, the population of Morocco is recorded as 29,878,000.

E.1.2 Health

- **Tuberculosis programs** started in the 1950s and DOTS was first introduced into the country in 1991. More detailed information was gathered re. TB incidence etc.. from around 1994 onwards.

- **Health care facilities** are considered good with both private and public health care available to the population.

- **Immigration:** There is some migration **out of** Morocco, but there is considerable **internal migration** from rural to urban areas. Large movements of people began around 1956 when Morocco gained independence. Since then urban towns have become very overcrowded.

- **Medical conditions:** There has been a considerable change in the diet of the general population and there has also been an increase in diabetes and cancer cases. HIV is not considered a large problem in Morocco although rates are beginning to rise.

- **Ageing population and TB epidemic:** The average age of a TB patient in Morocco is slowly increasing. People born in 1954 – 1960 are more likely to have a TB occurrence than those born in later years.

Appendix F

Exponential line fits to TB data from the Netherlands, Morocco and UK

F.1 Exponential line fits to the Dutch TB data

Figure F.1: (a)-(h): Plots of the Dutch TB case data for each of the 8 age ranges, with exponential line fits of the form: ln(TB cases/100,000) = A exp(-B age).

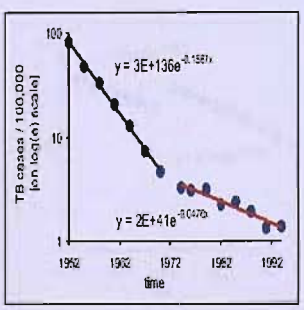

(a) Ages 0 to 14 years.

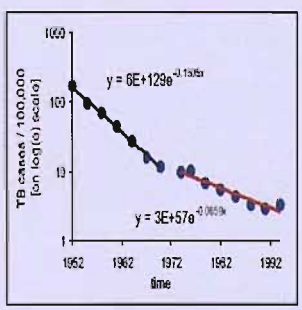

(b) Ages 15 to 24 years.

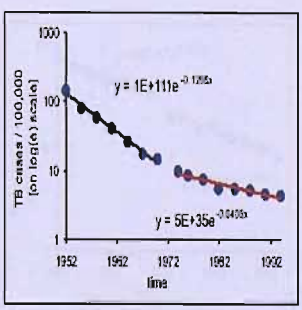

(c) Ages 25 to 34 years.

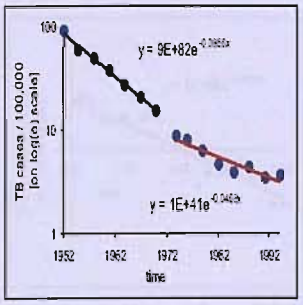

(d) Ages 35 to 44 years.

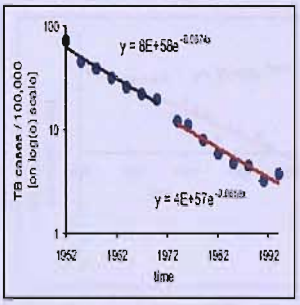

(e) Ages 45 to 54 years.

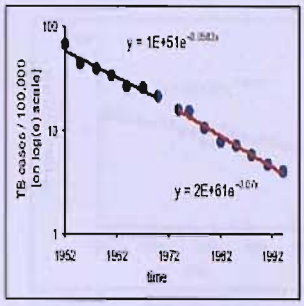

(f) Ages 55 to 64 years.

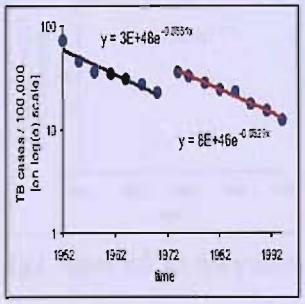

(g) Ages 65 to 69 years.

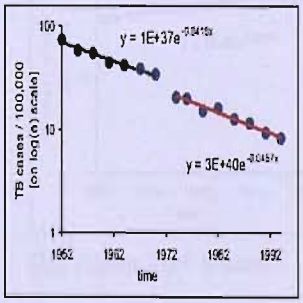

(h) Ages 70+ years.

F.2 Exponential line fits to the Moroccan PTB data

Figure F.2: (a)-(h): Plots of Moroccan PTB case data for each of the 8 age ranges, with exponential line fits of the form: ln(TB cases/100,000) = A exp(-B age).

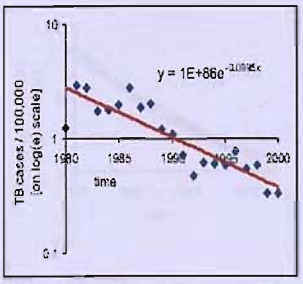

(a) Ages 0 to 14 years.

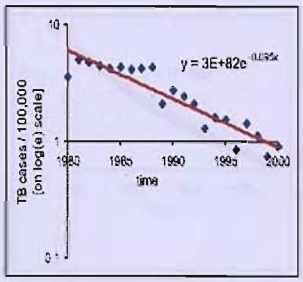

(b) Ages 15 to 24 years.

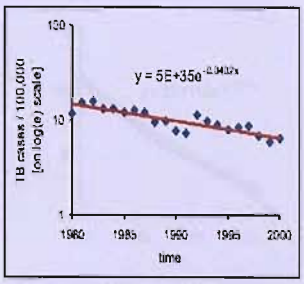

(c) Ages 25 to 34 years.

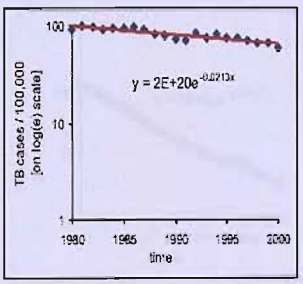

(d) Ages 35 to 44 years.

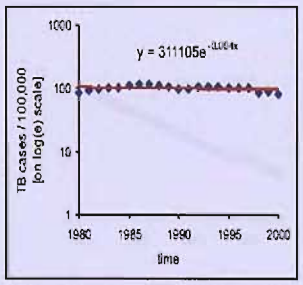

(e) Ages 45 to 54 years.

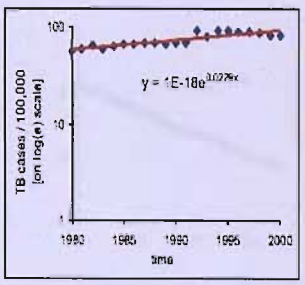

(f) Ages 55 to 64 years.

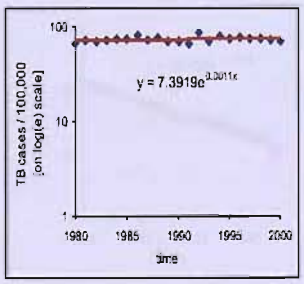

(g) Ages 65 to 69 years.

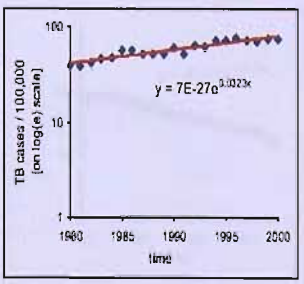

(h) Ages 70+ years.

F.3 Exponential line fits to UK white males TB data

Figure F.3: (a)-(h): Plots of UK (Male) TB case data for each of the 8 age ranges, with exponential line fits of the form: ln(TB cases/100,000) = A exp(-B age).

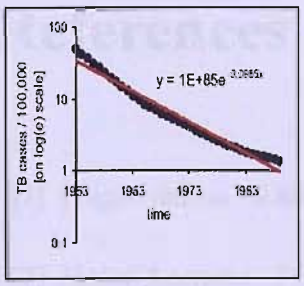

(a) Ages 0 to 14 years.

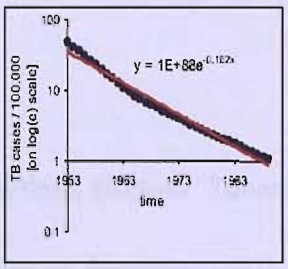

(b) Ages 15 to 24 years.

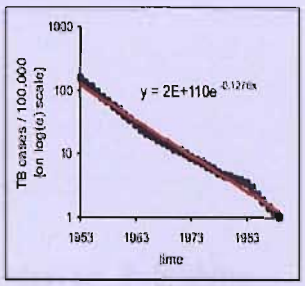

(c) Ages 25 to 34 years.

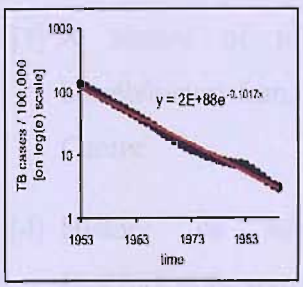

(d) Ages 35 to 44 years.

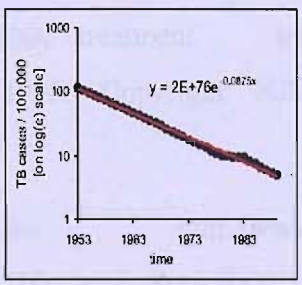

(e) Ages 45 to 54 years.

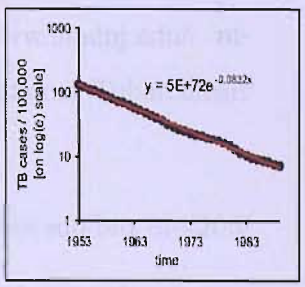

(f) Ages 55 to 64 years.

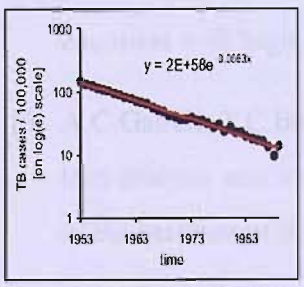

(g) Ages 65 to 69 years.

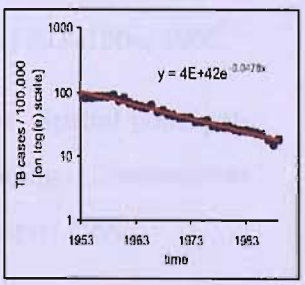

(h) Ages 70+ years.

References

[1] Plague nation - a history of three diseases: Tuberculosis.

[2] *Nobel Lectures, Physiology or Medicine 1901-1921*. Elsevier Publishing Company, Amsterdam, 1967.

[3] A history of tuberculosis treatment. http://www.umdnj.edu/ nt-bcweb/history.htm, July 1996. Copyright: NJMS National Tuberculosis Center.

[4] History of tuberculosis. http://www.goshen.edu/bio/Biol206/ Biol206LabProject/tricia/Tbhx.html, April 2000.

[5] A.Bermejo, H.Veeken, and A.Berra. Tuberculosis incidence in developing countries with high prevalence of hiv infection. *AIDS*, 6:1203–1206, 1992.

[6] A.C.Gatrell, T.C.Bailey, P.J.Diggle, and B.S.Rowlingson. Spatial point pattern analysis and its application in geographical epidemiology. *Transactions of the Institute of British Geographers*, 21(1):256–274, April 1996.

[7] A.D.Cliff and J.K.Ord. *Spatial Processes: Models and Applications (Chapters 1-5)*. London:Pion, 1981.

[8] B.Efron. Bootstrap methods: Another look at the jackknife. *Annals of Statistics*, 7:1–26, 1979.

[9] B.Efron and R.J.Tibshirani. *An introduction to the Bootstrap.* Chapman and Hall, 1 edition, 1993.

[10] B.Song, C.Castillo-Chavez, and J.P.Aparicio. Tuberculosis models with fast and slow dynamics: the role of close and casual contacts. *Mathematical Biosciences*, 180:187–205, 2002.

[11] B.Williams, E.Gouws, D.Wilkinson, and S.A.Karim. Estimating hiv incidence rates from age prevalence data in epidemic situations. *Statistics In Medicine*, 20:2003–2016, 2001.

[12] C.Castillo-Chavez and Z.Feng. To treat or not to treat: the case of tuberculosis. *Journal of Mathematical Biosciences*, 35:629–656, 1997.

[13] C.Dye and B.G.Williams. Criteria for the control of drug-resistant tuberculosis. *PNAS*, 97(14):8180–8185, July 2000.

[14] C.Dye, G.P.Garnett, K.Sleeman, and B.G.Williams. Prospects for global tuberculosis control under the who dots strategy. Global tuberculosis programme, World Health Organisation, Geneva, November 1998.

[15] C.Dye, G.P.Garnett, K Sleeman, and B.G.Williams. Prospects for worldwide tuberculosis control under the who dots strategy. *The Lancet*, 352:1886–1891, December 1998.

[16] C.Eberwein, R.J.Olsen, and P.B.Reagan. Intracluster correlation and complex sampling: Do geographic data lessen the problem? August 2003.

[17] C.J.Price, I.D.Coope, and D.Byatt. A convergent variant of the nelder-mead algorithm. *Journal of Optimisation Theory and Applications*, 113(1):5–19, April 2002.

[18] C.Murray, K.Styblo, and A.Rouillon. Tuberculosis: Disease control priorities in developing countries. *Oxford University Press*, 1993.

[19] C.S.M.Currie. A study of the effectiveness of different interventions in reducing the severity of tuberculosis epidemics in countries with a high prevalence of human immunodeficiency virus. A dissertation submitted in partial fulfilment of the requirements for the msc in operational research, University of Southampton, 2001.

[20] C.S.ReVelle, W.R.Lynn, and F.Feldmann. Mathematical models for the economic allocation of tuberculosis control activities in developing nations. *American Rev. Respiratory Disease*, 96(5):893–909, 1967.

[21] C.W.Koehler. Consumption, the great killer. *MDD*, 5(2):47–49, February 2002. (http://pubs.acs.org/subscribe/journals/mdd/v05/i02/html/02timeline.html).

[22] H.van Deutekom, S.P.Joijing, P.E.W.de Haas, M.W.Langendam, and A.Horsman. Clustered tuberculosis cases: Do they represent recent transmission and can they be detected earlier? *American Journal of Critical Care Medicine*, 169:806–810, 2004. www.atsjournals.org.

[23] E.Girardi, M.C.Raviglioni, G.Antonucci, P.Godfrey-Fausset, and G.Ippolito. Impact of the hiv epidemic on the spread of other diseases: the case of tuberculosis. *AIDS*, 14(suppl 3):S47–S56, 2000.

[24] E.G.Knox. The detection of space-time interactions. *Applied Statistics*, 13(1):25–29, 1964.

[25] E.Gouws. Modelling disease transmission, hiv in south africa, July 1998. Instructional notes, with help from B.Williams and C.Dye.

[26] E.L.Corbett, C.J.Watt, N.Walker, D.Maher, B.G.Williams, M.C.Raviglione, and C.Dye. The growing burden of tuberculosis: global trends and interactions with the hiv epidemic. *Arch Internal Medicine*, 12(163(9)):1009–21, 2003.

[27] E.Massad. Modeling the interaction between aids and tuberculosis. *Mathematical Computer Modelling*, 17(9):7–21, 1993.

[28] E.Vynnycky and P.E.M.Fine. The natural history of tuberculosis: the implications of age-dependent risks of disease and the role of reinfection. *Epidemiol Infect.*, 119:183–201, 1997.

[29] F.Marais. Tb history. http://www.ukcoalition.org/tb/history.html. Web page of the registered charity: UK Coalition of People Living with HIV and AIDS.

[30] F.W.O.Saporu. The use of a markov chain model in the analysis of data on the change in fertility status in cows. *The Statistician*, 43(3):403–412, 1994.

[31] G.Garnett and R.Anderson. Balancing sexual partnerships in an age and activity stratified model of hiv transmission in heterosexual populations. *IMA Journal of Mathematics*, 11:161–192, 1994.

[32] G.Jacquez. A k nearest neighbour test for space-time interaction. *Statistics in Medicine*, 15:1935–1949, 1996.

[33] G.J.Gibson, A.Kleczkowski, and C.A.Gilligan. Bayesian analysis of botanical epidemics using stochastic compartmental models. *Proc Natl Acad Sci USA*, 101(33):12120–12124, 2004.

[34] G.J.Gibson, C.A.Gilligan, and A.Kleczkowski. *Proc. R. Soc. London Series B*, 266:1743–1753, 1999.

[35] G.J.Gibson and E.Renshaw. *Stat Comput.*, 11:347–358, 2001.

[36] H.H.Chen, S.W.Duffy, and L.Tabar. A markov chain method to estimate the tumour progression rate from preclinical to clinical phase, sensitivity and positive predictive value for mammography in breast cancer screening. *The Statistician*, 45(3):307–317, 1996.

[37] H.T.Waaler and M.A.Piot. The use of an epidemiological model for estimating the effectiveness of tuberculosis control measures. *Bulletin World Health Organisation*, 41:75–93, 1969.

[38] H.Waaler, A.Geser, and S.Anderson. The use of mathematical models in the study of the epidemiology of tuberculosis. *American Journal of Public Health*, 52(6):1002 – 1013, 1962.

[39] J.A.Nelder and R.Mead. A simplex method for function minimization. *Computer Journal*, 7:308–313, 1965.

[40] J.A.N.Filipe and C.A.Gilligan. *Phys. Rev. E*, 67, 2003.

[41] J.A.Salomon and C.J.L.Murray. Modelling hiv/aids epidemics in sub-saharan africa using seroprevalence data from antenatal clinics. *Bulletin of the World Health Organisation*, 79(7):596–607, 2001.

[42] J.C.Lagarias, J.A.Reeds, M.H.Wright, and P.E.Wright. Convergence properties of the nelder-mead simplex method in low dimensions. *SIAM J.OPTIM.*, 9(1):112–147, 1998. Society for Industrial and Applied Mathematics.

[43] J.Fox. Bootstrapping regression models. *http://cran.r-project.org*, January 2002.

[44] J.O.Kephart, R.Das, and J.K.MacKie-Mason. Two-sided learning in an agent economy for information bundles. Website: www.research.ibm.com/infoecon/paps/html/amec99_bundle/node8.html.
A modified and extended version of a paper presented by Kephart at the Agent-mediated Electronic Commerce workshop at IJCAI'99, July 31, 1999 in Stockholm.

[45] J.P.Aparicio, A.F.Capurro, and C.Castillo-Chavez. Transmission and dynam-

ics of tuberculosis on generalised households. *Journal of Theoretical Biology*, 206:327–341, 2000.

[46] J.P.Aparicio, A.F.Capurro, and C.Castillo-Chavez. Markers of disease evolution: The case of tuberculosis. *Journal of Theoretical Biology*, 215:227–237, 2002.

[47] K.B.Arabas. Spatial and temporal relationships among fire frequency, vegetation, and soil depth in an eastern north american serpentine barren. *Journal of the Torrey Botanical Society*, 127(1):51–65, January-March 2000.

[48] K.Styblo. Epidemiology of tuberculosis. *The Hague: KNCV, Royal Netherlands Tuberculosis Association*, 1991.

[49] L.Getoor, J.T.Rhee, D.Koller, and P.Small. Understanding tuberculosis epidemiology using structured statistical models. *Artificial Intelligence in Medicine*, 30:233–256, 2004.

[50] L.Sattenspiel and C.P.Simon. The spread and persistence of infectious diseases in structured populations. *Mathematical Biosciences*, 90(1-2):341–366, July-August 1988.

[51] L.Smith. Washington post article. Washington Post, May 2003. Thursday May 01 2003 (Final Edition) Leef Smith Washington Post Staff Writer.

[52] M.A.Entin. Romance and tragedy of tuberculosis: Edward archibald's contribution to the surgical treatment of pulmonary tuberculosis. *The Canadian Journal of Plastic Surgery*, 3(4), Winter 1995.

[53] M.C.Pike and P.G.Smith. Disease clustering: A generalization of knox's approach to the detection of space-time interactions. *Biometrics*, 24(3):541–556, September 1968.

[54] N.Basgoz MD. http://patients.uptodate.com/. Assistant Professor of Medicine Harvard Medical School.

[55] M.J.Symons, R.C.Grimson, and Y.C.Yuan. Clustering of rare events. *Biometrics*, 39:193–205, 1983.

[56] M.K.Campbell, J.M.Grimshaw, and D.R.Elbourne. Intracluster correlation coefficients in cluster randomised trials: empirical insights into how should they be reported. *BMC Medical Research Methodology*, 4(9), April 2004. www.biomedcentral.com/1471-2288/4/9.

[57] M.K.Campbell, J.Mollison, and J.M.Grimshaw. Cluster trials in implementation research: estimation of intracluster correlation coefficients and sample size. *Statistics In Medicine*, 20:391–399, 2001.

[58] M.Kendall and A.Stuart. *The Advanced Theory of Statistics*, volume 2. Griffin, London, 4th edition, 1979.

[59] M.Kulldorff. A spatial scan statistic. *Communications in Statistics: Theory and Methods*, 26(6):1481–1496, 1997.

[60] M.Kulldorff. Satscan v4.0: Software for the spatial and space-time scan statistics. http://www.satscan.org/, 2003. In association with Information Management Services Inc.

[61] M.Kulldorff, F.Mostashari, J.Hartman, and R.Heffernan. A space-time permutation scan statistic for the early detection of disease outbreaks. 2003.

[62] M.Kulldorff and Inc. Information Management Services. Satscan v4.0: Software for the spatial and space-time scan statistics. Software, 2003. www.satscan.org.

[63] M.R.Chernick. *Bootstrap Methods: A Practitioners' Guide*. Wiley.

[64] M.Sampson. A markov chain model for unskilled workers and the highly mobile. *Journal of the American Statistical Association*, 85(409):177–180, March 1990.

[65] M.Schulzer, J.M.Fitzgerald, D.A.Enarson, and S.Grzybowski. An estimate of the future size of the tuberculosis problem in sub-saharan africa resulting from hiv infection. *Tubercle and Lung Disease*, 73:52–58, 1992.

[66] M.Schulzer, M.P.Radhamani, S.Grzybowski, E.Mak, and J.Mark. A mathematical model for the prediction of the impact of hiv infection on tuberculosis. *International Journal of Epidemiology*, 23(2):400–407, 1994.

[67] M.W.Borgdorff and N.Yamada. Who/wpro country/area profiles on possible stagnation of tuberculosis decline: Brunei, hong kong, japan, korea, macao, malaysia, and singapore. Draft report, World Health Organisation, January 2002.

[68] N.Mantel. The detection of disease clustering and a generalised regression approach. *Cancer Research*, 27:209–220, 1967.

[69] O.C.Ukoumunne, M.C.Gulliford, and S.Chinn. A note on the use of the variance inflation factor for determining sample size in cluster randomized trials. *The Statistician*, 51(4):479–484, 2002.

[70] O.C.Ukoumunne, M.C.Gulliford, S.Chinn, J.A.C.Sterne, P.G.J.Burney, and A.Donner. Methods in health service research: Evaluation of health interventions at area and organisation level. *British Medical Journal*, 319:376–379, August 1999.

[71] World Health Organisation. Global tuberculosis control: Surveillance, planning, financing, who report 2004. WHO Report 2004, Geneva, Switzerland, 2004. ISBN 920401S626401.

[72] P.Bratley, B.L.Fox, and L.E.Schrage. *A Guide to Simulation.* Springer-Verlag, 1983.

[73] P.Diggle, A.Chetwynd, R.Higgkvist, and S.Morris. Second-order analysis of space-time clustering. *Statistical methods in Medical Research*, 4(124-136), 1995.

[74] P.Humphreys. The magic mountain - a time capsule of tuberculosis treatment in the early twentieth century. *CBMH/BCHM*, 6:147–163, 1989.

[75] P.K.Moonan, M.Bayona, T.N.Quitugua, J.Oppong, D.Dunbar, K.C.Jost.Jnr, G.Burgess, K.P.Singh, and S.E.Weis. Using gis technology to identify areas of tuberculosis transmission and incidence. *International journal of Health Geographics*, 3(23), 2004.

[76] R.D.Baker. Testing for space-time clusters of unknown size. *Journal of Applied Statistics*, 23:543–554, 1996.

[77] R.E.LaPorte, F.Linkov, and M.Lovalekar et al. Supercourse epidemiology, the internet and global health. Website: www.pitt.edu/ super1/index.htm.

[78] R.F.Raubertas. Spatial and temporal analysis of disease occurrence for detection of clustering. *Biometrics*, 44(4):1121–1129, December 1988.

[79] R.Haining. Spatial and spatial-temporal interaction models and the analysis of patterns of diffusion. *Transactions of the Institute of British Geographers, New Series*, 8(2):158–186, 1983.

[80] R.J.Marshall. A review of methods for the statistical analysis of spatial patterns of disease. *Journal of the Royal Statistical Society. Series A (Statistics in Society)*, 154(3):421–441, 1991.

[81] R.J.Serfling. *Approximation Theorems of Mathematical Statistics*. John Wiley, New York, 1980.

[82] R.M.Lewis, V.Torczon, and M.W.Trosset. Direct search methods: then and now. *Journal of Computational and Applied Mathematics*, 124(1-2):191–207, December 2000.

[83] R.M.Turner, A.T.Prevost, and S.G.Thompson. Allowing for imprecision of the intracluster correlation coefficient in the design of cluster randomised trials.

[84] S.Brogger. Systems analysis in tuberculosis control: A model. *American Rev. Resp. Disease*, 95:419–434, 1965.

[85] S.J.Zyzanski, S.A.Flocke, and L.M.Dickinson. On the nature and analysis of clustered data. *Annals of Family Medicine*, 2(3):199–200, May/June 2004. www.ANNFAMMED.ORG.

[86] S.Killip, Z.Mahfoud, and K.Pearce. What is an intracluster correlation coefficient? crucial concepts for primary care researchers. *Annals of Family Medicine*, 2(3), May/June 2004. WWW.ANNFAMMED.ORG.

[87] S.M.Blower and H.Dowlatabadi. Sensitivity and uncertainty analysis of complex models of disease transmission: an hiv model, as an example. *International Statistical Review*, 62(2):229–243, 1994. *copywrite* International Statistical Institute.

[88] S.M.Blower and J.L.Gerberding. Understanding, predicting and controlling the emergence of drug-resistant tuberculosis: a theoretical framework. *Journal Mol. Med.*, 76:624–636, 1998.

[89] S.M.Debanne, R.A.Bielefeld, G.M.Cauthen, T.M.Daniel, and D.Y.Rowland. Multivariate markovian modeling of tuberculosis: Forecast for united states. *Emerging Infectious Diseases*, 6(2):148–157, March-April 2000.

[90] S.M.Kerry and J.M.Bland. Statistics notes: Sample size in cluster randomisation. *British Medical Journal*, 316(549), February 1998. http://bmj.bmjjournals.com.

[91] S.P.Brooks. *J.R.Stat.Soc D*, 47:69–100, 1998.

[92] S.Verver, R.M.Warren, Z.Munch, E.Vynnycky, P.D.van Helden, M.Richardson, G.D.van der Spuy, D.A.Enarson, M.W.Borgdorff, M.A.Behr, and N.Beyers. Transmission of tuberculosis in a high incidence urban community in south africa. *International Journal of Epidemiology*, 33(2):351–357, 2004.

[93] T.C.Porco, P.M.Small, and S.M.Blower. Amplification dynamics: Predicting the effect of hiv on tuberculosis outbreaks. *JAIDS Journal of Acquired Immune Deficiency Syndromes*, 28:437–444, 2001.

[94] The Cochrane Collaboration. Research glossary for consumers. Website: www.cochrane.org/cochrane/cngloss.htm. First draft prepared by the Australasian Cochrane Centre in April 1996.

[95] Y.Azuma. A simple simulation model of tuberculosis epidemiology for use without large scale computers. *Bulletin World Health Organisation*, 52:313–322, 1975.

[96] Z.Feng. A model for tuberculosis with exogenous reinfection. *Theoretical Population Biology*, 57:235–247, 2000.